Iron-sulfur cluster coordinating Glutaredoxins in neuroinflammatory degeneration and regeneration

Inaugural - Dissertation

Zur Erlangung des Doktorgrades
der Mathematisch-Naturwissenschaftlichen Fakultät
der Heinrich-Heine-Universität Düsseldorf

vorgelegt von

Klaudia Maria Lepka
aus Menden (Sauerland)

Düsseldorf, Januar 2017

Aus der Klinik für Neurologie
der Heinrich-Heine-Universität Düsseldorf

Gedruckt mit der Genehmigung der
Mathematisch-Naturwissenschaftlichen Fakultät der
Heinrich-Heine-Universität Düsseldorf

Referent: **Univ.-Prof. Dr. Orhan Aktas**
(Klinik für Neurologie der Heinrich-Heine-Universität Düsseldorf)

Korreferent: **Univ.-Prof. Dr. Dieter Willbold**
(Institut für Physikalische Biologie der Heinrich-Heine-Universität Düsseldorf)

Tag der mündlichen Prüfung: 07.02.2017

Data of this thesis have been published:

In published manuscripts:

Bräutigam L., Jensen LD, Poschmann G, Nyström S, Bannenberg S., Dreij K, **Lepka K**, Prozovoski T, Montano SJ, Aktas O, Uhlén P, Stühler K, Cao Y, Holmgren A, Berndt C, Glutaredoxin regulates vascular development by reversible glutathionylation of sirtuin 1. Proc Natl Acad Sci U S A. 110: 20057-20062 (2013)

Gellert M, Hanschmann EM, **Lepka K**, Berndt C, Lillig CH, Redox regulation of cytoskeletal dynamics during differentiation and de-differentiation. Biochim Biophys Acta. 1850: 1575-1587 (2015)

Lepka K, Berndt C, Hartung HP, Aktas O, Redox Events As Modulators of Pathology and Therapy of Neuroinflammatory Diseases. Front Cell Dev Biol. 4: 63 (2016)

Lepka K, Volbracht K, Bill E, Schneider R, Rios N, Hildebrandt T, Ingwersen J, Prozorovski T, Lillig CH, Hartung HP, Radi R, Holmgren A, Aktas O, Berndt C, Iron-sulfur Glutaredoxin 2 protects oligodendrocytes against damage induced by nitric oxide release from activated microglia (accepted in GLIA; see attachment)

Published manuscripts not included in this thesis:

Ingwersen J, Wingerath B, Graf J, **Lepka K**, Hofrichter M, Schröter F, Wedekind F, Bauer A, Schrader J, Hartung HP, Prozorovski T, Aktas O, Dual roles of the adenosine A2a receptor in autoimmune neuroinflammation. J Neuroinflammation. 13: 48 (2016)

As oral presentation (selected from abstract):

Lepka K, Volbracht K, Voevodskaya N, Bill E, Hartung HP, Aktas O, Berndt C, Glutaredoxin2 protection against oligodendroglial cell death during neuroinflammation. Society of Free Radical Research International (SFRRI 2014; Kyoto- Japan)

As poster contribution:

Lepka K, Volbracht K, Voevodskaya N, Bill E, Radi R, Hartung HP, Holmgren A, Aktas O, Berndt C, Holo Glutaredoxin2 protects oligodendrocytes during neuroinflammation. Current Topics in Myelin Research (2015, Kassel- Germany)

Lepka K, Volbracht K, Voevodskaya N, Bill E, Aktas O, Holmgren A, Berndt C, Holo Glutaredoxin2 protects against nitric oxide-mediated oligodendroglial cell death. 66. Mosbacher Kolloquium- “Metals in Biology- Cellular Functions and Diseases“ (GBM 2015, Mosbach- Germany)

Lepka K, Volbracht K, Schaberg E, Hartung HP, Goebels N, Aktas O, Berndt C, Glutaredoxin2 increases oligodendroglial capacity for regeneration. XII European Meeting on Glial Cells in Health and Disease (GLIA 2015, Bilbao- Spain)

Lepka K, Volbracht K, Voevodskaya N, Bill E, Radi R, Hartung HP, Aktas O, Holmgren A, Berndt C, Holo Glutaredoxin2 protects oligodendrocytes against neuroinflammatory cell death using an unconventional thiol switch. Thiol-based Redox Switches in Life Sciences (EMBO 2015, San Feliu de Guixols- Spain)

Table of content

Abstract

Multiple Sclerosis (MS) is a chronic inflammatory disease and the major cause for sustained neurological disabilities among young adults in western countries. Its pathology is characterized by focally appearing neuroinflammation via invading immune cells as well as focal demyelination. The concomitant activation of microglia, the resident immune cells of the central nervous system, leads to increased production of reactive oxygen and nitrogen species. Subsequent oxidative damage of lipids, nucleotides and proteins contributes to oligodendrocyte degeneration and hence, to demyelination. The oxidation of proteins can be reversed by oxidoreductases. Proteins of this family, like Glutaredoxins (Grxs), control various important signaling pathways via regulation of the protein thiol redox state. Grx2, for example, essentially contributes to brain development in vertebrates. However, the role of Grxs in neuroinflammatory diseases remains to be investigated. The aims of this study are firstly, to investigate the role of Grxs in neuroinflammation-mediated degeneration of oligodendrocytes and secondly, to examine the role of Grx2 in oligodendrocyte progenitor migration and differentiation, which are key properties for functional remyelination.

Our findings demonstrate that modulation of Grx2, via treatment with recombinant Grx2 or Grx2-specific si-RNA, affects the viability of primary mouse oligodendrocyte progenitors challenged by nitric oxide (NO). Decreased Grx2 levels enhanced the vulnerability of oligodendrocytes for NO while Grx2 treatment improved their viability in presence of NO. Of note, this was independent from the enzymatic activity of Grx2. UV-VIS spectroscopy and electron paramagnetic resonance spectroscopy revealed the NO-dependent disassembly of the Grx-specific iron-sulfur cluster (FeS) to result in formation of dinitrosyl-diglutathionyl-iron complexes. Thus, the Grx2-dependent NO-detoxification decreased nitrosative as well as oxidative damage in oligodendrocytes. Our results further demonstrate that Grx2 affects regeneration properties of oligodendrocytes. Treatment with Grx2 increased the transmigration of primary oligodendrocyte progenitors and blocked their differentiation in the migrating NG2-state. The systemic importance of the cell culture-based findings was verified using different *ex vivo* approaches. The expression of Grx2 was upregulated in acute human MS lesions as well as in the acute phase of experimental autoimmune encephalomyelitis, an animal model for MS, in mice. In cerebellar organotypic slice cultures, treatment with Grx2 protected against NO-mediated degeneration of myelin and increased the number of NG2- as well as ramified myelin-expressing cells under remyelinating conditions.

In conclusion, recombinant Grx2 enhanced oligodendrocyte progenitor migration and decreased their differentiation. Moreover, Grx2 is the first example to demonstrate a beneficial role of FeS disassembly, thus promoting cell survival via NO-detoxification.

We hypothesize FeS-coordinating Grxs to play a promising role in future therapies for inflammatory demyelinating diseases, such as MS.

Zusammenfassung

Multiple Sklerose (MS) ist eine chronisch-entzündliche Erkrankung des zentralen Nervensystems und stellt die Hauptursache für irreversible neurologische Beeinträchtigungen unter jungen Erwachsenen in der westlichen Welt dar. Pathologische Charakteristika sind fokale durch eingewanderte Immunzellen vermittelte Inflammations- sowie Demyelinisierungsherde. Die einhergehende Aktivierung der Mikroglia, der residenten Immunzellen des zentralen Nervensystems, führt zu einer verstärkten Produktion reaktiver Sauerstoff- und Stickstoff-Spezies. Diese Spezies tragen über oxidative Schädigungen von Lipiden, Nukleotiden und Proteinen in Oligodendrozyten zu deren Degeneration und somit zum Demyelinisierungsprozess bei. Entstandene Proteinoxidationen können durch Oxidoreduktasen aufgehoben werden. Mitglieder dieser Proteinfamilie, wie die Glutaredoxine (Grx), regulieren über den Protein-Thiol-Redox Status eine Vielzahl an wichtigen Signalwegen. Beispielsweise trägt Grx2 wesentlich zu der Hirnentwicklung in Vertebraten bei, doch ist der genaue Einfluss der Grx auf neuroinflammatorische Krankheitsverläufe bisher nicht untersucht. Die Ziele der vorliegenden Arbeit sind zum einen, die Untersuchung der Rolle von Grx in neuroinflammatorischen Degenerationsprozessen der Oligodendrozyten und zum anderen, die Untersuchung der Rolle von Grx2 auf die Migration und die Differenzierungsfähigkeit der Oligodendrozyten-Vorläuferzellen, Schlüsseleigenschaften für eine funktionsfähige Remyelinisierung.

Unsere Ergebnisse belegen einen Einfluss der Grx2-Konzentrationen auf die Stickstoffmonoxid(NO)-Resistenz primärer Oligodendrozyten-Vorläuferzellen aus der Maus, welche durch Behandlung mit rekombinantem Grx2 oder Grx2-spezifischer si-RNA moduliert wurden. Reduzierte Grx2-Konzentrationen verstärkten die Vulnerabilität von Oligodendrozyten gegenüber NO, während erhöhte Grx2-Konzentrationen die Überlebensfähigkeit der Oligodendrozyten in Gegenwart von NO steigerten. Zu beachten ist, dass dieser Vorgang nicht auf der enzymatischen Aktivität, sondern auf der NO-abhängigen Umwandlung des Grx-spezifischen Eisen-Schwefel-Zentrums (FeS) in Dinitrosyl-Diglutathionyl-Eisen-Komplexe beruht. Auf diese Weise schützt die Grx2-abhängige NO-Entgiftung Oligodendrozyten vor nitrosativen und oxidativen Schädigungen. Weiterhin belegen unsere Daten, dass Grx2 die Regenerationseigenschaften von Oligodendrozyten modifiziert. Die Behandlung primärer Oligodendrozyten-Vorläuferzellen mit Grx2 erhöhte die Fähigkeit zur Transmigration und blockierte deren Differenzierung im migrierenden NG2-Stadium. Zusätzliche *ex vivo* Ansätze verifizierten die systemische Relevanz der oben genannten zellkulturbasierten Resultate. Die Expression von Grx2 war sowohl in humanen MS-Läsionen wie auch in der akuten Phase der Experimentellen Autoimmunen Enzephalomyelitis, einem Tiermodell der MS, in Mäusen gesteigert. In organotypischen Schnittkulturen des Kleinhirns inhibierte eine Behandlung mit Grx2 die NO-induzierte Degeneration von Myelin und erhöhte die

Anzahl an NG2- sowie verzweigten myelinexprimierenden Zellen unter remyelinisierenden Bedingungen.

Zusammenfassend steigerte rekombinantes Grx2 die Migration von Oligodendrozyten-Vorläuferzellen und blockierte deren Differenzierung. Darüber hinaus stellt Grx2 das erste Beispiel eines FeS-koordinierenden Enzyms dar, dessen Cofaktor-Abbau über die beschriebene NO-Entgiftung einen protektiven Effekt auf die Zellviabilität hervorruft.

Die vorliegenden Daten bieten eine vielversprechende Grundlage für neue Therapieansätze in der Behandlung inflammatorisch demyelinisierender Ergkrankungen wie der MS.

1. Introduction

1.1 Redox biology

1.1.1 Reactive oxygen and nitrogen species

Reactive species comprise radicals like superoxide ($O_2^{\cdot -}$), hydroxyl- and nitric oxide-radicals ($OH\cdot$; $NO\cdot$) as well as non-radicals, such as hydrogen peroxide (H_2O_2) and peroxynitrite ($ONOO^-$). Every reactive molecule has its own chemical characteristics and thus distinct cellular reaction profiles (Gutteridge and Halliwell 1989). Under physiological conditions, they are mainly produced as side products of enzymatic reactions, predominantly by mitochondrial adenosine triphosphate (ATP) production. Under pathological conditions, for example upon inflammation, reactive oxygen species (ROS) and reactive nitrogen species (RNS) are increasingly produced. Immune cells (such as macrophages and microglia) enhance the generation of ROS/RNS after pathogen recognition of, for example, invading microbes as first cellular response (Paiva and Bozza 2014). This mechanism is known as “oxidative burst”, firstly discovered in plants, and represents both a toxic defense-machinery as well as an activator of further defense pathways (Doke et al. 1996). In general, pathological production of ROS and RNS is known as oxidative stress. The term “oxidative stress” was introduced in 1985, describing the imbalance between cellular pro- and antioxidant systems (Sies and Cadenas 1985). Pathological features comprise increased oxidative modifications of nucleotides, proteins, carbohydrates and lipids, which accumulate upon inflammation-mediated disorders of the central nervous system (CNS) like Multiple Sclerosis (MS) (Haider et al. 2011). Upon neuroinflammation (inflammatory processes in the CNS) extensive amounts of reactive species are generated by three major pathways: (I) Glial/macrophage iNOS upregulation leading to excessive NO synthesis, (II) mitochondrial alterations resulting in increased $O_2^{\cdot -}$ formation and further formation of H_2O_2 through superoxide dismutase (SOD) as well as (III) the Fenton reaction between H_2O_2 and metal ions generating $OH^{\cdot}$.

(I) One characteristic hallmark of inflammatory CNS lesions, as observed in the pathology of the autoimmune demyelinating disorder MS, is the increased generation of NO (Zipp and Aktas 2006). Remarkably, iNOS is significantly upregulated in lesion areas of MS patients (Bö et al. 1994; De Groot et al. 1997) and underlines its contribution to disease progression. NO is a gaseous and highly potent free radical that participates in a variety of chemical reactions and can freely diffuse across cell membranes. In this study, the term "NO" represents all three redox-active forms including the nitroxyl anion (NO^-),

the nitric oxide radical ($NO^{\cdot}$) and the nitrosonium cation (NO^{+}). In the brain, NO is synthesized by three different nitric oxide synthases (NOS): endothelial eNOS, neuronal nNOS and microglial iNOS, with iNOS being highly upregulated upon neuroinflammatory conditions (Hill et al. 2004). Via S-nitrosylation and cGMP modulation, NO functions as an intracellular messenger molecule and plays a role in neuronal functions such as memory, synaptic plasticity and sleep-wake rhythm (Palmer et al. 1987; Garthwaite et al. 1988; McCann et al. 1996; Xu et al. 1998; Guix et al. 2005). Increased concentrations of NO affect these signaling pathways detrimentally. Notably, since the 1990s a variety of reports have stressed the importance of NO-mediated degradation of FeS cluster proteins as an additional signaling pathway (Kennedy et al. 1997). FeS clusters are essential cofactors for a variety of cellular functions. One example is the iron regulatory protein 1 (IRP1). IRP1 is an FeS cluster protein itself that functions as active aconitase (ACO) in its holo-form or as iron regulatory element (IRE) in its apo-form. IREs regulate iron-dependent protein expression (Hirling et al. 1994). The FeS cluster degradation of ACO is modulated by NO and superoxide (Gardner et al. 1995; Kennedy et al. 1997), illustrating a correlation between increased NO concentrations and the regulation of iron homeostasis. Therefore, the concentration of NO determines its possible cell-toxic effect. Furthermore, NO can rapidly react with $O_2^{\cdot-}$ forming $ONOO^{-}$ by a diffusion-limited reaction (Huie and Padmaja 1993). There is evidence that most of the cytotoxic features of NO are rather caused by $ONOO^{-}$ and not by NO itself as NO is efficiently removed by the reaction with oxyhemoglobin to form nitrate (Joshi et al. 2002). Whether or not this mechanism is present in the CNS is yet unknown. $ONOO^{-}$ is able to damage nucleotides, to induce lipid peroxidation and to nitrate tyrosine residues of proteins leading to irreversible modifications. Pathologically, increased levels of both NO and $ONOO^{-}$ contribute to the loss of neural cells *in vitro* and *in vivo* (Jonnala and Buccafusco 2001; Li et al. 2005; Jack et al. 2007; Desai et al. 2016).

(II) Due to the enrichment of polyunsaturated fatty acids, the CNS parenchyma is highly sensitive to oxidative damage like lipid oxidation (Bazinet and Layé 2014). The low level of antioxidant molecules like SOD in comparison to other tissues is not sufficient to protect CNS tissue against oxidative damage. Thus, damage of mitochondrial deoxyribonucleic acid (DNA) is highly accumulated upon increased concentrations of ROS/RNS (Dringen 2000). The high metabolic activity of neural cells depends on oxidative phosphorylation in mitochondria, the energy producing organelles. Mitochondria constantly generate ROS as a byproduct of oxidative phosphorylation in the respiratory chain. This process leads to increased generation of $O_2^{\cdot-}$ and further to H_2O_2 catalyzed by SOD. Mitochondria themselves are highly vulnerable to oxidative DNA damage due to

their limited DNA repair capacity (Bohr et al. 2002). Dysfunctions of the respiratory chain are common consequences and cause impaired energy production as well as additional generation of reactive species. Extensive dysfunction of mitochondria was reported to contribute to the induction of apoptosis in neural cells under neuroinflammatory conditions in a variety of CNS disorders (Smigrodzki et al. 2004; Johri and Beal 2012) and in chronic progressive MS (Mahad et al. 2008; Campbell et al. 2011).

(III) Another important mechanism associated with pathological oxidative conditions is the Fenton reaction. H_2O_2 reacts with metal ions, mainly iron, to form highly reactive $OH^{\cdot}$. Therefore, iron uptake, distribution, storage and release are highly regulated in regard to its availability and need. In the CNS, these basics of iron homeostasis yet remain elusive. Iron, as a cofactor, is essential for basic processes like DNA replication, oxygen as well as electron transportation, glucose metabolism and ATP production (Beard et al. 1996). In regard to the CNS, iron is a cofactor for the synthesis of neurotransmitters and myelin, signal transduction and thus normal brain function (Youdim and Green 1978; Connor and Menzies 1996). For example, iron deficiency in rats led to hypomyelination and disturbance in brain function (Badaracco et al. 2008). Upon human aging, iron accumulates in brain tissue (Hallgren and Sourander 1958). However, the iron deposits observed under neuroinflammation are more pronounced compared to age-matched control groups (Craelius et al. 1982). It is yet unknown whether iron contributes to disease progression in MS and other neurodegenerative disorders such as Parkinson's disease Dexter et al. 1987) or iron depositions are a consequence of disease pathology. In contrast to MS, no comparable accumulation of iron in the CNS has been reported in an animal model of MS, the experimental autoimmune encephalomyelitis (EAE). However, iron chelation effectively decreases EAE severity in mice (Mitchell et al. 2007). Further evidences suggest a role of iron in disease pathology. Alterations in the expression levels of proteins, involved in iron homeostasis, have been reported. Here, concentrations of transferrin and ferritin, essential proteins for iron transport and uptake, were found to be elevated in the cerebrospinal fluid (CSF) of MS patients (Sfagos et al. 2005). Taken together, iron can contribute to MS pathology in two suggested ways: by increasing the formation of highly reactive $OH^{\cdot}$ molecules or by disturbance of essential cellular functions like myelin synthesis upon failure of iron homeostasis.

Although the term "oxidative stress" is still frequently used in science to describe general pathological oxidative processes, current research starts to specifically discriminate between the role of different reactive species and their different reduced forms in pathological and physiological cellular processes (Jones and Sies 2015).

1.1.2 Redox signaling and Glutaredoxins

During the last decade the importance of reactive species has shifted from an entirely detrimental view, when generated under pathological conditions, towards the increasingly accepted function of ROS and RNS as signaling molecules under physiological conditions (Jones and Sies 2015). At physiological concentrations, reactive species participate in cellular signaling as specific second messengers. The most important identified reactive second messengers are H_2O_2, NO and H_2S (Culotta and Koshland 1992; Bruce King 2013; Hancock and Whiteman 2014). Specific ROS/RNS-dependent signaling and in general aerobic life require the detoxification of reactive species including prevention, interception, repair and reversion of intended and unintended oxidative modifications. These mechanisms comprise non-enzymatic (ascorbic acid, flavonoids and α-Tocopherol) as well as enzymatic antioxidants (superoxide dismutases, glutathione (GSH) peroxidases, catalases and oxidoreductases). Specific redox events take place in all organisms. Under physiological conditions, reactive species act as specific and locally restricted prooxidant messengers. Thereby, they reversibly modulate protein stability, structure and activity. Thiol groups of cysteinyl residues are the major target (Hanschmann et al. 2013). Modifications include nitrosylation, thiol disulfide formation and glutathionylation. Essential cellular functions like proliferation (Zhang et al. 2008), differentiation (Gellert et al. 2013) as well as apoptosis (Enoksson et al. 2005) were already shown to be regulated by reversible redox events. Extrapolation by Go and Jones further suggested almost every signaling pathway to contain at least one redox regulated element (Go and Jones 2013).

Redox-dependent modification can be reversed by oxidoreductases like Thioredoxins (Trxs) and Glutaredoxins (Grxs). Grxs are members of the Trx family of proteins. This family comprises numerous enzymes and isoforms that differ in their active site composition as well as cellular localization (Fig. 1b). However, they share a structural motif, named the Trx fold. This motif consists of four stranded β-sheets and three surrounding α-helices. In higher organisms this motif can be expanded by additional helices and sheets. Grxs were first discovered as alternative electron donors for ribonucleotide reductase (RNR) (Holmgren 1979; Luthman et al. 1979). Recent findings indicate a participation of Grx2 in the susceptibility to apoptosis by preventing cytochrome c release (Enoksson et al. 2005) as well as a regulatory function in vascular and brain development (Bräutigam et al. 2011; Bräutigam et al. 2013). In detail, Grx2 is involved in the regulation of the thiol redox state of the collapsing response mediator protein 2 (CRMP2), an intracellular phosphoprotein

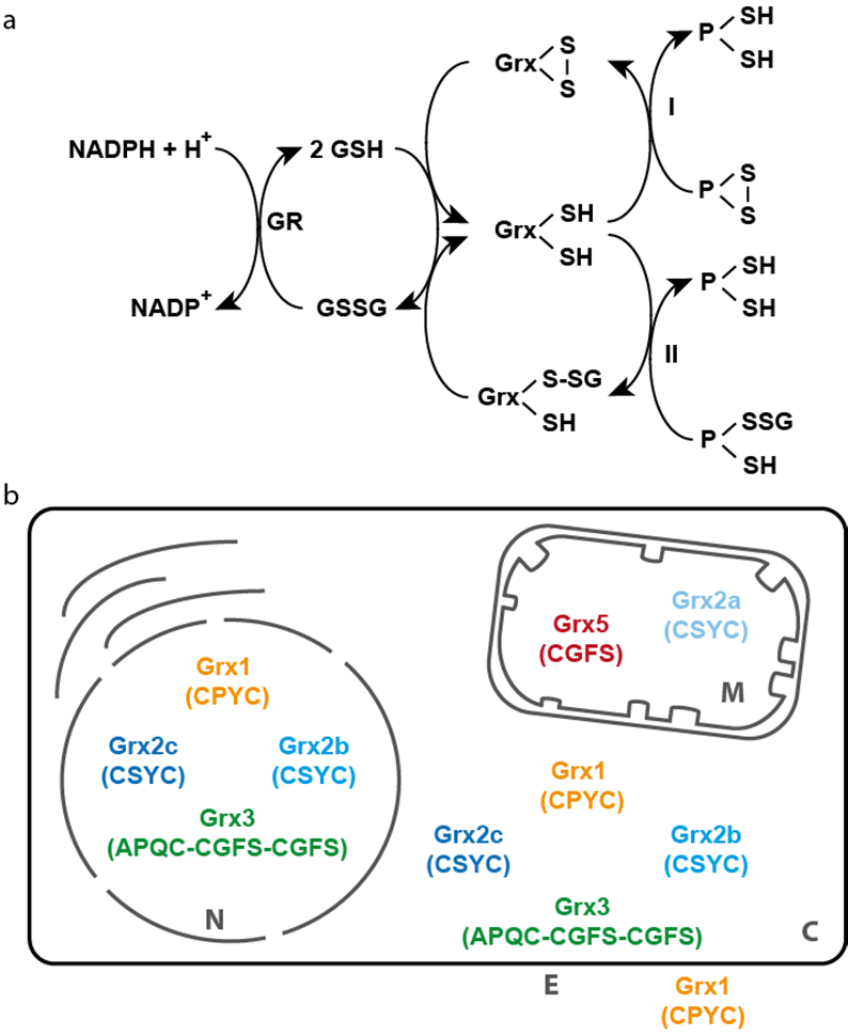

Figure 1. Reaction mechanism and cellular localization of Grxs in mammals. (a) The final electron source for Grxs is NADPH. The NADPH-dependent enzyme glutathione reductase (GR) generates two molecules of reduced glutathione (GSH) via the reduction of glutathione disulfide (GSSG). GSH delivers electrons to oxidized Grx. Thereby, Grx is able to reduce either a protein disulfide (dithiol mechanism; I) or a GSH-mixed disulfide (monothiol mechanism; II). (b) The isoforms and cellular localizations of mammalian Grxs are illustrated in addition to the active site sequence. C= cytosol, N= nucleus, M= mitochondrion, E= extracellular space (Hanschmann et al. 2013).

interacting with microtubules and involved in axon formation (Bräutigam et al. 2011). So far, four different Grxs were identified in mammalian cells: Grx1, Grx2, Grx3 and Grx5 (Fig. 1). Their active site motif enables the reaction of a dithiol (Grxs 1 and 2) or a monothiol mechanism (Grxs 3 and 5) involving either one or two active site cysteines. The monothiol reaction mechanism reduces glutathionylated substrates and the dithiol mechanism catalyzes the reduction of protein disulfides. The reconstruction of the reduced cysteines is ensured via two molecules of GSH (see Fig. 1a) (Johansson et al. 2004). Monothiol Grxs were shown to primarily contribute to iron homeostasis and biosynthesis of FeS clusters. Furthermore, they have a weak catalytic activity compared to the dithiol reaction mechanism. Cytosolic and nuclear located Grx3 was reported to be involved in iron trafficking and being a prerequisite for iron availability in zebrafish (Mühlenhoff et al. 2010; Haunhorst et al. 2013). Grx5 is located in mitochondria and is required for FeS cluster biosynthesis (Wingert et al. 2005). Besides Grx2, the monothiol

Grx3 and Grx5 are able to incorporate Grx-specific FeS clusters (Rodríguez-Manzaneque et al. 2002; Haunhorst et al. 2010).

1.1.2.1 Grx2 and its iron sulfur cluster

The active site of Grx2 is composed of a Cys-Ser-Tyr-Cys motif enabling Grx2 (I) to fulfill dithiol reaction mechanisms, (II) to be reduced not only by GSH but also by thioredoxin reductase (TrxR) and additionally (III) to coordinate an FeS cluster (Johansson et al. 2004; Enoksson et al. 2005). There are three different transcripts of Grx2 in mammalian cells: Grx2a, Grx2c and Grx2d, with Grx2d being only reported in mice and being unable to coordinate an FeS cluster (Lönn et al. 2008; Hudemann et al. 2009). So far, the specific function of Grx2d has not been investigated. Grx2a and Grx2c differ only in their localization with Grx2a in the mitochondria and Grx2c present in the cytosol and the nucleus. The mitochondrial translocation motif of Grx2a is finally cleaved resulting in an identical protein constitution of Grx2a and Grx2c. In contrast to other Grxs, Grx2 was not reported to be located in the extracellular space (Lundberg et al. 2004). The Grx-specific FeS cluster consists of two iron and two sulfur atoms, two Grx molecules and two non-covalently bound GSH molecules (Lillig et al. 2005; Berndt et al. 2007). Notably, this composition was not found in other FeS cluster coordinating protein so far. The cluster is bound via the N-terminal active site cysteine. Therefore, holo Grx2 dimers are enzymatically inactive (Berndt et al. 2007). In HeLa cells, more than 70 % of the intracellular Grx2 proteins are present in the holo-form (Lillig et al. 2005). However, the function of the cluster is still under debate. It is assumed to function as a redox sensor allowing the protein to switch between its enzymatically active and inactive form (Lillig et al. 2005). As mentioned before, the other FeS cluster coordinating Grxs 3 and 5 were shown to be essential for physiological iron homeostasis. A possible involvement of Grx2 in iron homeostasis was proposed in a cellular model of Parkinson's disease. Here, Grx2a silencing was connected to a decrease in free iron and an inefficient FeS cluster biosynthesis (Lee et al. 2009). A role of the cytosolic Grx2c in iron homeostasis has not been reported yet. Under physiological conditions immunohistochemical analysis revealed the expression of Grxs in all mouse tissues including the brain with predominant presence in neurons (Godoy et al. 2011). In addition, Grx2 was demonstrated to be ubiquitously expressed in glial cells in both mouse and human brain (Karunakaran et al. 2007). The participation of Grxs and oxidoreductases in general upon neuroinflammation is yet unclear although peripheral immune cell activation and guidance were shown to depend on oxidoreductase, for instance Trx1 (Bertini et al. 1999).

1.2 Neuroinflammation in Multiple Sclerosis

Neuroinflammation is characterized by the increased production of chemokines and cytokines, activation of the CNS-specific immune cells as well as peripheral immune cell infiltration. For a restricted period of time after disease onset, inflammation has clear beneficial effects and is essential for tissue regeneration (Morganti-Kossman et al. 1997; Finnie 2013). However, persistent neuroinflammation leads to neurodegeneration and neurological impairments (Lucin and Wyss-Coray 2009). The underlying cellular signaling mechanisms are yet barely understood. Oxidative events were reported to predominantly contribute to degenerative processes in neuroinflammatory disorders like MS, the prototype for a disorder of the CNS with inflammatory and degenerative aspects (Greco et al. 1999; Koch et al. 2006; Aktas et al. 2007; van Horssen et al. 2011). MS is a lymphocyte-mediated autoimmune disorder of the CNS (Hemmer et al. 2002a and b). It is the major cause of sustained neurological disability among young adults affecting approximately 2.5 million people worldwide. The early onsets, around the age of 30, as well as the subsequent life-long obstructions, underline the clinical as well as social importance of MS research. To this date, MS is not curable and existing therapeutic approaches are directed towards the suppression of immune attacks, omitting the regeneration of neural tissue. The etiology of MS is commonly believed to be related to genetic predisposition (indicated by familial aggregation of disease predisposition (Oksenberg 2013) and unknown environmental factors triggering autoimmunity against CNS myelin structures (Weinshenker 1996; Lutton et al. 2004). In line, a genome-wide association study (GWAS) verified previously suggested MS-specific genes and further identified 20 additional risk genes. These genes code for cytokine pathways, signaling molecules of immunological relevance and environmental MS risk factors such as vitamin D dependent metabolism (Sawcer et al. 2011). Notably, the involvement of viral infections as contributing factor to disease initiation and progression is under debate (Ascherio et al. 2001; Hernán et al. 2001). However, the molecular mechanisms as well as the exact antigen structure driving the specific immune reactivity towards myelin/oligodendrocytes are unclear (Hohlfeld et al. 2016).

1.2.1 Neuroinflammation-mediated demyelination

The most apparent pathological characteristic of MS is demyelination, the degradation of myelin. Oligodendrocytes are the myelinating cells of the CNS and maintain the myelin

sheets ensuring a saltatory signal transduction of action potentials. MS lesion areas are highly diverse. However, based on histological analyses they can be classified grossly into acute and chronic lesion areas (Fig. 2) (Frohman et al. 2006). Acute lesion areas are characterized by the presence of activated CNS immune cells (microglia and resident dendritic cells), reactive astrocytes, infiltrating peripheral immune cells (T cells, B cells and macrophages) and blood brain barrier (BBB) damage (Hemmer et al. 2002b; Alvarez et al. 2011). Chronic lesions show enhanced astrogliosis (hypertrophy of astrocytes), extended oligodendrocyte and neuronal/axonal loss and inefficient remyelination (Trapp et al. 1998; Zipp and Aktas 2006). Although MS is believed to be lymphocyte-driven, the contribution of microglia (CNS-resident immune cells) and astrocytes is gaining more and more attention regarding MS disease initiation and progression.

Under physiological conditions, astrocytes are required for the BBB integrity and control the glutamate as well as water homeostasis in the brain. In their activated state they were considered to contribute to failed regeneration via the formation of a glial scar with little influence in lesion formation or repair (Brosnan and Raine 2013). However, recent findings stress additional pro- as well as anti-inflammatory properties of reactive astrocytes potentially participating in lesion formation and demyelination (Farina et al. 2007; Correale and Farez 2015). Astrocytes show alterations already in early MS disease stages. They accumulate at acute inflammatory lesion borders and participate in the breakdown of the BBB, reinforcing peripheral immune cell infiltration (Chapouly et al. 2015). Therefore, their contribution to MS disease initiation is highly discussed but needs further investigations.

Similar to the involvement of astrocytes, the contribution of microglia to MS initiation and progression is controversial. Microglia represent the major inflammatory resident cell type of the CNS (Hanisch and Kettenmann 2007). They are likewise activated under pathological conditions and contribute to neuinflammatory disease progression via the release of pro-inflammatory factors such as cytokines, chemokines, proteases as well as ROS and RNS (Li et al. 2008; Di Penta et al. 2013). For example, increased iNOS expression in human MS lesion areas correlates with the amount of myelin damage (Hill et al. 2004). Furthermore, extensive secretion of NO by microglia is known to contribute to neural tissue damage and degeneration (Pacher et al. 2007). However, activated microglia are additionally contributing to the removal of myelin debris promoting regeneration (Kotter et al. 2006; Neumann et al. 2009). Clearance of myelin is an essential prerequisite for remyelination and axonal outgrowth that fail upon disease progression (Takahashi et al. 2007).

1.2.2 Remyelination

Regeneration after CNS demyelination is accomplished by migration and differentiation of oligodendrocyte progenitor cells (OPCs) (Adams et al. 1989; Franklin and Robin 2002). During embryonic development, OPCs arise in the ventral and later the dorsal neuroepithelium from neural progenitors. They proliferate and migrate throughout the CNS and finally differentiate via sequential stages into postmitotic, premyelinating (expressing 2',3'-cyclic nucleotide 3'-phosphodiesterase (CNPase), O4 and O1 proteins) and finally to myelinating oligodendrocytes (expressing myelin genes like myelin basic protein (MBP), proteolipid protein (PLP) and myelin oligodendrocyte glycoprotein (MOG). In the adult brain, PDGFα$^+$, $A_2B_5^+$ as well as NG2$^+$ OPCs persist in all brain structures and maintain their proliferative capacity throughout lifetime. In response to damage, OPCs proliferate, migrate and differentiate. However, under persistent neuroinflammatory conditions, as represented in chronic progressive MS, these properties are severely diminished. In the peripheral nervous system (PNS), remyelination is a quick and efficient process. After PNS demyelination, mature Schwann cells, the myelinating cells of the PNS, proliferate and contribute to regeneration (Arthur-Farraj et al. 2012). In the CNS, mature oligodendrocytes lose their capacity for remyelination after the process of demyelination (Keirstead and Blakemore 1997) and therefore OPC migration, differentiation and cell survival in lesion areas are crucial steps for functional remyelination.

MS lesions are characterized by an accumulation of multiple factors like myelin debris, chemokines, cytokines, growth factors, reactive species and semaphorins that reduce regeneration (Robinson and Miller 1999; Costa et al. 2015; Kremer et al. 2016). Thus, inhibition of OPC recruitment or extensive cell death of OPCs within lesion areas are discussed as crucial factors in remyelination failure (Fig. 2). Here, soluble factors expressed and secreted by activated astrocytes, like platelet-derived growth factor (PDGF) (Noble et al. 1988; Richardson et al. 1988), fibroblast growth factor (FGF) (Bögler et al. 1990) and leukemia inhibitory factor-like protein (LIF) (Gard et al. 1995) facilitates oligodendrocyte survival and proliferation and thereby protect oligodendrocytes as well as neurons from inflammatory damage (Bush et al. 1999; Sofroniew 2005). On the other hand, upon persistent activation of astrocytes, the extracellular matrix composition is changed via secretion of inhibitory factors (Back et al. 2005), leading to restricted migration of OPCs (Bannerman et al. 2007) and inhibition of neuronal and oligodendrocyte regeneration (Sabo et al. 2011). Semaphorins, for example, are repulsive guidance molecules especially important in embryonic brain development, regulating the direction of cell migration and axonal outgrowth. Semaphorins3a and 7a are highly present in demyelinated lesion areas (Costa et al. 2015). *In vitro* experiments revealed a

Semaphorin3a-dependent inhibition of OPC migration as possible cause for impaired remyelination (Syed et al. 2011). However, several other *in vivo* studies reported the presence of OPCs in both acute and chronic lesions accompanied with an absence of postmitotic as well as premyelinating OPCs (Cui et al. 2013). Further, therapeut application of antibodies against leucine rich repeat and immunoglobulin-like domain-containing protein 1 (LINGO-1), a negative regulator of myelin gene expression, revealed increased remyelination *in vitro* and *in vivo* (Rudick et al. 2008). These studies stress a possible misregulation in the process of differentiation as reason for failed remyelination. Comparable to embryonic differentiation, OPC differentiation in the adult brain involves sequential steps whose regulation is not yet fully understood. However, it is well established that histone methylation and acetylation are crucial initiation steps (Copray et al. 2009).

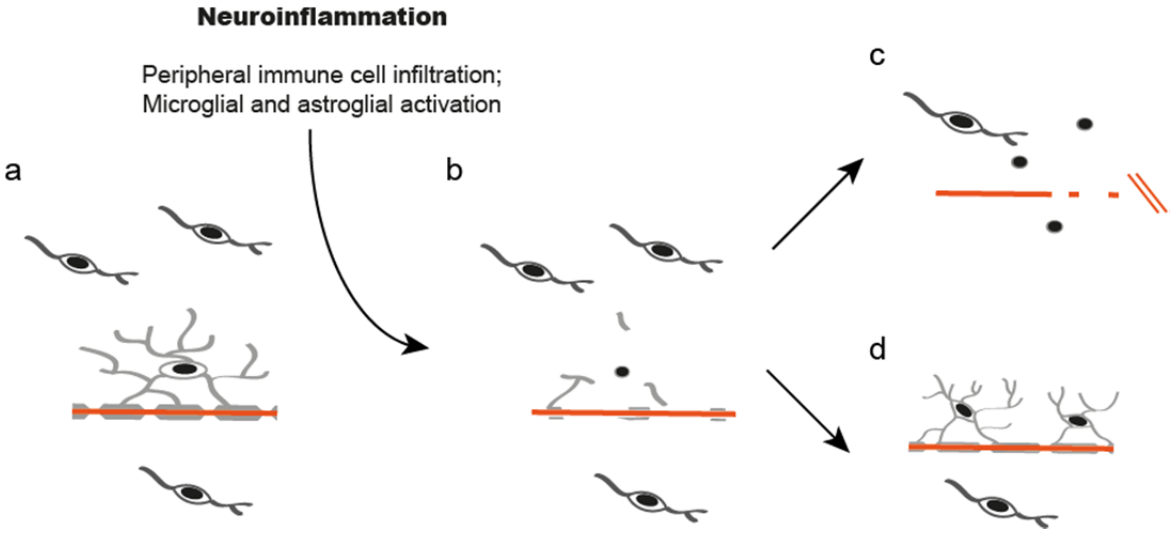

Figure 2. Oligodendrocyte lineage cells in MS progression. Under physiological conditions oligodendrocytes wrap their myelin-rich processes around axons and thus, ensuring saltatory signal transduction. Further, OPCs are present throughout the CNS (a). In MS peripheral immune cell infiltration, the activation of microglia and the activation of astrocytes trigger demyelination affecting myelin integrity and viability of mature oligodendrocytes (b). Depending on the progression of MS pathology either OPCs in the lesion area survive and remyelinate axons (d) or the accumulation of above mentioned inhibitory factors leads to impaired remyelination (c). Finally, the amount of dissected axons leads to persistent neurological disabilities. axons= orange; mature oligodendrocytes= light grey; OPCs= dark grey

1.2.2.1 Redox dependent events in neural differentiation

The contribution of different ROS/RNS to adult neural cell fate decision and neural stem cell maintenance was frequently reported. Here, reactive species contribute in a concentration-dependent manner to either maintain neural stem cell population or to

induce differentiation (Yuan et al. 2015). For example, anti-inflammatory treatment with minocycline that attenuates microglial activation (Henry et al. 2008) induces regenerative oligodendrogenesis from neural progenitors in a mouse Parkinson model rather than neurogenesis (Worlitzer et al. 2012). In addition, exposure to NO shifts the cell fate of neural progenitors from neurogenesis towards astrogliosis (Covacu et al. 2006). These observations stress the importance of redox regulated signaling pathways in early stem cell decision. Here, H_2O_2 was identified as essential signaling molecule, mediating self-renewal and thus maintaining neural stem population in the brain (Dickinson et al. 2011; Le Belle et al. 2011). In detail, increased neural progenitor proliferation and generation of both neurons and oligodendrocytes is regulated via H_2O_2-dependent up-regulation of the deacetylase Sirt2 (Pérez Estrada et al. 2014). As already mentioned in 1.1.1, activated microglia highly contribute to extensive ROS/RNS generation upon neuroinflammation and were thus, reported to induce both neurogenesis and oligogenesis (Butovsky et al. 2006a; Butovsky et al. 2006b). In contrast, extensive release of inflammatory mediators by activated microglia and immune cells was also found to decrease adult neurogenesis in mammals (Ekdahl et al. 2003; Packer et al. 2003). As already mentioned, concentration-dependent effects could explain these controversial results.

Concentrating on the oligodendrocyte lineage, a redox-dependent element in signaling pathways involved in glial precursor maintainance and differentiation is likely existing (Smith et al. 2000). In particular, myelin gene expression of mature oligodendrocytes was shown to be redox-sensitive (Jana and Pahan 2005). However, most reports showing alterations in oligodendrocyte maturation as cause of increased ROS and RNS levels are based on changes in early neural progenitor fate decision towards or against oligodendrocyte lineage with little direct effect on the oligodendrocyte lineage. Still, all mentioned references consider changes in the cellular overall redox state affecting ROS/RNS generation or depletion. Modulations in specific redox-dependent signaling pathways are yet not identified.

1.2.3 Model systems for neuroinflammatory demyelination and remyelination

MS pathogenesis is generally studied using animal models that manifest different characteristics of MS disease onset, progression and remission. EAE is the most frequently used animal model in rodents and primates, sharing MS-like disease progression as well as clinical symptoms of human MS (Mix et al. 2010). EAE is further the prototype for T cell-mediated autoimmune disorders in general. There are two ways to

induce EAE in rodents (active and passive). Active EAE is induced by the injection of a myelin-specific peptide in combination with Complete Freund's adjuvants and pertussis toxin. Similar to MS, the infiltration of peripheral immune cells triggers the activation of microglia and astrocytes, leading to severe neuroinflammation, demyelinated brain lesions and motoric impairments. Symptoms manifest within the first ten to fifteen days. Although the immunological backgrounds of rodents and humans differ (Mestas et. 2004) and a variety of medications show beneficial impact on EAE disease severity but fail to improve MS disease progression (Kipp et al. 2012), this model is the most useful model for MS therapeutic research as both diseases share common signaling events like accumulation of ROS/RNS ('t Hart et al. 2011). However, as the onset of MS is unknown, further animal models simulate the involvement of CNS resident cells as primary cause for demyelination. For example, toxin-induced (Ethidiumbromide, Cuprizone, Lysolecithin) as well as viral-induced (Theiler's murine encephalomyelitis virus) demyelination models are used to investigate pathogenic mechanisms leading to demyelination and being independent from the adaptive immune system. Notably, the underlying mechanisms of demyelination differ in each of these approaches.

Due to the complexity of animal models and to replace animal experiments, additional *ex vivo* systems like organotypic slice cultures (OSCs) are frequently used to study processes of demyelination and remyelination, omitting the influence of peripheral immune cells (Bin et al. 2012). OSCs represent a suitable interface between primary cultures and *in vivo* animal models (Cho et al. 2007) and possess a preserved multicellular physiology and cell connectivity. Furthermore, the experimental environment is easy to manipulate and thus diverse pathological situations can easily be simulated. Finally, the combination of *in vivo*, *ex vivo* and *in vitro* data combined with newly approved magnetic resonance studies in MS patients led to the approval of several disease modifying drugs for relapsing-remitting MS. Here, the increase in the CNS regeneration is a highly dedicated chalange in the present MS drug development.

1.2.4 Therapeutic approaches and redox signaling

Although none of the approved therapeutic treatments for relapsing-remitting MS is able to increase the repair of lesion areas in a direct manner, treatments may increase regeneration in an indirect manner via the modulation of redox processes. Therefore, new as well as existing therapeutic approaches were tested for possible antioxidant cellular defense mechanisms (Dubey et al. 2015). Here, recent findings underlined a redox-based neuro-protective effect of fingolimod (Ingwersen et al. 2012) and dimethyl fumarate (DMF)

(Albrecht et al. 2012). DMF was reported to act in a neuronal- and myelin-protective manner (Dubey et al. 2015) functioning via the translocation of nuclear factor like 2 (Nrf2) into the nucleus (Johnson and Johnson 2015; Buendia et al. 2016). Nrf2 is a transcription factor enhancing the expression of enzymes of the cellular antioxidant defense, like heme oxigenase-1 and glutathione S-transferase. In line, treatment with antioxidants like lipid peroxyl scavengers showed benefits in EAE disease progression, but so far a translation to MS patients only showed inefficient results. An insufficient supply to the CNS through the BBB is a possible explanation (Carvalho et al. 2016). It is worth mentioning that these clinical studies do not consider possible side effects of antioxidant donation. One example is reductive stress: In contrast to oxidative conditions that boost oxidative processes, molecules are pathologically reduced upon reductive stress (Rajasekaran et al. 2007; Zhang et al. 2010). However, both conditions can lead to cytotoxicity (Zhang et al. 2012; Korge et al. 2015). Furthermore, side effects on redox signaling events are not investigated yet. Specific targeting of redox dependent events represents promising new approaches, possibly overcoming the mentioned side effects (Fig. 3). Oxidoreductases participate in highly specific redox-dependent protein modifications. Here, Peroxiredoxins (Prxs) 3 and 5 as well as Trx2 were shown to be upregulated in MS lesions (Holley et al. 2007; Nijland et al. 2014). These studies stress the importance of specific redox events during MS disease progression.

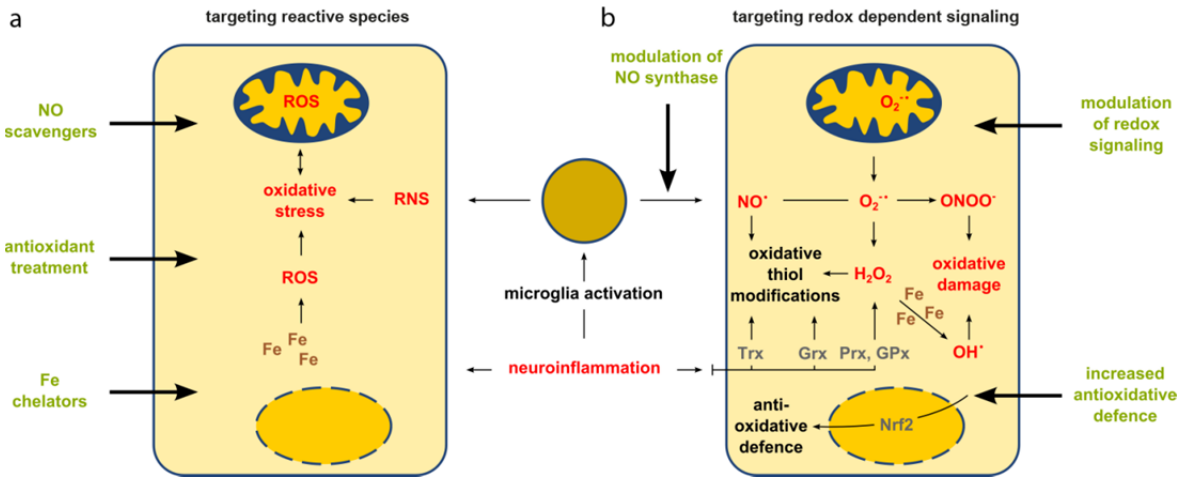

Figure 3. Global treatment against oxidative stress in comparison to targeted modulation of enzym-based thiol redox modifications. Increasing concentrations of ROS and RNS upon neuroinflammation affect the survival and function of neural cells. The current clinical studies aim in a overall change in the amount of ROS and RNS illustrated in a with a simplified view on the intracellular effects. A more specific approch is illustrated in b. The detailed intracellular redox responses to neuroinflammation introduces potential therapeutic strategies aiming rather in the control of specific enzym-based redox events (Lepka et al. 2016).

1.3 Aims of the study

Redox events are considered as major contributors to neuroinflammatory disease progression. In MS, ROS/RNS, such as peroxynitrite, participate in acute relapsing-remitting as well as in chronic progressive disease stages. The pathological increase of iron further accelerates the formation of ROS and RNS. Grxs were already connected to both redox regulation and iron homeostasis. However, the regulation and impact of Grxs upon neuroinflammation are not investigated so far. This study aims at:

(I) Characterizing the expression profiles of Grxs 2, 3, 5 and iron-dependent enzymes as well as their activities during neuroinflammatory disease progression.

(II) Elucidating the impact of Grx2 on neuroinflammation-mediated oligodendrocyte cell death.

(III) Investigating the effect of Grx2 on oligodendrocyte differentiation and migration as well as on oligodendrocyte regeneration capacities *in vitro* and *ex vivo*.

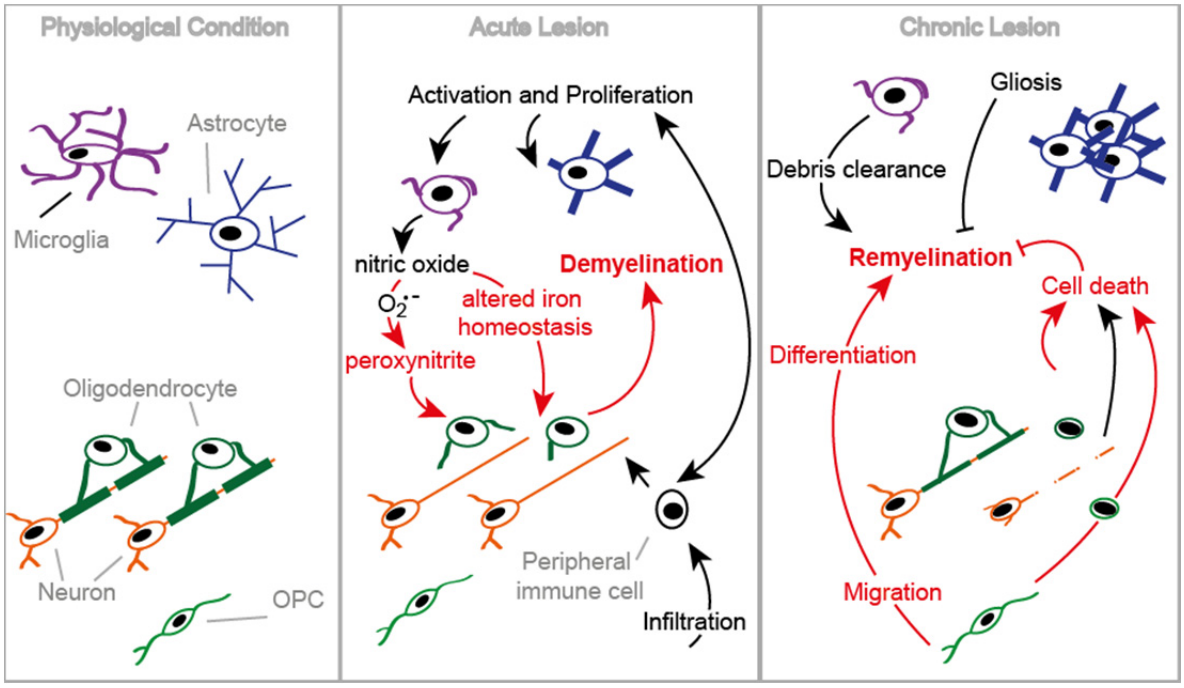

Figure 4. Contribution of CNS cell types to acute and chronic MS lesion progression with possible Grx2-dependent processes indicated in red. In acute lesion areas, the impact of Grx on NO-mediated demyelination will be investigated. Its role in oligodendrocyte progenitor migration, differentiation and cell death will be analyzed to determine the impact of Grx on the regeneration capacities of oligodendrocytes.

2. Materials and methods

2.1 Devices and chemicals

2.1.1 Chemicals and supplements

Table 1: List of chemicals and supplements

Chemicals and supplements	Company
Accutase	Thermo Fisher Scientific
Agarose	Biozym Scientific
Albumin fraction V, biotin-free	Sigma Aldrich
Anti-A_2B_5 MicroBeads	Miltenyi Biotech
CPTIO	Sigma-Aldrich
DMEM	Thermo Fisher Scientific
DMEM/F12	Thermo Fisher Scientific
DMSO	Sigma Aldrich
DNA ladder	PeqLab Biotechnologie
DNA loading buffer 6x	PeqLab Biotechnologie
Dulbecco's Phosphate Buffered Saline	Invitrogen Life Technologies
Envision+ Dual Link System	Dako
Ethidium bromide	Sigma-Aldrich
FCS	Thermo Fisher Scientific
Formaldehyde (4 %)	Sigma Aldrich
Glucose	Sigma Aldrich
Glutamax	Invitrogen Life Technologies
Griess Reagent	Molecular Probes
Grx2siRNA and fluorescent control siRNA	Thermo Fisher Scientific
Horse serum	Invitrogen Life Technologies
IFN gamma	Immuno Tools
Immunomount	Thermo Fisher Scientific
Lipopolysaccharide from E.coli O26B6	Sigma-Aldrich
Mini-PROTEAN TGX precast gels	Biorad
MK-571	Sigma-Aldrich
Modified Eagle's Medium	Invitrogen Life Technologies
MOG_{35-55} peptide	Pepceuticals

Chemicals and supplements	Company
NGS	Life Technologies
Nitrocellulose membrane	Biorad
NOC-5	Cayman Chemical
NOC-7	Cayman Chemical
NP40	Sigma Aldrich
PDGFα	Immuno Tools
Penicillin/Streptomycin	Invitrogen Life Technologies
Pierce 10x RIPA buffer	Thermo Fisher Scientific
Power SYBRGreen	Applied Biosystems
Prestained Protein Marker V peqGold	PeqLab Biotechnologie
Protease inhibitor cocktail tablets	Roche
Protein Loading buffer 4x	BioRad
SDS Loading Buffer	Biorad
SIN1	Cayman Chemical
StemPro Accutase	Invitrogen (GIBCO)
SYBRGreen PCR Master Mix	Applied Biosystems
TaqMan Reverse Transcription	Applied Biosystems
TaqMan Universal PCR Master Mix	Applied Biosystems
Tissue Tek	Sakura Fintek Europe B.V.
Triton-X-100	Merck
Tris/Glycerin running buffer	Biorad
Trypsin	Thermo Fisher Scientific
Tween 80	Sigma-Aldrich

2.1.2 Laboratory equipment

Table 2: List of used laboratory equipment

Laboratory equipment	Company
6 well Millicell-CM culture plate inserts	Millipore
7500 Pro Real-Time PCR Systems	Carl Zeiss Microscopy GmbH
Centrifuge 5417R	Eppendorf
Centrifuge Minispin	Eppendorf
CO_2 cell culture incubator	Thermo Scientific
F-View fluorescence camera	Soft Imaging System

Laboratory equipment	Company
HiTrap chelating column	GE healthcare
Horizontal laminar Flow	Heraeus
iBlot Dry Blotting System	Invitrogen
Leica CM1900 UV	Leica Microsystem
MACS Separation columns	Miltenyi Biotech
Microplate Reader	Tecan Group Ltd.
Nanodrop 2000 Spectrophotometer	Thermo Fisher Scientific
Neural Tissue Dissociation Kit	Miltenyi Biotech
Odyssey CLx Imaging System	LI-COR Biosciences
Olympus BX51	Olympus
Olympus U-RFL-T Burner	Olympus
Sonicator, UW 2070	Bandelin electronic
Standard Power Pack P25	Biometra
Sub Cell System	BioRAD
TC10 Automatic Cell Counter	BioRAD
Thermocycler T Gradient	Biometra
T-Personal Thermocycler	Biometra
Trans-O FLEX 24 well inserts (0.4 µm)	Greiner Bio-One
Trans-O FLEX 24 well inserts (8 µm)	Greiner Bio-One

2.1.3 Kits

Table 3: List of Kits used for sample analysis

Kit	Company	Cat #
Anti-A_2B_5 MicroBeads	MACS, Miltenyi Biotec	130-093-388
BC Assay Protein Quantification	Interchim	UP40840A
CellTiter-Blue® Cell Viability Assay	Promega	G8082
Fluor de lys-Green HDAC assay Kit	Enzo	AK555-0001
Multiscribe Reverse Transkriptase	Invitrogen	18064-014
Neural Tissue Dissociation Kit (P)	MACS, Miltenyi Biotec	130-092-628
Oxyblot Protein Oxidation Detection Kit	Merck Millipore	S7150

2.2 GSNO preparation

S-Nitrosoglutathione (GSNO) was synthesized following an adapted protocol published by (Hart 1985). Briefly, 1.54 g of glutathione was dissolved in 620 µl of concentrated HCl and diluted in 5.9 ml H_2O. Separately, 0.346 g $NaNO_2$ was dissolved in 1 ml H_2O and slowly added to the glutathione solution (vigorously stirring). After 5 min of stirring, the pH was set to 6.0 by addition of freshly prepared 10 M NaOH. For 500 mM GSNO the volume was adjusted to 10 ml using H_2O. The GSNO concentration was verified by spectroscopic analysis (mM extinction coefficient of GSNO= 0.92 at 335 nm). Preparation was performed in a light-protected environment as GSNO is highly light sensitive. Aliquots were kept at -80°C.

2.3 Grx2 purification and treatment

Mouse Grx2 as well as the Grx2-mutants mGrx2C37S and mGrx2S38P were recombinantly expressed in the BL21-CodonPlus-(DE3)-RIL *E. coli* strain (Stratagene) with an N-terminal 6xhistidine tag (pet15b, Novagen). Purification was performed using HiTrap chelating columns as described by (Lillig et al. 2005). Grx2-mutants were synthetized using site-directed mutagenesis with designed oligonucleotide primers introducing a single point mutation at the active site (Bosch 2015). Imidazole was exchanged via dialysis against 50 mM NaCl and 200 mM Na_2PO_4 (pH 7.6) over night. Finally, purity was examined by SDS-PAGE and concentration was determined using NanoDrop. Recombinant proteins were stored at -80 °C.

2.4 Cell culture

Cell culture work was performed under a sterile bench. Cell lines were cultured in DMEM culture medium and primary mouse cells were either cultured in proliferation or differentiation medium (Table 4). For cell de-attachment, Trypsin (for cell lines) or Accutase (for primary cells) was used. The reaction of Trypsin was stopped by addition of twice the amount of medium containing 10% fetal bovine serum (FCS). Accutase was diluted with twice the amount of phosphate buffered saline (PBS). Cultures were incubated at 5% CO_2 and 37°C. Poly-O coated dishes and plates were incubated with

0.001 % Poly-O overnight and thereafter washed three times with twice the amount of PBS. All experiments were performed in duplicates or triplicates.

2.4.1 BV2 and OLN-93 cell lines

Murine BV2 cells (mouse, microglia), rat OLN-93 cells (rat, oligodendroglia) as well as human HeLa wild type and Grx2c overexpressing cells (Enoksson et al. 2005) were cultured on un-coated petri dishes to a density of 80% confluence and splitted as described before. Cells were seeded at a density of 15,000 cells per cm^2. According to the read-out, experiments were terminated by either cell lysis in RIPA-Buffer for Western blot analysis (2.12), cell lysis in Trizol for quantitative real time PCR (q RT-PCR) analysis (2.11) or addition of CellTiter-Blue reagent for cell viability analysis (2.5). Further, BV2 cells were activated by addition of 1 µg/ml lipopolysaccharide (LPS) 2 h prior to co-culture experiments (2.4.3) triggering the release of chemokines, cytokines and NO. For the quantification of NO release, an additional condition of 1 µg/ml LPS and 10 units Interferone γ (IFNγ) was chosen as positive control. Griess Reagent was used following manufacturer's recommendation (absorbance measurement of culture supernatants at 540 nm using TECAN reader).

Table 4: List of cell culture media

DMEM culture medium	**A_2B_5 proliferation medium**	**A_2B_5 differentiation medium**
DMEM	DMEM/F12	DMEM/F12
100 U/ml Penicilin G	100 U/ml Penicilin G	100 U/ml Penicilin G
100 µg/ml Streptomycin	100 µg/ml Streptomycin	100 µg/ml Streptomycin
10% FCS	1x Glx	1x Glx
	10 ng/ml mFGF	400 ng/ ml T3
	20 ng/ml PDGFα	400 ng/ ml T4
	1x $B27^-$ (without vitamin A)	1x $B27^+$

2.4.2 Primary mouse oligodendrocyte progenitors

OPC-enriched cultures were derived from total brain single cell suspension of P1-P3 C57BL/6 wildtype mice using the Neuronal Tissue Dissociation Kit. Mice were decapitated, the brain was extracted, meninges were removed and tissue was further handled as described in manufacturer's protocol for manual dissociation. Single cell suspension was cultured for 3-5 days in A_2B_5 proliferation medium on poly-O coated petri dishes and afterwards sorted for A_2B_5-positive cell population using Anti-A_2B_5 MicroBeads obeying manufacturer's recommendation. Sorted cells were plated at 25,000 cells per cm^2 on Poly-O coated petri dishes and cultured in A_2B_5 proliferation medium (Table 4). Differentiation assays were only performed using cells from passage 1/2 whereas survival and migration assays were performed using cells up to passage 3.

2.4.3 BV2 and A_2B_5 co-culture

25,000 A_2B_5-positive progenitors per cm^2 were seeded in 24 wells. After 24 h under proliferating culture conditions, medium was replaced by DMEM supplemented with 5% FCS and 1% P/S generating tolerable culture conditions for both cell types. 2 h prior to co-culture, A_2B_5-positive progenitors were pretreated with 2 µM of recombinant mouse Grx2 and BV2 cells were pretreated with 1 µg/ ml LPS. Thereafter, BV2 cells were co-cultured on filter inserts with a pore size of 0.4 µm, allowing diffusion of soluble factors but preventing direct cell contact. Recombinant mouse Grx2 was additionally added 4 h after LPS treatment. After 24 h, filter inserts with the BV2 cells were removed and A_2B_5-positive progenitors were further cultured in 200 µl medium containing 20 % of CellTiter-Blue reagent (2.5). Here, absorbance of 100 µl conditioned mediun was measured in 96 well plates.

2.5 CellTiter-Blue® cell viability assay

Unless otherwise mentioned, A_2B_5-positive progenitors as well as OLN-93 and HeLa cells were plated at 25,000 cells per cm^2 in 96 wells. After 24 h under respective culture conditions, 2 µM Grx2 was supplemented 2 h prior and 4 h after treatment. Treatment comprised either the addition of NO-donors (GSNO, NOC5 and NOC7) or peroxynitrite donors (SIN1). After 24 h 20 % CellTiter-Blue reagent (Promega) was supplemented to the culture medium. After additional 4 h, absorption at 562 nm and at 612 nm (reference

wavelength) was measured using the TECAN microplate reader and survival rates in respect to untreated controls were determined following manufacturer's proposals using Excel.

2.6 Differentiation assay

Primary mouse A_2B_5-positive progenitors were cultured on petri dishes (for Western blot analysis), 6 well plates (for q RT-PCR analysis) or cover slips in 24 well plates (for immunocytochemical analysis) as described in 2.4.2. All items were coated with Poly-O (2.4). Cells were kept in proliferation medium for 24 h after seeding and further for additional 24 h in mixture of A_2B_5 proliferation medium and A_2B_5 differentiation medium (50:50) including 2 µM recombinant mouse Grx2. Thereafter, medium was replaced by 100% differentiation medium (see Table 1) either supplemented with or without 2 µM recombinant mouse Grx2. Cells were kept in A_2B_5 differentiation medium for no longer than 5 days due to extensive loss of cell viability. All read-outs were compared to untreated A_2B_5-positive control cells. According to the appropriate approach, cells were lysed in RIPA-buffer for Western blot analysis (2.12), lysed in Trizol for q RT-PCR analysis (2.11) or fixed with 4 % paraformaldehyde (PFA) for 15 min at room temperature, washed twice with PBS and kept in PBS at 4°C until immunocytochemical analysis (2.13). Matruration stages were distinguished using 5 distinct oligodendrocyte differentiation markers (Fig. 5)

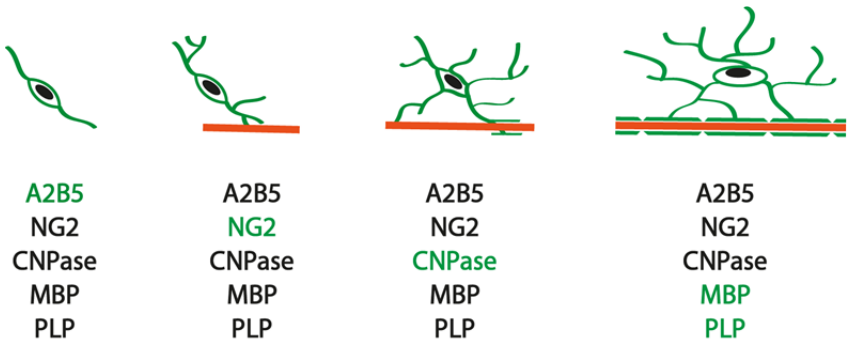

Figure 5. Maturation markers used for identification of oligodendrocyte differentiation stages. A_2B_5-postive oligodendrocyte progenitor cells (green) were MACS-sorted and differentiation was initiated by withdrawal of growth factors and addition of thyroid hormones (T3/T4) as well as retinoic acid. NG2 positive cells represent migrating progenitor cells, CNPase-positive cells represent premature oligodendrocytes and MBP- as well as PLP-positive cells represent mature oligodendocytes with the capacity to myelinate axons (organe) (Robinson et al. 2014).

2.7 Transmigration assay

Membrane inserts with a pore size of 8 µm were placed in Poly-O coated 24 well plates containing 300 µl A_2B_5 proliferation medium with an elevated PDGFα concentration of 0.1 µg/ml. 50,000 A_2B_5-positive progenitors were placed in 200 µl A_2B_5 proliferation medium on top of the insert. Semaphorin-3a was applied at a final concentration of 1 mg/ml into the lower chamber considering the final volume of 500 µl medium. 2 µM recombinant mouse Grx2 was applied at the beginning of the experiment as well as 4 h after cell seeding into the upper chamber. After 24 h the inserts were removed and migrated cells on the bottom of the 24 wells were fixed using 4 % PFA for 15 min. Wells were washed three times and further incubated with Hoechst (1:5,000 in PBS) for 5 min. To determine the amount of migrated cells, five pictures per well were recorded using Olympus Fluorescence microscope and stained nuclei were counted.

2.8 $ONOO^-$ quantification

Quantification of $ONOO^-$ was based on the reaction of Fluorescein-boronate (weak fluorescence) to Fluorescein (highly fluorescent) in the presence of $ONOO^-$ (Rios et al. 2016). The fluorescent probe was a kind gift of Prof. Dr. Rafael Radi, ("Departmento de Bioquímica" Universidad de la República, Montevideo, Uruguay). To obtain a stock solution of 4.5 mM, Fluorescein-boronate was diluted in dimethylsulfoxid (DMSO) and further diluted in PBS to a final concentration of 50 µM. Cells (primary mouse A_2B_5-positive progenitors or HeLa wild type as well as HeLa Grx2c overexpressing cells) were seeded in 96 wells, pre-incubated with or without 2 µM recombinant mouse Grx2 for 2 h and washed twice with PBS. Thereafter, cells were incubated with 50 µM Fluorescein-boronate for 30 min at 37°C and 5 % CO_2. Cells were washed three times with PBS and fluorescence was measured in a TECAN microplate reader (absorbance at 492 nm and emission at 515 nm) directly after addition of either PBS containing corresponding amounts of GSNO or PSB supplemented with 1 mM GSNO or 1 mM SIN1 in presence or absence of 50 µM Carboxyl-PTIO potasium salt (CPTIO; NO scavenger).

2.9 Cerebellar organotypic slice cultures

Cerebellar organotypic slice cultures (OSCs) were obtained from P9-10 C57BL/6 wild type mice. Here, a previously used method of (Stoppini et al. 1991) was slightly modified. Briefly, cerebellum and hindbrain were extracted and cut into 4000 µm sagittal sections (McIlwain tissue chopper). Slices were separated in OSC dissecting medium (Table 5), washed for 15 min in a mixture of Earle's balanced salt solution (HBSS) and minimal essential media (MEM) (50:50) containing 25 mM HEPES buffer and finally plated on Millipore-Millicel-CM culture inserts in OSC culture medium (Table 5). To allow the inflammatory processes to subside and the tissue homeostasis to recover, slices were cultured *in vitro* for two days at 5% CO_2 and 37 °C followed by 5 days under normal culture conditions (5 % CO_2 and 33 °C). Medium was exchanged every second day. Finally, experiments were initiated with the addition of 2 µM recombinant mouse Grx2 2 h prior to treatment. Treatment comprised either 750 µM GSNO or 10 µg/ml LPS for 24 h. All compounds were added to the culture medium. 4 h after treatment, 2 µM recombinant Grx2 was repeatedly added. Morphological analysis was performed by immunohistochemistry (2.13) after fixation with 4 % PFA followed by three washing steps using PBS.

Table 5: List of media used for cerebellar OSC preparation and culture

OSC culture medium	OSC dissecting medium
50 % MEM	HBSS +/+
25 % horse serum	1 mM kynurenic acid
25 % HBSS +/+	100 U/ml Penicilin G
0.5 % Glucose	100 µg/ml Streptomycinsulfate
2 mM L-glutamine	
100 U/ml Penicilin G	
100 µg/ml Streptomycinsulfate	

Remyelination experiments were performed as described in (Harrer et al. 2009). Briefly, OSCs were maintained for 7 days *in vitro* under normal culture conditions as described above. Thereafter, cultures were incubated with 5 % baby-rabbit complement and 5 µg/ml MOG-specific hu818C5 antibodies (kindly provided by Christine Baksmeier, AG Goebels, Klinik of Neurology, Heinrich-Heine-University Düsseldorf). Complete demyelination was

achieved after three days and medium was changed into normal OSC culture medium with or without 2 µM recombinant mouse Grx2 for additional three days allowing remyelination. Afterwards, OSCs were fixed with 4 % PFA for 30 min, washed for three times with PBS and finally stained against axonal, oligodendrocyte and oligodendrocyte progenitor structures (2.13).

2.10 Active EAE implementation

C57BL/6 wildtype mice were immunized as described earlier by (Schulze-Topphoff et al. 2009) and (Aktas et al. 2005). Briefly, six- to eight-week-old female mice were immunized subcutaneously on both sides of flanks and tails with 200 µg of recombinant myelin oligodendrocyte glycoprotein 35-55 ($MOG3_{5-55}$) and 800 µg mycobacterium tuberculosis emulsified in 100 µl complete Freund's adjuvans and 100 µl PBS (Schulze-Topphoff et al. 2009). Emulsion was performed by sonification. Additionally, 200 ng pertussis toxin (PTX) was injected intraperitoneally on the day of immunization as well as 2 days after immunization. Disease progression was quantified using a score-system from 0 to 5 with intervals of 0.5 evaluating animal mobility (0= no disease; 1= tail weakness; 2= paralysis; 3= paraplegia; 4= paraplegia with forelimb weakness; 5= moribund or dead animal) (Huehnchen et al. 2011). Daily evaluation and the sacrifice of mice were performed by several group members. All mice were housed in the animal research facility of the University of Düsseldorf under a dark/light cycle of 12 h, a stable temperature of 22- 24 °C, specific pathogen free conditions and unlimited access to food and water. Mice were either euthanized on day 7 (control animals), day 17 or day 27. Mice sacrificed at disease peak (d 17) had a score of three. Mice sacrificed at disease remission phase (day 27) recovered from a score of three on day 17 to a score of either 0 or 0.5 at the day of sacrifice. Mice were euthanized by lethal inhalation of isoflurane and perfused with ice cold PBS. Cerebellum was extracted and either directly frozen in liquid nitrogen and stored at -80 °C for further Western blot analysis (2.12), enzyme activity measurements (2.15) and q RT-PCR analysis (2.11) or handled as described in 2.13 for immunohistochemical analysis.

2.11 RNA isolation and quantitative RT-PCR

RNA isolation was performed with TRIzol reagent according to manufacturer's protocol. Quantity and quality of isolated RNA were determined using NanoDrop. cDNA was synthesized using TaqMan reverse transcription reagent in a TPersonal Thermocycler. Program was chosen as follows: 10 min at 25 °C, 45 min at 48 °C and 5 min at 95 °C. For q RT-PCR, Power SYBRGreen PCR Master Mix or TaqMan Universal PCR Master Mix was used with corresponding primer pairs (Table 6). Q RT-PCR program was as follows: 2 min at 50 °C, 10 min at 95 °C, 40 cycles of 15 sec at 95 °C and 1 min at 60 °C. For Power SYBRGreen measurements dissociation curve was attached from 60 °C to 95 °C. Fold induction values were calculated on the basis of the ΔCT validation. Glyceraldehyde3-phosphate dehydrogenase (GAPDH) was measured as housekeeping gene. Relative expressions to GAPDH and fold inductions to control were calculated using Microsoft Excel. All measurements were performed in duplicates.

Table 6: List of primer sequences for quantitative RT-PCR analysis

Target gene	Sequence
CNPase	Fw: 5'-TGCTGCACTGTACAACCAAATTC-3'
	Rw: 5'-GAGAGCAGAGATGGACAGTTTGAA-3'
GAPDH	Fw: 5'-CTCAACTACATGGTCTACATGTTCCA-3'
	Rw: 5'-CCATTCTCGGCCTTCACTAT-3'
	Probe: (Fam)TGACTCCACTCACGGCAAATTCAACGT(TAMRA)
Glrx2a	Fw: 5'-GGCGAGCGGGAGGATCTT-3'
	Rw: 5'-ATTGTTTCTTGGATCTGGTTCACA-3'
	Probe: (Fam)CGTGGCGCGGCTGGAGCT(TAMRA)
Glrx2c	Fw: 5'-CGGGGACCTTTGGCTATGTC-3'
	Rw: 5'-ATTGTTTCTTGGATCTGGTTCACA-3'
	Probe: (Fam)CGGCTTCGAATGGGAAACAGCACA(TAMRA)
Glrx3	Fw: 5'-AGCCTTCGCCTGAAAAAGCT-3'
	Rw: 5'-TCCACCATCTGCTTGCTGAA-3'
Glrx5	Fw: 5'-GCGACTATGCGGCCTACAA-3'
	Rw: 5'-TCGCCGTTGAGGTACACTTG-3'
iNOS	Fw: 5'-GGAAGTGGGCCGAAGGAT-3'
	Rw: 5'-ACTGGAGGGACCAGCCAAAT-3'

Target gene	Sequence
iNOS	Probe: (Fam)ACCGGGCTGTCACGGAGATCAATG(TAMRA)
MBP	Fw: 5'-CACAGAGACACGGGCATCCT-3'
	Rw: 5'-TCTGCTTTAGCCAGGGTACCTT-3'
MRP1	Fw: 5'-GTTCCCTCCGCATGAACTTG-3'
	Rw: 5'-CTGGCTCATGCCTGGACTCTG-3'
PLP	Fw: 5'-GTATAGGCAGTCTCTGCGCTGA-3'
	Rw: 5'-AAGTGGCAGCAATCATGAAGG-3'

2.12 Western blot analysis

Samples were lysed with 1x RIPA supplemented with 10 mM protease inhibitor for 10 min at RT. All following steps were performed at 4 °C. After vigorous vortexing, lysates were centrifuged for 20 min at 18,000 g. Supernatants were transferred into a new tube and kept at -80 °C. After thawing, protein concentration was quantified by BCA assay. 25-100 µg of boiled samples (5 min at 95 °C) were further separated on SDS-PAGE (150 V, any kD Mini-PROTEAN TGX Precast gels in Tris/Glycine/SDS buffer) in presence of 10 mM freshly prepared dithiothreitol (DTT) as well as 4x LDS sample loading buffer and blotted onto PVDF membranes using Trans-Blot Turbo Transfer System (Blot-program: mix kD). Membranes were blocked with 5 % Bovine serum albumin (BSA) in 1x PBS containing 0.005 % Tween for at least 2 h. Thereafter, membranes were incubated at 4 °C in primary antibody solution overnight while shaking moderately. Antibodies are listed in Table 7 and were diluted in 2.5 % BSA at respective concentrations. After three steps of washing with 0.005% PBSTween, membranes were incubated for 1 h at room temperature with IRDye secondary antibodies (Table 8). After three times of washing stained protein bands were detected using the Odyssey Infrared Imaging System. Quantification of band intensities was determined with Image Studio Lite analysis software. All intensities were normalized to β-actin as housekeeping protein. Protein carbonylation was detected using the Oxyblot protein oxidation detection kit according to manufacturer's protocol.

Table 7: List of primary antibodies for Western blot analysis

Antibody	Host	Dilution	Company	Cat #
B-actin	mouse	1:5,000	Sigma-Aldrich	A5316

Antibody	Host	Dilution	Company	Cat #
COX	rabbit	1:2,500	Abcam	
Ferritin	rabbit	1:1,000	Abcam	
mACO	rabbit	1:250	Abgent	
GFAP	guinea pig	1:2,000	Synaptic Systems	173 004
GPAT	rabbit	1:1,000	Santa Cruz Biotech.	sc-130698
Grx2	rabbit	1:400	(Godoy et al. 2011)	
Grx3	rabbit	1:400	(Godoy et al. 2011)	
Grx5	rabbit	1:400	(Godoy et al. 2011)	
MBP	rat	1:500	Merck Millipore	MAB386
MRP1	rat	1:500	Enzo Life Science	ALX-801-007
NG2	rabbit	1:500	Merck Millipore	AB5320
Nitrotyrosine	rabbit	1:5,000	Merck Millipore	05-233
SDH	mouse	1:1,000	Abcam	
TfR	mouse	1:1,000	Merck Millipore	GR08L

Table 8: List of secondary antibodies for Western blot analysis

Secondary antibody	Host	Company	Dilution
rabbit IgG 800	donkey	LI-Cor	1:15,000
rabbit IgG 680	donkey	LI-Cor	1:15,000

2.13 Immunohistochemistry and immunocytochemistry

After fixation using 4% PFA for 30 min (slice cultures) or 15 min (cell culture) at room temperature, samples were washed three times with PBS and blocked in PBS containing 5 % normal goat serum and 0.5 % triton (blocking solution) for 2 h at RT. Samples were incubated over night at 4 °C with primary antibodies in staining solution (1:1 = PBS:blocking solution). Primary and secondary antibodies are listed in Table 9 and Table 10. After three steps of washing with PBS, secondary antibodies were diluted likewise in staining solution and applied for 1 h at RT. Cell nuclei were visualized via Hoechst diluted 1:5,000 in PBS and added to samples for 5 min at room temperature. After three steps of washing, samples were mounted to preserve fluorescence. Pictures were taken either by

confocal scanning microscopy or by fluorescence microscopy. Disturbed myelin and neurofilament structures in slice cultures were quantified counting the total amount of cerebellar branches and the amount of disturbed branches stained against neurofilament-m (NF-M) or MBP.

Table 9: List of primary antibodies for immunohisto- and immunocytochemical analysis

Primary Antibody	Host	Dilution	Company	Cat #
A_2B_5	mouse	1:200	Sigma-Aldrich	A8229
Active caspase3	rabbit	1:200	Cell Signaling Tech.	9661
CNPase	mouse	1:500	Sigma-Aldrich	C5922
GFAP	guinea pig	1:2,000	Synaptic Systems	173 004
Grx2	rabbit	1:200	(Godoy et al. 2011)	
Grx3	rabbit	1:200	(Godoy et al. 2011)	
Grx5	rabbit	1:400	(Godoy et al. 2011)	
HisTag	mouse	1:200	Merck Millipore	05-531
MBP	rat	1:500	Merck Millipore	MAB386
MRP1	rat	1:500	Enzo Life Science	ALX-801-007
NG2	rabbit	1:200	Merck Millipore	AB5320
Nitrotyrosine	rabbit	1:100	Merck Millipore	05-233
NF-M	mouse	1:1,000	Sigma Aldrich	N0142
TfR	mouse	1:1,000	Merck Millipore	GR08L

Table 10: List of secondary antibodies for immunohisto- and immunocytochemical analysis

Fluorophor	secondary Antibody	Dilution	Company	Cat #
Cy2	goat anti- guinea pig	1:500	Life Technologies	A11073
Cy2	goat anti- mouse IgG	1:500	Merck Millipore	AP124J
Cy2	goat anti- rat IgG	1:500	Merck Millipore	AP202J
Cy3	goat anti- mouse IgM	1:500	Bioscience	bs3-0368G
Cy3	goat anti rabbit IgG	1:500	Merck Millipore	AP132C
Cy5	goat anti-mouse IgG	1:500	Merck Millipore	AP124S
Cy5	goat anti-rat IgG	1:500	Merck Millipore	AP136S

Staining of human brain paraffin sections was performed in the laboratory of Dr. Jack van Horssen (University Medical Center in Amsterdam) using the Dako Envision + Dual Link System. Briefly, brain samples were fixed for 10 min in acetone. Primary antibodies were diluted in 0.1 % BSA solved in PBS and incubated for 1 h at room temperature in a humidity chamber. After three steps of washing with PBS, sections were incubated with 100 µl Envision-HRP solution (1 h at room temperature) and Substrate Solution (~5 min at room temperature) consecutively. Thereafter, slides were incubated in Hematoxilin solution for 1 min to visualize nuclei and mounted after alcohol-dehydration procedure. Thereby, stained structures appeared brownish and nuclei were stained in blue. Brain samples were received from the Netherlands Brain Bank (Amsterdam). Documentation was performed with a Leica Microscope using bright field imaging. Paraffin sections for cerebellar mouse EAE tissue were stained against iron in the laboratory of Prof. Dr. Roland Lill ("Institut für Zytobiologie", Philipps-University in Marburg) in cooperation with Waltraud Ackermann in Marburg obeying Prussian blue staining protocol (potassium ferrocyanide reaction). In addition, nuclei were stained using red-aluminum sulfate solution.

2.14 EPR spectroscopy

Electron paramagnetic resonance (EPR) spectroscopy was performed in cooperation with Dr. Eckhard Bill (Max Planck Institute for Bioinorganic Chemistry in Mülheim Ruhr). Measurements were carried out to detect and quantify dinitrosyl-iron-complexes (DNIC) in OLN-93 oligodendrocyte cell line. Therefore, 25 x10^6 OLN-93 cells per condition were collected in 1 ml cell culture medium and treated in presence or absence of 2 µM recombinant mouse Grx2 with MK-571 to inhibit the activity of multidrug resistance-associated protein 1 (MRP1), a DNIC exporter, for 1 h at 37 °C. Afterwards, samples were centrifuged and resuspended in 200 µl PBS. In addition, one Grx2 treated sample was additionally washed twice to ensure extracellular Grx2 removal. Treatment with 5 mM GSNO was performed for 2 min directly before freezing. Samples were directly frozen in EPR tubes using a mixture of ethanol and dry ice. X-band EPR spectra were recorded at X-band (9.47 GHz) using a Bruker Elexsys E500 spectrometer with an NMR gaussmeter, a helium flow cryostat (Oxford Instruments), and a Hewlett-Packard frequency counter. Samples were measured at 30 K and deflections were characterized at a g value of 2.03. Quantification was calculated considering the double integral of the spectral area.

2.15 Protein activity measurements

Measurements were performed in the laboratory of Prof Dr. Roland Lill ("Institut für Zytobiologie", Philipps-University in Marburg) in cooperation with Dr. Ulrich Mühlenhoff. Activity measurements for aconitase, succinat dehydrogenase, malate dehydrogenase, cyclooxygenase and lactat dehydrogenase were performed as outlined in (Biederbick et al. 2006), (Stehling et al. 2009) and (Stehling et al. 2007). Therefore, cerebella of mice suffering from EAE (sacrificed at disease peak or at disease recovery phase) as well as cerebella from untreated control mice were lysed in SDS free lysis buffer, containing 50 mM Tris (ph8), 150 mM NaCl, 1% NP40, 0.5 % Deoxycholate, 0.1 mM cis-Aconitate, 5% Glycerin and 1x protease inhibitor. Tissue was sonificated three times for 5 sec. Lysates were kept on ice for 10 min and further centrifuged at 18,000 g for 20 min. Supernatants were transferred into a new tube and protein concentration was determined by BCA assay. 10 µg – 100 µg protein of lysed samples were used depending on the measurement sensibility and finally, enzyme activity was calculated as units per mg protein.

2.16 Software

Table 11: Software used for data analysis and presentation

Software	Company
Adobe Creative Suite 5	Adobe System Inc.
Citavi 4	Swiss Academic Software
GraphPad Prism 5	GraphPad Software
Image J	Rasband, W.S.
Megallan Data Analysis	Tecan Group Ltd.
Odyssey Image Studio Lite	LI-Cor
Office 2010	Microsoft Corporation
Primer Express software	Applied Biosystems

2.17 Ethical approvals

All animal experiments were conducted according to the guidelines and protocols approved by the local animal welfare committee "Landesamt für Natur, Umwelt und Verbraucherschutz Nordrhein- Westfalen" (LANUV) under the protocol numbers G363_09 and G197_09. EAE experimental procedures followed the EAE induction guideline and the ARRIVE criteria (Animal Research: Reporting of In Vivo Experiments) (Baker and Amor 2012).

Paraffin-embedded and formalin-fixed brain sections were obtained from patients with clinically diagnosed and neuropathologically confirmed MS from the Netherlands Brain Bank, Amsterdam. The Netherlands Brain Bank received the permission to perform autopsies for research purposes from the ethics committee of the VU Medical Center (Amsterdam, The Netherlands). All donors or their next of kin had given informed consent for brain autopsy and the use of material and clinical information for research purposes.

2.18 Statistical analysis

Statistics were performed using GraphPad Prism 6 (GraphPad Software). Descriptive statistic is displayed by the median (location scale) and the interquartile range (measures of dispersion). Groups comprising of $n \geq 4$ are graphically represented in form of Boxplots. The Boxplots themselves demonstrate data from the 25^{th} percentile to the 75^{th} percentile. The median (50^{th} percentile) is visualized by a horizontal line inside the Boxplot. Error bars indicate the range from the 5^{th} percentile to the 95^{th} percentile. For $n \leq 3$ all data-points are presented; here, the median is indicated by a horizontal line.

A normal distribution of the data could not be assumed since the number of samples was insufficient (sample-number smaller than 20). Therefore, the non-parametric Kruskal-Wallis h-test was performed for statistical analysis to compare three or more unmatched groups comprising $n \geq 4$ followed by Dunn's post test to compare statistical differences between two columns. To compare two unmatched groups the Mann Whitney u-test was performed. The level of significance was always set to $\alpha \leq 0.05$.

3. Results

The onset and progression of MS is insufficiently understood in detail. However, the importance of reactive species and redox-dependent events in neuroinflammatory disease progression was extensively elucidated in the last decade. This study illustrates the role of the mammalian iron-sulfur cluster coordinating oxidoreductases Grxs 2, 3 and 5 in neuroinflammatory de- and regeneration.

3.1 Grx levels and the activity of iron-dependent enzymes are altered in human MS and mouse EAE

To investigate a potential role of Grxs during neuroinflammation, the protein and mRNA expression profile of Grxs 2, 3 and 5 was measured in MS lesion areas and different stages of EAE progression. Grxs 3 and 5 are known to play an essential role in the assembly of iron-sulfur clusters and iron trafficking (Wingert et al. 2005; Haunhorst et al. 2013). Furthermore, iron homeostasis is disturbed in neuroinflammatory disorders including MS (Craelius et al. 1982). The contribution of iron to EAE progression is still under debate. Therefore, we measured the enzymatic activity and protein expression of proteins depending on iron cofactors in EAE disease progression. Another hallmark of neuroinflammation is the increased generation of NO in acute lesion areas (Oleszak et al. 1998; Liu et al. 2001). To combine both hallmarks, the impact of Grx2, the third FeS cluster coordinating mammalian Grx, on NO-mediated modulations of cellular iron homeostasis was analyzed using common parameters like transferrin-receptor localization and expression (Pantopoulos and Hentze 1995; Richardson et al. 1995).

3.1.1 Grxs 2, 3 and 5 are enriched at active lesion areas of human MS brain tissue

We analyzed the protein expression and localization of Grxs 2, 3 and 5 in human MS brain tissue in paraffin embedded sections from MS patients in cooperation with Prof. Dr. Jack van Horssen (VU University Medical Center, Amsterdam, Netherlands). Normal appearing white matter (NAWM) was used as reference. Here, three different lesion areas were analyzed according to their MHC class II HLA-DR (LN-3) and proteolipid protein (PLP) expression pattern: early lesions, acute lesions within the white matter and acute

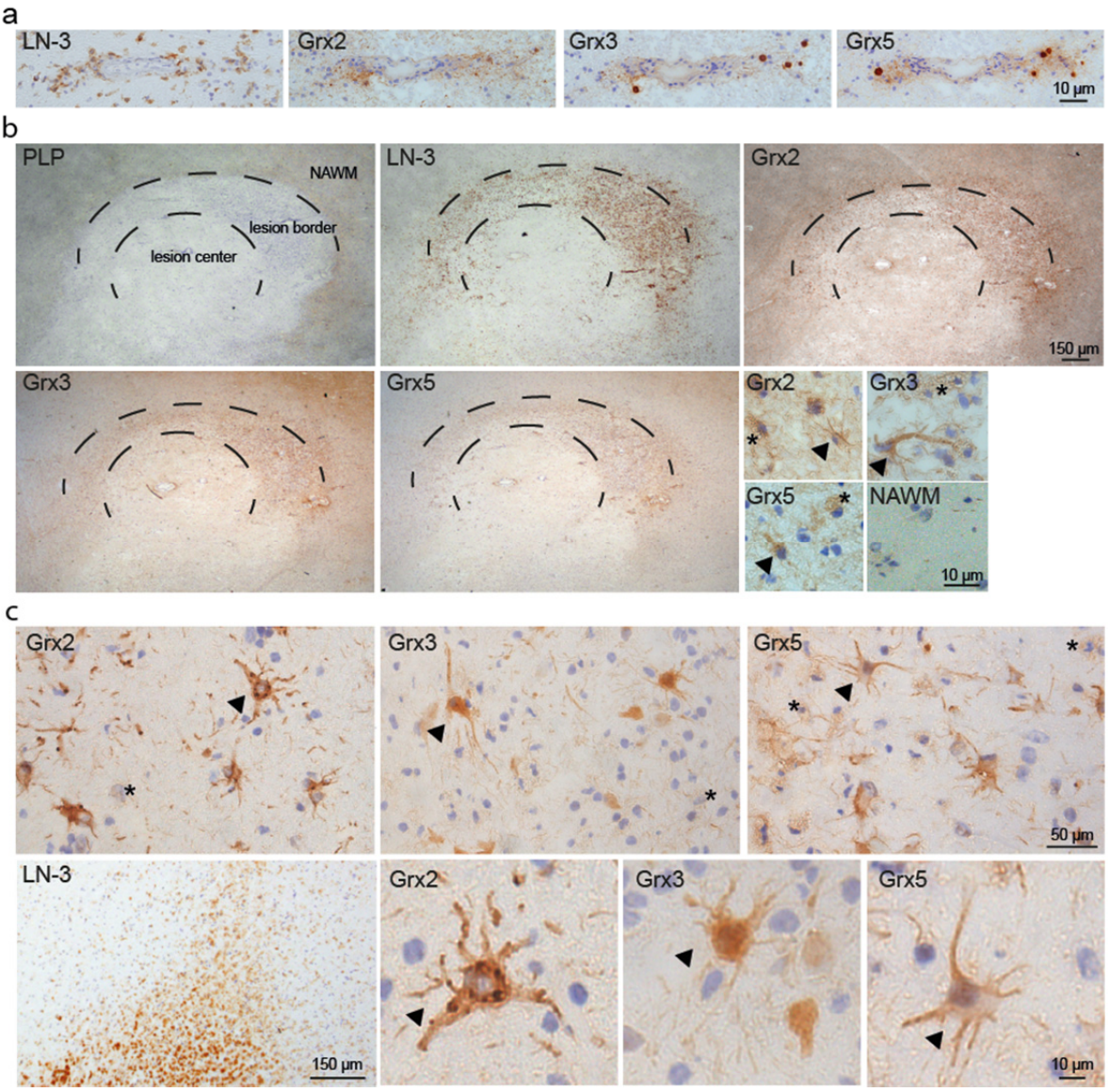

Figure 6. Protein expression patterns of Grxs 2, 3 and 5 in human MS white and grey matter brain tissue. Human paraffin sections were stained using Dako EnVision + Dual Link System. Nuclei were visualized by Hematoxylin staining. Lesion areas (acute lesion border and chronic lesion center) were identified using LN3 (antigen presenting cells, monocytes and macrophages) and PLP (myelin protein) staining. Three categories of lesion types were distinguished: early lesions (a; scale bar 10 µm), acute lesions in white matter brain tissue (b; NAWM: normal appearing white matter; scale bars 10 µm and 150 µm) and acute lesions in grey matter (c; scale bars 10 µm, 50 µm and 150 µm). The staining pattern for Grxs 2, 3 and 5 illustrates an increased level of all three proteins in demyelinated LN-3-positive lesion borders. The positively stained cells reveal morphological characteristics of astrocytes and phagocytic monocytes (b, c; star: cells with phagocytic monocyte-like morphology; arrow head: astrocyte-like morphology).

lesions within the grey matter (Fig. 6). Acute lesion areas were further distinguished into inflammatory active and inactive areas. Lesion sides were identified using immunohistochemical staining against PLP, a component of the myelin structure, and against LN3, illustrating activated antigen presenting cells (B cells, monocytes, macrophages, DCs, activated T cells). Inflammatory active lesion areas were characterized by LN3-positive staining and PLP-negative staining (Fig. 6 b and c). Furthermore, inflammatory inactive lesion centers were identified by double-negative staining (Fig. 6 b). Notably, all investigated Grxs showed nearly the same expression profile. Grx-positive staining was present in the inflammatory active areas of both early (Fig. 6 a) and acute lesions (Fig. 6 b and c). These areas are characterized by immune cell infiltration, the activation of microglia and astrocytes as well as an increased generation of proinflammatory cytokines and components (McFarland and Martin 2007). There was no staining visible for Grxs 2, 3 and 5 in the NAWM as well as in chronic lesion areas. However, less intensity of the overall staining pattern was observed in chronic lesion areas compared to the NAWM (Fig. 6 b).

3.1.2 Grx2 staining reveals morphological characteristics of astrocytes and co-localization with GFAP

The staining for Grxs 2, 3 and 5 in human MS brain tissue revealed increased protein levels mainly in acute lesion areas. These lesion areas are characterized, among others, by astrocytic and microglial activation and immune cell infiltration (Traugott and Lebon 1988; Lee et al. 1990). Morphological analyses of Grx-positive cells resembled cellular characteristics for activated astrocytes (Fig. 6 b and c, highlighted by arrow heads). These characteristics include cellular hypertrophy as well as thickened and shortened processes. Moreover, other cell types were identified showing cellular characteristics for phagocytic monocytes like macrophages and activated microglia (Fig. 6 b and c; highlighted by stars). To further underline the presence of Grxs in astrocytes we performed immunohistochemical analyses in MS brain tissue and looked for co-localization of Grx2 and an astrocytic marker, the glial fibrillary acidic protein (GFAP). As all Grxs revealed a similar expression pattern and the availability of human material was limited, we restricted the protein co-localization analysis to Grx2. Indeed, we found clear co-localization of Grx2 in hypertrophic GFAP-positive cells present only in acute lesion areas (Fig. 7). Furthermore, similar to the morphological analysis, we identified Grx2-positive but GFAP-negative cells, showing morphological similarities to phagocytic monocytes (Fig. 7; highlighted by arrow heads).

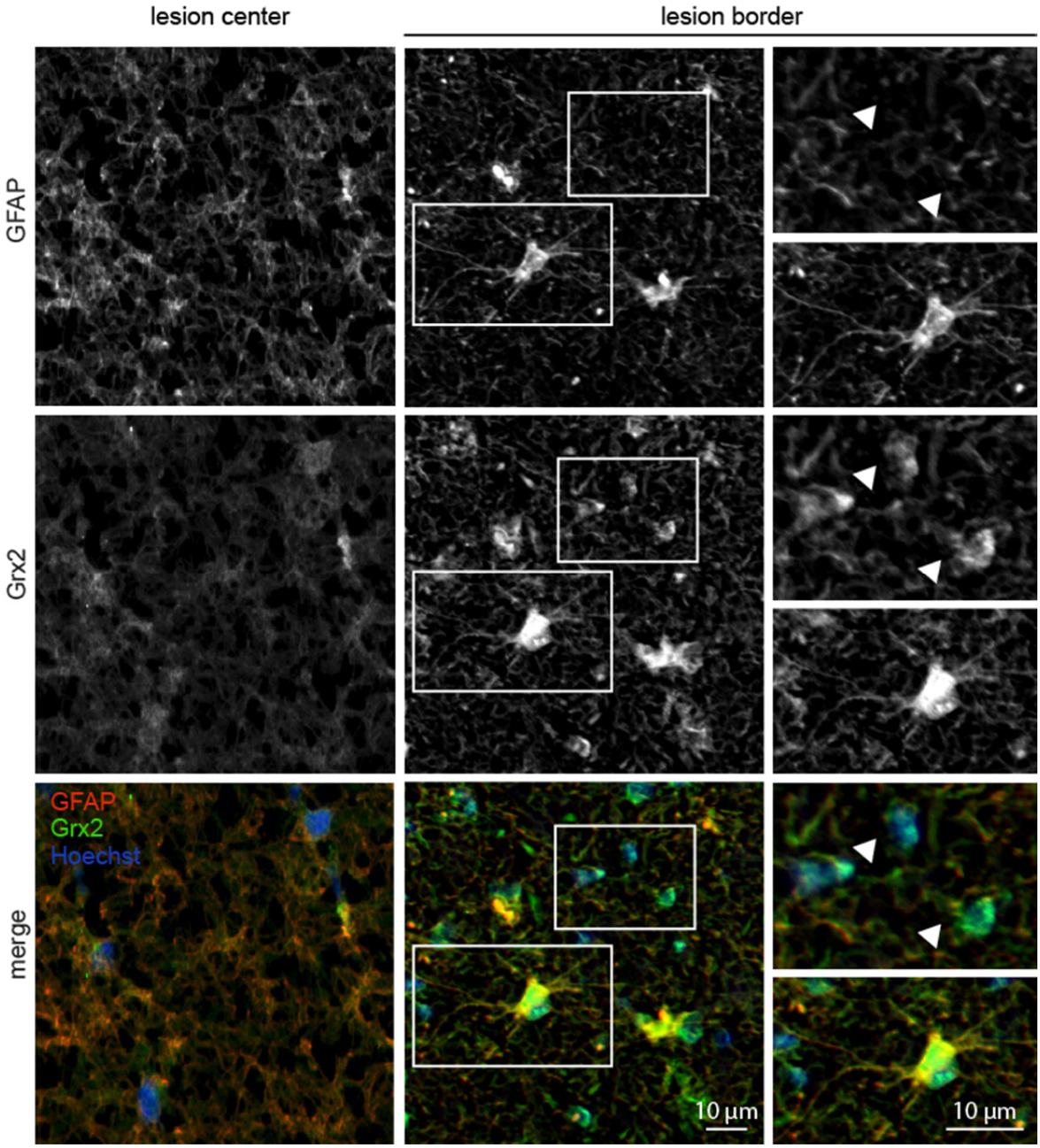

Figure 7. Grx2 staining reveals co-localization with GFAP-positive cells in human MS white matter brain tissue. Human paraffin sections were stained against GFAP (red) and Grx2 (green). Nuclei were visualized by Hoechst staining (blue). Immunohistochemical analysis revealed co-localization of Grx2 and GFAP-positive cells in lesion borders but not in lesion centers. Arrow heads highlight the presence of Grx2-positive but GFAP-negative cells. Scale bar 10 µm.

3.1.3 Expression levels of Grxs 2, 3 and 5 are altered during EAE disease progression

To further characterize the expression pattern of Grxs 2, 3 and 5 in the progression of neuroinflammatory demyelination we concentrated on EAE, an animal model of MS, performed in mice. For additional experiments the access to human MS brain tissue was restricted. Therefore, all following analyses are based on EAE samples. We analyzed the expression levels of Grxs 2, 3 and 5 on protein and mRNA levels, comparing cerebellar brain tissue from EAE mice in acute disease peak (day 17, clinical score 3-4) and in chronic disease phase (day 27, clinical score 2.5). Brain tissue from immunized animals before disease onset (day 7) was used as control. The applied score system was assigned determining symptom manifestation as described in 2.10. Protein and mRNA analyses of EAE cerebellar brain tissue demonstrated two different expression patterns. Cerebellar Grx2 was upregulated in the acute disease stage on mRNA levels compared to control with a significant upregulation for the cytosolic isoform Grx2c (Grx2c $p= 0.022$) (Fig. 8 e). However, the protein level of cerebellar Grx2 showed no upregulation in the acute disease phase compared to control. In chronic EAE phase, Grx2 was downregulated on both mRNA and protein level. Here, mRNA expression was decreased for both isoforms, Grx2a and Grx2c (Fig. 8 d and e). Grx5 protein level was likewise not regulated in the acute disease phase and showed a downregulation in the chronic disease phase. Unlike, Grx3 showed a different expression pattern (Fig. 8 b and f). On protein level, Grx3 was reproducibly downregulated in the acute disease phase. In the chronic disease phase Grx5 protein levels returned to control levels. However, mRNA analyses for Grxs 3 and 5 allow no conclusions due to high variety of the data (acute phase: Grx3 $p> 0.99$; Grx5 $p> 0.99$; chronic disease phase: Grx3 $p> 0.99$; Grx5 $p> 0.99$).

Taken together, Grx2c was significantly upregulated in the cerebellum of EAE mice in the disease peak on mRNA level. In chronic disease phase Grx2 was downregulated both on protein and mRNA level. Further, protein analysis revealed a reproducible downregulation of Grx3 in acute disease phase and of Grx5 in chronic disease phase.

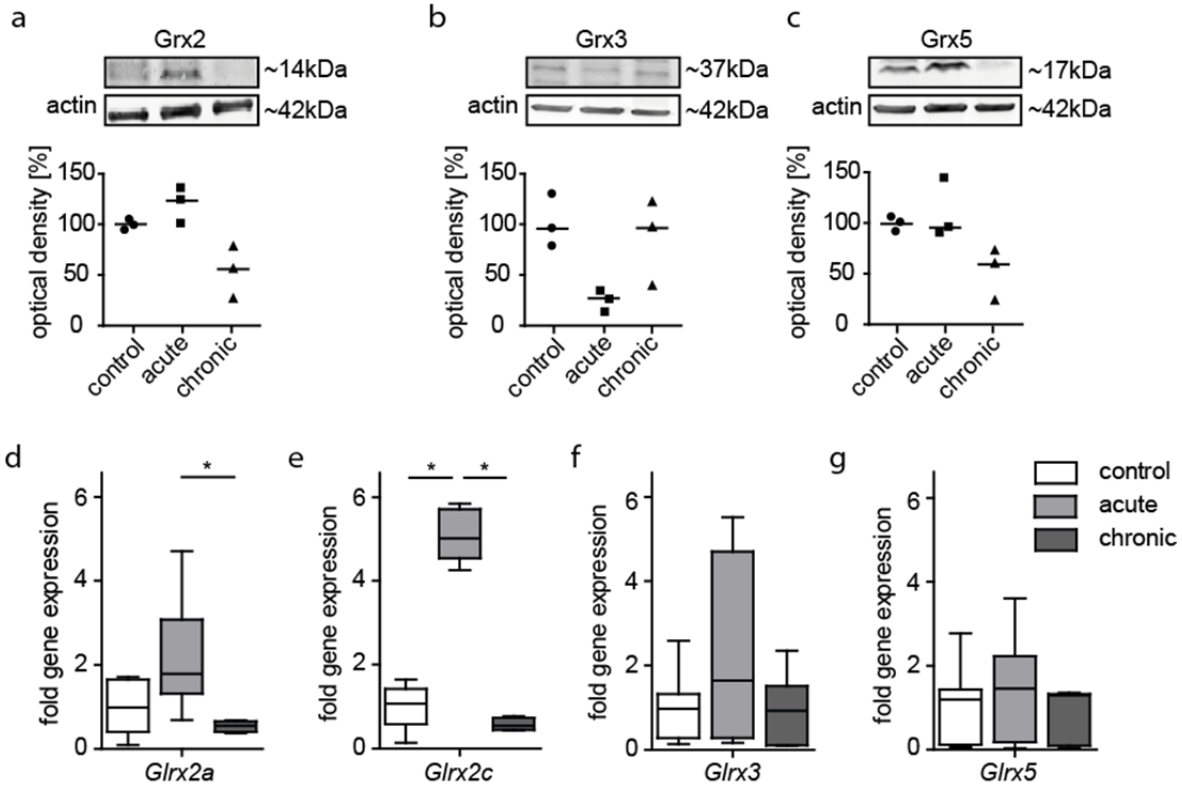

Figure 8. Protein and mRNA expression levels of Grxs 2, 3 and 5 in the progression of mouse EAE. Mouse EAE cerebellar brain tissue from control (before disease onset, day 7 post immunization), acute (day 17 post immunization, mean clinical score 3.5) and chronic (day 27 post immunization, mean clinical score 2.5) disease phase was either lysed using RIPA buffer to detect protein levels of Grxs 2, 3 and 5 by Western blot and optic density analyses (a, b and c; n= 3) or mRNA was isolated by phenol-chloroform extraction and quantified using q RT-PCR (d,e and f, n= 4 - 8). All data points are shown for n≤ 3; Boxplots are shown for n≥ 4; non-parametric Kruskal-Wallis h-test (α≤ 0.05).

3.1.4 The activity of iron-dependent enzymes is altered during EAE disease progression

As Grxs 3 and 5 are both involved in FeS cluster homeostasis as well as iron trafficking (Mühlenhoff et al. 2010), we investigated the activity of several iron-dependent enzymes and the function of FeS biosynthesis in the cerebellum during EAE disease progression. Notably, the activity measurements were performed from total cellular extracts. Therefore, mitochondrial and cytosolic activities cannot be distinguished. Two different activity patterns were detected (Fig. 9). The activities of aconitase (ACO, present both in the mitochondria and as holo IRP1 protein in the cytosol) and succinat-dehydrogenase (SDH, mitochondrial localization) were significantly reduced in disease peak (ACO p= 0.005; SDH p= 0.018) and consistently downregulated in the chronic disease phase compared to

healthy control tissue (Fig. 9 a and b). The activities of cytochrome C oxidase (COX, mitochondrial localization) and lactat-dehydrogenase (LDH, cytosolic localization) were decreased in disease peak (COX p= 0.018; LDH p= 0.005) and restored in the chronic disease phase comparable to control tissue (Fig. 9 d and e). Malate-dehydrogenase (MDH) is present in both the cytosol as well as in the mitochondria. Its enzymatic activity is independent from iron. To display the observed changes in enzymatic activity to depend on specific alteration in iron cofactors, the MDH activity was measured as reference and showed no significant alteration (disease peak: p> 0.99 and chronic disease phase: p= 0.98) (Fig. 9 c). Further, to exclude variations in protein content like degradation and/ or expression upon EAE progression, we examined the protein level for ACO, SDH and COX. None of these proteins showed alterations upon disease progression on protein level (Fig. 9 a, b and d; illustrated by grey bars). As obstructions in the iron homeostasis could result in the observed decrease in iron-dependent protein activity, I further investigated whether or not subtle changes in iron homeostasis are present during EAE disease progression. A prominent candidate known to be regulated upon alterations in iron homeostasis is glycerol-3-phosphate acyltransferase (GPAT). GPAT shows rapid protein degradation when its FeS cluster is disassembled *in vitro* and *in vivo* (Grandoni et al. 1989; Martelli et al. 2007). Furthermore, the IRP pathway is rapidly activated under iron starving conditions (Pantopoulos and Hentze 1995), regulating the expression of ACO, Ferritin and Transferin receptor (TfR) (Cairo and Recalcati 2007). Western blot analysis, using the entire cerebellar protein extract, indicated no significant regulation for any of the mentioned iron-dependent proteins (Fig. 9 g- k; illustrated by grey bars). Further, potassium ferrocyanide staining displayed no visible iron staining in cerebellar brain tissue; neither in animals of the acute EAE state nor in animals of the chronic EAE phase (Fig. 9 f).

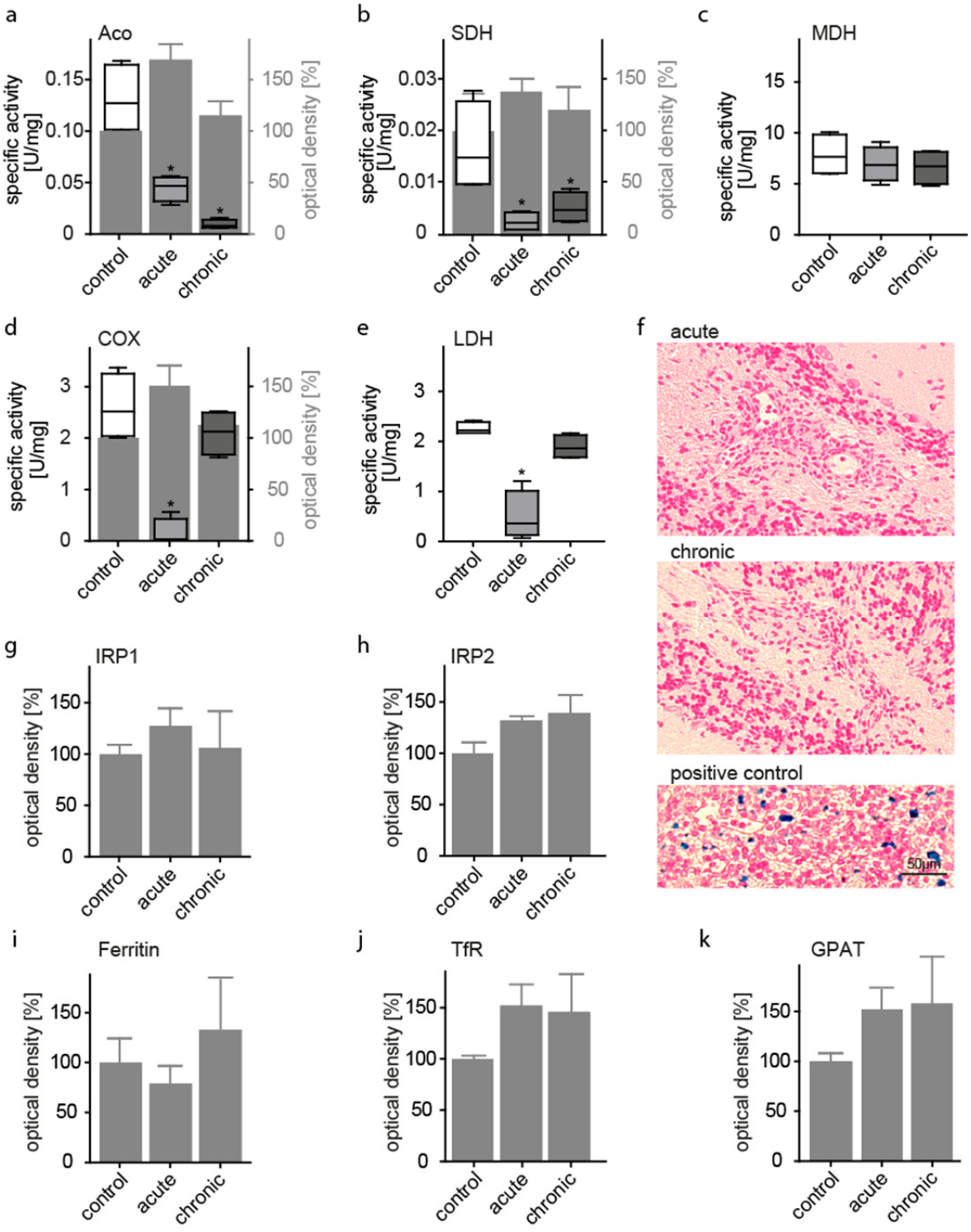

Figure 9. The activities but not the protein levels of iron-dependent enzymes are significantly affected during the progression of mouse EAE. Mouse EAE cerebellar brain tissue from control (before disease onset), acute (peak of disease, clinical score 3- 4) and chronic (remission, clinical score 2.5) disease phase was either lysed using SDS-free lysis buffer for Western blot and protein activity analyses or fixed with 4% PFA for histochemical analysis. Aconitase (Aco, a), sodium dehydrogenase (SDH, b), malate dehydrogenase (MDH, c), cytochrome c oxidase (COX, d) and lactate dehydrogenase (LDH, e) activities were measured in total cerebellar extract (n= 4). MDH was measured as an iron-independent control protein.

Appropriate protein levels for the mentioned enzymes and further for glycerol-3-phosphate acyltransferase (GPAT, k), ferritin (i), iron responsive protein 1/ 2 (IRP1/ 2, g and h) and transferrin receptor (TfR, j) were determined using Western blot analyses (grey bars; n= 3-4). Protein levels were normalized to respective control samples. Histological iron staining in paraffin sections showed no positive staining in neither acute nor chronic cerebellar EAE tissue. Spleen tissue was simultaneously stained as positive control to prove proper staining procedure (f; scale bar 50 µm). Data show median with range for Western blot analyses. Datasets of the activity measurements are illustrated as boxplots; non-parametric Kruskal-Wallis h-test ($\alpha \leq 0.05$).

3.1.5 Grx2 can reverse NO-mediated alterations in the localization pattern of the transferrin receptor in OLN-93 cells

One hallmark of MS lesion areas is the increased generation of NO (Oleszak et al. 1998; Liu et al. 2001). To verify whether this is also the case for our chosen animal model, the EAE, we performed an immunohistochemical analysis for nitrated tyrosines and indeed, we found increased nitrotyrosine staining close to cells with enhanced immunoreactivity for ionized calcium-binding adapter molecule1 (Iba1). Here, the Iba1 staining was used to identify activated microglia and macrophages as hallmarks for lesion areas (Fig. 11). Our findings indicate the presence of nitrosative stress in EAE lesion areas. As previously reported, the oligodendrocyte lineage is dramatically affected in EAE lesions and exhibits a clear histological staining pattern for iron (Benkovic and Connor 1993). Furthermore, as increased generation of NO was shown to cause changes in the iron metabolism (Weiss et al. 1993; Oria et al. 1995), we investigated a possible impact of Grx2 on NO-mediated alterations of iron homeostasis using the rat oligodendrocyte OLN-93 cell line. As the role of Grxs 3 and 5 in iron homeostasis is already published (Wingert et al. 2005; Haunhorst et al. 2013) and the regulation of both proteins was rather diverse on protein and mRNA level during the progression of EAE, we concentrated on a possible impact of Grx2 (upregulation in disease peak and downregulation in chronic disease phase; Fig. 8). Protein analysis of iron-dependent enzymes showed no significant regulation of neither TfR nor Ferritin nor GPAT in cultures, treated with GSNO or a combination of GSNO and Grx2 (Fig. 10 c, d and e). These results are consistent with the protein expression measurements during EAE progression (see 3.1.4), underlining a possible coherence. Due to the observed changes in the activity of iron-dependent enzymes during EAE progression, we further characterized the subcellular distribution of the TfR in OLN-93 cells using immuocytochemistry. Confocal microscopy revealed a significant redistribution of the TfR from the endosomes to the cytosol induced by non-toxic concentrations of GSNO for 24 h ($p= 0.001$) (Fig. 10 a and b). Quantification of cells with a cellular

distribution of the TfR underline the impact of Grx2 on the NO-mediated redistribution of the TfR. Here, the addition of 2 µM recombinant Grx2 into the culture medium diminished the NO-mediated TfR translocation (p= 0.28).

Summarizing, Grx2 is regulated on protein and mRNA levels in both acute and chronic disease phases of human MS and mouse EAE. Further, treatment with recombinant Grx2 protected against the NO-mediated alteration of the cellular distribution of the TfR pointing to an involvement of Grx2 in iron dependent pathways of oligodendrocytes.

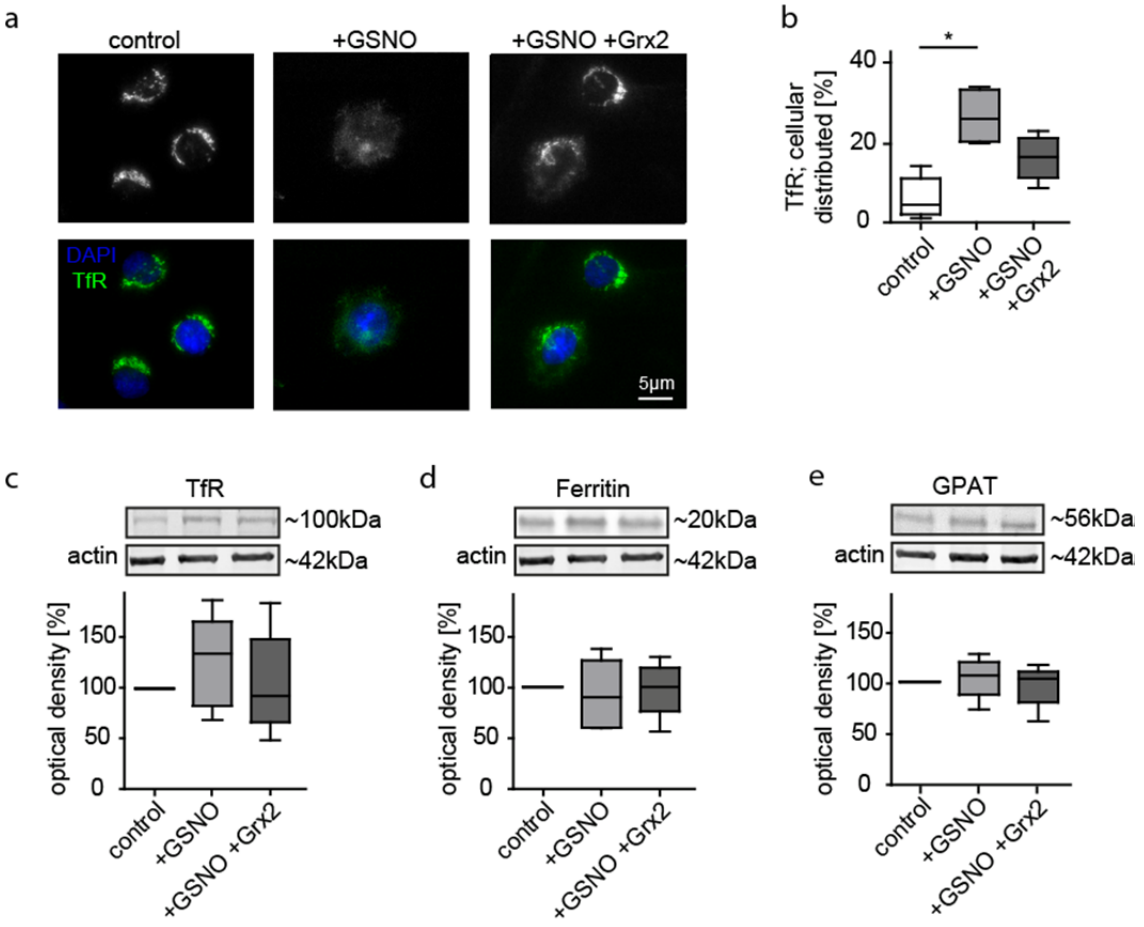

Figure 10. GSNO induces alteration of TfR expression and localization in OLN-93 cells. OLN-93 oligodendroglial cell line was incubated with 500 µM GSNO in presence or absence of 2 µM recombinant Grx2. After 24 h cells were either fixed with 4 % PFA (a) or cell lysates were prepared using RIPA buffer (c- e, n= 5). Fixed cells were stained against transferrin receptor (TfR, green) and nuclei were visualized using Hoechst (blue) (a, scale bar 5 µm). Immunocytochemistry was quantified according to the localization of stained protein (b, either concentrated in vacuoles or cellular distributed, n= 6). Cell lysates were examined using Western blot analysis against TfR (c), Ferritin (d) and GPAT (e). Intensities were calculated using ImageJ and normalized to actin. Datasets are illustrated as boxplots; non-parametric Kruskal-Wallis h-test ($\alpha \leq 0.05$).

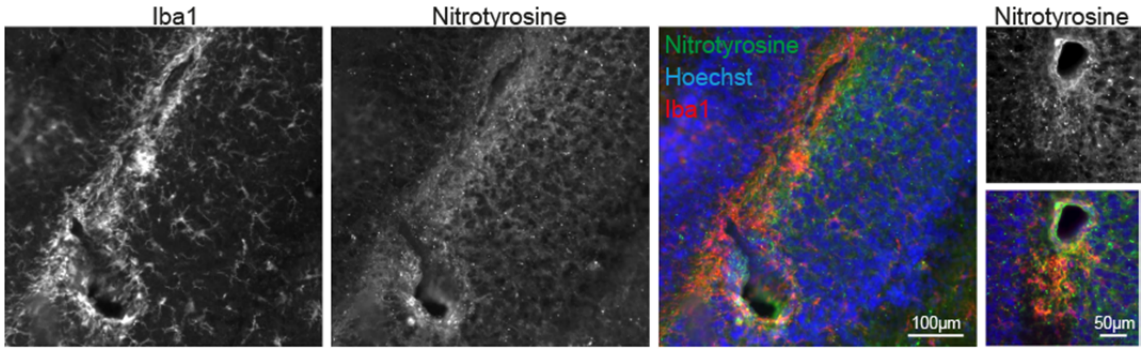

Figure 11. Nitrotyrosine is increased in mouse EAE lesion areas. Cryosections of chronic mouse EAE brain tissue (clinical score 3-4) were stained for Iba1 (microglia, red) and Hoechst (nuclei, blue) to visualize lesion areas and for anti-nitrotyrosine antibody (green) to visualize nitrated proteins. Comparison to non-lesion areas reveals accumulation of nitrated proteins in EAE lesion areas. Scale bars 100 µm and 50 µm.

3.2 Recombinant Grx2 protects oligodendrocyte lineage cells against NO-mediated cell death

Mature myelinating oligodendrocytes undergo cell death inside MS and EAE lesion areas (Dowling et al. 1997). Furthermore, pre-existing mature oligodendrocytes do not contribute to remyelination (Keirstead and Blakemore 1997) and oligodendrocyte progenitors are highly vulnerable to increased concentrations of NO *in vitro* (Pang et al. 2010). As NO is increasingly produced in MS lesions (Oleszak et al. 1998; Liu et al. 2001), the inhibition of oligodendrocyte death became a promising target for therapeutic approaches to inhibit degeneration and improve regeneration. In 3.1 we observed a Grx2-dependent inhibition of NO-mediated alterations in cellular TfR localization. Hence, we further investigated the impact of recombinant Grx2 treatment on the survival of NO-mediated oligodendrocyte cell death.

3.2.1 Recombinant Grx2 treatment results in increased Grx2 protein concentrations in cell cultures as well as OSCs

First, the amount and localization of recombinant Grx2 after supplementation into the culture medium was determined using Western blot analysis and immunocytochemistry. For all experiments, culture medium was supplemented with 2 µM recombinant Grx2 2 h

before treatment with GSNO or LPS. The final readout was performed after 24 h. Therefore, primary A_2B_5-positive mouse cells, OLN-93 cell line and OSCs were analyzed using Western blot analysis either 2 h or 24 h after Grx2 treatment. To avoid detection of extracellular Grx2, all cultures were carefully washed before cell lysis. Western blot analyses revealed an increased level of Grx2 in A_2B_5-positive progenitors of 144 % and 120 % (two independent experiments) after 2 h and of 135 % and 150 % after 24 h (n= 2) (Fig. 15 b). For OSCs an increased Grx2 protein level of 660 % and 720 % was detected (n= 2) (Fig. 12 d) and in OLN-93 cells Grx2 protein level was increased to 473 % ± 113 %. To further investigate the localization of externally added recombinant Grx2, we took advantage of the hisTag coupled to the recombinant protein and performed immunohisto- and immunocytochemical analyses in A_2B_5-positive progenitors and OSCs. Here, primary mouse A_2B_5-positive progenitors clearly co-localized with the hisTag staining (Fig. 15 a). Further, the hisTag staining in OSCs revealed a co-localization with GFAP (astrocytic marker), Iba1 (marker for microglial cells) and MBP (oligodendrocyte marker) (Fig. 12 a). These results indicate that externally applied recombinant Grx2 accumulates in all investigated cell types both 2 and 24 h after treatment.

3.2.2 Influence of recombinant Grx2 on NO-mediated OSC myelin damage

OSCs enable simultaneous modulation of the Grx2 concentrations and the amount of associable NO in an *ex vivo* model maintaining the complex multicellular nature of the *in vivo* situation. Here, we increased the concentration of NO, using either 750 µM GSNO as physiological NO donor, or 10 µg/ ml LPS, a toll-like receptor 4 agonist, to activate local microglia and stimulate NO release (Simmons and Murphy 1992). In both setups, we observed a destruction of myelin structures visualized by immunohistochemical staining against MBP (Fig. 12 b and Fig. 13 a and b) as well as a reduction in the number of A_2B_5-positive OPCs (Fig. 12 e). Untreated control slices revealed a consistent number of approximately 40 % damaged white mater branches, whereas GSNO treatment increased the number of damaged branches up significantly to approximately 55 % and LPS to 65 % (LPS p= 0.001; GSNO p= 0.005). The addition of 2 µM recombinant Grx2 prevented from both GSNO and LPS-mediated myelin destruction (LPS p= 0.003; GSNO p= 0.12) (Fig. 12 c). Further, addition of recombinant Grx2 increased the number of A_2B_5-positive progenitors per white matter branch significantly compared to LPS treated slices (p= 0.001). In OSCs treated with LPS alone the number of A_2B_5-positive progenitors decreased significantly to approximately 65 % (Fig. 12 e). To underline that the observed

LPS induced myelin destruction is mediated by NO, we additionally applied the NO scavenger CPTIO. Here, the experiments indicated a concentration-dependent protection of CPTIO from LPS-mediated myelin damage (Fig. 13 d). Notably, despite myelin damage, neuronal structures were not affected by the increased generation of NO ($p > 0.99$) (Fig. 13 b). To further investigate the role of Grx2 in oligodendrocyte survival, viability measurements with primary mouse A_2B_5-positive OPCs were performed.

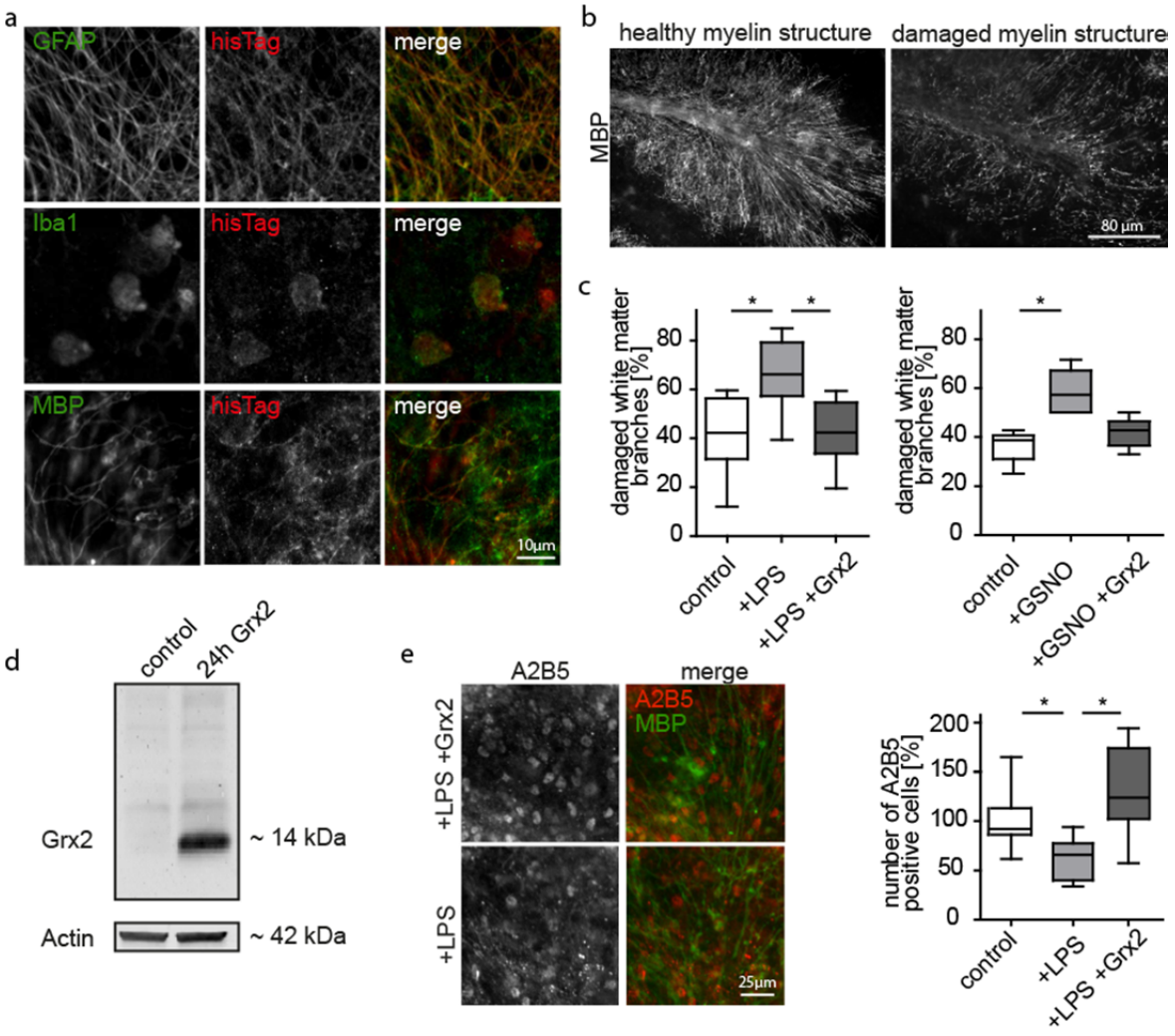

Figure 12. Recombinant Grx2 is taken up by organotypic slice cultures and protects mature oligodendrocytes as well as oligodendrocyte progenitors from NO-mediated cell death. Cerebellar organotypic slice cultures (OSCs) were treated with 750 µM GSNO or 10 µg/ ml LPS in the presence or absence of 2 µM recombinant Grx2. After 24 h, OSCs were stained against MBP (myelin), A_2B_5 (oligodendrocyte progenitors), GFAP (astrocytes), Iba1 (microglia) or hisTag (recombinant Grx2). Immunohistochemical analysis illustrated the uptake of recombinant Grx2 into astrocytes, microglia and oligodendrocytes (MBP) (a, scale bar 10 µm) which was further underlined by Western blot analysis (d). Percentage of damaged myelin branches per slice was analyzed and quantified via MBP staining (b and c, GSNO: n= 5- 6; LPS: n= 12- 18; scale bar 80 µm). The number of A_2B_5-positive progenitors was quantified per myelin branch (e, n= 11, scale bar 25 µm). Datasets are illustrated as boxplots; non-parametric Kruskal-Wallis h-test ($\alpha \leq 0.05$).

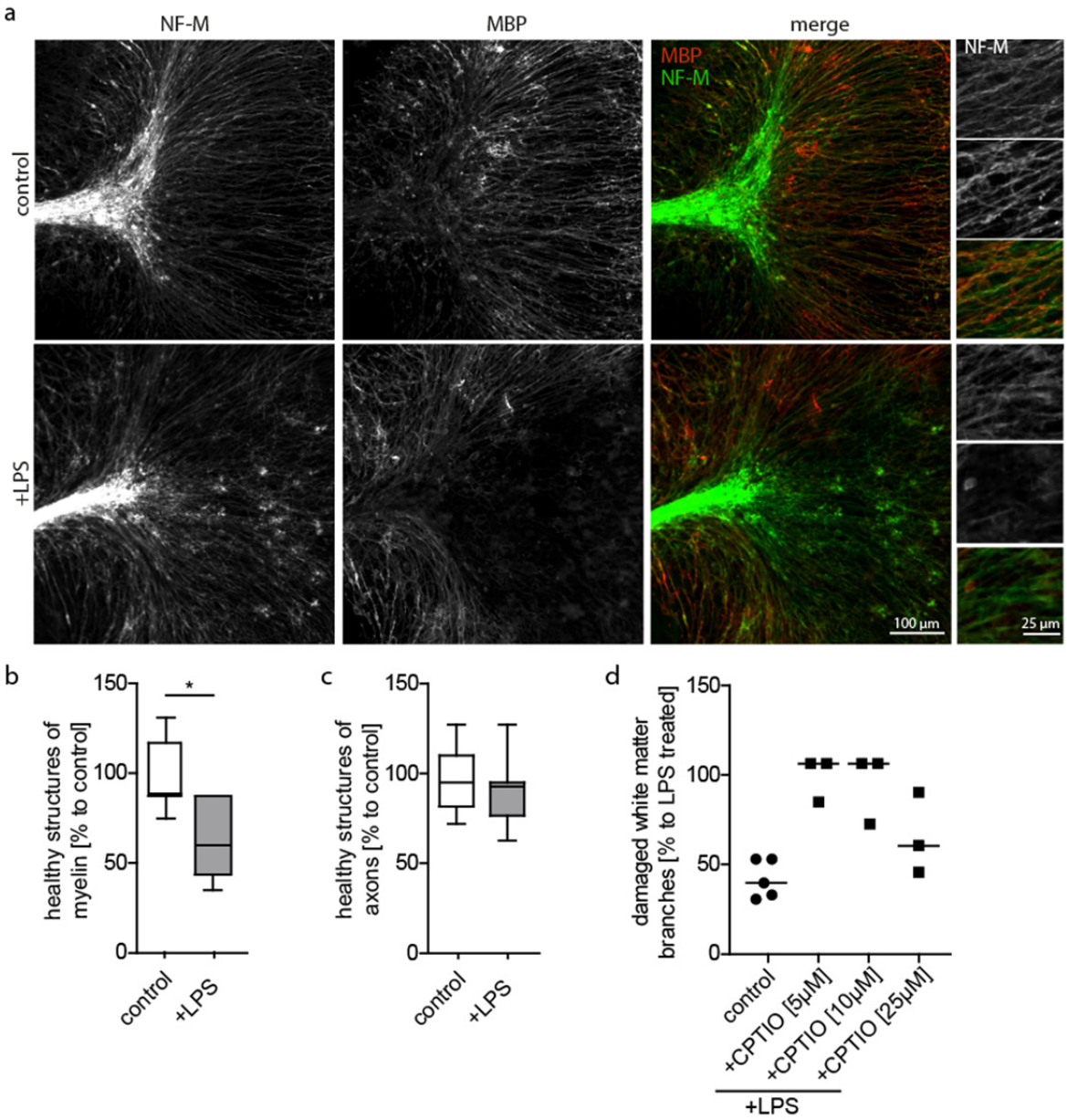

Figure 13. LPS treatment affects myelin structure but not axonal structure and can be rescued by NO scavenging. Cerebellar OSCs were treated with 10 µg/ ml LPS in the presence of 0, 5, 10 or 25 µM CPTIO. After 24 h OSCs were stained against MBP (myelin) and NF-M (axons) (a, scale bar 100 µm and 25 µm). The integrity of both axonal and myelin structure was calculated per slice (b and c, n= 7- 11). Additional treatment with the NO scavenger CPTIO revealed a concentration-dependent decrease in myelin destruction (d, n= 3- 6). All data points are shown for n≤ 3. Boxplots are shown for n≥ 4; non-parametric Mann Whitney u-test (α≤ 0.05).

3.2.3 Influence of Grx2 on NO-mediated cell death of primary A_2B_5-positive progenitors and HeLa Grx2 overexpressing cells

First, the sensitivity of primary mouse A_2B_5-positive progenitors against GSNO treatment was investigated. The concentration-dependent cell viability revealed an IC_{50} value of 1.1 mM after 24 h (Fig. 14 a). Therefore, all further viability experiments were performed using 1 mM GSNO. To ensure that our observations are NO-dependent, we performed control experiments using the NO scavenger CPTIO. Treatment with CPTIO decreased GSNO-mediated cell death in a concentration-dependent manner underlining direct contribution of NO to the observed effects (Fig. 14 b). To mimic the condition present in the OSC setup, A_2B_5-positive cells were co-cultured with LPS activated BV2 cells. Direct cell-to-cell contact was prevented by Trans O FLEX 24 well inserts with a pore size of 0.4 µm. LPS treatment induced iNOS expression and increased microglial NO release measured by Griess reagent reaction (Fig. 16 a and b). Here, LPS-induced secretion of NO decreased the survival rate of A_2B_5-positive progenitors to approximately 65 % in the co-culture system (Fig. 15 c). Similar to the observations in the OSC, treatment with recombinant Grx2 prevented BV2-induced cell death similar to untreated control cultures (Fig. 15 c). Next, we investigated whether knockdown of endogenous Grx2 promotes NO-mediated cell death. Grx2-specific siRNA silencing emphasized the repellent effect of Grx2 on NO-mediated cell death (Fig. 15 f). The decreased expression of Grx2 (mRNA level: Grx2a 27 % and Grx2c 33 %; n= 3) diminished the viability of A_2B_5-positive progenitors in the BV2 co-culture system ($p= 0.085$). To further strengthen this observation, we repeated the GSNO toxicity experiments using Grx2c overexpressing HeLa cells (Fig. 14 c). The GSNO-dependent cell death of HeLa cells revealed an increase in the IC_{50} value from 1.1 mM to 3.4 mM based on the 3 fold overexpression of Grx2c (Enoksson et al. 2005) (Fig. 14 c).

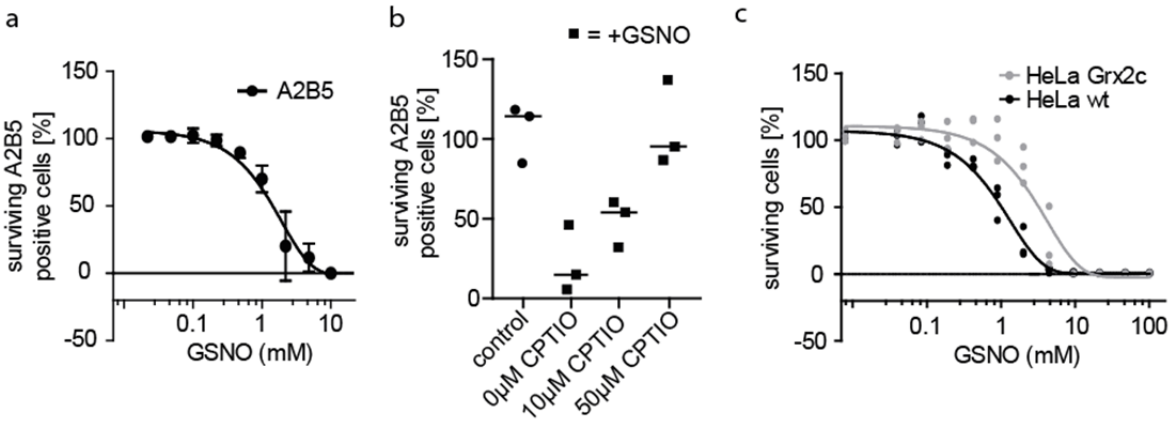

Figure 14. GSNO-mediated oligodendrocyte cell death is attenuated by NO scavenging and intracellular Grx2c. Primary mouse A_2B_5-positive progenitors (a, b), HeLa wt or HeLa Grx2c overexpressing cells (c) were incubated with increasing amounts of GSNO (a, n= 4, IC_{50}= 1.1 mM; b, n= 3; c, n= 3, HeLa wt: IC_{50}= 1.1 mM, HeLa Grx2c: IC_{50}= 3.4 mM). Cell survival rate was measured using CellTiter-Blue® assay and normalized to control condition. The influence of CPTIO was investigated in the presence of 1 mM GSNO (b). Datasets are illustrated as median with range for n≥ 4 or by all data points presented for n≤ 3.

3.2.4 Recombinant Grx2 treatment shows no alteration of NO release and iNOS expression in activated BV2 cells

The evaluation of the A_2B_5/ BV2 co-culturing experiments assumed an influence of recombinant Grx2 on primary mouse A_2B_5-positive progenitors. However, it is unknown whether or not Grx2 has an effect on microglia activation. To exclude a direct influence of Grx2 on LPS-activated BV2 cell functions in our experimental co-culture setup, the impact of recombinant Grx2 on cell viability, *iNOS* transcription and NO release was investigated. Here, LPS alone significantly increased *iNOS* mRNA expression two-fold (p= 0.012) and further raised NO release to approximately to 380 % compared to untreated control cells but showed no influence on BV2 cell viability. Additional treatment of recombinant Grx2 showed no significant effect on the observed readouts (iNOS expression: p> 0.9) (Fig. 16 a, b and c). These results underline a Grx2-dependent increase in A_2B_5 cell viability independent of the modification of BV2 cell functions.

Summarizing, the findings revealed a protective effect of recombinant Grx2 against NO-mediated cell death of mature oligodendrocytes and their A_2B_5-positive progenitors in OSCs. No effect was detectable on neuronal NF-M immunohistochemical integrity in OSCs upon NO challenge.

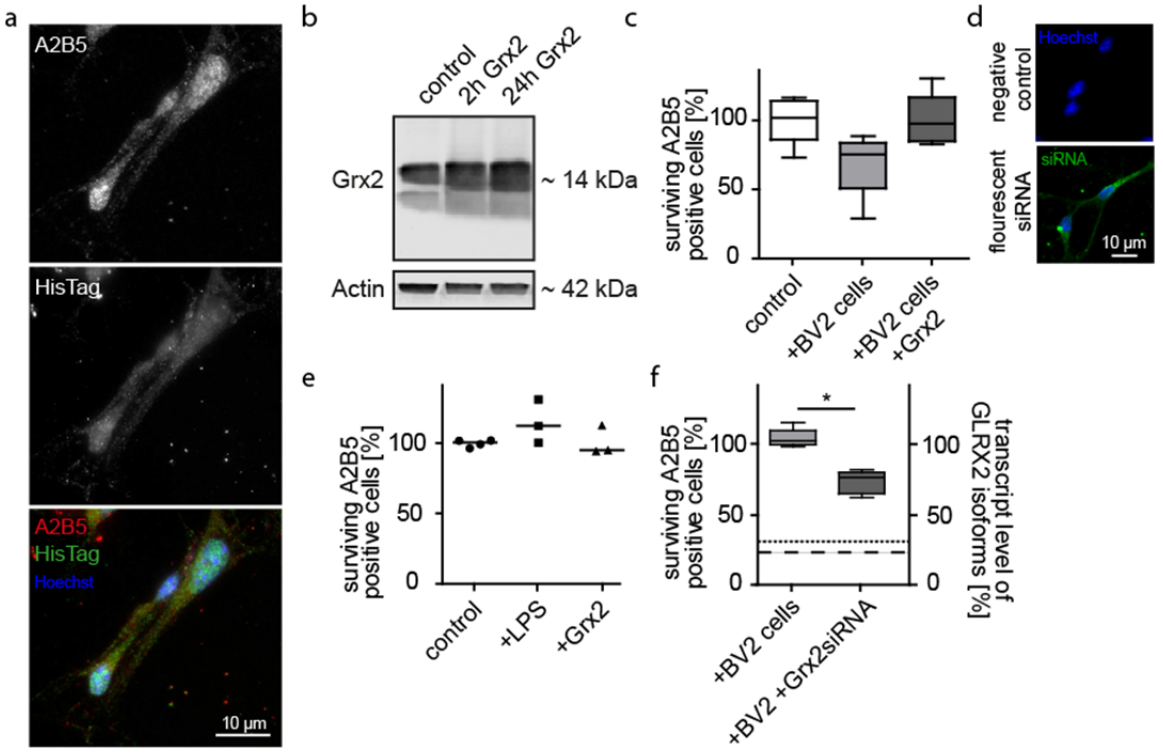

Figure 15. Intracellular Grx2 is required for the detoxification of NO in primary A_2B_5-positive progenitors. Primary mouse A_2B_5-positive progenitors were treated with either 1 mM GSNO or co-cultured (without direct cell contact) with LPS activated BV2 microglial cells (1 µg/ ml LPS, 50.000 BV2 cells) in the presence or absence of 2 µM recombinant Grx2 (c, BV2 co-cultured: n= 5) or Grx2-specific siRNA (f, BV2 co-cultured: n= 5; GSNO treated: n= 4). Immunocytochemistry (a) and Western blot analyses (b) reveal an uptake of recombinant Grx2 by cultured A_2B_5-positive progenitors. The uptake of siRNA is visualized using fluorescent siRNA (d). Transcription levels of the cytosolic (Grx2c) and the mitochondrial (Grx2a) Grx2 isoform after incubation with Grx2-specific siRNA for 3 days was analyzed by q RT-PCR (f, n= 5, dashed line: Grx2a, dotted line: Grx2c). Cell survival rate were quantified after 24 h using CellTiter-Blue® assay and normalized to untreated control cells. LPS treatment as well as Grx2 treatment alone showed no influence on the survival rate of A_2B_5-positive progenitors (e, n= 3). Boxplots are shown for n≥ 4; non-parametric Kruskal-Wallis h-test (α≤ 0.05).

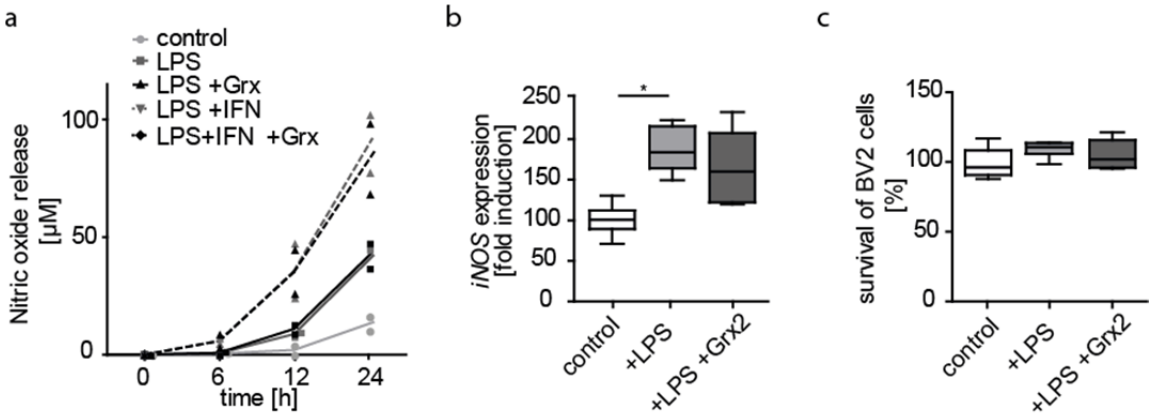

Figure 16. Recombinant Grx2 has no effect on LPS-induced NO secretion by BV2 cells. The influence of recombinant Grx2 treatment on the amount of NO released by BV2 microglial cell line was analyzed according to three readouts: LPS (1 µg/ ml +/- 100 U/ ml IFNγ) induced NO release in the presence or absence of 2 µM Grx2 was quantified using Griess reagent (a, n= 2, measured in triplicates). *iNOS* mRNA expression level was analyzed by q RT-PCR (b, n= 6) and BV2 survival rate was measured using the CellTiter-Blue® assay (c, n= 8). All data points are shown for n≤ 3. Boxplots are shown for n≥ 4; non-parametric Kruskal-Wallis h-test (α≤ 0.05).

3.3 Grx2 promotes oligodendrocyte cell survival by FeS-dependent detoxification of NO

This chapter further characterizes the connection between the enzymatic activity of Grx2 and the cell-protective effects observed in 3.2. We purified two Grx2 mutants: One being enzymatically hyper-active without the ability to coordinate FeS clusters (Grx2S38P) and one being enzymatically inactive and further lacking the ability to generate FeS clusters (Grx2C37S) (Berndt et al. 2007). Surprisingly, Grx2S38P although hyper-active showed no protective effect stressing the importance of the Grx2 feature to assemble an iron-sulfur (FeS) cluster. Finally, we further characterized the protective mechanism of Grx2 and its influence on NO-dependent $ONOO^-$ formation.

3.3.1 Recombinant Grx2 protects against NO but not $ONOO^-$

Exposing cells to an increased amount of NO resulted in diverse protein modifications like formation of nitrotyrosine that was previously reported to be increased in MS (Bö et al. 1994) as well as EAE lesions (Fig. 11). Western blot analysis using both primary mouse

A_2B_5-positive progenitors and the oligodendrocyte OLN-93 cell line revealed increased protein nitration and carbonylation in presence of GSNO and SIN1, a $ONOO^-$ donor (Fig. 17 a-d and 18 a and b). Following GSNO treatment the formation of nitrotyrosine increased to approximately 170 % in OLN-93 cells compared to untreated control cells. In presence of recombinant Grx2 the formation was significantly repealed (p= 0.016) (Fig. 17 c). A similar pattern was observed measuring the amount of protein carbonyls (Fig. 17 a). GSNO treatment increased protein carbonyls to approximately 170 % in OLN-93 cells compared to control cultures, whereas the addition of recombinant Grx2 significantly decreased the amount of protein carbonyls almost to control level (p= 0.046). Examinations were confirmed in A_2B_5-positive progenitors (147 % protein carbonyls in presence of GSNO and 62 % after the addition of recombinant Grx2) (Fig. 18 b). Since NO reacts rapidly with $O_2^{\cdot-}$ forming $ONOO^-$, oxidative as well as nitrosative protein damage is thought to be mainly mediated by $ONOO^-$ (Pacher et al. 2007). Treatment with SIN1, as $ONOO^-$ donor, displayed a comparable increase in oxidative and nitrosative protein damage in OLN-93 cells (amount of protein carbonyls: 210 %; protein nitration: 145 %). However, recombinant Grx2 treatment showed no protective effects on cells exposed to SIN1 (amount of protein carbonyls: 190 %; protein nitration: 155 %). Again, the limited protection of recombinant Grx2 against SIN1 induced protein nitration was validated in A_2B_5-positive progenitors (SIN1 treatment: 170 %; SIN1 and Grx2 treatment: 180 %) (Fig. 18 a). Conclusively, Grx2 showed a limited effect on SIN1-mediated cell death. A_2B_5-positive progenitors displayed a concentration-dependent sensitivity in cell survival against SIN1 without protective effects in presence of recombinant Grx2 (Fig. 18 c). Next, we analyzed the immunohistochemical reactivity of active caspase3, as marker for apoptotic cell death, in OLN-93 cells. In line, recombinant Grx2 reduced the amount of active caspase3 after GSNO treatment but not after SIN1 treatment (Fig. 17 e). These results indicate that recombinant Grx2 prevents from NO-mediated protein damage and further inhibits the induction of apoptosis.

3.3.2 Recombinant Grx2 decreases $ONOO^-$ formation

The results described in 3.3.1 stress a Grx2-dependent detoxification of NO and the subsequent inhibition of $ONNO^-$ formation. In this case Grx2 treatment should reduce the amount of $ONOO^-$ formation in presence of GSNO. Indeed, a newly developed probe (Fluorescein-boronate, kindly provided by Prof. Dr. Rafael Radi, Universidad de la República, Uruguay (Rios et al. 2016) for $ONOO^-$ detection revealed a Grx2-dependent inhibition of $ONNO^-$ formation in GSNO treated A_2B_5-positive progenitors (n= 2; 70 % and

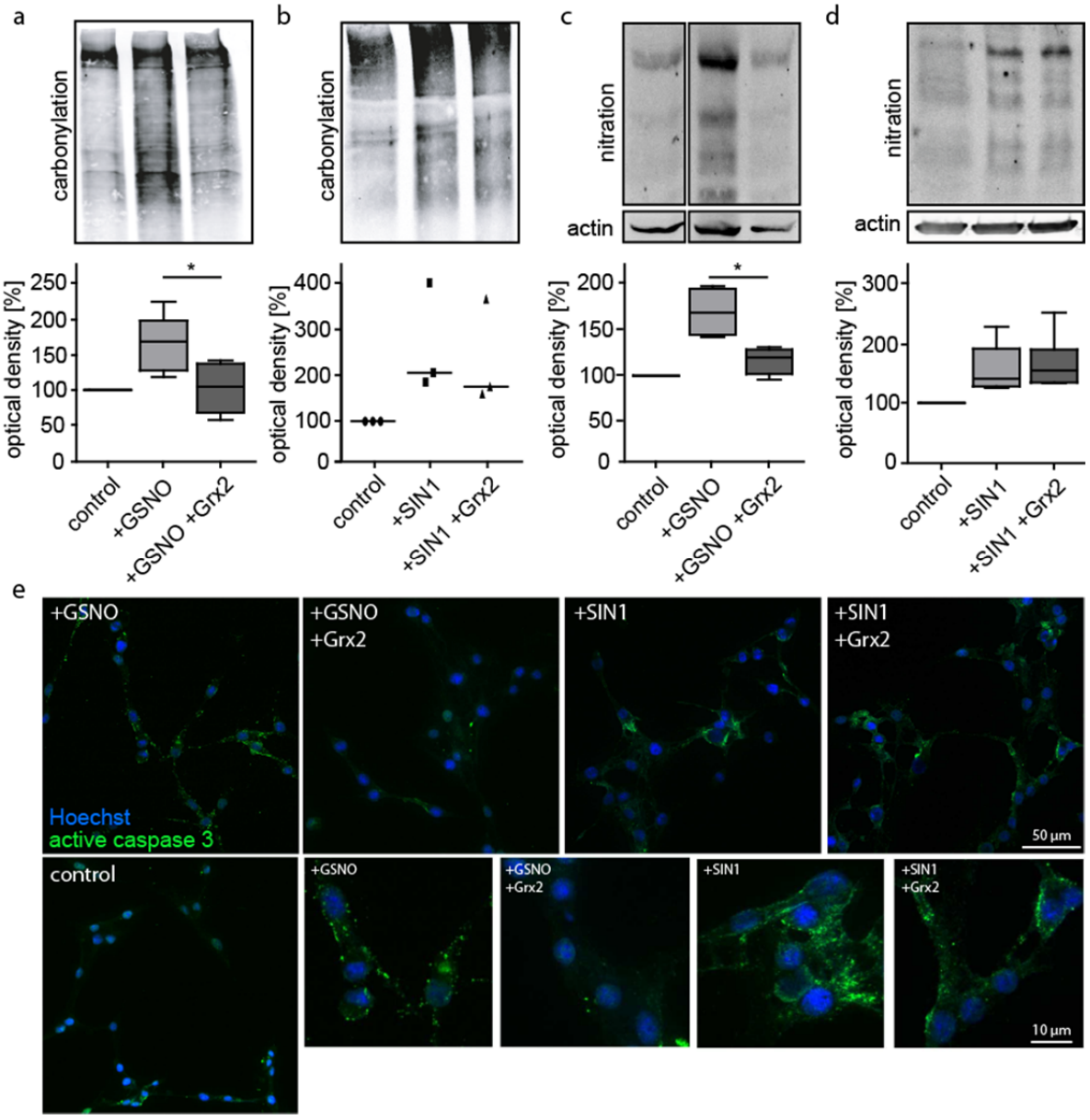

Figure 17. Grx2-dependent detoxification of NO protects against protein nitration and carbonylation via inhibition of peroxynitrite formation and caspase-dependent apoptosis. OLN-93 oligodendrocyte cell line was incubated with 500 µM GSNO or 500 µM SIN1 in presence or absence of 2 µM recombinant Grx2. After 24 h cells were fixed with 4 % PFA (e) or cell lysates were prepared using RIPA buffer (a- d). Cell lysates were examined using Western blot analyses and nitrotyrosine-specific antibody (c- d, normalization to actin, GSNO: n= 4, SIN1: n= 6) or using a protein carbonylation detection assay (a- b, GSNO: n= 5, SIN1: n= 3) to visualize protein bound carbonyl groups. Intensity was calculated using ImageJ. Fixed cells were stained against active caspase3 (green) and nuclei were visualized using Hoechst (blue) (e, scale bars 50 µm and 10 µm). All data points are shown for n≤ 3. Boxplots are shown for n≥ 4; non-parametric Kruskal-Wallis h-test (α≤ 0.05).

52 % compared to GSNO treated cells). Notably, treatment with recombinant Grx2 alone revealed no impact compared to control cells (n= 2; 119 % and 71 %) (Fig. 18 d). Collectively, treatment with Grx2 showed no effect on SIN1-dependent $ONOO^-$ formation, whereas a protective effect was present in cells treated with GSNO (n= 2, 78 % and 92 % compared to cells only treated with SIN1). Since Fluorescein-boronate is known to react also with peroxides, we verified the impact of NO by addition of CPTIO. Indeed, the CPTIO-dependent inhibition of $ONOO^-$ formation in SIN1 treated A_2B_5-positive progenitors indicates a NO-dependent effect (n= 2, 48 % and 40 % compared to SIN1 treated cells) (Fig. 18 d). These observations were confirmed using HeLa cells (n= 3, Fig. 19 c). Of note, experiments with HeLa Grx2c overexpressing cells showed a severe effect after GSNO treatment compared to parental HeLa wt cells treated with recombinant Grx2 underlining the role of intracellular Grx2c (n= 3, Grx2c overexpressing HeLa cells: 27 %, wt HeLa treated with recombinant Grx2: 77 % compared to untreated control cells, Fig. 19 c).

3.3.3 Recombinant Grx2S38P has no protective effect on NO-mediated alterations in OLN-93 cells

To further clarify the impact of the enzymatic activity of Grx2 on the protective role in oligodendrocyte lineage cells, the effects of two Grx2 mutant proteins were analyzed. Neither the enzymatic inactive mutant (Grx2C37S) nor the mutant exhibiting an elevated level of enzymatic function but missing the ability to coordinate FeS clusters (Grx2S38P) showed protective capacities (Fig. 19). Both mutants showed no increase in cell viability of A_2B_5-positive progenitors utilizing the BV2 co-culture model (Fig. 19 b). In line, Grx2S38P lacked the ability to reduce the amount of protein carbonyls in OLN-93 cells (GSNO: 210 %; GSNO and Grx2S38P 240 % and 140 % with the addition of Grx2 wt recombinant protein) (Fig. 19 a). Finally, Grx2S38P was not able to abolish the formation of $ONOO^-$ (Grx2S38P treated HeLa cells: 110 % and Grx2wt: 75 % compared to untreated control cells, Fig. 19 c). However, wild type Grx2 was able to modify all three parameters. These findings suggest the importance of FeS cluster coordination in Grx2-dependent detoxification of NO.

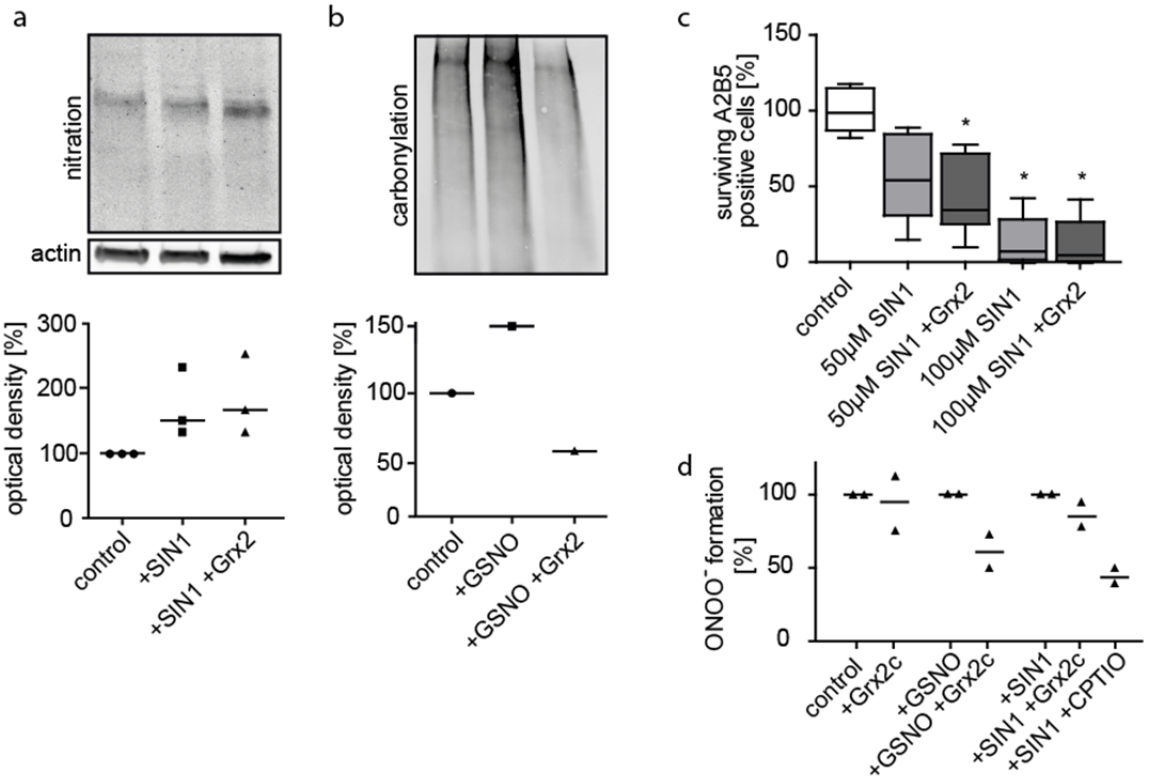

Figure 18. Grx2 does not protect A_2B_5-positive progenitors against peroxynitrite. Primary mouse A_2B_5-positive progenitors were incubated with 250 µM GSNO (b), 50 µM (a+ c) or 100 µM (c) SIN1 in the presence or absence of 2 µM recombinant Grx2. After 24 h, cell survival was determined using CellTiter-Blue® assay (c, n= 13- 18) or cells were lysed using RIPA buffer. Lysates were further analyzed using Western blot analyses and nitrotyrosine-specific antibody (a, n= 3) or using a protein carbonylation detection assay (b, n= 1). Intensity was calculated using ImageJ and normalized to actin. For the measurement of $ONOO^-$ formation, A_2B_5-positive progenitors were incubated with 50 µM Fluorescein-boronate and further incubated with either 1 mM GSNO or 1 mM SIN1 with or without 2 h pre-incubation of 2 µM Grx2 or 50 µM of the NO-scavenger CPTIO. $ONOO^-$ formation was measured in a TECAN plate reader (d, absorbance= 492 nm, emission= 515 nm, n= 2 measured in triplicates). All data points are shown for n≤ 3. Boxplots are shown for n≥ 4; non-parametric Kruskal-Wallis h-test compared to control (α≤ 0.05).

3.3.4 NO donors disassemble the FeS cluster of recombinant Grx2 leading to formation of dinitrosyl-iron-complexes

To further analyze the importance of the FeS cluster, recombinant Grx2 protein was incubated with different concentrations of two distinct NO donors having customized half-life times. The destruction of the Grx2-specific FeS cluster by NO was visualized by absorbance measurement at 428 nm (Fig. 20 a). In detail, NOC5 with a half-life time of 25 min and NOC7 with a half-life time of 5 min revealed a time-dependent degradation of the FeS cluster that was further dependent of the applied concentration. In presence of 5 mM

NOC5 only 93 % of holo Grx2 was detectable and only 87 % of holo Grx2 was detectable in presence of 5 mM NOC7 compared to 98 % without the addition of an NO donor. EPR spectroscopy from OLN-93 cells treated with GSNO in presence and absence of recombinant Grx2 revealed a specific signal at a g value of 2.03. This signal illustrates the formation of DNICs upon NO-mediated FeS destruction in OLN-93 cells (Fig. 20 b- h). For quantification, the double integral of the spectral area was determined. Further, the double integral of OLN-93 cells treated with GSNO and recombinant Grx2 was set to 100 % (Fig 20 b). Here, cells treated either with GSNO alone or recombinant Grx2 alone displayed a decreased EPR signal of 25 % and 32 % (Fig. 20 b, c and e). To underline the responsibility of intracellular located Grx2 two washing steps were included prior to GSNO treatment. However, this intervention showed on change in the EPR signal (Fig. 20 b and g). Finally, we investigated the effect of Grx1, the second mammalian dithiol Grx, on GSNO-dependent DNIC formation. Grx1 displays 34 % homology in its sequence compared to Grx2 but cannot coordinate FeS cluster due to its active site motif (Berndt et al. 2007). EPR measurements revealed an increase in signal quantity compared to GSNO treatment alone (GSNO: 33 %, GSNO + Grx1: 52 %). However compared to Grx2, Grx1 treatment revealed only a signal intensity of 38 % (Fig. 20 b and h).

3.3.5 MRP1 inhibition increases the level of intracellular DNIC in OLN-93 cells

To further address the fate of the intracellular located DNICs we characterized the expression profile of MRP1 in oligodendrocyte lineage cells. MRP1 was described as DNIC exporter in a variety of cell types (Watts et al. 2006; Lok et al. 2012). However, the expression of MRP1 in oligodendrogial lineage cell is controversial (Hirrlinger et al. 2002; Hartz and Bauer 2011). The examination of the protein level and localization as well as mRNA level illustrated the expression of MPR1 using three independent methods in primary A_2B_5-positive mouse cells and oligodendrocyte OLN-93 cell line (Fig. 21). Moreover, an involvement of MRP1 in the export of DNICs in OLN-93 cells was displayed using EPR spectroscopy. The inhibition of MRP1 increased the intracellular level of DNICs slightly to 125 % only in presence of recombinant Grx2 (Fig. 20 b and f). Here, the addition of MK 571, an inhibitor of MRP1, without GSNO treatment revealed no change in GSNO-dependent DNIC formation (GSNO: 33 %, GSNO + MK571: 33 %) (Fig. 20 b and d).

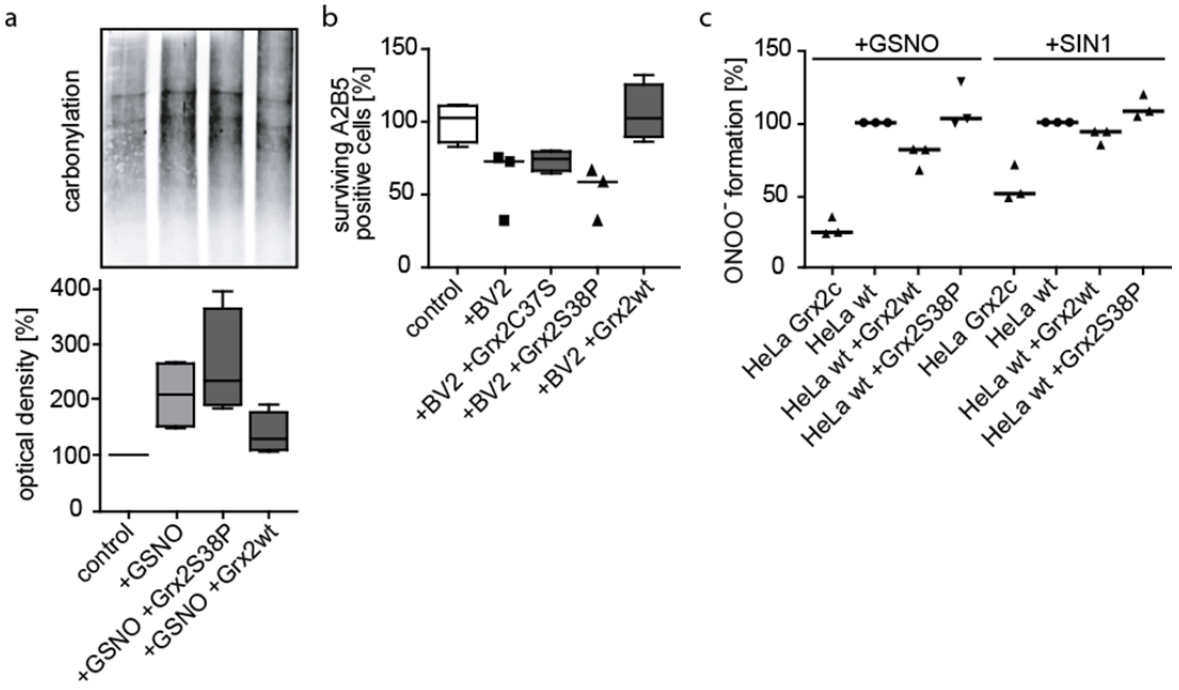

Figure 19. FeS cluster coordination, not enzymatic activity, is required for Grx2-dependent detoxification of NO. OLN-93 cells were incubated with 1 mM GSNO or 1 mM SIN1 in the presence or absence of 2 µM recombinant Grx2 or Grx2S38P (no cluster coordination but enzymatic active) (a). Cells were lysed using RIPA buffer and analyzed for protein bound carbonyl groups. Intensity was calculated using ImageJ (a, n= 4- 9). Primary mouse A_2B_5-positive progenitors were co-cultured (without direct cell contact) with LPS activated BV2 microglial cells (1 µg/ ml LPS, 50.000 BV2 cells) in the presence or absence of 2 µM recombinant Grx2 wild type, Grx2C37S (neither cluster coordination, nor enzymatic activity) or Grx2S38P. After 24 h cell survival rate was measured using CellTiter-Blue® assay (b, n= 6- 8). The amount of $ONOO^-$ was measured using HeLa wt and HeLa Grx2c overexpressing cells (c). HeLa cells were incubated with 50 µM Fluorescein-boronate and further incubated with either 1 mM GSNO or 1 mM SIN1 with or without 2 h pre-incubation of 2 µM Grx2wt or 2 µM Grx2S38P. $ONOO^-$ formation was measured in a TECAN plate reader (c, absorbance= 492 nm, emission= 515 nm; n= 3 measured in triplicates). All data points are shown for n≤ 3. Boxplots are shown for n≥ 4; non-parametric Kruskal-Wallis h-test revealed no significance.

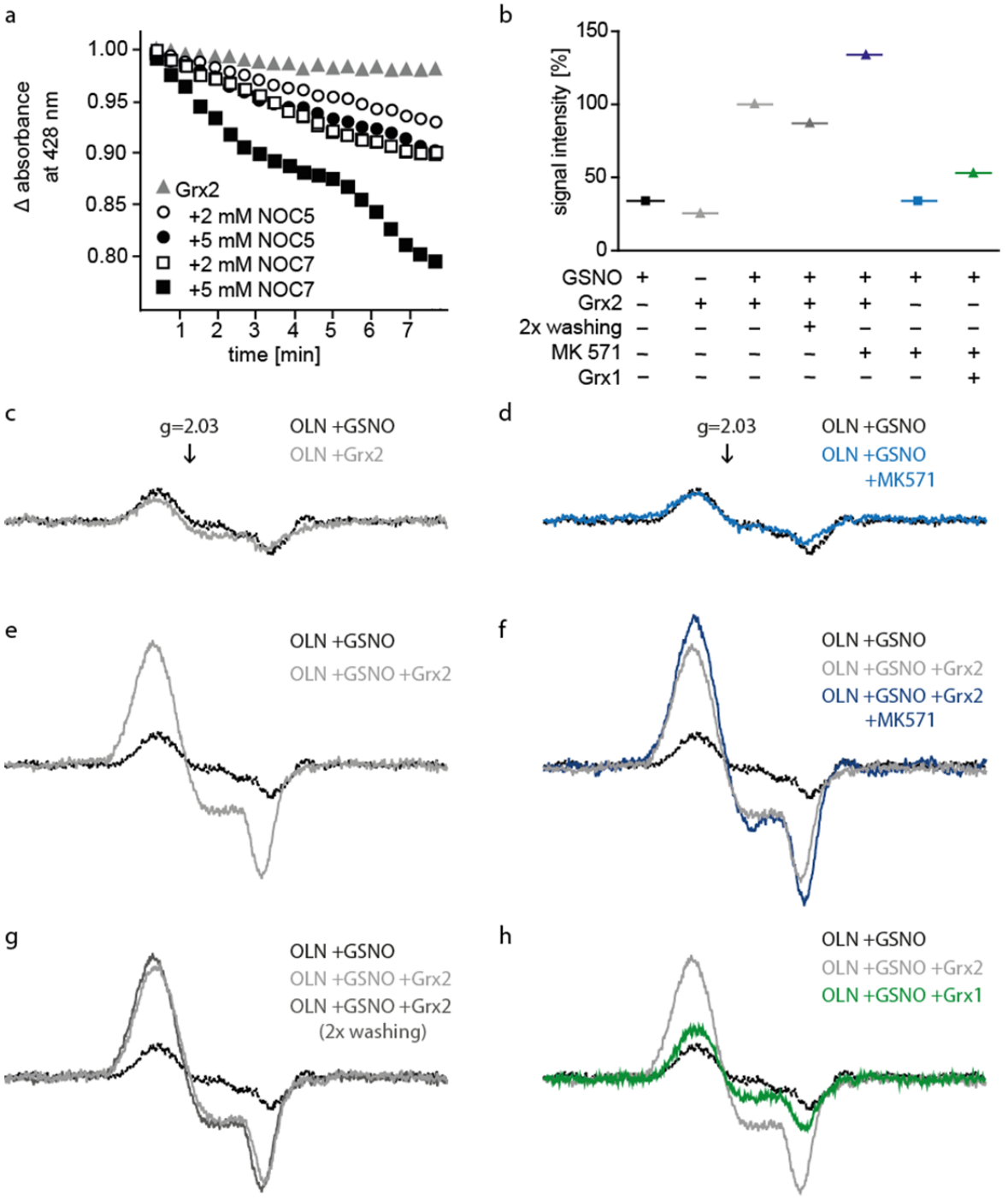

Figure 20. NO disassembles the FeS cluster of Grx2 leading to the formation of dinitrosyl-iron-complexes. 50 µM recombinant mouse Grx2 was incubated with 2 or 5 mM of either NOC5 (t_2= 25 min) or NOC7 (t_2= 5 min). Decrease in absorbance at 428 nm (detecting holo Grx2) was measured over a time period of 7 min using a TECAN plate reader (a). OLN-93 cells (2x 10^7 cells/ condition) were collected and incubated in 1 ml culture medium for 2 h in the presence or absence of 100 µM recombinant mouse Grx1 or 100 µM recombinant Grx2 +/- 20 µM MK572 (an inhibitor for the MRP1 transporter). Cells were further washed twice with PBS and incubated with or without 5 mM GSNO for 3 min. EPR spectroscopy revealed a signal at a g-value of 2.03 that is specific for dinitrosyl-iron-complexes (c- h, 9.64 GHz, 1 mW, 7.5 G modulation, 20 K). Bars represent integrated signal intensity (b).

Taking together, these findings indicate a direct detoxification of NO via the disassembly of Grx2 FeS cluster resulting in intracellular formation of DNICs. Further, MRP1 inhibition showed a slight increase in DNICs levels in presence of Grx2 and GSNO. In line, the expression of MRP1 was demonstrated in primary A_2B_5-positive progenitors and OLN-93 cell line.

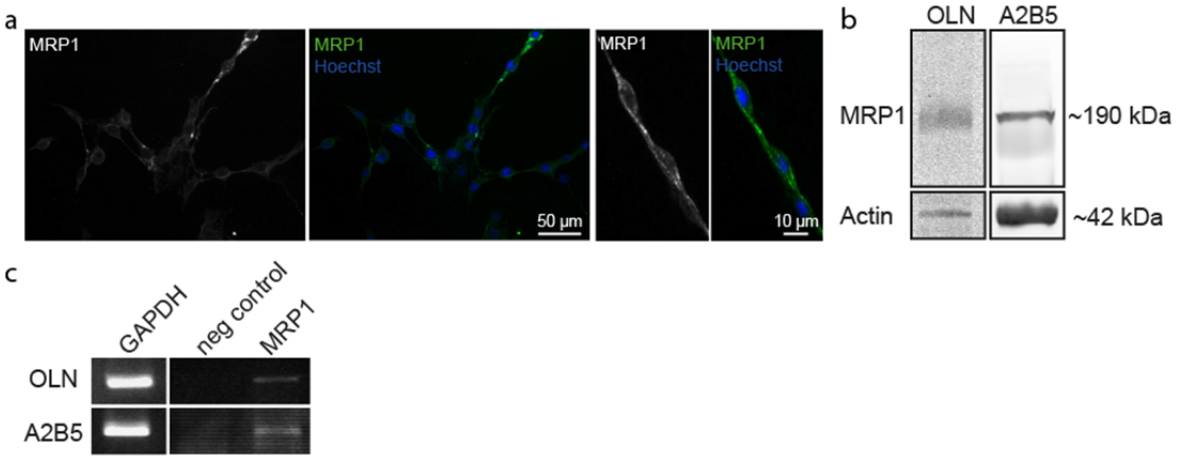

Figure 21. MRP1 transporter is expressed in oligodendrocyte lineage cells. OLN-93 cells were cultured on cover slips and fixed with 4 % PFA. Immunocytochemical analyses against MRP1 transporter (green) and Hoechst (blue) revealed a cellular staining pattern (a, scale bar 50 µm and 10 µm). Western blot analyses of both OLN-93 and primary A_2B_5-positive cell lysates illustrated only one band in the previously reported height of MRP1 (~190 kDa) using an MRP1-specific antibody (b). In line, using PCR analysis, MRP1 mRNA was debatable (c, neg control= no template control).

3.4 Recombinant Grx2 alters the ability for differentiation and migration of oligodendrocyte progenitors in OSCs and primary cell cultures

Previous findings indicated that Grx2 significantly prevented NO-mediated myelin destruction and oligodendrocyte cell death. Thus, we hypothesized a beneficial effect of Grx2 treatment in neuroinflammation-mediated demyelination and remyelination. Concentrating on regenerative processes following demyelination, we further determined the impact of recombinant Grx2 treatment on the myelin repair capacity including

migration and differentiation of OPCs. Notably, redox signaling was previously reported to play a major role in HeLe cell migration (Hurd et al. 2012; Berndt et al. 2014) and neuronal differentiation (Gellert et al. 2015). Its role in oligodendrocyte lineage cells has so far not been investigated.

3.4.1 Recombinant Grx2 treatment affects MBP-positive cell morphology and the number of NG2 expressing cells in an OSC remyelination model

To date, the molecular mechanisms of myelination and remyelination upon MS and EAE disease progression are barley understood (Kremer et al. 2016). Here, we assumed and further examined an involvement of Grx2 in OPC remyelination capacities. Indeed, using an antibody-mediated OSC remyelination model (Harrer et al. 2009), we identified a Grx2-dependent impact on oligodendrocyte differentiation using immunohistochemical analysis against two differentiation markers. MBP was chosen for analysis of mature oligodendrocytes, whereas NG2 staining was chosen to illustrate migrating pre-mature oligodendrocytes possessing the ability to differentiate into myelinating mature oligodendrocytes *in vivo* (Watanabe et al. 2002). Immunohistochemical analysis after 3 days of remyelination following complete demyelination revealed Grx2-dependent alterations in MBP-positive cell morphology (Fig. 22 a and b). Using quantitative fluorescent based remyelination analysis, we could not detect any significant differences between Grx2 treated and untreated fluorescence intensity for the MBP myelin gene. However, using higher magnifications we could distinguish between two cell morphologies: on the one hand, branched MBP-positive cells showing contact to NF-M-positive axons and on the other hand, roundish and hypertrophic MBP positive cells characterized by unramified morphology (Fig. 22 b). Quantification illustrated a significant Grx2-dependent decrease in unramified MBP-positive cells compared to untreated control slices ($p= 0.001$) (Fig. 22 c). Additionally, the treatment with recombinant Grx2 significantly increased the number of NG2 expressing cells per branch ($p= 0.004$) (Fig. 22 e). Here, the morphology of the NG2-expressing cells remained unaffected (Fig. 22 d).

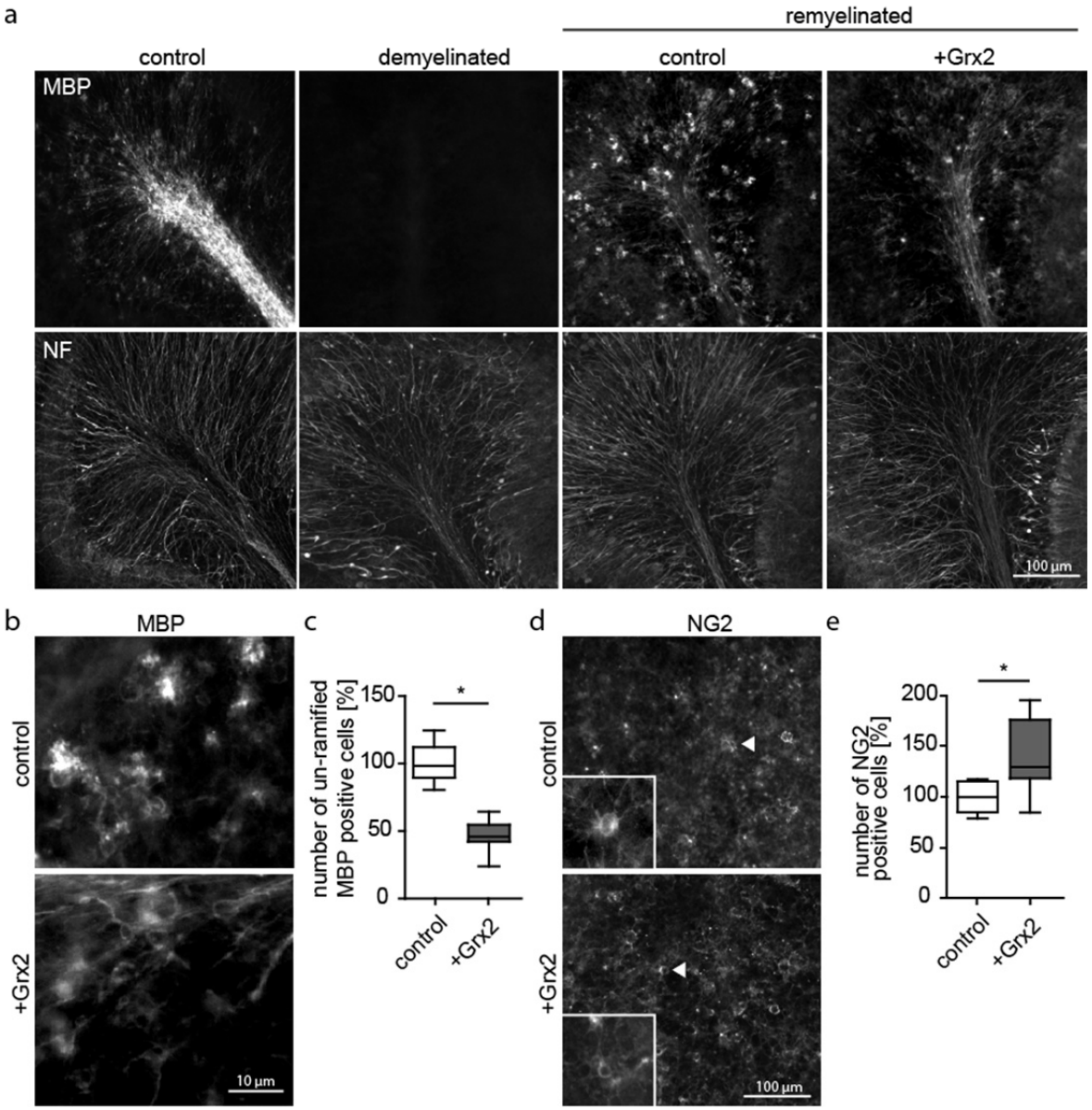

Figure 22. Recombinant Grx2 shows the capacity to increase proper remyelination in OSCs. Cerebellar OSCs were demyelinated for 3 days using MOG-specific hu818C5 antibody (kindly provided by Christine Baksmeier, AG Goebels, Klinik of Neurology, Heinrich-Heine-University Düsseldorf) and 5- 6 % baby-rabbit complement. Thereafter, slices were kept for additional 3 days under normal culture conditions in the presence or absence of 2 µM recombinant Grx2 allowing remyelination. Representative images are shown in a, b and d (arrow heads highlight NG2-positive cells, scale bars 100 µm and 10 µm). Slices were fixed with 4 % PFA and stained against MBP, NF-M and NG2 to visualize remyelination, axons and oligodendrocyte progenitors. Quantification was performed using ImageJ (c and e, n= 10 with two independent experiments). Data are shown in boxplots; non-parametric Mann Whitney u-test ($\alpha \leq 0.05$).

3.4.2 Grx2 is not regulated during the differentiation of primary A_2B_5-positive progenitors

To determine whether the alterations in OSC remyelination are based on an influence of Grx2 on OPC differentiation, a differentiation assay for primary mouse A_2B_5-positive OPCs was established initiated by mitogen withdrawal (see methods part 2.6). The process of differentiation was induced by mitogen withdrawal and monitored by three different readouts: Western blot, q RT-PCR and cytochemical analyses. All three read-outs revealed a feasible documentation of OPC differentiation. The expression levels of three differentiation markers were documented using q RT-PCR and Western blot (Fig. 23 b- i). Furthermore, the cell morphology was documented using bright-field microscopy showing an increase in process formation until day 3 and an increase in branch formation until day 5 (Fig. 23 a). The chosen readouts revealed an increase in differentiation markers (CNPase, MBP and PLP) until day 5 on both protein and mRNA level (Fig. 23 b- d, f- i), whereas NG2 protein expression showed a slight increase on day 1 followed by reduction in protein expression until day 5 (Fig. 23 e). To further investigate whether the expression level of Grx2 is altered during OPC differentiation, Grx2 protein level was measured using Western blot analysis and Grx2 mRNA level was measured by q RT-PCR (Fig. 23 b, h and i). Quantification revealed no significant regulation of Grx2 protein expression as well as Grx2 mRNA expression during OPC differentiation. Notably, Grx2 demonstrated a high endogenous level in differentiated as well as undifferentiated OPCs compared to OSC cultures (Fig. 12 d and Fig. 15 b).

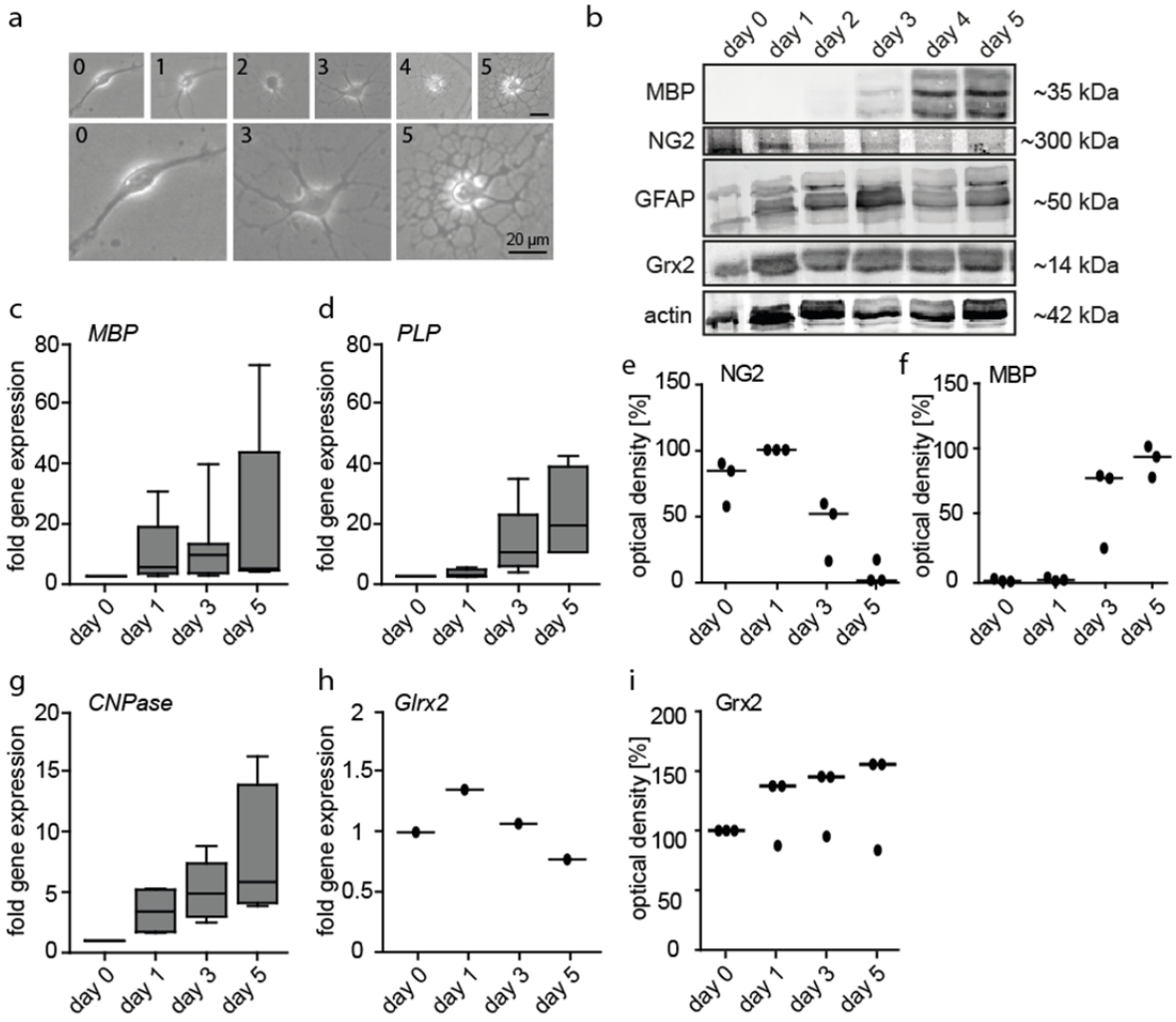

Figure 23. Identification of oligodendrocyte differentiation stages in primary mouse A_2B_5-positive progenitors. Primary mouse A_2B_5-positive progenitors were differentiated by addition of thyroid hormones (T3/T4) and retinoic acid as well as the removal of proliferation factors FGF and PDGFα. Differentiation was monitored morphologically using bright-field microscopy (a, day 0- day 5, scale bar 20 µm), on protein level using Western blot analysis (e, f and i: n= 3) and on mRNA level using q RT-PCR (c, d and g: n= 4- 5 and h: n= 1). At indicated time points A_2B_5-positive progenitors were either lysed using RIPA buffer or mRNA was isolated by phenol-chloroform extraction. Quantification of GFAP illustrates the presence of astrocytes. The stages of differentiation are illustrated by quantification of NG2 (progenitors), CNPase (pre-mature oligodendrocytes) and MBP as well as PLP (mature oligodendrocytes). All data points are shown for n≤ 3. Boxplots are shown for n≥ 4; non-parametric Kruskal-Wallis h-test revealed no significance.

3.4.3 Differentiation capacity of primary A_2B_5-positive progenitors is altered by recombinant Grx2

Although, there was no regulation of Grx2 expression level during OPC differentiation the treatment with recombinant Grx2 affected remyelination in OSC cultures. To further clarify

the influence of Grx2 on OPC differentiation, recombinant protein was externally added during the differentiation assay using primary mouse A_2B_5-positive progenitors. Examination of the three mentioned readouts (immunocytochemistry, q RT-PCR and Western blot) revealed a Grx2-dependent inhibition of differentiation. Quantification of the immunocytochemical analysis after 5 days of differentiation for NG2 (migrating progenitor), CNPase (pre-mature oligodendrocyte) and MBP (mature oligodendrocyte) expressing cells further demonstrated a Grx2-dependent increase in NG2-positive cells ($p= 0.012$). In line, the amount of CNPase- and MBP-positive cells decreased (CNPase: $p= 0.057$; MBP: $p= 0.057$) (Fig. 24 a and b). These results were verified by Western blot analysis. Here, protein levels for NG2 and MBP were likewise regulated by treatment with recombinant Grx2 (Fig. 24 d and e). NG2 protein level was reproducibly upregulated and MBP protein level was reproducibly downregulated compared to untreated control cells. In line, mRNA levels of same differentiation markers were downregulated after recombinant Grx2 treatment (Fig. 24 c). We further distinguished between two different applications for Grx2: (1) Differentiation medium was supplemented with Grx2 only on day 1 and (2) Differentiation medium was supplemented with Grx2 every day. Both treatments induced a reproducible decrease on mRNA level for CNPase, MBP and PLP as markers for mature oligodenddrocytes. However, the persistent presence of Grx2 during differentiation slightly enhanced the inhibitory effect on differentiation of A_2B_5-positive progenitors (Fig. 24 c). Notably, A_2B_5 expressing progenitors are able to differentiate to GFAP-positive astrocytes *in vitro*. To exclude a possible impact on cell fate decision towards astrocytes, Western blot analysis was additionally performed for GFAP (Fig. 24 d and e). The quantification illustrates rather a decrease than an increase of GFAP protein level after recombinant Grx2 treatment (Fig. 24 e).

Taking together, these findings illustrate that recombinant Grx2 blocks differentiation of A_2B_5-positive progenitors in a NG2-positive state *in vitro*.

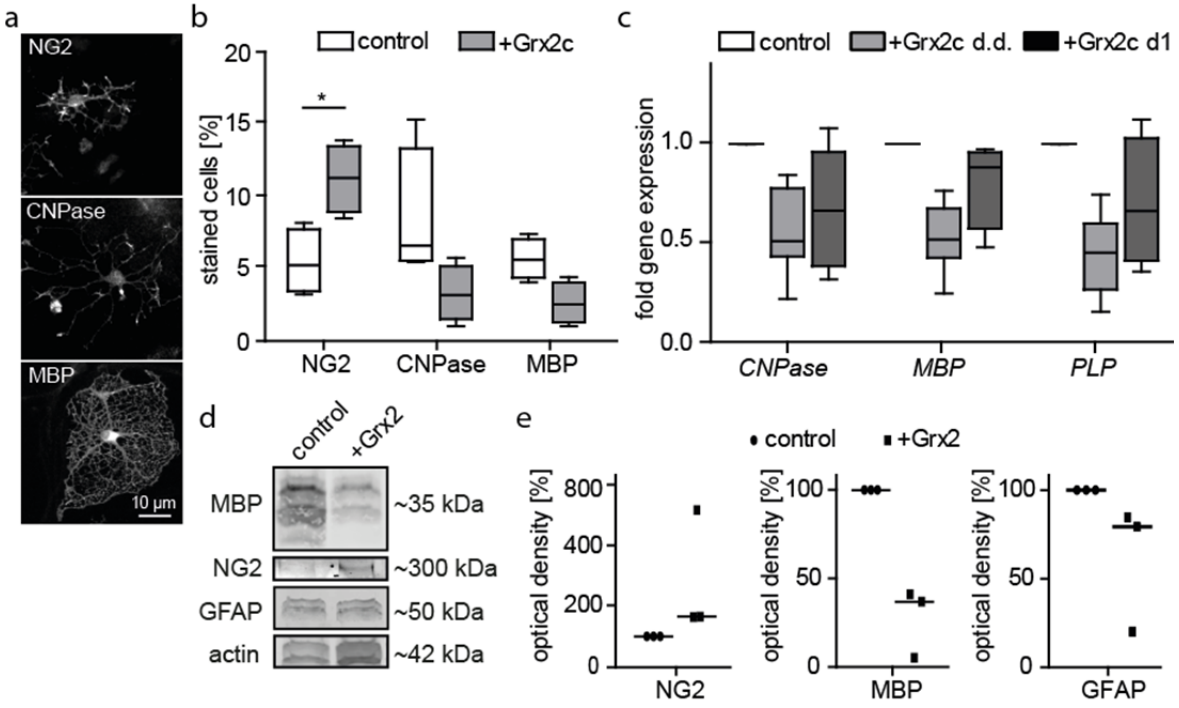

Figure 24. Recombinant Grx2 blocks the differentiation of A_2B_5-positive progenitors. Primary mouse A_2B_5-positive progenitors were differentiated by the addition of thyroid hormones (T3/T4) and retinoic acid and the removal of proliferation factor FGF. Immunocytochemical analysis was performed after 5 days of differentiation. Cells were stained against NG2 (progenitor marker), CNPase (pre-mature oligodendrocyte) and MBP (mature oligodendrocyte). Representative images are shown in a and quantification in b (n= 4). Furthermore, cells were either lysed using RIPA buffer to detect protein levels for MBP, NG2 and GFAP by Western blot analysis (d and e; n= 3) or mRNA was isolated by phenol-chloroform extraction and CNPase, MBP and PLP transcripts were quantified by q RT-PCR (c, d.d.= during differentiation, n= 8; d1= Grx2 supplementation only once at differentiation initiation, n= 4- 9). All data points are shown for n≤ 3. Boxplots are shown for n≥ 4; non-parametric Kruskal-Wallis h-test or Mann Whitney u-test (α≤ 0.05).

3.4.4 Possible molecular mechanism of Grx2-dependent oligodendrocyte differentiation block

One identified substrate of Grx2 is the histone deacetylase Sirt1 that was previously shown to be involved in redox-dependent cell fate decision of neural progenitors (Prozorovski et al. 2008). Furthermore, our group characterized a Grx2-dependent S-glutathionylation of Sirt1 (Bräutigam et al. 2013). Therefore, we investigated whether the Grx2-dependent redox modification of Sirt1 influences the differentiation of A_2B_5-positive oligodendrocyte progenitors. Previously performed Sirt1 activity measurements indicated a concentration-dependent correlation between recombinant Grx2 and Sirt1 activity (Bräutigam et al. 2013). To examine the role of this redox-dependent enzyme in the differentiation of primary mouse A_2B_5-positive progenitors, mRNA analysis was performed

after 3 days of differentiation in presence and absence of recombinant Grx2 or the Sirt1 inhibitor EX257. We examined three different markers for mature oligodendrocytes (CNPase, MBP, PLP) on mRNA level. Here, MBP and CNPase mRNA was non-significantly downregulated in presence of EX257, whereas, as described before, the treatment with recombinant Grx2 decreased all three observed differentiation markers (CNPase: p= 0.014; MBP: p= 0.09; PLP: p= 0.019) (Fig. 25, n= 4- 6). Co-treatment with Grx2 and EX257 did not further increase the effect of Grx2 alone compared to control (CNPase: p= 0.045; MBP: p= 0.0018; PLP: p= 0.063).

Taken together, treatment with EX257 likewise decreased the differentiation of A_2B_5-positive progenitors towards mature oligodendrocytes.

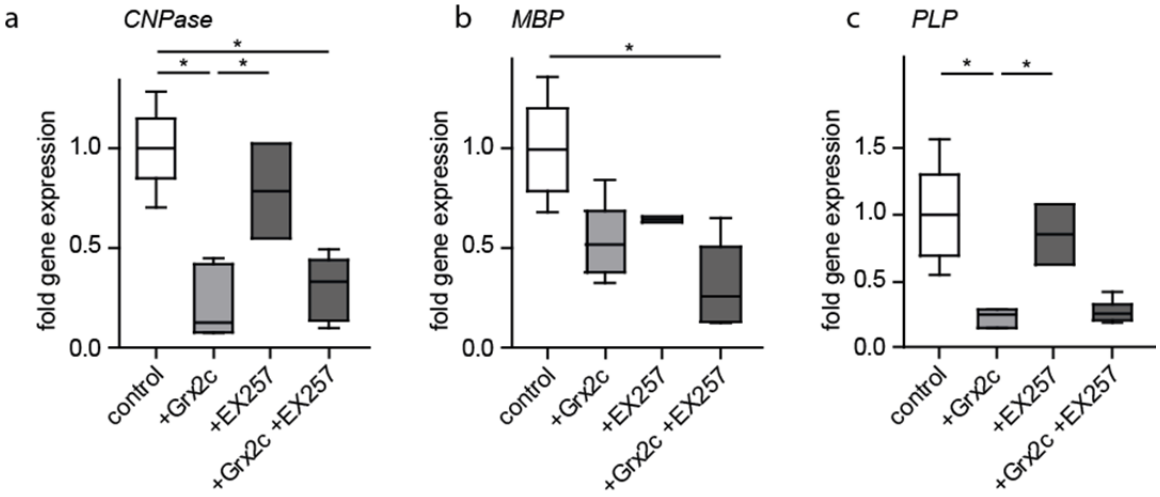

Figure 25. Sirt1 alters A_2B_5 cell differentiation. mRNA analysis after 3 days of differentiation revealed a downregulation of CNPase, MBP and PLP in presence of recombinant Grx2 and the Sirt1 inhibitor EX257. Of note, in presence of EX257 alone no significant effect was measured for the mRNA level of the observed differentiation markers (a, b and c: n= 4- 6). Datasets are illustrated as boxplots; non-parametric Kruskal-Wallis h-test (α≤ 0.05).

3.4.5 Recombinant Grx2 influences the migration capacity of primary A_2B_5-positive progenitors

The observation of Grx2-dependent alterations in OSC remyelination could also be explained by a promotion in cell migration. Therefore, the migration capacity of primary mouse A_2B_5-positive progenitors was examined using a transmigration assay. Notably, repulsive compounds like extracellular matrix components or semaphorins are known to

be accumulated in MS (Costa et al. 2015). Furthermore, semaphorin3a was demonstrated to contribute to remyelination failure (Syed et al. 2011). The treatment of 1 mg/ ml semaphorin3a reduced the ability of A_2B_5-positive progenitors reproducibly to approximately 70 % compared to untreated cells (Fig. 26). Further, supplementation of recombinant Grx2 in absence or presence of semaphorin3a increased the transmigration capacity significantly (p= 0.045 and p= 0.0034).

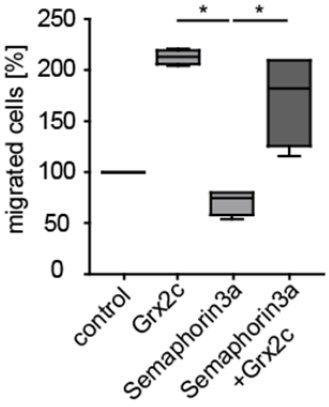

Figure 26. A_2B_5 cell migration capacity is increased by recombinant Grx2 treatment. Primary mouse A_2B_5-positive progenitors were plated on filters with a pore size of 8 µm in presence or absence of 2 µM recombinant Grx2 with or without 1 mg/ ml Semaphorin3a (oligodendrocyte chemotactic retraction) in the lower culture chamber (n= 4- 5). Datasets are illustrated as boxplots; non-parametric Kruskal-Wallis h-test (α≤ 0.05).

Summarizing, the observed effect of recombinant Grx2 on antibody-induced remyelination in OSCs is characterized by a decrease in the amount of mature oligodendrocytes with a hypertrophic un-ramified morphology (3.4.1). These observations could be explained by a Grx2-dependent differentiation block of primary A_2B_5-positive progenitors in the NG2-positive migratory differentiation state. Furthermore, treatment with recombinant Grx2 increased the migration capacity of A_2B_5-positive progenitors along with the ability to overcome the repelling effect of semaphorin3a.

4. Discussion

The aim of the present study was to gain insights into the role of FeS-coordinating Grxs in the process of neuroinflammatory demyelination and their influence on properties of oligodendrocyte progenitors, which are important for remyelination. Therefore, the expression pattern of Grxs 2, 3 and 5 upon neuroinflammation as well as the impact of Grx2 on oligodendrocyte lineage cell survival, differentiation and migration was investigated using neuroinflammatory mouse *in vivo* and *in vitro* models as well as in human MS samples.

4.1 Grxs in neuroinflammatory degeneration and regeneration

Histologically, MS as well as EAE are characterized by focal demyelinated brain lesions associated with neuroinflammation, including the infiltration of peripheral immune cells and activated microglia and astrocytes. These areas can be grossly distinguished into inflammatory active acute and inflammatory inactive chronic lesion areas. Disturbed oxidative events, like the increase in reactive species production, contribute to MS lesion formation and lesion maintenance (van Horssen et al. 2011). The Trx family of proteins is highly involved in oxidative defense as well as redox-dependent signaling (Hanschmann et al. 2013). However, there is only one descriptive study in human MS indicating an increase in immunoreactivity of members of the Trx family of proteins, namely Prx3 and Trx2, in acute lesion areas (Nijland et al. 2014). The present thesis identified a beneficial effect of recombinant Grx2 treatment on OPC survival and myelin integrity upon NO challenge. Furthermore, I observed an impact on the regeneration capacity of oligodendrocyte progenitors *in vitro* and in OSCs. Investigating the participating cell types, we observed a Grx2-dependent block of oligodendrocyte differentiation, increased oligodendrocyte progenitor migration as well as increased Grx2 expression in phagocytes and reactive astrocytes.

4.1.1 Microglia and astrocytes

Activated microglia and astrocytes are present in all neuroinflammatory CNS pathologies including MS and contribute to the progress of de- and regeneration. Our findings reveal a so far unknown regulation of Grxs 2, 3 and 5 in MS lesion progression with predominant

levels in activated astrocytes and phagocytes located in acute lesion areas (Fig. 6). Further immunohistological studies of our group confirmed a co-localization of Grx2 with the microglia/macrophage marker Iba1, classical neuroinflammatory phagocytes, in active lesions of EAE mice (Conforti 2014). In chronic MS lesions the histological analyses further revealed a decreased staining pattern of all observed Grxs (Fig. 6). Notably, chronic lesion areas show extensive astrogliosis with increased neuronal and oligodendrocyte cell death (Zipp and Aktas 2006). As the staining patterns for all observed markers were decreased in these areas, the extensive cell loss could result in an overall decreased immunoreactivity. Therefore, the downregulation of Grx2 in the chronic stage as well as the upregulation in the inflammatory active acute stage was further verified in EAE brain tissue by Western blot and q-RT PCR analysis (Fig. 8). The increased expression of Grx2 in inflammatory active lesions is in line with a study reporting the upregulation of Grx2 only in the acute phase of the MTPT-induced animal model for the neuroinflammatory and neurodegenerative Parkinson's disease (Karunakaran et al. 2007). Similar to the inflammatory reaction in Parkinson's disease, acute MS lesion areas are characterized by a strong neuroinflammatory reaction comprised of microglia activation (Hemmer et al. 2002a). Upon inflammatory-mediated activation, both cell types, astrocytes and microglia, were reported to upregulate proteins important for the cellular oxidative defense including members of the Trx family of proteins like Trxs 1 and 2 as well as Prxs (Wang et al. 2007; Nijland et al. 2014; Wang et al. 2016). Recent findings illustrating a higher resistance against ROS/RNS displayed by a delayed cell death of astrocytes and microglia compared to oligodendrocyte lineage cells and neurons support the results of Wang et al. (Oshiro et al. 2000). In line, upon ischemia in mouse hippocampus, areas of increased survival rates correlated with increased expression of Prx3 and Trx2, while in comparison Prx3 and Trx2 non-expressing areas showed high neural cell death (Hwang et al. 2010). Grxs 3 and 5 catalyze the monothiol reaction mechanism possibly contributing to antioxidant defense as monothiol Grxs regulate stress resistance in yeast (Rodríguez-Manzaneque et al. 1999). In detail, Grx3 was shown to deglutathionylate Sir2, the yeast homologue of Sirt1, and thereby increases stress resistance (Vall-Llaura et al. 2016). Furthermore, Nrf2, a transcriptional activator of the cellular redox defense mechanism, contributes to the ability of astrocytes to increase neuronal survival (Jimenez-Blasco et al. 2015). Taking these findings into account, the increased expression of Grxs 2, 3 and 5 in activated astrocytes and microglia could be part of the previously reported upregulated cellular defense against increased amounts of reactive species in neuroinflammatory lesion areas. Therefore, Grxs in activated astrocytes could either act via ROS/RNS detoxification (see 4.1) or modification of specific

redox events. I suggest to further address the impact of specific redox-dependent protein modifications during Grx upregulation in EAE or MS in the future.

Notably, the activation of both astrocytes and microglia ambivalently contributes to lesion progression. The expression of Grx2 in reactive astrocytes present in acute but not in chronic lesion areas underlines the possibility of a redox-dependent regulation in the manifestation of an activated astroglial phenotype. Research on microglial activation revealed specific factors regulating the activation towards either the M1 (IFNγ, TNFα) or the M2 (IL-4, IL-13) phenotype. For astrocytes, possible trigger molecules are yet unknown. Depending on the microglial M1 or M2 activation stage, the cells can promote regeneration through debris clearance and secretion of anti-inflammatory cytokines or they can contribute to tissue degeneration by secretion of pro-inflammatory molecules and ROS/RNS. A recent study stresses the involvement of redox regulated components in the production of NO by activated microglia. In detail, the activity of endothelial NOS (eNOS) was found to be inhibited by S-glutathionylation which was reversed by Grx1 in mice (Chen et al. 2013; Shang et al. 2016). A possible regulatory mechanism based on S-glutathionylation is not reported for microglial iNOS yet. Our experiments using LPS activated BV2 cells (microglial mouse cell line) show no effect of recombinant Grx2 treatment (Fig. 16). However, further experiments need to investigate a possible influence of Grx1. Unlike Grx2, Grx1 is deactivated by addition of GSNO (Hashemy et al. 2007), indicating a controversial regulation of the two mammalian dithiol Grxs upon neuroinflammation. During EAE, the expression of Grx2 is decreased in the chronic stage of the disease, whereas the Grx1 expression is increased (Lepka et al., submitted). Research by Miller et al. indicate a Grx1-dependent activation of microglia leading to increased neurodegeneration (Miller et al. 2016), which would correspond to the microglial M1 proinflammatory phenotype. However, Miller et al. did not consider the M2 phenotype at all and thus, further experiments have to clarify the role of Grxs 1 and 2 in microglia activation with a defined distinction between M1 and M2 manifestation.

Our data underline a redox-dependent component in the mechanism of astrocyte and microglia activation. However, based on our data and the present literature, further investigations need to evaluate whether the upregulation of redoxins is indeed a regulator/ prerequisite for glial activation and activation state decision or only a consequence causing higher resistance to pathological ROS/RNS concentrations.

4.1.2 Oligodendrocyte lineage cell survival

It is evident that next to inflammatory stimuli, such as INFγ and TNFα (Horwitz et al. 1997; Owens et al. 2001), the generation of NO and $ONNO^-$ contributes to demyelination promoting MS pathology in a multitude of ways. For instance, NO induces oligodendrocyte cell death and inhibits remyelination (Kremer et al. 2011; Miron et al. 2011; Miron et al. 2013). In line, oligodendrocyte cell death occurs in MS lesions (Ozawa et al. 1994) accompanied by increased expression of iNOS and increased generation of NO, detected in chronic active MS lesions and the cerebrospinal fluid of MS patients (Bö et al. 1994; DeGroot et al. 1997; Hill et al. 2004). Using the EAE mouse model of MS, we and others were able to confirm the involvement of NO in EAE pathology by immunohistochemical analysis of nitrotyrosine protein modifications inside cerebellar brain lesions (Fig. 11) (Ljubisavljevic et al. 2012). A recent publication further supports the contribution of NO to demyelination (Desai et al. 2016): Here, LPS injection into the CNS white matter of mice led to microglial activation and increased expression of iNOS in early disease phase resulting in demyelinated lesion areas (Desai et al. 2016). To investigate the impact of Grx2 on previously reported microglia-mediated oligodendrocyte damage (Pang et al. 2010), I performed viability assays co-culturing LPS activated microglial BV2 cells and primary mouse cultures of OPCs. Furthermore, to address the impact of Grx2 on demyelination, I established a GSNO- as well as LPS-mediated demyelination model in cerebellar OSCs. I could confirmed the major impact of NO in LPS-/GSNO-mediated OPC toxicity since CPTIO, a NO scavenger, was able to prevent OSC demyelination and GSNO induced cell death of primary mouse A_2B_5-positive progenitors in a concentration-dependent manner. Notably, unlike in humans, in mice only microglia express the LPS-specific toll-like receptor 4 and thus, a direct effect of LPS on oligodendrocytes can be excluded (Bsibsi et al. 2002). The effect of LPS and increased levels of NO on neuronal cell viability is controversial. Studies in hippocampal OSCs underlined a NMDA-mediated neuronal cytotoxicity upon NO treatment, whereas others stressed a high resistance of neurons to NO treatment (Dawson et al. 1991; Keynes et al. 2004). In our OSC model, neither LPS nor GSNO treatment led to neuronal destruction and morphological changes, assessed by histological analysis using the neuronal marker NF-M (Fig. 13). Changes on molecular level in neurons were not investigated and require further analysis. However, the NO-mediated changes on myelin integrity in OSCs challenged with GSNO as well as LPS were profound. These results confirm the vulnerability of oligodendrocytes and their progenitors to NO and $ONOO^-$ previously reported *in vitro* and *in vivo* (Li et al. 2005; Jack et al. 2007; Pacher et al. 2007) and stress a beneficial effect of recombinant Grx2 against NO-mediated oligodendrocyte toxicity. The mechanism is based on the detoxification of

NO preventing nitrosative cell damage. However, NO-mediated alterations in oligodendrocyte iron homeostasis are also possible.

Oligodendrocytes are more robustly stained for iron than any other cell type of the CNS (Benkovic and Connor 1993). One reason could be that myelin maintenance requires high amounts of iron as essential cofactor in its synthesis (Connor and Menzies 1996). However, free iron is detrimental for brain function stressing the importance of functional iron homeostasis including chelation and storage in physiological and pathophysiological processes. Under neuroinflammatory conditions, NO can mobilize iron from its ferritin-bound storage and increase ROS generation and cytotoxicity through the Fenton reaction (Reif and Simmons 1990). The contribution of iron to neuroinflammatory progression is further stressed by the beneficial effect of deferiprone, an iron-chelator, on EAE progression (Mitchell et al. 2007). Although iron accumulations increase in the brain upon aging, additionally increased iron deposits were reported for numerous chronic diseases of the CNS, including Parkinson's disease, Alzheimer's disease and MS (Stankiewicz et al. 2007; Rouault 2013). Due to the delay between the onset of MS, MS symptoms manifestation and the diagnosis, the contribution of dysregulated iron homeostasis in MS initiation and early MS stages is unknown. Similar to other studies, we could not observe massive iron depositions in mice suffering from EAE, neither in the acute, nor in the chronic EAE disease stage (Fig. 9 f) (Schuh et al. 2014). However, this does not exclude the involvement of subtle alterations in iron homeostasis. Our findings demonstrate a significant breakdown of the activity of iron-dependent enzymes upon EAE disease progression (Fig. 9). However, the reason for the decrease in enzymatic activity needs to be further analyzed. Global metabolic failure is rather unlikely, as the activity of MDH, an iron-independent key enzyme in the citric acid cycle, was not affected at all. A specific effect on FeS cluster biosynthesis is also not supported by our data as GPAT, a protein that is rapidly degraded upon disassembly of its FeS cluster (Grandoni et al. 1989; Martelli et al. 2007), showed no regulation on protein level. Furthermore, whether or not the IRP system is affected remains elusive. The breakdown of ACO activity most likely results in the disassembly of its FeS cluster resulting in IRP1 protein. However, IRP1 regulated proteins showed no significant changes on protein level. Notably, we performed our analyses in total cerebellar EAE mouse lysates. As mentioned before, oligodendrocytes are robustly stained for iron (Benkovic and Connor 1993). Therefore, we hypothesized that the observed changes in enzyme activity and protein expression occur most likely in oligodendrocytes. We further estimated the presence of unaffected cell types in the lysate to obscure the specific effect on oligodendrocytes. This hypothesis is supported by our *in vitro* experiments. Immunocytochemical analysis revealed a shift in cellular TfR

localization in OLN-93 cells upon GSNO treatment which is characteristic for iron starvation conditions (Haunhorst et al. 2013). Treatment with recombinant Grx2 repealed this effect (Fig. 10). In line, the analysis of two different mouse MS models previously revealed a significant upregulation of TfR but not IRP1 and 2 (Sands et al. 2015). Our Western blot analyses demonstrated on regulation of TfR in OLN-93 cells treated with NO. Furthermore, the TfR was likewise not regulated upon EAE on protein level (Fig. 9). Although the determination of TfR expression in EAE mice showed no significant alterations, we hypothesize that the major effect of neuroinflammation-mediated alterations of TfR expression is on oligodendrocytes and are, as mentioned before, obscured by the usage of total cerebellar lysates. The observed downregulation of Grx3 in the acute phase of EAE further underlines alterations in iron trafficking (Haunhorst et al. 2013) and points towards the dysregulation of iron uptake and transport upon neuroinflammation. In a cell model of Parkinson's disease an interaction between mitochondrial Grx2a, free iron and FeS cluster biosynthesis was already hypothesized (Lee et al. 2009). Although our findings point towards a contribution of Grx2 as modulator for NO-mediated alterations in oligodendrocyte-dependent iron homeostasis, we hypothesise the protective effect to be based on a Grx2-specific detoxification of NO rather than on an involvement of Grx2 in iron homeostasis.

Taken together, Grx2 decreases NO-mediated oligodendrocyte cell death and myelin disturbance by either the inhibition of cytotoxic $ONOO^-$ generation or the prevention of NO-mediated alterations in iron homeostasis. For both mechanisms, the detoxification of NO is a prerequisite.

4.1.2.1 Grx2-dependent detoxification of NO

Peroxynitrite is a highly potent oxidant that interacts with DNA, lipids and proteins. Upon neuroinflammation, increased levels of $ONOO^-$ result in extensive nitration of protein tyrosine residues and mitochondrial dysfunction leading to induction of cell death in oligodendrocytes and neurons (Li et al. 2005; Mander and Brown 2005). Peroxynitrite is formed by the reaction of NO and $O_2^{\bullet-}$. Vice versa, the prevention of either NO or $O_2^{\bullet-}$ formation inhibits $ONOO^-$ generation and cytotoxicity (Mander and Brown 2005). Our findings demonstrate a so far unknown Grx2-dependent mechanism for detoxification of NO. The mechanism depends on the ability of Grx2 to coordinate an FeS cluster. My experiments showed that the NO-mediated disassembly of the FeS cluster results in the inhibition of $ONOO^-$ formation and prevention of $ONOO^-$-mediated cytotoxicity. In this regard we showed that the physiological NO donor GSNO leads to protein nitration as well

as protein carbonylation in oligodendrocytes subsequently inducing cell death. This was demonstrated in primary mouse A_2B_5-positive progenitors and OLN-93 cells. Here, recombinant Grx2 affected both GSNO-mediated protein damage and cell viability of cultures treated with GSNO. In contrast, we did not observe any effects of recombinant Grx2 in cultures treated with the $ONOO^-$ donor SIN1. These findings suggest that the protective effect of Grx2 takes place before formation of $ONOO^-$.

Next, we verified the importance of FeS cluster disassembly for the Grx2-dependent detoxification of NO. Like Grxs 3 and 5, Grx2 is able to coordinate FeS clusters. Intriguingly, due to the coordination of the cluster via their N-terminal active site cysteine (Berndt et al. 2007), Grxs are the only FeS cluster proteins that are enzymatically inactive in their holo-form. The FeS cluster of Grxs 3 and 5 is well-known to function in iron homeostasis of both eukaryotes as well as prokaryotes. In particular, Grx3 participates in iron trafficking (Haunhorst et al. 2013) and Grx5 is involved in the FeS cluster biosynthesis (Rodríguez-Manzaneque et al. 2002; Mühlenhoff et al. 2003; Wingert et al. 2005). First evidence by Lee et al. in 2009 indicated an involvement of Grx2 in mitochondrial FeS cluster biosynthesis. Here, silencing of mitochondrial Grx2a was associated with changes in FeS cluster biosynthesis in yeast and mammalian dopaminergic cells (Lee et al. 2009; McDonagh et al. 2011). However, whether the FeS cluster or the enzymatic activity of Grx2a led to the observed alterations in iron homeostasis was not investigated. Until now, only a single further function of the FeS cluster of Grx2 is hypothesized: as redox sensor allowing Grx2 to switch between its enzymatically active apo-form (protein lacking its cofactor) and enzymatically inactive holo-form (protein conjugated with cofactor) (Lillig et al. 2005; Berndt et al. 2007). This function is based on experiments in cell-free systems and has not been studied in cell cultures yet. Our findings indicate an additional function of the Grx2-coordinated FeS cluster that was verified in both cell-free systems and *in vitro* cultures. NO was previously reported to react with metal centers including FeS clusters (Foster and Cowan 1999). In our experimental setup, the treatment with the NO donors NOC5 and NOC7 led to the disassembly of the FeS cluster coordinated by Grx2 in a concentration- and time-dependent manner, indicating the NO-dependent decrease in Grx2 FeS cluster stability. We confirmed the importance of FeS cluster disassembly for the detoxification of NO using the Grx2 mutant Grx2S38P. In this mutant, the active site motif was exchanged to that of Grx1 (Johansson et al. 2004) retaining its enzymatic activity while lacking the ability to coordinate FeS clusters (Berndt et al. 2007). Here, the Grx2S38P mutant showed no protective role against GSNO-mediated protein nitration and cytotoxicity in oligodendrocytes. Due to the Grx-specific cluster coordination that involves two non-covalently bound GSH molecules as non-protein ligands (Berndt et al. 2007), we

propose the NO-mediated disassembly to result in two apo Grxs (I) (Hashemy et al. 2007; Johansson et al. 2007), the formation of dinitrosyl-diglutathionyl-iron-complexes (DNGICs) (II) and most likely H_2S (III) (Fitzpatrick and Kim 2015) (Fig. 27). In the following paragraphs, all mentioned reaction products are discussed in detail.

(I) The cytotoxic effect of $ONOO^-$ is partly mediated via cytochrome c-/caspase 3-dependent apoptosis (Shacka et al. 2006). We confirmed that GSNO treatment leads to apoptotic events in oligodendrocytes. Furthermore, our immunocytochemical analysis of OLN-93 cells revealed a GSNO-mediated accumulation of active caspase 3. Co-treatment with recombinant Grx2 inhibited GSNO-mediated apoptosis. Our data are in accordance with findings that demonstrate Grx2 to inhibit apoptosis in a variety of cell types including cerebellar granule neurons (Daily et al. 2001). In HeLa cells, the enzymatic activity of Grx2 prevents apoptosis via the inhibition of cytochrome c release (Lillig et al. 2004; Enoksson et al. 2005). Although the treatment with the Grx2S38P mutant showed no protective effect against GSNO-mediated protein nitration and cytotoxicity in oligodendrocytes, the incorporation of a point mutation could inhibit the reduction of protein GSH disulfides (Johansson et al. 2004) and thereby result in a failed substrate recognition. It was previously reported that a change in the active site composition prevents cluster assembly and results in a 2.3 times higher enzymatic activity compared to wild type Grx2 (Berndt et al. 2007). However, the binding efficacy of interaction partners could be specifically important for the Grx2-dependent protective function against GSNO-mediated oligodendrocyte apoptosis and could be inhibited. Therefore, although our data underline a minor involvement of the enzymatic activity, its contribution cannot be excluded completely.

(II) Similar to the enzymatic active Grx2, the formation of DNGICs, DNIC with thiolate ligands, decrease the induction of apoptosis (Kim et al., 2000; Giliano et al. 2011). However, the underlying mechanism is yet unknown. DNGICs were previously reported to beneficially influence diverse pathological conditions like MS (Chazov et al. 2012; Tsai et al. 2015). Even though NO reacts with other FeS cluster proteins to form DNICs (Ren et al. 2008), their functionality is limited to global NO transport and storage as well as iron mobilization (Tsai et al. 2015). To our knowledge, non-protein ligands of FeS clusters are only used by Grxs. Their FeS clusters possess two molecules of GSH (Berndt et al. 2007; Johansson et al. 2007) and thereby highly support the formation of DNGICs upon FeS cluster disassembly. To verify the formation of DNGICs rather than of DNICs upon Grx2 FeS disassembly, we exploited the DNGIC-specific inhibition of GST activity (Keese et al. 1997; Cesareo et al. 2005). Here, in HeLa cell extracts and in cell-free systems, the enzymatic inhibition of GST upon GSNO treatment was increased in a Grx2-dependent

manner (Lepka et al., submitted). Furthermore, GST is known to support the cellular export of iron via the MRP1 iron exporter (Lok et al. 2012). MRP1-mediated iron export is GSH-dependent (Watts and Richardson 2001) and exports iron in form of DNGICs (Watts et al. 2006; Lok et al. 2012). In line, our EPR analysis with GSNO treated OLN-93 cells revealed a DNGIC-specific signal at g= 2.03 (Vanin et al. 1998) that is increased upon pharmacological inhibition of MRP1. However, in tumor cells the MRP1-mediated efflux of iron and GSH induced apoptosis (Lok et al. 2012). Furthermore, the formation of DNGICs protects from iron-mediated DNA damage (Lewandowska et al. 2015) and $OH^{\cdot}$ formation via the inhibition of the Fenton reaction (Lu and Koppenol 2005). Therefore, it has to be clarified whether the formation and export of DNGICs or its contribution as signaling molecule participate in the observed effects.

(III) In addition, the disassembly of holo Grxs results in the release of sulfur. The present study did not investigate a possible contribution of the released sulfur to the observed effects. However, recent synthetic modeling studies by Fritzpatrick and Kim revealed the formation of H_2S upon NO-dependent disassembly of FeS cluster proteins (Fitzpatrick and Kim 2015). In the last two decades H_2S has been described as regulatory molecule in a variety of neurodegenerative and neuroinflammatory disorders, such as Alzheimer's disease and MS (Whiteman et al. 2004; Whiteman et al. 2005; Gong et al. 2011; Kida and Ichinose 2015). Increased concentrations of H_2S via the donation of NaHS inhibit apoptosis in early brain lesions in rats (Kida and Ichinose 2015; Li et al. 2016). In our study, the release of H_2S upon NO-mediated FeS cluster disassembly may provide an additional mechanism to suppress apoptotic cascades. However, similar to NO, H_2S is highly toxic and its contribution as signaling molecule is barely understood. For example, H_2S competes with ROS and RNS affecting a multitude of signaling pathways (reviewed by (Hancock and Whiteman 2016)).

Taken together, the Grx-specific FeS cluster provides iron, GSH and sulfur molecules in close proximity, favoring the formation of DNGICs and H_2S upon detoxification of NO along with the release of enzymatic active apo Grx. All three components have the potential to be responsible for the Grx2-dependent inhibition of $ONOO^-$-mediated cytotoxicity in oligodendrocytes. However, further experiments need to clarify their contribution to our proposed mechanism. If merely the generation of H_2S is essential for the inhibition of apoptosis, any FeS cluster coordinating protein could replace the role of Grx2 in the observed detoxification mechanism of NO. If the formation of DNGICs is needed, GSH as non-protein ligand is essential. Here, the function of Grx2 could be replaced by the two other FeS cluster coordinating Grxs 3 and 5 or the $[[Fe_2S_2]^{2+}(GS^-)^4]^{2-}$ complex in which GSH molecules alone coordinate an FeS cluster (Qi et al. 2012). The

third possibility is the contribution of Grx2's enzymatic function. In this case only Grx2-coordinated FeS clusters could prevent $ONOO^-$-mediated cytotoxicity.

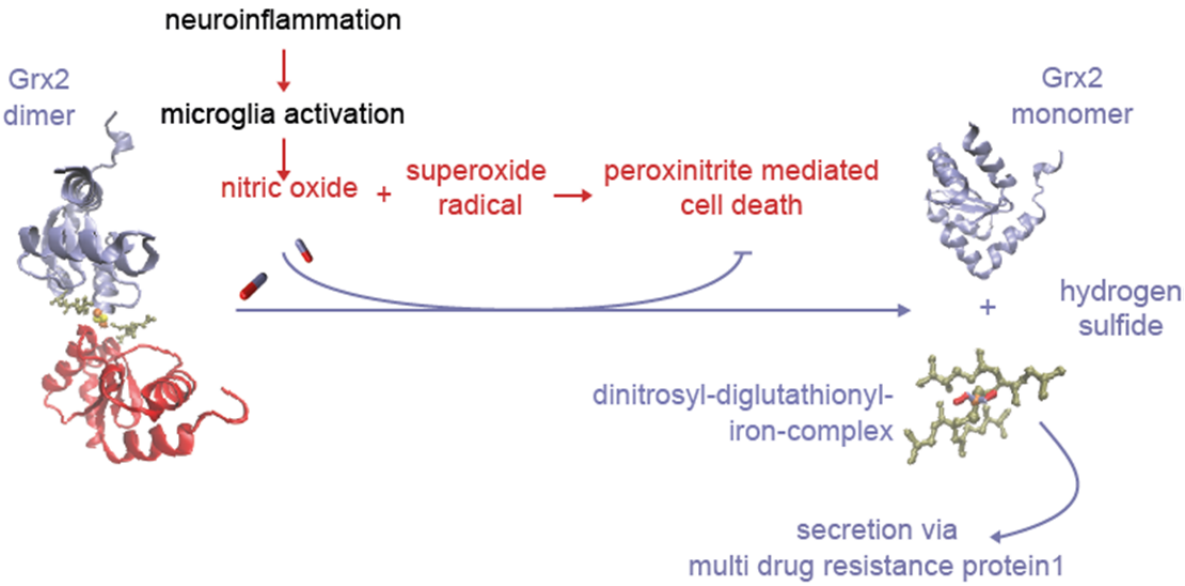

Figure 27. Grx2-dependent detoxification of NO protects oligodendrocyte progenitors from $ONOO^-$-mediated cell death. Upon neuroinflammation, activated microglia secrete toxic amounts of NO that lead to oligodendrocyte cell death based on the formation of $ONOO^-$. In the presence of holo Grx2, NO is detoxified by the disassembly of the FeS cluster, resulting in the formation of DNGICs which are further exported from the cell via the MRP1 transporter. Also and most likely H_2S is formed. The release of enzymatic active apo Grx2 as well as DNGICs and H_2S could in parallel contribute to the observed increase in cell viability.

4.1.3 Oligodendrocyte progenitor migration and differentiation

Functional remyelination requires, besides the survival of OPCs, their efficient migration into demyelinated areas and differentiation into myelin-producing oligodendrocytes. In contrast to Schwann cells of the peripheral nervous system that undergo a de-differentiation program, pre-existing mature oligodendrocytes do not contribute to remyelinaiton (Crawford et al. 2016). Hence, the existence of OPCs inside lesion areas is essential for proper regeneration, as shown in EAE mice (Crawford et al. 2016). Examination of the OPC differentiation state inside lesion areas after lysolecithin-mediated demyelination in mice identified OPCs inside lesion areas as NG2-expressing cells (Kucharova and Stallcup 2015). Our experiments revealed that upon recombinant Grx2 treatment the number of NG2-positive cells increased in remyelinated OSCs. This

increase is not linked to enhanced proliferation of OPCs but is rather related to a Grx2-dependent inhibition of OPC differentiation. Thus, the number of mature oligodendrocytes that express myelin genes is decreased upon Grx2 treatment *in vitro*, supporting the hypothesis of a Grx2-mediated differentiation block. The process of oligodendrocyte differentiation is complex and still under investigation. Redox modifications are able to regulate glial differentiation (Smith et al. 2000) and myelin gene expression of mature oligodendrocytes (Jana and Pahan 2005). However, these studies only investigated changes in the global cellular redox state without the identification of specific redox regulatory events. Our findings introduce a so far unexplored Grx2-dependent differentiation block of oligodendrocytes. Western blot analyses underline a high basal level of Grx2 in primary A_2B_5-positive progenitors (Fig. 23) and stress the contribution of Grx2 in OPC progenitor maintenance and/or differentiation. Notably, we did not observe any changes in the level of Grx2 expression during OPC differentiation, underlining the involvement of additional regulatory factors. Among other regulatory mechanisms, histone deacetylation is a well-established and frequently reviewed initiation process for differentiation in general and especially in neural cell fate (Teng et al. 2009; Hu et al. 2014). Previous results of our group identified the activity of Sirt1, a histone deacetylase, to regulate neural stem cell differentiation under oxidative conditions (Prozorovski et al. 2008). In addition, our findings revealed the activation of Sirt1 via Grx2-dependent deglutathionylation in both HeLa cell lysates and zebrafish (Bräutigam et al. 2013). Sirt1 is the only histone modifying enzyme so far known to be Grx-regulated and thus, I examined its contribution to oligodendrocyte differentiation. In our A_2B_5 differentiation assay, recombinant Grx2 treatment decreased the amount of mature oligodendrocytes. Based on these findings I hypothesized that the inhibition of Sirt1 would increase the number of differentiated mature oligodendrocytes in this assay. However, the treatment with Ex571, a Sirt1 inhibitor, induced the same differentiation block as recombinant Grx2 treatment, underlining active Sirt1 as initiator for OPC differentiation. Interestingly, cell fate decisions in glial restricted progenitors and neural progenitors differ in their molecular mechanism. The current literature on the role of Sirt1 in differentiation is restricted to neural stem cell decision. Research by Rafalski and colleagues showed the inactivation of Sirt1 to ameliorate remyelination and to delay EAE symptom progression by the increase of OPC generation from neural stem cells (Rafalski et al. 2013). However, this study did not detect an influence of Sirt1 on OPC differentiation (Rafalski et al. 2013). Sirt1 was further shown to promote Wnt signaling (Holloway et al. 2010) whose contribution to OPC differentiation is likewise controversial (Guo et al. 2015). Although our findings are in contrast to current

publications neglecting an involvement of Sirt1 in OPC differentiation, the complexity of the involved signaling pathways stress the need for further investigations.

As the NG2-positive cell population failed to continue differentiation upon recombinant Grx2 treatment, another possible mechanism for the Grx2-dependent differentiation block is the modulation of NG2 protein expression or degradation. NG2 cells generate mature myelinating oligodendrocytes as well as astrocytes (Rivers et al. 2008; Zhu et al. 2008). Moreover, NG2 is essential for cell migration and cytoskeleton interactions (Jamil et al. 2016; Sakry and Trotter 2016). In particular, guided OPC migration is NG2-dependent (Chatterjee et al. 2008). Furthermore, in the adult brain this cell type shows additional functions: NG2 cells migrate towards lesion areas and contribute essentially to wound closure and healing (Dimou and Götz 2014). Inside lesion areas, the majority remains NG2-positive and does not differentiate (Dimou and Götz 2014; Viganò et al. 2016). Summerizing, the current literature supports the direct involvement of NG2-expresing cells in regeneration and therefore stresses migration rather than differentiation as essential feature of this cell type for primary regeneration. Our experiments revealed a Grx2-dependent increase in the migration capacity of mouse OPCs. In our OSC remyelination model the number of NG2 cells increased per demyelinated branch upon Grx2 treatment, indicating an enhanced migration capacity towards areas of demyelinated axons (Fig. 22). Notably, we previously excluded the influence of recombinant Grx2 on OPC proliferation (Volbracht 2012). Regarding oligodendrocyte differentiation, recombinant Grx2 treatment decreased the number of MBP expressing cells *in vitro*. Although, the number was not affected *ex vivo*, we observed a Grx2-dependent alteration in the morphology of MBP expressing cells upon remyelination. Grx2-dependent redox signaling is highly established in the process of migration. The identification of interaction partners in brain tissue for Grx2 revealed a variety of proteins involved in cytoskeletal rearrangement (Schütte et al. 2013). Next to Trx1, cytosolic Grx2 was confirmed as regulator of CRMP2 affecting the migration capacity in HeLa cells (Bräutigam et al. 2011; Gellert et al. 2013). Interestingly, not only the structure and function of CRMP2 is known to be regulated via a dithiol-disulfide switch but also other cytoskeletal components like actin as well as tubulin were shown to be redox regulated downstream of the semaphorin3a signaling pathway (Gellert et al. 2015) (Fig. 28). Semaphorin3a is highly accumulated in neuroinflammatory MS and EAE lesions, inhibiting OPC migration (Costa et al. 2015; Gutiérrez-Franco et al. 2016). Further, semaphorin3a contributes to immune cell activation, to neural degeneration and failed regeneration (Syed et al. 2011; Eixarch et al. 2013; Gutiérrez-Franco et al. 2016). A promising approach for drug development in MS regeneration is to overcome the semaphorin3a-dependent repellant effect on OPC migration (Villoslada 2016). Our

experiments reveal a semaphorin3a-dependent inhibition of A_2B_5 cell migration. This observation was abolished by recombinant Grx2 treatment. In line, recombinant Grx2 treatment alone increased the transmigration of A_2B_5-positive progenitors significantly (Fig. 26). Whether or not the previous identification of a CRMP2-Grx2 interaction is the basis for our observations has to be further analysed. In line with our findings of GSNO-mediated protein modification in EAE lesion areas, S-nitrosylation of actin as well as tubulin contributes to EAE progression (Smerjac and Bizzozero 2008; Bizzozero and Zheng 2009). We identified a Grx2-dependent detoxification mechanism of NO (discussed in 4.1) that could prevent NO-dependent S-nitrosylation of cytoskeletal proteins. This could likewise increase the oligodendrocyte progenitor migration capacity *in vivo*. The application of a global approach to identify interaction partners of Grx2 in OPCs and mature oligodendrocytes could identify new pathways important for both Grx2-dependent oligodendrocyte progenitor migration and differentiation.

Our e*x vivo* experiments in OSCs supported our *in vitro* results regarding migration as well as differentiation. Here, Grx2-dependent alterations on OPC maturation and remyelination were detected but not reflected in the fluorescence based quantification of the MBP staining. Although co-localization and quantitative fluorescence studies are commonly used for the quantification of remyelination, current research is discussing the reliability of this method (Keough et al. 2015). Alternatively, the number of mature oligodendrocytes per defined area was taken into consideration for quantification. However, the number of internodes per oligodendrocyte is inconsistent underlining the limitation of this method to quantify functional remyelination (Keough et al. 2015). In our experiments the overall cell number of MBP-positive mature oligodendrocytes was neither changed by the treatment of recombinant Grx2 nor was the fluorescence intensity of the MBP signal. However, we faced clear differences in cell morphology of MBP expressing cells and considered the existence of mature oligodendrocytes that do not contribute to functional remyelination. This fact though is not included in the mentioned quantification methods. Our experiments highlight that the maturation alone is insufficient to ensure remyelination. Untreated control slices revealed the presence of mature non-myelinating oligodendrocytes, underlining the essential impact of the defined time- and place-dependent initiation of OPC differentiation. Hence, the induction of OPC maturation without an axon in close proximity would not lead to remyelination. In our experimental setup, the existence of mature, non-myelinating oligodendrocytes therefore distort and prohibit fluorescence based quantification of remyelination. Counting the number and length of internodes is another commonly used method to quantify remyelination which considers the existence of mature oligodendrocytes not contributing to remyelination. In future evaluations of our

experiments we will consider the quantification of connection points between NG2-positive cells and axons (quantifying migration capacity) as well as the number and length of the nodes of Ranvier co-localized to axonal structures using additional caspr staining for functional paranodes (quantifying functional remyelination).

Taken together, Grx2 regulates the migration capacity of various cell types including OPCs. The underlying mechanism most likely suppresses the differentiation of OPCs in the state of NG2 expression. Later differentiation stages discard migratory capacity along with the termination of NG2 expression (Nishiyama et al. 2009; Kukley et al. 2010). Therefore, Grx2 could simultaneously increase migration capacity while preventing differentiation of OPCs, resulting in an increased regeneration capacity upon different neuroinflammatory pathological situations like CNS wound healing after stroke or trauma.

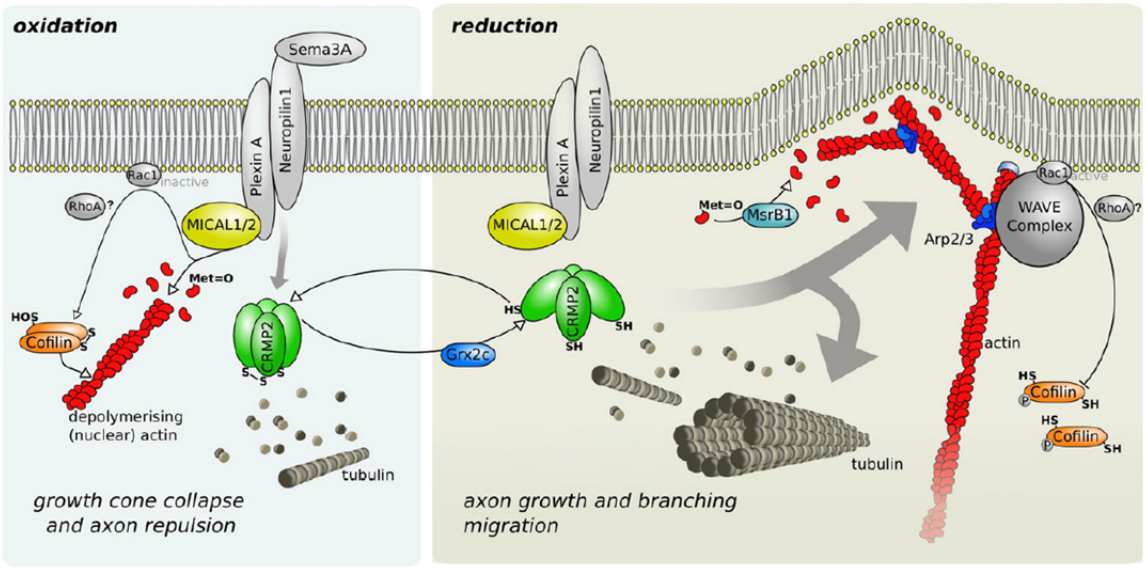

Figure 28. Redox-dependent modifications in cytoskeletal components downstream of semaphorin3a signaling. Semaphorin3a binding to its specific receptor leads through MICAL1/2 and/or cofilin to actin de-polymerization. Through CRMP2, Semaphorin3a induces growth cone collapse and axon repulsion. The Grx2-dependent reduction leads to conformational changes of the homo-tetramer, causing the polymerization of actin and tubulin. Absence of Sema3a leads to axonal outgrowth and further enables migration (Gellert et al., 2015).

4.2 Perspectives for therapeutic applications

Grx2 is an FeS cluster coordinating oxidoreductase affecting neuroinflammatory degeneration and oligodendrocyte progenitor migration and differentiation - two major processes for functional remyelination. This study underlines distinct roles of Grx2 for both features: NO-detoxification and inhibition of $ONOO^-$-formation via FeS cluster disassembly as well as increased migration capacity via its enzymatic activity. These data stress a possible application of Grx2 as therapeutic compound against neuroinflammatory diseases characterized by increased NO production, including Parkinson's disease and MS. Previous therapeutic MS research already focused on the detoxification of reactive species. For example, the administration of NOX-100, a NO scavenger, beneficially affected EAE disease progression (Jolivalt et al. 2003). However, these results were not translated to human disease models yet underlining the challenge of a successful translation from animal models to humans (Mix et al. 2010). Neglected side effects of ROS/RNS scavenger donation are unexplored but meight interfere with essential redox-dependent signaling pathways (Lepka et al. 2016). Therefore, possible side effects of Grx2 have to be investigated. Grx2 is a specific redox-active enzyme involved in a variety of cellular processes. Our findings displayed its contribution to NO-mediated changes in iron homeostasis and DNGICs synthesis in oligodendrocytes. However, this effect could simultaneously affect other cell types. Previous characterization of a variety of interaction partners underlined its contribution to pathways important for cell migration, survival and differentiation that are not restricted to one cell type (Hurd et al. 2012; Berndt et al. 2014; Gellert et al. 2015). Furthermore, efforts to translate antioxidant treatment from animal model to human beings show little success in preclinical MS studies (Carvalho et al. 2016; Lepka et al. 2016). Donation of, for instance, low molecular weight antioxidants (Hansen et al. 1995) showed beneficial effects in the MS animal models, whereas, a beneficial contribution was not reported in preclinical studies. One possible reason could be an inappropriate application method. Upon peripheral donation, a successful therapeutic agent for CNS diseases, has to cross the BBB in sufficient amounts (Carvalho et al. 2016). Although recombinant human Trx1, showing structural similarities to Grx2, crosses the BBB (Hattori et al. 2004), it is unknown whether or not Grx2 is able to pass the BBB. In addition, the cellular uptake of Grx2 is entirely unexplored. However, my results point towards a cellular uptake of externally added recombinant Grx2. Likewise to exogen Grx2 treatment, Grx2c overexpression in HeLa cells as well as Grx2-specific siRNA silencing in primary A_2B_5-positive progenitors modulated cellular NO resistance supporting an endogenous existence of the introduced mechanism. Finally, the systemic distribution of

exogen Grx needs to be further investigated *in vivo*. In acute MS lesion areas, Grxs were only expressed by reactive astrocytes and activated microglia. Whether or not the Grxs are secreted and therefore affect surrounding cells is unknown and has to be further investigated. Finally, the translation of recombinant Grx2 treatment into the EAE mouse model will help to clarify the impact of Grx2 as therapeutic agent in neuroinflammatory disorders like MS.

4.3 Summary

Increased production of NO and concomitant nitrosative damage to oligodendrocytes and their progenitors is an early event during neuroinflammatory diseases. Therefore, the detoxification of NO represents a promissing tool to prevent cellular damage and neuroinflammatory demyelination. This study characterizes for the first time the beneficial role of Grx2 in the detoxification of NO. Furthermore, it is the first description of a beneficial effect of iron-sulfur cluster disassembly. Moreover, within this thesis, I identified a new potential function of iron-sulfur cluster coordinating Grxs during neuroinflammation; especially of Grx2 in oligodendrocyte progenitor functions important for regeneration. In detail, my thesis revealed the following results:

(I) The expression of Grxs 2, 3 and 5 as well as the activity of various iron-dependent enzymes was regulated upon neuroinflammation illustrated by human MS and mouse EAE disease progression. Immunohistochemical analysis of MS lesion areas revealed the presence of Grxs 2, 3 and 5 in activated astrocytes and microglia only in acute lesion areas. In line, Grx2 was upregulated in the inflammatory active acute EAE phase and down-regulated in the chronic disease phase. Whereas overall protein levels were not affected upon EAE, the enzymatic activity of iron-dependent enzymes decreased.

(II) Grx2 promotes oligodendrocyte viability and myelin integrity upon NO treatment via a newly identified detoxification mechanism. Our results demonstrate an iron-sulfur cluster-dependent detoxification of NO, preventing cytotoxic $ONOO^-$ formation. This mechanism results in the formation of apo Grx, DNGICs and most likely H_2S. All products were previously reported to inhibit the induction of apoptosis. Furthermore, Grx2 attenuated the NO-mediated pathological alteration of the transferrin receptor localization in oligodendrocytes. The systemic relevance was further verified in mouse *ex vivo* and *in vitro* approaches.

(III) Grx2 increases OPC migration capacity and decreases their differentiation capacity. OPC transmigration was significantly promoted even in presence of semaphorin3a, a repellent guidance molecule accumulating in neuroinflammatory lesion areas. Oligodendrocyte differentiation capacity was blocked in the state of NG2-expressing cells. NG2 cells were reported to actively migrate towards lesion areas and to contribute significantly to their regeneration, previously shown for wound closure and healing.

These findings indicate a promissing benefit of Grx2 as feasible therapeutic agent for both a decrease in neuroinflammatory degeneration and an increase in regeneration.

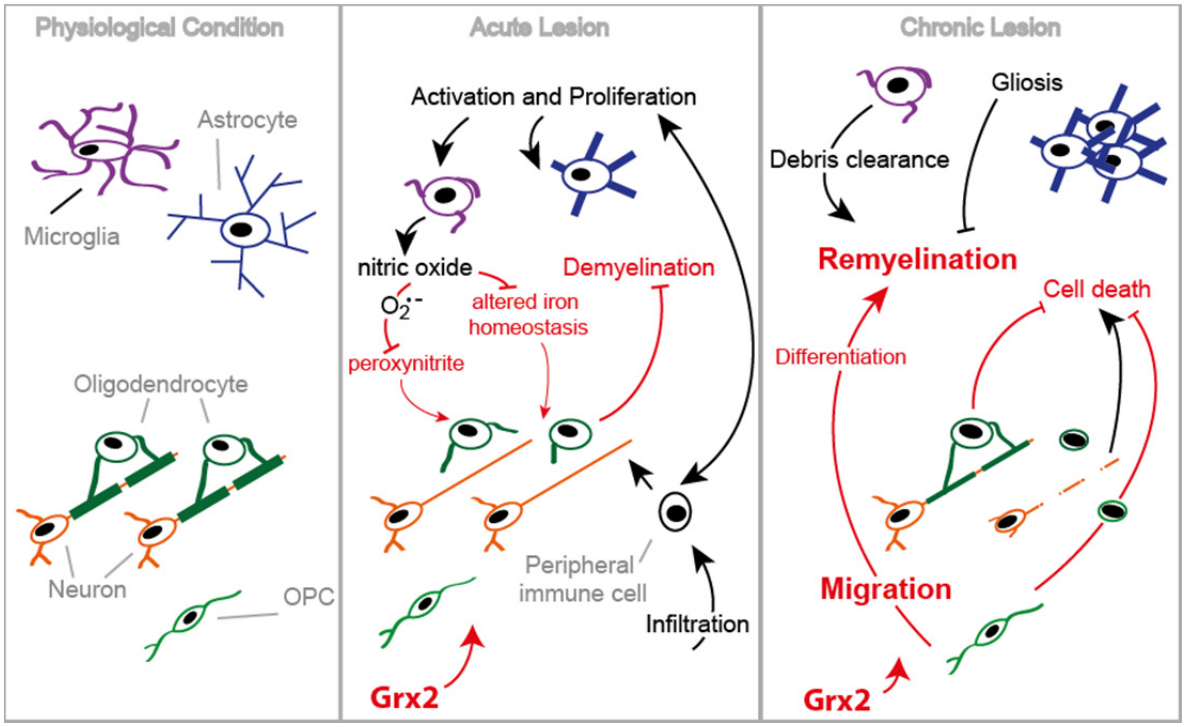

Figure 29. Confirmed contributions of Grx2 to acute and chronic neuroinflammatory lesion area progression. Grx2 revealed an increased expression in the acute EAE phase and a decreased expression in the chronic phase indicating a function in both the de- and remyelination. Grx2 inhibited peroxynitrite generation and was able to prevent NO-mediated alterations in iron homeostasis resulting in myelin maintainance. Furthermore, Grx2 promoted oligodendrocyte progenitor prerequisites for regeneration including survival, migration and differentiation.

5. References

Adams, C. W.; Poston, R. N.; Buk, S. J. (1989): Pathology, histochemistry and immunocytochemistry of lesions in acute multiple sclerosis. In: *Journal of the neurological sciences* 92 (2-3), S. 291–306.

Aktas, Orhan; Smorodchenko, Alina; Brocke, Stefan; Infante-Duarte, Carmen; Schulze Topphoff, Ulf; Vogt, Johannes et al. (2005): Neuronal damage in autoimmune neuroinflammation mediated by the death ligand TRAIL. In: *Neuron* 46 (3), S. 421–432. DOI: 10.1016/j.neuron.2005.03.018.

Aktas, Orhan; Ullrich, Oliver; Infante-Duarte, Carmen; Nitsch, Robert; Zipp, Frauke (2007): Neuronal damage in brain inflammation. In: *Archives of neurology* 64 (2), S. 185–189. DOI: 10.1001/archneur.64.2.185.

Albrecht, Philipp; Bouchachia, Imane; Goebels, Norbert; Henke, Nadine; Hofstetter, Harald H.; Issberner, Andrea et al. (2012): Effects of dimethyl fumarate on neuroprotection and immunomodulation. In: *Journal of neuroinflammation* 9, S. 163. DOI: 10.1186/1742-2094-9-163.

Alvarez, Jorge Ivan; Cayrol, Romain; Prat, Alexandre (2011): Disruption of central nervous system barriers in multiple sclerosis. In: *Biochimica et biophysica acta* 1812 (2), S. 252–264. DOI: 10.1016/j.bbadis.2010.06.017.

Arthur-Farraj, Peter J.; Latouche, Morwena; Wilton, Daniel K.; Quintes, Susanne; Chabrol, Elodie; Banerjee, Ambily et al. (2012): c-Jun reprograms Schwann cells of injured nerves to generate a repair cell essential for regeneration. In: *Neuron* 75 (4), S. 633–647. DOI: 10.1016/j.neuron.2012.06.021.

Ascherio, A.; Munger, K. L.; Lennette, E. T.; Spiegelman, D.; Hernán, M. A.; Olek, M. J. et al. (2001): Epstein-Barr virus antibodies and risk of multiple sclerosis: a prospective study. In: *JAMA* 286 (24), S. 3083–3088.

Back, Stephen A.; Tuohy, Therese M F; Chen, Hanqin; Wallingford, Nicholas; Craig, Andrew; Struve, Jaime et al. (2005): Hyaluronan accumulates in demyelinated lesions and inhibits oligodendrocyte progenitor maturation. In: *Nature medicine* 11 (9), S. 966–972. DOI: 10.1038/nm1279.

Badaracco, M. E.; Ortiz, E. H.; Soto, E. F.; Connor, J.; Pasquini, J. M. (2008): Effect of transferrin on hypomyelination induced by iron deficiency. In: *Journal of neuroscience research* 86 (12), S. 2663–2673. DOI: 10.1002/jnr.21709.

Baker, David; Amor, Sandra (2012): Publication guidelines for refereeing and reporting on animal use in experimental autoimmune encephalomyelitis. In: *Journal of neuroimmunology* 242 (1-2), S. 78–83. DOI: 10.1016/j.jneuroim.2011.11.003.

Bannerman, Peter; Hahn, Ashleigh; Soulika, Athena; Gallo, Vittorio; Pleasure, David (2007): Astrogliosis in EAE spinal cord: derivation from radial glia, and relationships to oligodendroglia. In: *Glia* 55 (1), S. 57–64. DOI: 10.1002/glia.20437.

Bazinet, Richard P.; Layé, Sophie (2014): Polyunsaturated fatty acids and their metabolites in brain function and disease. In: *Nature reviews. Neuroscience* 15 (12), S. 771–785. DOI: 10.1038/nrn3820.

Beard, J. L.; Dawson, H.; Piñero, D. J. (1996): Iron metabolism: a comprehensive review. In: *Nutrition reviews* 54 (10), S. 295–317.

Benkovic, S. A.; Connor, J. R. (1993): Ferritin, transferrin, and iron in selected regions of the adult and aged rat brain. In: *The Journal of comparative neurology* 338 (1), S. 97–113. DOI: 10.1002/cne.903380108.

Berndt, Carsten; Hudemann, Christoph; Hanschmann, Eva-Maria; Axelsson, Rebecca; Holmgren, Arne; Lillig, Christopher Horst (2007): How does iron-sulfur cluster coordination regulate the activity of human glutaredoxin 2? In: *Antioxidants & redox signaling* 9 (1), S. 151–157. DOI: 10.1089/ars.2007.9.151.

Berndt, Carsten; Poschmann, Gereon; Stühler, Kai; Holmgren, Arne; Bräutigam, Lars (2014): Zebrafish heart development is regulated via glutaredoxin 2 dependent migration and survival of neural crest cells. In: *Redox biology* 2, S. 673–678. DOI: 10.1016/j.redox.2014.04.012.

Bertini, R.; Howard, O. M.; Dong, H. F.; Oppenheim, J. J.; Bizzarri, C.; Sergi, R. et al. (1999): Thioredoxin, a redox enzyme released in infection and inflammation, is a unique chemoattractant for neutrophils, monocytes, and T cells. In: *The Journal of experimental medicine* 189 (11), S. 1783–1789.

Biederbick, Annette; Stehling, Oliver; Rösser, Ralf; Niggemeyer, Brigitte; Nakai, Yumi; Elsässer, Hans-Peter; Lill, Roland (2006): Role of human mitochondrial Nfs1 in cytosolic iron-sulfur protein biogenesis and iron regulation. In: *Molecular and cellular biology* 26 (15), S. 5675–5687. DOI: 10.1128/MCB.00112-06.

Bin, Jenea M.; Leong, Soo Yuen; Bull, Sarah-Jane; Antel, Jack P.; Kennedy, Timothy E. (2012): Oligodendrocyte precursor cell transplantation into organotypic cerebellar shiverer slices: a model to study myelination and myelin maintenance. In: *PloS one* 7 (7), S. e41237. DOI: 10.1371/journal.pone.0041237.

Bizzozero, Oscar A.; Zheng, Jianzheng (2009): Identification of major S-nitrosylated proteins in murine experimental autoimmune encephalomyelitis. In: *Journal of neuroscience research* 87 (13), S. 2881–2889. DOI: 10.1002/jnr.22113.

Bö, L.; Dawson, T. M.; Wesselingh, S.; Mörk, S.; Choi, S.; Kong, P. A. et al. (1994): Induction of nitric oxide synthase in demyelinating regions of multiple sclerosis brains. In: *Annals of neurology* 36 (5), S. 778–786. DOI: 10.1002/ana.410360515.

Bögler, O.; Wren, D.; Barnett, S. C.; Land, H.; Noble, M. (1990): Cooperation between two growth factors promotes extended self-renewal and inhibits differentiation of oligodendrocyte-type-2 astrocyte (O-2A) progenitor cells. In: *Proceedings of the National Academy of Sciences of the United States of America* 87 (16), S. 6368–6372.

Bohr, Vilhelm A.; Stevnsner, Tinna; de Souza-Pinto, Nadja C (2002): Mitochondrial DNA repair of oxidative damage in mammalian cells. In: *Gene* 286 (1), S. 127–134.

Bosch, Bastian (2015): Redox-regulated aspects of axonal outgrowth and regeneration. Master Thesis, Department of Neurology, Heinrich-Heine-University Düsseldorf

Bräutigam, Lars; Jensen, Lasse Dahl Ejby; Poschmann, Gereon; Nyström, Staffan; Bannenberg, Sarah; Dreij, Kristian et al. (2013): Glutaredoxin regulates vascular development by reversible glutathionylation of sirtuin 1. In: *Proceedings of the National Academy of Sciences of the United States of America* 110 (50), S. 20057–20062. DOI: 10.1073/pnas.1313753110.

Bräutigam, Lars; Schütte, Lena Dorothee; Godoy, José Rodrigo; Prozorovski, Timour; Gellert, Manuela; Hauptmann, Giselbert et al. (2011): Vertebrate-specific glutaredoxin is essential for brain development. In: *Proceedings of the National Academy of Sciences of the United States of America* 108 (51), S. 20532–20537. DOI: 10.1073/pnas.1110085108.

Brosnan, Celia F.; Raine, Cedric S. (2013): The astrocyte in multiple sclerosis revisited. In: *Glia* 61 (4), S. 453–465. DOI: 10.1002/glia.22443.

Bruce King, S. (2013): Potential biological chemistry of hydrogen sulfide (H2S) with the nitrogen oxides. In: *Free radical biology & medicine* 55, S. 1–7. DOI: 10.1016/j.freeradbiomed.2012.11.005.

Bsibsi, Malika; Ravid, Rivka; Gveric, Djordje; van Noort, Johannes M (2002): Broad expression of Toll-like receptors in the human central nervous system. In: *Journal of neuropathology and experimental neurology* 61 (11), S. 1013–1021.

Buendia, Izaskun; Michalska, Patrycja; Navarro, Elisa; Gameiro, Isabel; Egea, Javier; León, Rafael (2016): Nrf2-ARE pathway: An emerging target against oxidative stress and neuroinflammation in neurodegenerative diseases. In: *Pharmacology & therapeutics* 157, S. 84–104. DOI: 10.1016/j.pharmthera.2015.11.003.

Bush, T. G.; Puvanachandra, N.; Horner, C. H.; Polito, A.; Ostenfeld, T.; Svendsen, C. N. et al. (1999): Leukocyte infiltration, neuronal degeneration, and neurite outgrowth after ablation of scar-forming, reactive astrocytes in adult transgenic mice. In: *Neuron* 23 (2), S. 297–308.

Butovsky, Oleg; Landa, Gennady; Kunis, Gilad; Ziv, Yaniv; Avidan, Hila; Greenberg, Nadav et al. (2006a): Induction and blockage of oligodendrogenesis by differently activated microglia in an animal model of multiple sclerosis. In: *The Journal of clinical investigation* 116 (4), S. 905–915. DOI: 10.1172/JCI26836.

Butovsky, Oleg; Ziv, Yaniv; Schwartz, Adi; Landa, Gennady; Talpalar, Adolfo E.; Pluchino, Stefano et al. (2006b): Microglia activated by IL-4 or IFN-gamma differentially induce neurogenesis and oligodendrogenesis from adult stem/progenitor cells. In: *Molecular and cellular neurosciences* 31 (1), S. 149–160. DOI: 10.1016/j.mcn.2005.10.006.

Cairo, Gaetano; Recalcati, Stefania (2007): Iron-regulatory proteins: molecular biology and pathophysiological implications. In: *Expert reviews in molecular medicine* 9 (33), S. 1–13. DOI: 10.1017/S1462399407000531.

Campbell, Graham R.; Ziabreva, Iryna; Reeve, Amy K.; Krishnan, Kim J.; Reynolds, Richard; Howell, Owen et al. (2011): Mitochondrial DNA deletions and neurodegeneration in multiple sclerosis. In: *Annals of neurology* 69 (3), S. 481–492. DOI: 10.1002/ana.22109.

Carvalho, Andreia Neves; Firuzi, Omidreza; Gama, Maria João; van Horssen, Jack; Saso, Luciano (2016): Oxidative stress and antioxidants in neurological diseases: is there still hope? In: *Current drug targets*.

Cesareo, E.; Parker, L. J.; Pedersen, J. Z.; Nuccetelli, M.; Mazzetti, A. P.; Pastore, A. et al. (2005): Nitrosylation of Human Glutathione Transferase P1-1 with Dinitrosyl Diglutathionyl Iron Complex in Vitro and in Vivo. In: *Journal of Biological Chemistry* 280 (51), S. 42172–42180. DOI: 10.1074/jbc.M507916200.

Chapouly, Candice; Tadesse Argaw, Azeb; Horng, Sam; Castro, Kamilah; Zhang, Jingya; Asp, Linnea et al. (2015): Astrocytic TYMP and VEGFA drive blood-brain barrier opening in inflammatory central nervous system lesions. In: *Brain : a journal of neurology* 138 (Pt 6), S. 1548–1567. DOI: 10.1093/brain/awv077.

Chatterjee, Nivedita; Stegmüller, Judith; Schätzle, Philipp; Karram, Khalad; Koroll, Michael; Werner, Hauke B. et al. (2008): Interaction of syntenin-1 and the NG2 proteoglycan in migratory oligodendrocyte precursor cells. In: *The Journal of biological chemistry* 283 (13), S. 8310–8317. DOI: 10.1074/jbc.M706074200.

Chazov EI, Rodnenkov OV, Zorin AV, Lakomkin VL, Gramovich VV, Vyborov ON, Dragnev AG, Timoshin, Capital A Cyrilliclexander A, Buryachkovskaya LI, Abramov AA, Massenko VP, Arzamastsev EV, Kapelko VI, Vanin AF. 2012. Hypotensive effect of Oxacom® containing a dinitrosyl iron complex with glutathione: animal studies and clinical trials on healthy volunteers. Nitric oxide : biology and chemistry / official journal of the Nitric Oxide Society 26(3):148–156.

Chen, Chun-An; Pascali, Francesco de; Basye, Ariel; Hemann, Craig; Zweier, Jay L. (2013): Redox modulation of endothelial nitric oxide synthase by glutaredoxin-1 through reversible oxidative post-translational modification. In: *Biochemistry* 52 (38), S. 6712–6723. DOI: 10.1021/bi400404s.

Cho, Seongeun; Wood, Andrew; Bowlby, Mark R. (2007): Brain slices as models for neurodegenerative disease and screening platforms to identify novel therapeutics. In: *Current neuropharmacology* 5 (1), S. 19–33.

Connor, J. R.; Menzies, S. L. (1996): Relationship of iron to oligodendrocytes and myelination. In: *Glia* 17 (2), S. 83–93. DOI: 10.1002/(SICI)1098-1136(199606)17:2<83::AID-GLIA1>3.0.CO;2-7.

Conforti, Andreas (2014): Redox-Regulation in reaktiven Astrozyten. Bachelor Thesis, Department of Neurology, Heinrich-Heine-University Düsseldorf

Copray, Sjef; Huynh, Jimmy Long; Sher, Falak; Casaccia-Bonnefil, Patrizia; Boddeke, Erik (2009): Epigenetic mechanisms facilitating oligodendrocyte development, maturation, and aging. In: *Glia* 57 (15), S. 1579–1587. DOI: 10.1002/glia.20881.

Correale, Jorge; Farez, Mauricio F. (2015): The Role of Astrocytes in Multiple Sclerosis Progression. In: *Frontiers in neurology* 6, S. 180. DOI: 10.3389/fneur.2015.00180.

Costa, C.; Martínez-Sáez, E.; Gutiérrez-Franco, A.; Eixarch, H.; Castro, Z.; Ortega-Aznar, A. et al. (2015): Expression of semaphorin 3A, semaphorin 7A and their receptors in multiple sclerosis lesions. In: *Multiple sclerosis (Houndmills, Basingstoke, England)* 21 (13), S. 1632–1643. DOI:

10.1177/1352458515599848.

Covacu, Ruxandra; Danilov, Alexandre I.; Rasmussen, Bo Sonnich; Hallén, Katarina; Moe, Morten C.; Lobell, Anna et al. (2006): Nitric oxide exposure diverts neural stem cell fate from neurogenesis towards astrogliogenesis. In: *Stem cells (Dayton, Ohio)* 24 (12), S. 2792–2800. DOI: 10.1634/stemcells.2005-0640.

Craelius, W.; Migdal, M. W.; Luessenhop, C. P.; Sugar, A.; Mihalakis, I. (1982): Iron deposits surrounding multiple sclerosis plaques. In: *Archives of pathology & laboratory medicine* 106 (8), S. 397–399.

Crawford, Abbe H.; Tripathi, Richa B.; Foerster, Sarah; McKenzie, Ian; Kougioumtzidou, Eleni; Grist, Matthew et al. (2016): Pre-Existing Mature Oligodendrocytes Do Not Contribute to Remyelination following Toxin-Induced Spinal Cord Demyelination. In: *The American journal of pathology* 186 (3), S. 511–516. DOI: 10.1016/j.ajpath.2015.11.005.

Cui, Qiao-Ling; Kuhlmann, Tanja; Miron, Veronique E.; Leong, Soo Yuen; Fang, Jun; Gris, Pavel et al. (2013): Oligodendrocyte progenitor cell susceptibility to injury in multiple sclerosis. In: *The American journal of pathology* 183 (2), S. 516–525. DOI: 10.1016/j.ajpath.2013.04.016.

Culotta, E.; Koshland, D. E. (1992): NO news is good news. In: *Science (New York, N.Y.)* 258 (5090), S. 1862–1865.

Daily, D.; Vlamis-Gardikas, A.; Offen, D.; Mittelman, L.; Melamed, E.; Holmgren, A.; Barzilai, A. (2001): Glutaredoxin protects cerebellar granule neurons from dopamine-induced apoptosis by dual activation of the ras-phosphoinositide 3-kinase and jun n-terminal kinase pathways. In: *The Journal of biological chemistry* 276 (24), S. 21618–21626. DOI: 10.1074/jbc.M101400200.

Dawson, V. L.; Dawson, T. M.; London, E. D.; Bredt, D. S.; Snyder, S. H. (1991): Nitric oxide mediates glutamate neurotoxicity in primary cortical cultures. In: *Proceedings of the National Academy of Sciences of the United States of America* 88 (14), S. 6368–6371.

De Groot, C J; Ruuls, S. R.; Theeuwes, J. W.; Dijkstra, C. D.; Van der Valk, P (1997): Immunocytochemical characterization of the expression of inducible and constitutive isoforms of nitric oxide synthase in demyelinating multiple sclerosis lesions. In: *Journal of neuropathology and experimental neurology* 56 (1), S. 10–20.

Desai, Roshni A.; Davies, Andrew L.; Tachrount, Mohamed; Kasti, Marianne; Laulund, Frida; Golay, Xavier; Smith, Kenneth J. (2016): Cause and prevention of demyelination in a model multiple sclerosis lesion. In: *Annals of neurology* 79 (4), S. 591–604. DOI: 10.1002/ana.24607.

Dexter, D. T.; Wells, F. R.; Agid, F.; Agid, Y.; Lees, A. J.; Jenner, P.; Marsden, C. D. (1987): Increased nigral iron content in postmortem parkinsonian brain. In: *Lancet (London, England)* 2 (8569), S. 1219–1220.

Di Penta, Alessandra; Moreno, Beatriz; Reix, Stephanie; Fernandez-Diez, Begoña; Villanueva, Maite; Errea, Oihana et al. (2013): Oxidative stress and proinflammatory cytokines contribute to demyelination and axonal damage in a cerebellar culture model of neuroinflammation. In: *PloS one* 8 (2), S. e54722. DOI: 10.1371/journal.pone.0054722.

Dickinson, Bryan C.; Peltier, Joseph; Stone, Daniel; Schaffer, David V.; Chang, Christopher J. (2011): Nox2 redox signaling maintains essential cell populations in the brain. In: *Nature chemical biology* 7 (2), S. 106–112. DOI: 10.1038/nchembio.497.

Dimou, Leda; Götz, Magdalena (2014): Glial cells as progenitors and stem cells: new roles in the healthy and diseased brain. In: *Physiological reviews* 94 (3), S. 709–737. DOI: 10.1152/physrev.00036.2013.

Doke, N.; Miura, Y.; Sanchez, L. M.; Park, H. J.; Noritake, T.; Yoshioka, H.; Kawakita, K. (1996): The oxidative burst protects plants against pathogen attack: mechanism and role as an emergency signal for plant bio-defence--a review. In: *Gene* 179 (1), S. 45–51.

Dowling, P.; Husar, W.; Menonna, J.; Donnenfeld, H.; Cook, S.; Sidhu, M. (1997): Cell death and birth in multiple sclerosis brain. In: *Journal of the neurological sciences* 149 (1), S. 1–11.

Dringen, R. (2000): Metabolism and functions of glutathione in brain. In: *Progress in neurobiology* 62 (6), S. 649–671.

Dubey, Duvyanshu; Kieseier, Bernd C.; Hartung, Hans P.; Hemmer, Bernhard; Warnke, Clemens; Menge, Til et al. (2015): Dimethyl fumarate in relapsing-remitting multiple sclerosis: rationale, mechanisms of action, pharmacokinetics, efficacy and safety. In: *Expert review of neurotherapeutics* 15 (4), S. 339–346. DOI: 10.1586/14737175.2015.1025755.

Eixarch, Herena; Gutiérrez-Franco, Ana; Montalban, Xavier; Espejo, Carmen (2013): Semaphorins 3A and 7A: potential immune and neuroregenerative targets in multiple sclerosis. In: *Trends in molecular medicine* 19 (3), S. 157–164. DOI: 10.1016/j.molmed.2013.01.003.

Ekdahl, Christine T.; Claasen, Jan-Hendrik; Bonde, Sara; Kokaia, Zaal; Lindvall, Olle (2003): Inflammation is detrimental for neurogenesis in adult brain. In: *Proceedings of the National Academy of Sciences of the United States of America* 100 (23), S. 13632–13637. DOI: 10.1073/pnas.2234031100.

Enoksson, Mari; Fernandes, Aristi Potamitou; Prast, Stefanie; Lillig, Christopher Horst; Holmgren, Arne; Orrenius, Sten (2005): Overexpression of glutaredoxin 2 attenuates apoptosis by preventing cytochrome c release. In: *Biochemical and biophysical research communications* 327 (3), S. 774–779. DOI: 10.1016/j.bbrc.2004.12.067.

Farina, Cinthia; Aloisi, Francesca; Meinl, Edgar (2007): Astrocytes are active players in cerebral innate immunity. In: *Trends in immunology* 28 (3), S. 138–145. DOI: 10.1016/j.it.2007.01.005.

Finnie, J. W. (2013): Neuroinflammation: beneficial and detrimental effects after traumatic brain injury. In: *Inflammopharmacology* 21 (4), S. 309–320. DOI: 10.1007/s10787-012-0164-2.

Fitzpatrick, Jessica; Kim, Eunsuk (2015): Synthetic modeling chemistry of iron-sulfur clusters in nitric oxide signaling. In: *Accounts of chemical research* 48 (8), S. 2453–2461. DOI: 10.1021/acs.accounts.5b00246.

Foster, Matthew W.; Cowan, J. A. (1999): Chemistry of Nitric Oxide with Protein-Bound Iron Sulfur Centers. Insights on Physiological Reactivity. In: *J. Am. Chem. Soc.* 121 (17), S. 4093–4100. DOI: 10.1021/ja9901056.

Franklin, Robin J M (2002): Why does remyelination fail in multiple sclerosis? In: *Nature reviews. Neuroscience* 3 (9), S. 705–714. DOI: 10.1038/nrn917.

Frohman, Elliot M.; Racke, Michael K.; Raine, Cedric S. (2006): Multiple sclerosis--the plaque and its pathogenesis. In: *The New England journal of medicine* 354 (9), S. 942–955. DOI: 10.1056/NEJMra052130.

Gard, A. L.; Burrell, M. R.; Pfeiffer, S. E.; Rudge, J. S.; Williams, W. C. (1995): Astroglial control of oligodendrocyte survival mediated by PDGF and leukemia inhibitory factor-like protein. In: *Development (Cambridge, England)* 121 (7), S. 2187–2197.

Gardner, P. R.; Raineri, I.; Epstein, L. B.; White, C. W. (1995): Superoxide radical and iron modulate aconitase activity in mammalian cells. In: *The Journal of biological chemistry* 270 (22), S. 13399–13405.

Garthwaite, J.; Charles, S. L.; Chess-Williams, R. (1988): Endothelium-derived relaxing factor release on activation of NMDA receptors suggests role as intercellular messenger in the brain. In: *Nature* 336 (6197), S. 385–388. DOI: 10.1038/336385a0.

Gellert, Manuela; Hanschmann, Eva-Maria; Lepka, Klaudia; Berndt, Carsten; Lillig, Christopher Horst (2015): Redox regulation of cytoskeletal dynamics during differentiation and de-differentiation. In: *Biochimica et biophysica acta* 1850 (8), S. 1575–1587. DOI: 10.1016/j.bbagen.2014.10.030.

Gellert, Manuela; Venz, Simone; Mitlöhner, Jessica; Cott, Catherine; Hanschmann, Eva-Maria; Lillig, Christopher Horst (2013): Identification of a dithiol-disulfide switch in collapsin response mediator protein 2 (CRMP2) that is toggled in a model of neuronal differentiation. In: *The Journal of biological chemistry* 288 (49), S. 35117–35125. DOI: 10.1074/jbc.M113.521443.

Giliano NY, Konevega LV, Noskin LA, Serezhenkov VA, Poltorakov AP, Vanin AF. 2011. Dinitrosyl iron complexes with thiol-containing ligands and apoptosis: studies with HeLa cell cultures. Nitric oxide : biology and chemistry / official journal of the Nitric Oxide Society 24(3):151–159.

Go, Young-Mi; Jones, Dean P. (2013): The redox proteome. In: *The Journal of biological chemistry* 288 (37), S. 26512–26520. DOI: 10.1074/jbc.R113.464131.

Godoy, José Rodrigo; Funke, Maria; Ackermann, Waltraud; Haunhorst, Petra; Oesteritz, Sabrina; Capani, Francisco et al. (2011): Redox atlas of the mouse. Immunohistochemical detection of glutaredoxin-, peroxiredoxin-, and thioredoxin-family proteins in various tissues of the laboratory mouse. In: *Biochimica et biophysica acta* 1810 (1), S. 2–92. DOI: 10.1016/j.bbagen.2010.05.006.

Gong, Qi-Hai; Shi, Xue-Ru; Hong, Zhen-Yi; Pan, Li-Long; Liu, Xin-Hua; Zhu, Yi-Zhun (2011): A new hope for neurodegeneration: possible role of hydrogen sulfide. In: *Journal of Alzheimer's disease : JAD* 24 Suppl 2, S. 173–182. DOI: 10.3233/JAD-2011-110128.

Grandoni, J. A.; Switzer, R. L.; Makaroff, C. A.; Zalkin, H. (1989): Evidence that the iron-sulfur cluster of Bacillus subtilis glutamine phosphoribosylpyrophosphate amidotransferase determines stability of the enzyme to degradation in vivo. In: *The Journal of biological chemistry* 264 (11), S. 6058–6064.

Greco, A.; Minghetti, L.; Sette, G.; Fieschi, C.; Levi, G. (1999): Cerebrospinal fluid isoprostane shows oxidative stress in patients with multiple sclerosis. In: *Neurology* 53 (8), S. 1876–1879.

Guix, F. X.; Uribesalgo, I.; Coma, M.; Muñoz, F. J. (2005): The physiology and pathophysiology of nitric oxide in the brain. In: *Progress in neurobiology* 76 (2), S. 126–152. DOI: 10.1016/j.pneurobio.2005.06.001.

Guo, Fuzheng; Lang, Jordan; Sohn, Jiho; Hammond, Elizabeth; Chang, Marcello; Pleasure, David (2015): Canonical Wnt signaling in the oligodendroglial lineage--puzzles remain. In: *Glia* 63 (10), S. 1671–1693. DOI: 10.1002/glia.22813.

Gutiérrez-Franco, Ana; Costa, Carme; Eixarch, Herena; Castillo, Mireia; Medina-Rodríguez, Eva M.; Bribián, Ana et al. (2016): Differential expression of sema3A and sema7A in a murine model of multiple sclerosis: Implications for a therapeutic design. In: *Clinical immunology (Orlando, Fla.)* 163, S. 22–33. DOI: 10.1016/j.clim.2015.12.005.

Gutteridge, J. M.; Halliwell, B. (1989): Iron toxicity and oxygen radicals. In: *Baillière's clinical haematology* 2 (2), S. 195–256.

Haider, Lukas; Fischer, Marie T.; Frischer, Josa M.; Bauer, Jan; Höftberger, Romana; Botond, Gergö et al. (2011): Oxidative damage in multiple sclerosis lesions. In: *Brain : a journal of neurology* 134 (Pt 7), S. 1914–1924. DOI: 10.1093/brain/awr128.

HALLGREN, B.; SOURANDER, P. (1958): The effect of age on the non-haemin iron in the human brain. In: *Journal of neurochemistry* 3 (1), S. 41–51.

Hancock, J. T.; Whiteman, M. (2014): Hydrogen sulfide and cell signaling: team player or referee? In: *Plant physiology and biochemistry : PPB / Société française de physiologie végétale* 78, S. 37–42. DOI: 10.1016/j.plaphy.2014.02.012.

Hancock, John T.; Whiteman, Matthew (2016): Hydrogen sulfide signaling: interactions with nitric oxide and reactive oxygen species. In: *Annals of the New York Academy of Sciences* 1365 (1), S. 5–14. DOI: 10.1111/nyas.12733.

Hanisch, Uwe-Karsten; Kettenmann, Helmut (2007): Microglia: active sensor and versatile effector cells in the normal and pathologic brain. In: *Nature neuroscience* 10 (11), S. 1387–1394. DOI: 10.1038/nn1997.

Hanschmann, Eva-Maria; Godoy, José Rodrigo; Berndt, Carsten; Hudemann, Christoph; Lillig, Christopher Horst (2013): Thioredoxins, glutaredoxins, and peroxiredoxins--molecular mechanisms and health significance: from cofactors to antioxidants to redox signaling. In: *Antioxidants & redox signaling* 19 (13), S. 1539–1605. DOI: 10.1089/ars.2012.4599.

Hansen, L. A.; Willenborg, D. O.; Cowden, W. B. (1995): Suppression of hyperacute and passively transferred experimental autoimmune encephalomyelitis by the anti-oxidant, butylated hydroxyanisole. In: *Journal of neuroimmunology* 62 (1), S. 69–77.

Harrer, Melanie D.; Büdingen, Hans-Christian von; Stoppini, Luc; Alliod, Chantal; Pouly, Sandrine; Fischer, Katja; Goebels, Norbert (2009): Live imaging of remyelination after antibody-mediated demyelination in an ex-vivo model for immune mediated CNS damage. In: *Experimental neurology* 216 (2), S. 431–438.

Hart, Terance W. (1985): Some observations concerning the S-nitroso and S-phenylsulphonyl derivatives of L-cysteine and glutathione. In: *Tetrahedron Letters* 26 (16), S. 2013–2016. DOI: 10.1016/S0040-4039(00)98368-0.

Hartz, A M S; Bauer, B. (2011): ABC transporters in the CNS - an inventory. In: *Current pharmaceutical biotechnology* 12 (4), S. 656–673.

Hashemy, Seyed Isaac; Johansson, Catrine; Berndt, Carsten; Lillig, Christopher Horst; Holmgren, Arne (2007): Oxidation and S-nitrosylation of cysteines in human cytosolic and mitochondrial glutaredoxins: effects on structure and activity. In: *The Journal of biological chemistry* 282 (19), S. 14428–14436. DOI: 10.1074/jbc.M700927200.

Hattori, Itaro; Takagi, Yasushi; Nakamura, Hajime; Nozaki, Kazuhiko; Bai, Jie; Kondo, Norihiko et al. (2004): Intravenous administration of thioredoxin decreases brain damage following transient focal cerebral ischemia in mice. In: *Antioxidants & redox signaling* 6 (1), S. 81–87. DOI: 10.1089/152308604771978372.

Haunhorst, Petra; Berndt, Carsten; Eitner, Susanne; Godoy, José R.; Lillig, Christopher Horst (2010): Characterization of the human monothiol glutaredoxin 3 (PICOT) as iron-sulfur protein. In: *Biochemical and biophysical research communications* 394 (2), S. 372–376. DOI: 10.1016/j.bbrc.2010.03.016.

Haunhorst, Petra; Hanschmann, Eva-Maria; Bräutigam, Lars; Stehling, Oliver; Hoffmann, Bastian; Mühlenhoff, Ulrich et al. (2013): Crucial function of vertebrate glutaredoxin 3 (PICOT) in iron homeostasis and hemoglobin maturation. In: *Molecular biology of the cell* 24 (12), S. 1895–1903. DOI: 10.1091/mbc.E12-09-0648.

Hemmer, Bernhard; Archelos, Juan J.; Hartung, Hans-Peter (2002a): New concepts in the immunopathogenesis of multiple sclerosis. In: *Nature reviews. Neuroscience* 3 (4), S. 291–301. DOI: 10.1038/nrn784.

Hemmer, Bernhard; Cepok, Sabine; Nessler, Stefan; Sommer, Norbert (2002b): Pathogenesis of multiple sclerosis: an update on immunology. In: *Current opinion in neurology* 15 (3), S. 227–231.

Henry, Christopher J.; Huang, Yan; Wynne, Angela; Hanke, Mark; Himler, Justin; Bailey, Michael T. et al. (2008): Minocycline attenuates lipopolysaccharide (LPS)-induced neuroinflammation, sickness behavior, and anhedonia. In: *Journal of neuroinflammation* 5, S. 15. DOI: 10.1186/1742-2094-5-15.

Hernán, M. A.; Zhang, S. M.; Lipworth, L.; Olek, M. J.; Ascherio, A. (2001): Multiple sclerosis and age at infection with common viruses. In: *Epidemiology (Cambridge, Mass.)* 12 (3), S. 301–306.

Hill, Kenneth E.; Zollinger, Lauren V.; Watt, Hilary E.; Carlson, Noel G.; Rose, John W. (2004): Inducible nitric oxide synthase in chronic active multiple sclerosis plaques: distribution, cellular expression and association with myelin damage. In: *Journal of neuroimmunology* 151 (1-2), S. 171–179. DOI: 10.1016/j.jneuroim.2004.02.005.

Hirling, H.; Henderson, B. R.; Kühn, L. C. (1994): Mutational analysis of the [4Fe-4S]-cluster converting iron regulatory factor from its RNA-binding form to cytoplasmic aconitase. In: *The EMBO journal* 13 (2), S. 453–461.

Hirrlinger, Johannes; König, Jörg; Dringen, Ralf (2002): Expression of mRNAs of multidrug resistance proteins (Mrps) in cultured rat astrocytes, oligodendrocytes, microglial cells and neurones. In: *Journal of neurochemistry* 82 (3), S. 716–719.

Hohlfeld, Reinhard; Dornmair, Klaus; Meinl, Edgar; Wekerle, Hartmut (2016): The search for the target antigens of multiple sclerosis, part 2: CD8+ T cells, B cells, and antibodies in the focus of reverse-translational research. In: *The Lancet. Neurology* 15 (3), S. 317–331. DOI: 10.1016/S1474-4422(15)00313-0.

Holley, J. E.; Newcombe, J.; Winyard, P. G.; Gutowski, N. J. (2007): Peroxiredoxin V in multiple sclerosis lesions: predominant expression by astrocytes. In: *Multiple sclerosis (Houndmills, Basingstoke, England)* 13 (8), S. 955–961. DOI: 10.1177/1352458507078064.

Holloway, Kimberly R.; Calhoun, Tara N.; Saxena, Madhurima; Metoyer, Cheynita F.; Kandler, Ethan F.; Rivera, Chantal A.; Pruitt, Kevin (2010): SIRT1 regulates Dishevelled proteins and promotes transient and constitutive Wnt signaling. In: *Proceedings of the National Academy of Sciences of the United States of America* 107 (20), S. 9216–9221. DOI: 10.1073/pnas.0911325107.

Holmgren, A. (1979): Glutathione-dependent synthesis of deoxyribonucleotides. Characterization of the enzymatic mechanism of Escherichia coli glutaredoxin. In: *The Journal of biological chemistry* 254 (9), S. 3672–3678.

Horwitz, M. S.; Evans, C. F.; McGavern, D. B.; Rodriguez, M.; Oldstone, M. B. (1997): Primary demyelination in transgenic mice expressing interferon-gamma. In: *Nature medicine* 3 (9), S. 1037–1041.

Hu, Bin; Guo, Ye; Chen, Chunyuan; Li, Qing; Niu, Xin; Guo, Shangchun et al. (2014): Repression of SIRT1 promotes the differentiation of mouse induced pluripotent stem cells into neural stem cells. In: *Cellular and molecular neurobiology* 34 (6), S. 905–912. DOI: 10.1007/s10571-014-0071-8.

Hudemann, Christoph; Lönn, Maria Elisabet; Godoy, José Rodrigo; Zahedi Avval, Farnaz; Capani, Francisco; Holmgren, Arne; Lillig, Christopher Horst (2009): Identification, expression pattern, and characterization of mouse glutaredoxin 2 isoforms. In: *Antioxidants & redox signaling* 11 (1), S. 1–14. DOI: 10.1089/ars.2008.2068.

Huehnchen, Petra; Prozorovski, Timour; Klaissle, Philipp; Lesemann, Anne; Ingwersen, Jens; Wolf, Susanne A. et al. (2011): Modulation of adult hippocampal neurogenesis during myelin-directed autoimmune neuroinflammation. In: *Glia* 59 (1), S. 132–142. DOI: 10.1002/glia.21082.

Huie, R. E.; Padmaja, S. (1993): The reaction of no with superoxide. In: *Free radical research communications* 18 (4), S. 195–199.

Hurd, Thomas Ryan; DeGennaro, Matthew; Lehmann, Ruth (2012): Redox regulation of cell migration and adhesion. In: *Trends in cell biology* 22 (2), S. 107–115. DOI: 10.1016/j.tcb.2011.11.002.

Hwang, In Koo; Yoo, Ki-Yeon; Kim, Dae Won; Lee, Choong Hyun; Choi, Jung Hoon; Kwon, Young-Guen et al. (2010): Changes in the expression of mitochondrial peroxiredoxin and thioredoxin in neurons and glia and their protective effects in experimental cerebral ischemic damage. In: *Free radical biology & medicine* 48 (9), S. 1242–1251. DOI: 10.1016/j.freeradbiomed.2010.02.007.

Ingwersen, Jens; Aktas, Orhan; Kuery, Patrick; Kieseier, Bernd; Boyko, Alexey; Hartung, Hans-Peter (2012): Fingolimod in multiple sclerosis: mechanisms of action and clinical efficacy. In: *Clinical immunology (Orlando, Fla.)* 142 (1), S. 15–24. DOI: 10.1016/j.clim.2011.05.005.

Jack, Carolyn; Antel, Jack; Brück, Wolfgang; Kuhlmann, Tanja (2007): Contrasting potential of nitric oxide and peroxynitrite to mediate oligodendrocyte injury in multiple sclerosis. In: *Glia* 55 (9), S. 926–934. DOI: 10.1002/glia.20514.

Jamil, Nuor S M; Azfer, Asim; Worrell, Harrison; Salter, Donald M. (2016): Functional roles of CSPG4/NG2 in chondrosarcoma. In: *International journal of experimental pathology* 97 (2), S. 178–186. DOI: 10.1111/iep.12189.

Jana, Malabendu; Pahan, Kalipada (2005): Redox regulation of cytokine-mediated inhibition of myelin gene expression in human primary oligodendrocytes. In: *Free radical biology & medicine* 39 (6), S. 823–831. DOI: 10.1016/j.freeradbiomed.2005.05.014.

Jimenez-Blasco, D.; Santofimia-Castaño, P.; Gonzalez, A.; Almeida, A.; Bolaños, J. P. (2015): Astrocyte NMDA receptors' activity sustains neuronal survival through a Cdk5-Nrf2 pathway. In: *Cell death and differentiation* 22 (11), S. 1877–1889. DOI: 10.1038/cdd.2015.49.

Johansson, Catrine; Kavanagh, Kathryn L.; Gileadi, Opher; Oppermann, Udo (2007): Reversible sequestration of active site cysteines in a 2Fe-2S-bridged dimer provides a mechanism for glutaredoxin 2 regulation in human mitochondria. In: *The Journal of biological chemistry* 282 (5), S. 3077–3082. DOI: 10.1074/jbc.M608179200.

Johansson, Catrine; Lillig, Christopher Horst; Holmgren, Arne (2004): Human mitochondrial glutaredoxin reduces S-glutathionylated proteins with high affinity accepting electrons from either glutathione or thioredoxin reductase. In: *The Journal of biological chemistry* 279 (9), S. 7537–7543. DOI: 10.1074/jbc.M312719200.

Johnson, Delinda A.; Johnson, Jeffrey A. (2015): Nrf2--a therapeutic target for the treatment of neurodegenerative diseases. In: *Free radical biology & medicine* 88 (Pt B), S. 253–267. DOI: 10.1016/j.freeradbiomed.2015.07.147.

Johri, Ashu; Beal, M. Flint (2012): Mitochondrial dysfunction in neurodegenerative diseases. In: *The Journal of pharmacology and experimental therapeutics* 342 (3), S. 619–630. DOI: 10.1124/jpet.112.192138.

Jolivalt, Corinne G.; Howard, Randy B.; Chen, Long S.; Mizisin, Andrew P.; Lai, Ching-San (2003): A novel nitric oxide scavenger in combination with cyclosporine A ameliorates experimental autoimmune encephalomyelitis progression in mice. In: *Journal of neuroimmunology* 138 (1-2), S. 56–64.

Jones, Dean P.; Sies, Helmut (2015): The Redox Code. In: *Antioxidants & redox signaling* 23 (9), S. 734–746. DOI: 10.1089/ars.2015.6247.

Jonnala, R. R.; Buccafusco, J. J. (2001): Inhibition of nerve growth factor signaling by peroxynitrite. In: *Journal of neuroscience research* 63 (1), S. 27–34.

Joshi, Mahesh S.; Ferguson, T. Bruce; Han, Tae H.; Hyduke, Daniel R.; Liao, James C.; Rassaf, Tienush et al. (2002): Nitric oxide is consumed, rather than conserved, by reaction with

oxyhemoglobin under physiological conditions. In: *Proceedings of the National Academy of Sciences of the United States of America* 99 (16), S. 10341–10346. DOI: 10.1073/pnas.152149699.

Karunakaran, Smitha; Saeed, Uzma; Ramakrishnan, Sujanitha; Koumar, Ratnacaram Chandrahaas; Ravindranath, Vijayalakshmi (2007): Constitutive expression and functional characterization of mitochondrial glutaredoxin (Grx2) in mouse and human brain. In: *Brain research* 1185, S. 8–17. DOI: 10.1016/j.brainres.2007.09.019.

Keese, M. A.; Böse, M.; Mülsch, A.; Schirmer, R. H.; Becker, K. (1997): Dinitrosyl-dithiol-iron complexes, nitric oxide (NO) carriers in vivo, as potent inhibitors of human glutathione reductase and glutathione-S-transferase. In: *Biochemical pharmacology* 54 (12), S. 1307–1313.

Keirstead, H. S.; Blakemore, W. F. (1997): Identification of post-mitotic oligodendrocytes incapable of remyelination within the demyelinated adult spinal cord. In: *Journal of neuropathology and experimental neurology* 56 (11), S. 1191–1201.

Kennedy, M. C.; Antholine, W. E.; Beinert, H. (1997): An EPR investigation of the products of the reaction of cytosolic and mitochondrial aconitases with nitric oxide. In: *The Journal of biological chemistry* 272 (33), S. 20340–20347.

Keough, Michael B.; Jensen, Samuel K.; Yong, V. Wee (2015): Experimental demyelination and remyelination of murine spinal cord by focal injection of lysolecithin. In: *Journal of visualized experiments : JoVE* (97). DOI: 10.3791/52679.

Keynes, Robert G.; Duport, Sophie; Garthwaite, John (2004): Hippocampal neurons in organotypic slice culture are highly resistant to damage by endogenous and exogenous nitric oxide. In: *The European journal of neuroscience* 19 (5), S. 1163–1173. DOI: 10.1111/j.1460-9568.2004.03217.x.

Kida, Kotaro; Ichinose, Fumito (2015): Hydrogen Sulfide and Neuroinflammation. In: *Handbook of experimental pharmacology* 230, S. 181–189. DOI: 10.1007/978-3-319-18144-8_9.

Kim YM, Chung HT, Simmons RL, Billiar TR. 2000. Cellular non-heme iron content is a determinant of nitric oxide-mediated apoptosis, necrosis, and caspase inhibition. The Journal of biological chemistry 275(15):10954–10961.

Kipp, Markus; van der Star, Baukje; Vogel, Daphne Y S; Puentes, Fabìola; van der Valk, Paul; Baker, David; Amor, Sandra (2012): Experimental in vivo and in vitro models of multiple sclerosis: EAE and beyond. In: *Multiple sclerosis and related disorders* 1 (1), S. 15–28. DOI: 10.1016/j.msard.2011.09.002.

Koch, Marcus; Ramsaransing, Geeta S M; Arutjunyan, Alexander V.; Stepanov, Michael; Teelken, Albert; Heersema, Dorothea J.; Keyser, Jacques de (2006): Oxidative stress in serum and peripheral blood leukocytes in patients with different disease courses of multiple sclerosis. In: *Journal of neurology* 253 (4), S. 483–487. DOI: 10.1007/s00415-005-0037-3.

Korge, Paavo; Calmettes, Guillaume; Weiss, James N. (2015): Increased reactive oxygen species production during reductive stress: The roles of mitochondrial glutathione and thioredoxin reductases. In: *Biochimica et biophysica acta* 1847 (6-7), S. 514–525. DOI: 10.1016/j.bbabio.2015.02.012.

Kotter, Mark R.; Li, Wen-Wu; Zhao, Chao; Franklin, Robin J M (2006): Myelin impairs CNS remyelination by inhibiting oligodendrocyte precursor cell differentiation. In: *The Journal of neuroscience : the official journal of the Society for Neuroscience* 26 (1), S. 328–332. DOI: 10.1523/JNEUROSCI.2615-05.2006.

Kremer, David; Aktas, Orhan; Hartung, Hans-Peter; Küry, Patrick (2011): The complex world of oligodendroglial differentiation inhibitors. In: *Ann Neurol.* 69 (4), S. 602–618. DOI: 10.1002/ana.22415.

Kremer, David; Göttle, Peter; Hartung, Hans-Peter; Küry, Patrick (2016): Pushing Forward: Remyelination as the New Frontier in CNS Diseases. In: *Trends in neurosciences* 39 (4), S. 246–263. DOI: 10.1016/j.tins.2016.02.004.

Kucharova, Karolina; Stallcup, William B. (2015): NG2-proteoglycan-dependent contributions of oligodendrocyte progenitors and myeloid cells to myelin damage and repair. In: *Journal of neuroinflammation* 12, S. 161. DOI: 10.1186/s12974-015-0385-6.

Kukley, Maria; Nishiyama, Akiko; Dietrich, Dirk (2010): The fate of synaptic input to NG2 glial cells: neurons specifically downregulate transmitter release onto differentiating oligodendroglial cells. In: *The Journal of neuroscience : the official journal of the Society for Neuroscience* 30 (24), S. 8320–8331. DOI: 10.1523/JNEUROSCI.0854-10.2010.

Le Belle, Janel E; Orozco, Nicolas M.; Paucar, Andres A.; Saxe, Jonathan P.; Mottahedeh, Jack; Pyle, April D. et al. (2011): Proliferative neural stem cells have high endogenous ROS levels that regulate self-renewal and neurogenesis in a PI3K/Akt-dependant manner. In: *Cell stem cell* 8 (1), S. 59–71. DOI: 10.1016/j.stem.2010.11.028.

Lee, Donna W.; Kaur, Deepinder; Chinta, Shankar J.; Rajagopalan, Subramanian; Andersen, Julie K. (2009): A disruption in iron-sulfur center biogenesis via inhibition of mitochondrial dithiol glutaredoxin 2 may contribute to mitochondrial and cellular iron dysregulation in mammalian glutathione-depleted dopaminergic cells: implications for Parkinson's disease. In: *Antioxidants & redox signaling* 11 (9), S. 2083–2094. DOI: 10.1089/ars.2009.2489.

Lee, S. C.; Moore, G. R.; Golenwsky, G.; Raine, C. S. (1990): Multiple sclerosis: a role for astroglia in active demyelination suggested by class II MHC expression and ultrastructural study. In: *Journal of neuropathology and experimental neurology* 49 (2), S. 122–136.

Lepka, Klaudia; Berndt, Carsten; Hartung, Hans-Peter; Aktas, Orhan (2016): Redox Events As Modulators of Pathology and Therapy of Neuroinflammatory Diseases. In: *Frontiers in cell and developmental biology* 4, S. 63. DOI: 10.3389/fcell.2016.00063.

Lewandowska, Hanna; Sadło, Jarosław; Męczyńska, Sylwia; Stępkowski, Tomasz M.; Wójciuk, Grzegorz; Kruszewski, Marcin (2015): Formation of glutathionyl dinitrosyl iron complexes protects against iron genotoxicity. In: *Dalton transactions (Cambridge, England : 2003)* 44 (28), S. 12640–12652. DOI: 10.1039/c5dt00927h.

Li, Jianrong; Baud, Olivier; Vartanian, Timothy; Volpe, Joseph J.; Rosenberg, Paul A. (2005): Peroxynitrite generated by inducible nitric oxide synthase and NADPH oxidase mediates microglial toxicity to oligodendrocytes. In: *Proceedings of the National Academy of Sciences of the United States of America* 102 (28), S. 9936–9941. DOI: 10.1073/pnas.0502552102.

Li, Jianrong; Ramenaden, E. Radhika; Peng, Jie; Koito, Hisami; Volpe, Joseph J.; Rosenberg, Paul A. (2008): Tumor necrosis factor alpha mediates lipopolysaccharide-induced microglial toxicity to developing oligodendrocytes when astrocytes are present. In: *The Journal of neuroscience : the official journal of the Society for Neuroscience* 28 (20), S. 5321–5330. DOI: 10.1523/JNEUROSCI.3995-07.2008.

Li, Tong; Liu, Hansen; Xue, Hao; Zhang, Jinsen; Han, Xiao; Yan, Shaofeng et al. (2016): Neuroprotective effects of hydrogen sulfide against early brain injury and secondary cognitive deficits following subarachnoid hemorrhage. In: *Brain pathology (Zurich, Switzerland). DOI:* 10.1111/bpa.12361.

Lillig, Christopher Horst; Berndt, Carsten; Vergnolle, Olivia; Lönn, Maria Elisabet; Hudemann, Christoph; Bill, Eckhard; Holmgren, Arne (2005): Characterization of human glutaredoxin 2 as iron-sulfur protein: a possible role as redox sensor. In: *Proceedings of the National Academy of Sciences of the United States of America* 102 (23), S. 8168–8173. DOI: 10.1073/pnas.0500735102.

Lillig, Christopher Horst; Lönn, Maria Elisabet; Enoksson, Mari; Fernandes, Aristi Potamitou; Holmgren, Arne (2004): Short interfering RNA-mediated silencing of glutaredoxin 2 increases the sensitivity of HeLa cells toward doxorubicin and phenylarsine oxide. In: *Proceedings of the National Academy of Sciences of the United States of America* 101 (36), S. 13227–13232. DOI: 10.1073/pnas.0401896101.

Liu, J. S.; Zhao, M. L.; Brosnan, C. F.; Lee, S. C. (2001): Expression of inducible nitric oxide synthase and nitrotyrosine in multiple sclerosis lesions. In: *The American journal of pathology* 158 (6), S. 2057–2066. DOI: 10.1016/S0002-9440(10)64677-9.

Ljubisavljevic, Srdjan; Stojanovic, Ivana; Pavlovic, Dusica; Milojkovic, Maja; Vojinovic, Slobodan; Sokolovic, Dusan; Stevanovic, Ivana (2012): Correlation of nitric oxide levels in the cerebellum and spinal cord of experimental autoimmune encephalomyelitis rats with clinical symptoms. In: *Acta neurobiologiae experimentalis* 72 (1), S. 33–39.

Lok, Hiu Chuen; Suryo Rahmanto, Yohan; Hawkins, Clare L.; Kalinowski, Danuta S.; Morrow, Charles S.; Townsend, Alan J. et al. (2012): Nitric oxide storage and transport in cells are mediated by glutathione S-transferase P1-1 and multidrug resistance protein 1 via dinitrosyl iron complexes. In: *The Journal of biological chemistry* 287 (1), S. 607–618. DOI: 10.1074/jbc.M111.310987.

Lönn, Maria Elisabet; Hudemann, Christoph; Berndt, Carsten; Cherkasov, Valeria; Capani, Francisco; Holmgren, Arne; Lillig, Christopher Horst (2008): Expression pattern of human glutaredoxin 2 isoforms: identification and characterization of two testis/cancer cell-specific isoforms. In: *Antioxidants & redox signaling* 10 (3), S. 547–557. DOI: 10.1089/ars.2007.1821.

Lu, Changyuan; Koppenol, Willem H. (2005): Inhibition of the Fenton reaction by nitrogen monoxide. In: *Journal of biological inorganic chemistry : JBIC : a publication of the Society of Biological Inorganic Chemistry* 10 (7), S. 732–738. DOI: 10.1007/s00775-005-0019-z.

Lucin, Kurt M.; Wyss-Coray, Tony (2009): Immune activation in brain aging and neurodegeneration: too much or too little? In: *Neuron* 64 (1), S. 110–122. DOI: 10.1016/j.neuron.2009.08.039.

Lundberg, Mathias; Fernandes, Aristi Potamitou; Kumar, Sushil; Holmgren, Arne (2004): Cellular and plasma levels of human glutaredoxin 1 and 2 detected by sensitive ELISA systems. In: *Biochemical and biophysical research communications* 319 (3), S. 801–809. DOI: 10.1016/j.bbrc.2004.04.199.

Luthman, M.; Eriksson, S.; Holmgren, A.; Thelander, L. (1979): Glutathione-dependent hydrogen donor system for calf thymus ribonucleoside-diphosphate reductase. In: *Proceedings of the National Academy of Sciences of the United States of America* 76 (5), S. 2158–2162.

Lutton, J. D.; Winston, R.; Rodman, T. C. (2004): Multiple sclerosis: etiological mechanisms and future directions. In: *Experimental biology and medicine (Maywood, N.J.)* 229 (1), S. 12–20.

Mahad, Don; Ziabreva, Iryna; Lassmann, Hans; Turnbull, Douglas (2008): Mitochondrial defects in acute multiple sclerosis lesions. In: *Brain : a journal of neurology* 131 (Pt 7), S. 1722–1735. DOI: 10.1093/brain/awn105.

Mander, Palwinder; Brown, Guy C. (2005): Activation of microglial NADPH oxidase is synergistic with glial iNOS expression in inducing neuronal death: a dual-key mechanism of inflammatory neurodegeneration. In: *Journal of neuroinflammation* 2, S. 20. DOI: 10.1186/1742-2094-2-20.

Martelli, Alain; Wattenhofer-Donzé, Marie; Schmucker, Stéphane; Bouvet, Samuel; Reutenauer, Laurence; Puccio, Hélène (2007): Frataxin is essential for extramitochondrial Fe-S cluster proteins in mammalian tissues. In: *Human molecular genetics* 16 (22), S. 2651–2658. DOI: 10.1093/hmg/ddm163.

McCann, S. M.; Karanth, S.; Kimura, M.; Yu, W. H.; Rettori, V. (1996): The role of nitric oxide (NO) in control of hypothalamic-pituitary function. In: *Revista brasileira de biologia* 56 Su 1 Pt 1, S. 105–112.

McDonagh, Brian; Padilla, C. Alicia; Pedrajas, José Rafael; Bárcena, José Antonio (2011): Biosynthetic and iron metabolism is regulated by thiol proteome changes dependent on glutaredoxin-2 and mitochondrial peroxiredoxin-1 in Saccharomyces cerevisiae. In: *The Journal of biological chemistry* 286 (17), S. 15565–15576. DOI: 10.1074/jbc.M110.193102.

McFarland, Henry F.; Martin, Roland (2007): Multiple sclerosis: a complicated picture of autoimmunity. In: *Nature immunology* 8 (9), S. 913–919. DOI: 10.1038/ni1507.

Mestas, Javier; Hughes, Christopher C W (2004): Of mice and not men: differences between mouse and human immunology. In: *Journal of immunology (Baltimore, Md. : 1950)* 172 (5), S. 2731–2738.

Miller, Olga Gorelenkova; Behring, Jessica Belle; Siedlak, Sandra L.; Jiang, Sirui; Matsui, Reiko; Bachschmid, Markus M. et al. (2016): Upregulation of Glutaredoxin-1 Activates Microglia and Promotes Neurodegeneration: Implications for Parkinson's Disease. In: *Antioxidants & redox signaling. DOI:* 10.1089/ars.2015.6598.

Miron, Veronique E.; Boyd, Amanda; Zhao, Jing-Wei; Yuen, Tracy J.; Ruckh, Julia M.; Shadrach, Jennifer L. et al. (2013): M2 microglia and macrophages drive oligodendrocyte differentiation during CNS remyelination. In: *Nat Neurosci* 16 (9), S. 1211–1218. DOI: 10.1038/nn.3469.

Miron, Veronique E.; Kuhlmann, Tanja; Antel, Jack P. (2011): Cells of the oligodendroglial lineage, myelination, and remyelination. In: *Biochimica et Biophysica Acta (BBA) - Molecular Basis of Disease* 1812 (2), S. 184–193. DOI: 10.1016/j.bbadis.2010.09.010.

Mitchell, K. M.; Dotson, A. L.; Cool, K. M.; Chakrabarty, A.; Benedict, S. H.; LeVine, S. M. (2007): Deferiprone, an orally deliverable iron chelator, ameliorates experimental autoimmune encephalomyelitis. In: *Multiple sclerosis (Houndmills, Basingstoke, England)* 13 (9), S. 1118–1126. DOI: 10.1177/1352458507078916.

Mix, Eilhard; Meyer-Rienecker, Hans; Hartung, Hans-Peter; Zettl, Uwe K. (2010): Animal models of multiple sclerosis--potentials and limitations. In: *Progress in neurobiology* 92 (3), S. 386–404. DOI: 10.1016/j.pneurobio.2010.06.005.

Morganti-Kossman, M. C.; Lenzlinger, P. M.; Hans, V.; Stahel, P.; Csuka, E.; Ammann, E. et al. (1997): Production of cytokines following brain injury: beneficial and deleterious for the damaged tissue. In: *Molecular psychiatry* 2 (2), S. 133–136.

Mühlenhoff, Ulrich; Gerber, Jana; Richhardt, Nadine; Lill, Roland (2003): Components involved in assembly and dislocation of iron-sulfur clusters on the scaffold protein Isu1p. In: *The EMBO journal* 22 (18), S. 4815–4825. DOI: 10.1093/emboj/cdg446.

Mühlenhoff, Ulrich; Molik, Sabine; Godoy, José R.; Uzarska, Marta A.; Richter, Nadine; Seubert, Andreas et al. (2010): Cytosolic monothiol glutaredoxins function in intracellular iron sensing and trafficking via their bound iron-sulfur cluster. In: *Cell metabolism* 12 (4), S. 373–385. DOI: 10.1016/j.cmet.2010.08.001.

Neumann, H.; Kotter, M. R.; Franklin, R J M (2009): Debris clearance by microglia: an essential link between degeneration and regeneration. In: *Brain : a journal of neurology* 132 (Pt 2), S. 288–295. DOI: 10.1093/brain/awn109.

Nijland, Philip G.; Witte, Maarten E.; van het Hof, Bert; van der Pol, Susanne; Bauer, Jan; Lassmann, Hans et al. (2014): Astroglial PGC-1alpha increases mitochondrial antioxidant capacity and suppresses inflammation: implications for multiple sclerosis. In: *Acta neuropathologica communications* 2, S. 170. DOI: 10.1186/s40478-014-0170-2.

Nishiyama, Akiko; Komitova, Mila; Suzuki, Ryusuke; Zhu, Xiaoqin (2009): Polydendrocytes (NG2 cells): multifunctional cells with lineage plasticity. In: *Nature reviews. Neuroscience* 10 (1), S. 9–22. DOI: 10.1038/nrn2495.

Noble, M.; Murray, K.; Stroobant, P.; Waterfield, M. D.; Riddle, P. (1988): Platelet-derived growth factor promotes division and motility and inhibits premature differentiation of the oligodendrocyte/type-2 astrocyte progenitor cell. In: *Nature* 333 (6173), S. 560–562. DOI: 10.1038/333560a0.

Oksenberg, Jorge R. (2013): Decoding multiple sclerosis: an update on genomics and future directions. In: *Expert review of neurotherapeutics* 13 (12 Suppl), S. 11–19. DOI: 10.1586/14737175.2013.865867.

Oleszak, E. L.; Zaczynska, E.; Bhattacharjee, M.; Butunoi, C.; Legido, A.; Katsetos, C. D. (1998): Inducible nitric oxide synthase and nitrotyrosine are found in monocytes/macrophages and/or

astrocytes in acute, but not in chronic, multiple sclerosis. In: *Clinical and diagnostic laboratory immunology* 5 (4), S. 438–445.

Oria, R.; Sánchez, L.; Houston, T.; Hentze, M. W.; Liew, F. Y.; Brock, J. H. (1995): Effect of nitric oxide on expression of transferrin receptor and ferritin and on cellular iron metabolism in K562 human erythroleukemia cells. In: *Blood* 85 (10), S. 2962–2966.

Oshiro, S.; Kawahara, M.; Kuroda, Y.; Zhang, C.; Cai, Y.; Kitajima, S.; Shirao, M. (2000): Glial cells contribute more to iron and aluminum accumulation but are more resistant to oxidative stress than neuronal cells. In: *Biochimica et biophysica acta* 1502 (3), S. 405–414.

Owens, T.; Wekerle, H.; Antel, J. (2001): Genetic models for CNS inflammation. In: *Nature medicine* 7 (2), S. 161–166. DOI: 10.1038/84603.

Ozawa, K.; Suchanek, G.; Breitschopf, H.; Brück, W.; Budka, H.; Jellinger, K.; Lassmann, H. (1994): Patterns of oligodendroglia pathology in multiple sclerosis. In: *Brain : a journal of neurology* 117 (Pt 6), S. 1311–1322.

Pacher, Pál; Beckman, Joseph S.; Liaudet, Lucas (2007): Nitric oxide and peroxynitrite in health and disease. In: *Physiological reviews* 87 (1), S. 315–424. DOI: 10.1152/physrev.00029.2006.

Packer, Michael A.; Stasiv, Yuri; Benraiss, Abdellatif; Chmielnicki, Eva; Grinberg, Alexander; Westphal, Heiner et al. (2003): Nitric oxide negatively regulates mammalian adult neurogenesis. In: *Proceedings of the National Academy of Sciences of the United States of America* 100 (16), S. 9566–9571. DOI: 10.1073/pnas.1633579100.

Paiva, Claudia N.; Bozza, Marcelo T. (2014): Are reactive oxygen species always detrimental to pathogens? In: *Antioxidants & redox signaling* 20 (6), S. 1000–1037. DOI: 10.1089/ars.2013.5447.

Palmer, R. M.; Ferrige, A. G.; Moncada, S. (1987): Nitric oxide release accounts for the biological activity of endothelium-derived relaxing factor. In: *Nature* 327 (6122), S. 524–526. DOI: 10.1038/327524a0.

Pang, Y.; Campbell, L.; Zheng, B.; Fan, L.; Cai, Z.; Rhodes, P. (2010): Lipopolysaccharide-activated microglia induce death of oligodendrocyte progenitor cells and impede their development. In: *Neuroscience* 166 (2), S. 464–475. DOI: 10.1016/j.neuroscience.2009.12.040.

Pantopoulos, K.; Hentze, M. W. (1995): Rapid responses to oxidative stress mediated by iron regulatory protein. In: *The EMBO journal* 14 (12), S. 2917–2924.

Pérez Estrada, Cynthia; Covacu, Ruxandra; Sankavaram, Sreenivasa R.; Svensson, Mikael; Brundin, Lou (2014): Oxidative stress increases neurogenesis and oligodendrogenesis in adult neural progenitor cells. In: *Stem cells and development* 23 (19), S. 2311–2327. DOI: 10.1089/scd.2013.0452.

Prineas, J. (1975): Pathology of the early lesion in multiple sclerosis. In: *Human pathology* 6 (5), S. 531–554.

Prozorovski, Timour; Schulze-Topphoff, Ulf; Glumm, Robert; Baumgart, Jan; Schröter, Friederike; Ninnemann, Olaf et al. (2008): Sirt1 contributes critically to the redox-dependent fate of neural progenitors. In: *Nature cell biology* 10 (4), S. 385–394. DOI: 10.1038/ncb1700.

Qi, Wenbin; Li, Jingwei; Chain, C. Y.; Pasquevich, G. A.; Pasquevich, A. F.; Cowan, J. A. (2012): Glutathione Complexed Fe–S Centers. In: *J. Am. Chem. Soc.* 134 (26), S. 10745–10748. DOI: 10.1021/ja302186j.

Rafalski, Victoria A.; Ho, Peggy P.; Brett, Jamie O.; Ucar, Duygu; Dugas, Jason C.; Pollina, Elizabeth A. et al. (2013): Expansion of oligodendrocyte progenitor cells following SIRT1 inactivation in the adult brain. In: *Nature cell biology* 15 (6), S. 614–624. DOI: 10.1038/ncb2735.

Rajasekaran, Namakkal S.; Connell, Patrice; Christians, Elisabeth S.; Yan, Liang-Jun; Taylor, Ryan P.; Orosz, András et al. (2007): Human alpha B-crystallin mutation causes oxido-reductive stress and protein aggregation cardiomyopathy in mice. In: *Cell* 130 (3), S. 427–439. DOI: 10.1016/j.cell.2007.06.044.

Reif, D. W.; Simmons, R. D. (1990): Nitric oxide mediates iron release from ferritin. In: *Archives of biochemistry and biophysics* 283 (2), S. 537–541.

Ren, Binbin; Zhang, Nianhui; Yang, Juanjuan; Ding, Huangen (2008): Nitric oxide-induced bacteriostasis and modification of iron-sulphur proteins in Escherichia coli. In: *Molecular microbiology* 70 (4), S. 953–964. DOI: 10.1111/j.1365-2958.2008.06464.x.

Richardson, D. R.; Neumannova, V.; Nagy, E.; Ponka, P. (1995): The effect of redox-related species of nitrogen monoxide on transferrin and iron uptake and cellular proliferation of erythroleukemia (K562) cells. In: *Blood* 86 (8), S. 3211–3219.

Richardson, W. D.; Pringle, N.; Mosley, M. J.; Westermark, B.; Dubois-Dalcq, M. (1988): A role for platelet-derived growth factor in normal gliogenesis in the central nervous system. In: *Cell* 53 (2), S. 309–319.

Rios, Natalia; Piacenza, Lucía; Trujillo, Madia; Martínez, Alejandra; Demicheli, Verónica; Prolo, Carolina et al. (2016): Sensitive detection and estimation of cell-derived peroxynitrite fluxes using fluorescein-boronate. In: *Free radical biology & medicine. DOI:* 10.1016/j.freeradbiomed.2016.08.033.

Rivers, Leanne E.; Young, Kaylene M.; Rizzi, Matteo; Jamen, Françoise; Psachoulia, Konstantina; Wade, Anna et al. (2008): PDGFRA/NG2 glia generate myelinating oligodendrocytes and piriform projection neurons in adult mice. In: *Nature neuroscience* 11 (12), S. 1392–1401. DOI: 10.1038/nn.2220.

Robinson, Andrew P.; Rodgers, Jane M.; Goings, Gwendolyn E.; Miller, Stephen D. (2014): Characterization of oligodendroglial populations in mouse demyelinating disease using flow cytometry: clues for MS pathogenesis. In: *PloS one* 9 (9), S. e107649. DOI: 10.1371/journal.pone.0107649.

Robinson, S.; Miller, R. H. (1999): Contact with central nervous system myelin inhibits oligodendrocyte progenitor maturation. In: *Developmental biology* 216 (1), S. 359–368. DOI: 10.1006/dbio.1999.9466.

Rodríguez-Manzaneque, M. T.; Ros, J.; Cabiscol, E.; Sorribas, A.; Herrero, E. (1999): Grx5 glutaredoxin plays a central role in protection against protein oxidative damage in Saccharomyces cerevisiae. In: *Molecular and cellular biology* 19 (12), S. 8180–8190.

Rodríguez-Manzaneque, María Teresa; Tamarit, Jordi; Bellí, Gemma; Ros, Joaquim; Herrero, Enrique (2002): Grx5 is a mitochondrial glutaredoxin required for the activity of iron/sulfur enzymes. In: *Molecular biology of the cell* 13 (4), S. 1109–1121. DOI: 10.1091/mbc.01-10-0517.

Rouault, Tracey A. (2013): Iron metabolism in the CNS: implications for neurodegenerative diseases. In: *Nature reviews. Neuroscience* 14 (8), S. 551–564. DOI: 10.1038/nrn3453.

Rudick, Richard A.; Mi, Sha; Sandrock, Alfred W. (2008): LINGO-1 antagonists as therapy for multiple sclerosis: in vitro and in vivo evidence. In: *Expert opinion on biological therapy* 8 (10), S. 1561–1570. DOI: 10.1517/14712598.8.10.1561.

Sabo, Jennifer K.; Aumann, Tim D.; Merlo, Daniel; Kilpatrick, Trevor J.; Cate, Holly S. (2011): Remyelination is altered by bone morphogenic protein signaling in demyelinated lesions. In: *The Journal of neuroscience : the official journal of the Society for Neuroscience* 31 (12), S. 4504–4510. DOI: 10.1523/JNEUROSCI.5859-10.2011.

Sakry, Dominik; Trotter, Jacqueline (2016): The role of the NG2 proteoglycan in OPC and CNS network function. In: *Brain research* 1638 (Pt B), S. 161–166. DOI: 10.1016/j.brainres.2015.06.003.

Sands, Scott A.; Tsau, Sheila; LeVine, Steven M. (2015): The habenula and iron metabolism in cerebral mouse models of multiple sclerosis. In: *Neuroscience letters* 606, S. 204–208. DOI: 10.1016/j.neulet.2015.09.003.

Sawcer, Stephen; Hellenthal, Garrett; Pirinen, Matti; Spencer, Chris C A; Patsopoulos, Nikolaos A.; Moutsianas, Loukas et al. (2011): Genetic risk and a primary role for cell-mediated immune mechanisms in multiple sclerosis. In: *Nature* 476 (7359), S. 214–219. DOI: 10.1038/nature10251.

Schuh, Cornelia; Wimmer, Isabella; Hametner, Simon; Haider, Lukas; van Dam, Anne-Marie; Liblau, Roland S. et al. (2014): Oxidative tissue injury in multiple sclerosis is only partly reflected in experimental disease models. In: *Acta neuropathologica* 128 (2), S. 247–266. DOI: 10.1007/s00401-014-1263-5.

Schulze-Topphoff, Ulf; Prat, Alexandre; Prozorovski, Timour; Siffrin, Volker; Paterka, Magdalena; Herz, Josephine et al. (2009): Activation of kinin receptor B1 limits encephalitogenic T lymphocyte recruitment to the central nervous system. In: *Nature medicine* 15 (7), S. 788–793. DOI: 10.1038/nm.1980.

Schütte, Lena Dorothee; Baumeister, Stefan; Weis, Benjamin; Hudemann, Christoph; Hanschmann, Eva-Maria; Lillig, Christopher Horst (2013): Identification of potential protein dithiol-disulfide substrates of mammalian Grx2. In: *Biochimica et biophysica acta* 1830 (11), S. 4999–5005. DOI: 10.1016/j.bbagen.2013.07.009.

Sfagos, Constantinos; Makis, Alexandros C.; Chaidos, Aristeidis; Hatzimichael, Eleftheria C.; Dalamaga, Androniki; Kosma, Katerina; Bourantas, Konstantinos L. (2005): Serum ferritin, transferrin and soluble transferrin receptor levels in multiple sclerosis patients. In: *Multiple sclerosis (Houndmills, Basingstoke, England)* 11 (3), S. 272–275.

Shacka, J. J.; Sahawneh, M. A.; Gonzalez, J. D.; Ye, Y-Z; D'Alessandro, T. L.; Estévez, A. G. (2006): Two distinct signaling pathways regulate peroxynitrite-induced apoptosis in PC12 cells. In: *Cell death and differentiation* 13 (9), S. 1506–1514. DOI: 10.1038/sj.cdd.4401831.

Shang, Qingjuan; Bao, Lei; Guo, Hongjie; Hao, Fabao; Luo, Qianfu; Chen, Jiaping; Guo, Chunbao (2016): Contribution of glutaredoxin-1 to S-glutathionylation of endothelial nitric oxide synthase for mesenteric nitric oxide generation in experimental necrotizing enterocolitis. In: *Translational research : the journal of laboratory and clinical medicine. DOI:* 10.1016/j.trsl.2016.01.004.

Sies, H.; Cadenas, E. (1985): Oxidative stress: damage to intact cells and organs. In: *Philosophical transactions of the Royal Society of London. Series B, Biological sciences* 311 (1152), S. 617–631.

Simmons, M. L.; Murphy, S. (1992): Induction of nitric oxide synthase in glial cells. In: *Journal of neurochemistry* 59 (3), S. 897–905.

Smerjac, Suzanne M.; Bizzozero, Oscar A. (2008): Cytoskeletal protein carbonylation and degradation in experimental autoimmune encephalomyelitis. In: *Journal of neurochemistry* 105 (3), S. 763–772. DOI: 10.1111/j.1471-4159.2007.05178.x.

Smigrodzki, Rafal; Parks, Janice; Parker, W. Davis (2004): High frequency of mitochondrial complex I mutations in Parkinson's disease and aging. In: *Neurobiology of aging* 25 (10), S. 1273–1281. DOI: 10.1016/j.neurobiolaging.2004.02.020.

Smith, J.; Ladi, E.; Mayer-Proschel, M.; Noble, M. (2000): Redox state is a central modulator of the balance between self-renewal and differentiation in a dividing glial precursor cell. In: *Proceedings of the National Academy of Sciences of the United States of America* 97 (18), S. 10032–10037. DOI: 10.1073/pnas.170209797.

Sofroniew, Michael V. (2005): Reactive astrocytes in neural repair and protection. In: *The Neuroscientist : a review journal bringing neurobiology, neurology and psychiatry* 11 (5), S. 400–407. DOI: 10.1177/1073858405278321.

Stankiewicz, James; Panter, S. Scott; Neema, Mohit; Arora, Ashish; Batt, Courtney E.; Bakshi, Rohit (2007): Iron in chronic brain disorders: imaging and neurotherapeutic implications. In: *Neurotherapeutics : the journal of the American Society for Experimental NeuroTherapeutics* 4 (3), S. 371–386. DOI: 10.1016/j.nurt.2007.05.006.

Stehling, Oliver; Sheftel, Alex D.; Lill, Roland (2009): Chapter 12 Controlled expression of iron-sulfur cluster assembly components for respiratory chain complexes in mammalian cells. In: *Methods in enzymology* 456, S. 209–231. DOI: 10.1016/S0076-6879(08)04412-1.

Stehling, Oliver; Smith, Paul M.; Biederbick, Annette; Balk, Janneke; Lill, Roland; Mühlenhoff, Ulrich (2007): Investigation of iron-sulfur protein maturation in eukaryotes. In: *Methods in molecular biology (Clifton, N.J.)* 372, S. 325–342. DOI: 10.1007/978-1-59745-365-3_24.

Stoppini, L.; Buchs, P. A.; Muller, D. (1991): A simple method for organotypic cultures of nervous tissue. In: *Journal of neuroscience methods* 37 (2), S. 173–182.

Syed, Yasir A.; Hand, Elisabeth; Möbius, Wiebke; Zhao, Chao; Hofer, Matthias; Nave, Klaus A.; Kotter, Mark R. (2011): Inhibition of CNS remyelination by the presence of semaphorin 3A. In: *The Journal of neuroscience : the official journal of the Society for Neuroscience* 31 (10), S. 3719–3728. DOI: 10.1523/JNEUROSCI.4930-10.2011.

't Hart, Bert A; Gran, Bruno; Weissert, Robert (2011): EAE: imperfect but useful models of multiple sclerosis. In: *Trends in molecular medicine* 17 (3), S. 119–125. DOI: 10.1016/j.molmed.2010.11.006.

Takahashi, Kazuya; Prinz, Marco; Stagi, Massimiliano; Chechneva, Olga; Neumann, Harald (2007): TREM2-transduced myeloid precursors mediate nervous tissue debris clearance and facilitate recovery in an animal model of multiple sclerosis. In: *PLoS medicine* 4 (4), S. e124. DOI: 10.1371/journal.pmed.0040124.

Teng, Felicia Yu Hsuan; Hor, Catherine Hong Huan; Tang, Bor Luen (2009): Emerging cues mediating astroglia lineage restriction of progenitor cells in the injured/diseased adult CNS. In: *Differentiation; research in biological diversity* 77 (2), S. 121–127. DOI: 10.1016/j.diff.2008.09.013.

Trapp, B. D.; Peterson, J.; Ransohoff, R. M.; Rudick, R.; Mörk, S.; Bö, L. (1998): Axonal transection in the lesions of multiple sclerosis. In: *The New England journal of medicine* 338 (5), S. 278–285. DOI: 10.1056/NEJM199801293380502.

Traugott, U.; Lebon, P. (1988): Interferon-gamma and Ia antigen are present on astrocytes in active chronic multiple sclerosis lesions. In: *Journal of the neurological sciences* 84 (2-3), S. 257–264.

Tsai, Ming-Li; Tsou, Chih-Chin; Liaw, Wen-Feng (2015): Dinitrosyl iron complexes (DNICs): from biomimetic synthesis and spectroscopic characterization toward unveiling the biological and catalytic roles of DNICs. In: *Accounts of chemical research* 48 (4), S. 1184–1193. DOI: 10.1021/ar500459j.

Vall-Llaura, Núria; Reverter-Branchat, Gemma; Vived, Celia; Weertman, Naomi; Rodríguez-Colman, María José; Cabiscol, Elisa (2016): Reversible glutathionylation of Sir2 by monothiol glutaredoxins Grx3/4 regulates stress resistance. In: *Free radical biology & medicine* 96, S. 45–56. DOI: 10.1016/j.freeradbiomed.2016.04.008.

van Horssen, Jack; Witte, Maarten E.; Schreibelt, Gerty; de Vries, Helga E (2011): Radical changes in multiple sclerosis pathogenesis. In: *Biochimica et biophysica acta* 1812 (2), S. 141–150. DOI: 10.1016/j.bbadis.2010.06.011.

Vanin, Anatoly F.; Serezhenkov, Vladimir A.; Mikoyan, Vasak D.; Genkin, Michael V. (1998): The 2.03 Signal as an Indicator of Dinitrosyl–Iron Complexes with Thiol-Containing Ligands. In: *Nitric Oxide* 2 (4), S. 224–234. DOI: 10.1006/niox.1998.0180.

Viganò, Francesca; Schneider, Sarah; Cimino, Mauro; Bonfanti, Elisabetta; Gelosa, Paolo; Sironi, Luigi et al. (2016): GPR17 expressing NG2-Glia: Oligodendrocyte progenitors serving as a reserve pool after injury. In: *Glia* 64 (2), S. 287–299. DOI: 10.1002/glia.22929.

Villoslada, Pablo (2016): Neuroprotective therapies for multiple sclerosis and other demyelinating diseases. In: *Mult Scler Demyelinating Disord* 1 (1), S. 19067. DOI: 10.1186/s40893-016-0004-0.

Volbracht, Katrin (2012): Effect of glutaredoxin2 on cellular functions of oligodendrocytes. Master Thesis, Department of Neurology, Heinrich-Heine-University Düsseldorf

Wang, Mengfei; Zhu, Kunting; Zhang, Luyu; Li, Lingyu; Zhao, Jing (2016): Thioredoxin 1 protects astrocytes from oxidative stress by maintaining peroxiredoxin activity. In: *Molecular medicine reports* 13 (3), S. 2864–2870. DOI: 10.3892/mmr.2016.4855.

Wang, Xiaoyang; Svedin, Pernilla; Nie, Chunxia; Lapatto, Risto; Zhu, Changlian; Gustavsson, Malin et al. (2007): N-acetylcysteine reduces lipopolysaccharide-sensitized hypoxic-ischemic brain injury. In: *Annals of neurology* 61 (3), S. 263–271. DOI: 10.1002/ana.21066.

Watanabe, Masahiko; Toyama, Yoshiaki; Nishiyama, Akiko (2002): Differentiation of proliferated NG2-positive glial progenitor cells in a remyelinating lesion. In: *Journal of neuroscience research* 69 (6), S. 826–836. DOI: 10.1002/jnr.10338.

Watts, R. N.; Richardson, D. R. (2001): Nitrogen Monoxide (NO) and Glucose: UNEXPECTED LINKS BETWEEN ENERGY METABOLISM AND NO-MEDIATED IRON MOBILIZATION FROM CELLS. In: *Journal of Biological Chemistry* 276 (7), S. 4724–4732. DOI: 10.1074/jbc.M006318200.

Watts, Ralph N.; Hawkins, Clare; Ponka, Prem; Des Richardson, R. (2006): Nitrogen monoxide (NO)-mediated iron release from cells is linked to NO-induced glutathione efflux via multidrug resistance-associated protein 1. In: *Proceedings of the National Academy of Sciences of the United States of America* 103 (20), S. 7670–7675. DOI: 10.1073/pnas.0602515103.

Weinshenker, B. G. (1996): Epidemiology of multiple sclerosis. In: *Neurologic clinics* 14 (2), S. 291–308.

Weiss, G.; Goossen, B.; Doppler, W.; Fuchs, D.; Pantopoulos, K.; Werner-Felmayer, G. et al. (1993): Translational regulation via iron-responsive elements by the nitric oxide/NO-synthase pathway. In: *The EMBO journal* 12 (9), S. 3651–3657.

Whiteman, Matthew; Armstrong, Jeffrey S.; Chu, Siew Hwa; Jia-Ling, Siau; Wong, Boon-Seng; Cheung, Nam Sang et al. (2004): The novel neuromodulator hydrogen sulfide: an endogenous peroxynitrite 'scavenger'? In: *Journal of neurochemistry* 90 (3), S. 765–768. DOI: 10.1111/j.1471-4159.2004.02617.x.

Whiteman, Matthew; Cheung, Nam Sang; Zhu, Yi-Zhun; Chu, Siew Hwa; Siau, Jia Ling; Wong, Boon Seng et al. (2005): Hydrogen sulphide: a novel inhibitor of hypochlorous acid-mediated oxidative damage in the brain? In: *Biochemical and biophysical research communications* 326 (4), S. 794–798. DOI: 10.1016/j.bbrc.2004.11.110.

Wingert, Rebecca A.; Galloway, Jenna L.; Barut, Bruce; Foott, Helen; Fraenkel, Paula; Axe, Jennifer L. et al. (2005): Deficiency of glutaredoxin 5 reveals Fe-S clusters are required for vertebrate haem synthesis. In: *Nature* 436 (7053), S. 1035–1039. DOI: 10.1038/nature03887.

Worlitzer, Maik Ma; Bunk, Eva C.; Hemmer, Kathrin; Schwamborn, Jens C. (2012): Anti-inflammatory treatment induced regenerative oligodendrogenesis in parkinsonian mice. In: *Stem cell research & therapy* 3 (4), S. 33. DOI: 10.1186/scrt124.

Xu, Y. Z.; Ruan, D. Y.; Wu, Y.; Jiang, Y. B.; Chen, S. Y.; Chen, J.; Shi, P. (1998): Nitric oxide affects LTP in area CA1 and CA3 of hippocampus in low-level lead-exposed rat. In: *Neurotoxicology and teratology* 20 (1), S. 69–73.

Youdim, M. B.; Green, A. R. (1978): Iron deficiency and neurotransmitter synthesis and function. In: *The Proceedings of the Nutrition Society* 37 (2), S. 173–179.

Yuan, Ti-Fei; Gu, Simeng; Shan, Chunlei; Marchado, Sergio; Arias-Carrión, Oscar (2015): Oxidative Stress and Adult Neurogenesis. In: *Stem cell reviews* 11 (5), S. 706–709. DOI: 10.1007/s12015-015-9603-y.

Zhang, Huali; Limphong, Pattraranee; Pieper, Joel; Liu, Qiang; Rodesch, Christopher K.; Christians, Elisabeth; Benjamin, Ivor J. (2012): Glutathione-dependent reductive stress triggers mitochondrial oxidation and cytotoxicity. In: *FASEB journal : official publication of the Federation of American Societies for Experimental Biology* 26 (4), S. 1442–1451. DOI: 10.1096/fj.11-199869.

Zhang, Li; Wang, Ning-Li; Zhang, Wei; Chang, Zhi-Jie (2008): [Suppression of cell proliferation by inhibitors to redox signaling in human lens epithelial cells]. In: *[Zhonghua yan ke za zhi] Chinese journal of ophthalmology* 44 (7), S. 622–628.

Zhang, Xia; Min, Xiaoyan; Li, Chuanfu; Benjamin, Ivor J.; Qian, Bo; Zhang, Xiaojin et al. (2010): Involvement of reductive stress in the cardiomyopathy in transgenic mice with cardiac-specific overexpression of heat shock protein 27. In: *Hypertension* 55 (6), S. 1412–1417. DOI: 10.1161/HYPERTENSIONAHA.109.147066.

Zhu, Xiaoqin; Bergles, Dwight E.; Nishiyama, Akiko (2008): NG2 cells generate both oligodendrocytes and grey matter astrocytes. In: *Development (Cambridge, England)* 135 (1), S. 145–157. DOI: 10.1242/dev.004895.

Zipp, Frauke; Aktas, Orhan (2006): The brain as a target of inflammation: common pathways link inflammatory and neurodegenerative diseases. In: *Trends in neurosciences* 29 (9), S. 518–527. DOI: 10.1016/j.tins.2006.07.006.

6. Appendix

6.1 List of Figures

6.2 List of Tables

6.3 Abbreviations

ACO	Aconitase
ATP	Adenosine triphosphate
BBB	Blood brain barrier
BSA	Bovine serum albumin
CNPase	2',3'-cyclic nucleotide 3'-phosphodiesterase
CNS	Central nervous system
COX	Cyclooxygenase
CPTIO	Carboxyl-PTIO potasium salt
CRMP2	Collapsin response mediator protein 2
CSF	Cerebrospinal fluid
DMF	Dimethylformamid
DMSO	Dimethylsulfoxid
DNA	Deoxyribonucleic acid
DNIC	Dinitrosyl iron complexes
DNGIC	Glutathionyl dinitrosyl-iron-complexes
DTT	Dithiothreitol
EAE	Experimental autoimmune encephalomyelitis
EPR	Electron Paramagnetic resonance
FCS	Fetal Bovine Serum
FGF	Fibroblast growth factor
GAPDH	Glycerinaldehyd-3-phosphat-dehydrogenase
GFAP	Glial Fibrillary acidic protein
GR	Glutathione reductase
Glx	Glutamax
Grx	Glutaredoxin
GPAT	Glycerol-3-phosphate acyltransferase
GSH	Glutathion
GSNO	S-Nitrosoglutathione
GSSG	Glutathione disulfide
H_2O_2	Hydrogen peroxide
HBSS	Hank's Balanced Salt Solution
Iba1	Ionized calcium-binding adapter molecule 1
IFN	Interferone

IL-4	Interleukin-4
IRP	Iron regulatory protein
LDH	Lactat-Dehydrogenase
LIF	Leukemia inhibitory factor
LINGO-1	Leucine rich repeat and immunoglobulin-like domain-containing protein 1
LPS	Lipopolysaccharide
MBP	Myelin basic protein
MDH	Malate-Dehydrogenase
MEM	Minimum Essential Media
min	minute
MOG	Myelin oligodendrocyte glycoprotein
MRP1	Multidrug resistance-associated protein 1
MS	Multiple sclerosis
NADPH	Nicotinamide adenine dinucleotide phosphate
NAWM	Normal Appearing white matter
NG2	Neural/glial antigen 2
NGS	Normal Goat Serum
NF-M	Neurofilament M
NO	Nitric oxide
NOS	Nitric oxide synthase
Nrf2	Nuclear Factor-E2-related factor 2
O_2	Superoxide
$OH^{\cdot}$	Hydroxyl radicals
$ONOO^{-}$	Peroxinitrate
OPC	oligodendrocyte progenitor
OSC	Organotypic slice cultures
PBS	Phosphate Buffered Saline
PDGFα	Platelet-derived growth factor α
PFA	Paraformaldehyde
PLP	Proteolipid protein
Prx	Peroxiredoxin
PTX	Pertussis toxin
q RT-PCR	quantitative Real Time Polymerase Chain Reaction
RNA	Ribonucleic acid

RNR	Ribonucleotide reductase
RNS	Reactive nitrogen species
ROS	Reactive oxygen species
SDH	Succinat-Dehydrogenase
SOD	Superoxide dismutase
TfR	Transferrin receptor
Trx	Thioredoxin
TrxR	Thioredoxin Reductase

6.4 Manuscript

Iron-sulfur Glutaredoxin 2 protects oligodendrocytes against damage induced by nitric oxide release from activated microglia

Klaudia Lepka[1], Katrin Volbracht[1], Eckhard Bill[2], Reiner Schneider[1], Natalia Rios[3], Thomas Hildebrandt[1], Jens Ingwersen[1], Timur Prozorovski[1], Christopher Horst Lillig[4], Jack van Horssen[5], Lawrence Steinman[6], Hans-Peter Hartung[1], Rafael Radi[3], Arne Holmgren[7], Orhan Aktas[1*], Carsten Berndt[1*]

[1]Department of Neurology, Medical Faculty, Heinrich-Heine Universität, 40225 Düsseldorf, Germany, [2]Max-Planck-Institut für Chemische Energiekonversion, 45470 Mülheim/Ruhr, Germany, [3]Departmento de Bioquímica and Center for Free Radical and Biomedical Research, Facultad de Medicina, Universidad de la República, CP 11800, Montevideo, Uruguay, [4]Universitätsmedizin Greifswald, Institute for Medical Biochemistry and Molecular Biology, 17475 Greifswald, Germany, [5]Department of Molecular Cell Biology and Immunology, VU University Medical Center, 1007 MB Amsterdam, The Netherlands, [6]Department of Neurology and Neurological Sciences, Stanford University School of Medicine, Stanford, CA 94305-5316, USA, [7]Department for Medical Biochemistry and Biophysics, Karolinska Institutet, 17177 Stockholm, Sweden

*addresses for correspondence: Carsten Berndt, Department of Neurology, Medical Faculty, Heinrich-Heine Universität, Life Science Center, Merowingerplatz 1a, 40225 Düsseldorf, Germany, tel.: +49 211 302039220, fax: +49 211 302039227, email: carsten.berndt@hhu.de; ORCID: 0000-0001-8583-7966, Orhan Aktas, Department of Neurology, Medical Faculty, Heinrich-Heine Universität, Moorenstr. 5, 40225 Düsseldorf, Germany, tel.: +49 211 8118464, fax: +49 211 8118469, email: orhan.aktas@hhu.de; ORCID: 0000-0002-2020-9210

running title: Holo-Glutaredoxin detoxifies nitric oxide

key words: dinitrosyl-iron-complex, glutathione, oxidation, myelin, oxidoreductase

number of words: 10437, Introduction: 518, Material and Methods: 1471, Results: 2560, Discussion: 1437, Figure legends: 1541, References: 2200
number of Figures: 7, number of tables: 0, number of supplementary figures: 4

Main points

- Unique FeS protein Grx2 inhibits damage of myelin and oligodendrocyte progenitor cells induced by NO
- FeS disassembly allows formation of dinitrosyl-diglutathionyl-iron-complexes and prevents $ONOO^-$ formation and subsequent oxidative damage

Table of Contents Image

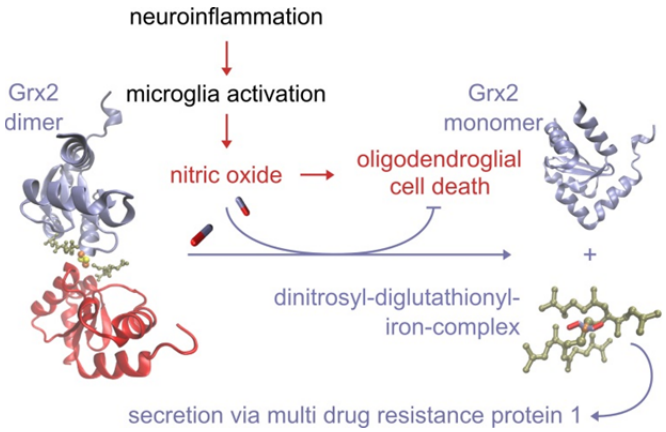

Abstract

Demyelinated brain lesions, a hallmark of autoimmune neuroinflammatory diseases like multiple sclerosis, result from oligodendroglial cell damage. Activated microglia are considered a major source of nitric oxide and subsequent peroxynitrite-mediated damage of myelin. Here, we provide biochemical and biophysical evidence that the oxidoreductase glutaredoxin 2 inhibits peroxynitrite formation by transforming nitric oxide into dinitrosyl-diglutathionyl-iron-complexes. Glutaredoxin 2 levels influence both survival rates of primary oligodendrocyte progenitor cells and preservation of myelin structure in cerebellar organotypic slice cultures challenged with activated microglia or nitric oxide donors. Of note, glutaredoxin 2-mediated protection is not linked to its enzymatic activity as oxidoreductase, but to the disassembly of its uniquely coordinated iron-sulfur cluster using glutathione as non-protein ligand. The protective effect of glutaredoxin 2 is connected to decreased protein carbonylation and nitration. In line, brain lesions of mice suffering from experimental autoimmune encephalomyelitis, an animal model of multiple sclerosis, show decreased glutaredoxin 2 expression and increased nitrotyrosine formation indicating that this type of protection is missing in the inflamed central nervous system. Our findings link inorganic biochemistry to neuroinflammation and identify glutaredoxin 2 as a protective factor against neuroinflammation-mediated myelin damage. Thus, improved availability of glutathione-coordinated iron-sulfur clusters emerges as a potential therapeutic approach in inflammatory demyelination.

Introduction

Multiple sclerosis (MS) is the major, non-traumatic cause of neurological disability in young adults in Western countries and is characterized by a persistent, inflammatory process in the central nervous system (CNS) (Compston & Coles, 2002). According to current paradigms, MS is considered an autoimmune disease that is mediated by myelin-reactive lymphocytes invading the CNS (Hohlfeld & Wekerle, 2004). This leads to immune-mediated demyelination (Ip et al., 2006), axonal degeneration and neuronal loss (Lassmann, Brück, & Lucchinetti, 2007). The presence of activated microglia and their secretion of the nitric oxide radical ($^{\bullet}$NO) is a characteristic feature of MS lesions and contributes to chronic neuroinflammation (Trapp, 2004; Zipp & Aktas, 2006). Of note, oligodendrocytes as well as oligodendroglial precursor cells (OPCs) are highly susceptible to reactive nitrogen species (RNS)-induced cell death leading to damage of myelinating

oligodendrocytes and subsequent myelin loss, especially via the formation of peroxynitrite (Jack, Antel, Brück, & Kuhlmann, 2007; Li, Baud, Vartanian, Volpe, & Rosenberg, 2005). Peroxynitrite ($ONOO^-$) is the product of $^{\bullet}NO$ and the superoxide radical ($O_2^{\bullet-}$) and leads to oxidative damage of proteins via tyrosine nitration and cysteine oxidation (Radi, 2013).

Consistent with the traditional perspective, “oxidative stress” and increased formation of reactive oxygen species (ROS) and RNS are linked to many pathological conditions (Sies, 2015) as described above for MS, including myelin damage (O'Sullivan, Velasco-Estevez, & Dev, 2017). However, the “oxidative stress” paradigm evolved from the concept of a general disruption in the balance of oxidants and antioxidants towards specific enzymatic redox events (Berndt, Lillig, & Flohé, 2014). Oxidative thiol modifications are the main targets for these redox events. Research in recent years has established that certain ROS and RNS at physiological concentrations are not generally detrimental but can actually regulate a variety of processes at cellular and organismal levels, e.g. embryonic development (Bräutigam et al., 2013; Bräutigam et al., 2011). As a prominent example, the identification of NO as a signaling molecule resulted in the Nobel Prize in 1998. Reduction of oxidized cysteine residues is facilitated by oxidoreductases of the thioredoxin family (Hanschmann, Godoy, Berndt, Hudemann, & Lillig, 2013). First identified as electron donors of ribonucleotide reductase, thioredoxins (Trxs) and glutaredoxins (Grxs) are now recognized as general thiol oxidoreductases (Hanschmann et al., 2013). Mammalian Grx2 exists in isoforms that are located in both the mitochondria (Grx2a) and cytosol (Grx2c) (Hudemann et al., 2009; Lönn et al., 2008), and human Grx2 was the first discovered example of an FeS cluster coordinating Grx (Lillig et al., 2005). The cofactor is coordinated between two monomers using the N-terminal active site cysteines and two non-covalently bound glutathione (GSH) molecules as ligands (Berndt et al., 2007). The existence of this enzymatically inactive holo-complex was confirmed through crystallization studies (Johansson, Kavanagh, Gileadi, & Oppermann, 2007). In cells, holo-Grx2 is the dominant form as confirmed by determination of bound radioactive ^{55}Fe after immunoprecipitation and a fluorescence resonance energy transfer (FRET)-based method (Hoff et al., 2009; Lillig et al., 2005).

Here, we describe that Grx2 detoxifies $^{\bullet}NO$ in mature oligodendrocytes and OPCs via the formation of dinitrosyl-iron-complexes, inhibiting the formation of harmful peroxynitrite and reducing subsequent oligodendroglial damage.

Materials and Methods

GSNO was prepared as previously reported by the reaction of acidified sodium nitrite and glutathione (Hart, 1985). NOC-5 and NOC-7 were purchased from Enzo Life Science; SIN-1 and CPTIO from Cayman Chemicals; Accell Grx2-si-RNA and non-targeting Accell siRNA with or without Dy-547 labeling from Thermo Fisher; LPS, DTT, 1-chloro-2,4-dinitrobenzene (CDNB), and MK-571 from Sigma-Aldrich. Primary antibodies were from Merck Millipore (mouse anti-NF-M, rat anti-MBP, mouse anti-nitrotyrosine, rabbit anti-acetylated histone 3, rabbit anti-Olig2), Chemicon (mouse anti-A2B5, mouse anti-BrdU), Wako Chemicals (rabbit anti-Iba1), Sigma-Aldrich (mouse anti-β-actin), Enzo Life Science (rat anti-MRP1), and Cell Signaling Technology (rabbit anti-active caspase 3). Anti-Grx2 is a selfmade antibody (Godoy et al., 2011). Secondary antibodies for Western blots were from Li-COR (IRDye) and secondary antibodies conjugated to Cy2, Cy3, or Cy5 for immunofluorescence as well as Hoechst were purchased from Invitrogen.

Recombinant protein expression and purification

Human and mouse Grx2 and the mutants mGrx2C37S and mGrx2S38P were recombinantly expressed in the BL21-CodonPlus-(DE3)-RIL *E. coli* strain (Stratagene) with N-terminal histidine tags (pet15b, Novagen) and purified on HiTrap chelating columns (GE Healthcare) as described before (Lillig et al., 2005). After dialysis to remove imidazole and removal of endotoxins (Pierce high capacity endotoxin removal spin columns, Thermo Scientific), purity of proteins was analyzed by SDS-PAGE (Bio-Rad). GST from *Schistosoma japonicum* was expressed and purified using vector pGEX-3X and GST-sepharose (GE Healthcare).

Glutathione S-transferase assay

GST activity was measured as described previously (Habig, Pabst, & Jakoby, 1974) in a microplate reader (Molecular Devices) at 20ºC using either HeLa cell extracts (20-60 µg) or recombinant *Schistosoma japonicum* GST (75 or 150 ng). Activity was determined using the increase in absorbance at 340 nm following GST-mediated conjugation of glutathione to 1-chloro-2,4-dinitrobenzene (CDNB).

Cerebellar organotypic slice cultures

Cerebellar organotypic slice cultures were obtained from postnatal day 10 C57BL/6 mice by modifying a previously used method (Stoppini, Buchs, & Muller, 1991). Briefly, cerebellum with attached hindbrain was dissected and cut into 350 µm sagittal sections

using a McIlwain tissue chopper (Gala Instruments). Slices were dissociated in dissecting medium containing 1 mM kynurenic acid (Sigma Aldrich), penicillin/streptomycin (100 U/ml, Invitrogen) and Glutamax (Gibco) in Hanks´ balanced salt solution (HBSS, Invitrogen), washed for 15 min in 1:1 HBSS:minimal essential media (MEM) containing 25 mM HEPES buffer and plated on Millipore-Millicel-CM culture inserts. Culture medium was MEM containing 25% heat inactivated horse serum (Gibco), 25% HBSS, 5 mg/ml glucose, Glutamax, and penicillin/streptomycin (100 U/ml). After 7 days *in vitro* (5% CO_2 and 33°C) slices were incubated with 2 µM Grx2 for 2 h prior and 4 h after treatment initiation. Treatment comprised either 750 µM GSNO or 10 µg/ml LPS for 24 h. Morphological analysis was performed by immunofluorescence.

Cell cultures

Oligodendroglial precursor cell (OPC) enriched cultures were derived from postnatal day 1 C57BL/6 mice using the Neuronal Tissue Dissociation Kit for total brain single cell suspension (Miltenyi Biotec) and anti-A2B5 MicroBeads (Miltenyi Biotec) obeying manufacturer´s recommendation. Sorted cells were plated at 50,000 cells/cm^2 on poly-L-ornithine (Sigma Aldrich) coated petri-dishes and purity (94 ± 1% A2B5 cells) was determined by immunofluorescence (Fig. S1). A2B5 cells were cultivated in DMEM/F12 (Gibco) complemented with Glutamax, penicillin/streptomycin (100 U/ml), B27 supplement (Gibco), FGF (20 ng/ml, Immunotools) and PDGFa (20 ng/ml, Immunotools). OLN93 (rat oligodendroglial cell line), BV2 (mouse microglia cell line), and HeLa cells (human epitheloid cervix cancer cell line) were cultivated in DMEM (Gibco) containing 10% heat inactivated fetal bovine serum (Invitrogen) and penicillin/streptomycin (100 U/ml). Cells were treated with H_2O_2 (30 min in HBSS), $^{\bullet}NO$ (GSNO: 24 h in medium, NOCs: 20 min in medium) or peroxynitrite donors (SIN-1: 2 h in PBS) or co-cultured without direct cell contact in a transwell system (Thin Certs, Greiner) for 24 h with BV2 cells in presence of LPS (1 µg/ml).

Survival assay

A2B5 cells were plated at 25,000 cells/cm^2, OLN93 and HeLa cells at 15,000 cells/cm^2 in either 96 or 24 well plates (co-cultures). The viability of cultured cells was determined either by the cell titer blue assay (Promega) or the XTT assay (Roche). Absorbance was measured in a microplate reader (Tecan, Molecular Devices).

Nitric oxide and peroxynitrite measurement

Measurement of nitric oxide was performed with the Griess Reagent from Molecular Probes according to manufacturer´s protocol using a microplate reader (Tecan, Molecular Devices, absorbance at 540 nm). Measurement of peroxynitrite was based on the reaction of fluorescein-boronate to fluorescein in the presence of peroxynitrite (Rios et al., 2016). The probe was synthesized and solved in DMSO and further diluted and measured in PBS at a final concentration of 50 µM. Cells were pre-incubated with 2 µM recombinant Grx2 for 2 h. After washing with PBS, the peroxynitrite concentration was measured in the living cells in a microplate reader (Tecan, Molecular Devices, absorbance at 492 nm and emission at 515 nm) directly after the addition of fluorescein-boronate and 1 mM GSNO, 100 µM H_2O_2 or 1 mM SIN-1 in the presence or absence of 50 µM CPTIO.

Immunofluorescence

Following GSNO or LPS treatment as well as treatment with 10 µM BrdU for 2 h ± incubation with 2 µM Grx2 for 24 h to follow proliferation, slice cultures and single cells were fixed at RT with 4% PFA for 30 or 10 min, respectively, washed twice with PBS and blocked in 5% horse or goat serum and 0.5% Triton-X-100 in PBS for 2 h at RT. Samples were incubated over night at 4°C with primary antibodies in staining solution (1:1 PBS:blocking solution). After three washing steps, samples were incubated with secondary antibodies for 1 h at RT. Cell nuclei were visualized using Hoechst. Pictures were taken by confocal microscopy (Zeiss LSM510) or fluorescence microscopy (Olympus BX51). Disturbed myelin structures in slice cultures were quantified counting the total amount and the amount of damaged cerebellar white matter tracts.

Western Blot analysis

Protein concentrations of cell lysates were quantified using the BCA assay (Interchim), separated on SDS-PAGE (mini-PROTEAN TGX precast gels, Bio-Rad) and blotted onto nitrocellulose membranes (Bio-Rad). After blocking in 2.5% milk powder or 5% BSA in PBS-Tween for 2 h at RT, membranes were incubated with primary antibodies overnight at 4°C followed by IRDye-coupled secondary antibodies (LI-COR) for 1 h at RT. Intensity quantification was normalized to β-actin. Protein carbonyls were determined using the Protein Oxidation Detection Kit (Chemicon).

Quantitative real time PCR

RNA isolation was performed using TRIzol solution according to manufacture instructions (Invitrogen). For cDNA synthesis TaqMan reverse transcription reagent (Applied Biosystems) and for qRTPCR Power SYBRGreen fluorescent dye or TaqMan probe (Applied Biosystems) were used. Glyceraldehyde3-phosphate dehydrogenase (GAPDH) was measured as housekeeping gene. Relative gene expression ratio was calculated based on the $2^{-deltaCt}$ method. Measurements were performed in duplicates. Negative control for identification of MRP1 transcription was water.

Spectroscopy

UV-visible spectra were recorded with a Shimadzu UV-2100 spectrophotometer. Decrease in absorbance at 480 nm was followed using the same UV-VIS spectrophotometer or a microplate reader (Tecan). Mössbauer spectra were recorded with a spectrometer of the alternating constant acceleration type. The minimum experimental line width was 0.24 mm x s^{-1} (full width at half height). The sample temperature was maintained constant either in an Oxford Instruments Variox or an Oxford Instruments Mössbauer Spectromag cryostat. X-band EPR spectra were recorded with a Bruker Elexsys E500 spectrometer equipped with a helium flow cryostat (Oxford Instruments ESR 910), an NMR gaussmeter, and a Hewlett-Packard frequency counter.

Experimental autoimmune encephalomyelitis

Experimental autoimmune encephalomyelitis (EAE) induction was performed as described previously, e.g. (Schneider et al., 2016). Briefly, for actively-induced EAE, C57BL/6 female mice were immunized with 200 µg of myelin oligodendrocyte glycoprotein ($MOG_{35–55}$) peptide in Complete Freund´s Adjuvant (CFA) with additionally supplemented heat-inactivated 800 µg *M. tuberculosis* H37RA (Difco) followed by pertussis toxin (PTX, Sigma Aldrich) injections (200 ng on the days 0 and 2). For adoptive transfer (or passively-induced) EAE, spleen and lymph node cells were isolated form SJL/J mice treated similar as for active EAE, i.e. upon immunization with proteolipid protein (PLP) peptide $PLP_{139-151}$ (but without PTX). After re-stimulation with $PLP_{139-151}$ cells were harvested and injected i.p. into naïve female SJL/J mice. Disease severity was scored from 0 to 5 (0: no clinical signs, 1: tail plegia, 2: abnormal gait, 3: hind limb paralysis, 4: complete paralysis, 5: death or euthanasia) (Huehnchen et al., 2011). Animals investigated in this study had a clinical score of at least 3 during the acute phase, thus displayed established disease. All

animal experiments were approved by the local animal welfare committee (G363/09 and G197/09).

Data analysis and availability

Optical densities were measured using ImageJ (www.imagej.nih.gov). Regression was calculated using Grace (www.plasma-gate.weizmann.ac.il). Values are presented as mean ± SEM (when $n \geq 3$). Statistical significance was calculated using GraphPad Prism 5 (GraphPad Software) when $n \geq 4$ using Student´s t-test or - for more than two treated groups - ANOVA (with Bonferroni post-test) (*: $p<0.05$; **: $p<0.005$; ***: $p<0.001$). All requested data are available via the corresponding authors.

Results

Decreased Grx2 expression in EAE lesions

•NO levels are enhanced within MS lesions upon increased iNOS expression in microglia/macrophages leading to subsequent secretion of •NO (Jack et al., 2007). The death of mature and differentiating oligodendrocytes, which are particularly sensitive to •NO induced damage, critically contributes to persisting damage in neuroinflammatory diseases like MS. EAE as an inflammatory model of MS is characterized by macrophage infiltration and activated microglia, which contribute to the pathogenesis (Prinz, Priller, Sisodia, & Ransohoff, 2011). As shown in Fig. 1A, increased nitrotyrosine staining was observed in areas with activated microglia and macrophage infiltration in the chronic stage of this animal model. At the same stage, transcription of *GLRX2a* and *GLRX2c* is diminished in the brain after induction of adoptive transfer (Fig. 1B; *GLRX2a*: 62 ± 8%, *GLRX2c*: 27 ± 9%, all values mean ± SEM) and actively induced EAE (Fig. 1C; *GLRX2a*: 80 ± 6%, *GLRX2c*: 72 ± 9%) compared to brains of control mice but not the transcription of *GLRX1* (adoptive EAE: 94 ± 19%, active EAE: 132 ± 29%). In line, the protein level of Grx2 is decreased to 54 ± 15% (Fig. 1D). Therefore, we investigated next whether Grx2 has a protective effect against myelin damage under these inflammatory conditions.

Grx2 preserves the myelin structure

We prepared cerebellar organotypic slice cultures, modulated intracellular Grx2 levels, and exposed them to the physiological •NO-donor nitroso-glutathione (GSNO). We took

advantage of the cellular uptake of recombinant Grx2 to enhance the intracellular levels of this protein (treatment with 2 µM Grx2 resulted in an increase to 690 ± 30% of intracellular Grx2, Fig. S2A and C). Compared to the untreated control slices, GSNO treatment resulted in substantial damage of white matter tracts (increase from 29 ± 5% to 63 ± 4%), whereas the myelin structure was preserved in the presence of Grx2 (38 ± 3% damaged white matter tracts, Fig. 2A). During neuroinflammation, activated microglia are considered a major source of •NO. We stimulated •NO release by local microglia via exposing the slice cultures to the toll-like receptor 4 agonist lipopolysaccharide (LPS), an experimental approach to investigate myelin integrity in MS (Desai et al., 2016). Treatment with LPS increased the amount of damaged myelin structures (63 ± 3% compared to 40 ± 3% in untreated cultures), while Grx2 conferred again protection of the white matter tracts, similar to control conditions (43 ± 4% damaged white matter tracts) (Fig. 2A). The importance of •NO formation for myelin damage in our experimental set-up was demonstrated by the concentration-dependent protection of white matter tracts following the treatment of tissue slices with the •NO scavenger CPTIO (Fig. 2B). Of note, in contrast to myelin structures, neuroaxonal structures showed no structural damage upon LPS challenge (Fig. 2C).

Grx2 protects OPCs

The accumulation of •NO within lesions does not only damage the myelin structure, but moreover inhibits remyelination of axons by induction of cell death of OPCs (Pang et al., 2010). Therefore, we investigated the ability of Grx2 to protect OPCs. Again, we treated cerebellar slice cultures with or without Grx2 and LPS. Then, we counted the number of A2B5 positive cells (glial precursor cells). Indeed, the number of A2B5 positive cells in the area of white matter tracts was strongly reduced under •NO-releasing conditions (33 ± 4 compared to 52 ± 5 in control slices), whereas additional treatment with Grx2 abolished this effect (67 ± 7 A2B5 cells/white matter tract, Fig. 2D). We further investigated this effect in primary A2B5 cells that were isolated from mouse brains. The uptake of recombinant Grx2 in these cells was confirmed by immunocytochemistry (Fig. S2B) and Western blot analyses that revealed an increase to 132 ± 12% after 2 h and 143 ± 8% after 24 h treatment (Fig. S2D). Upon GSNO treatment, transcription and expression of endogenous Grx2 was not affected in A2B5 cells (mRNA levels of treated compared to untreated cells: *GLRX2a*: 101 ± 2%, *GLRX2c*: 114 ± 12%, Fig. S3A) and in oligodendroglial cell line OLN93 (protein level of treated compared to untreated cells: 95 ± 10%, Fig. S3B). To mimic the experimental set-up of the organotypic slice cultures, A2B5 positive cells were treated with GSNO or co-cultured with LPS-activated BV2 cells, a

microglial cell line, without direct cell-to-cell contact. As observed in slice cultures, the increased levels of Grx2 led to an enhanced survival rate of A2B5 positive cells compared to •NO-treated cells without Grx2 (Fig. 2E and F). OPCs that were incubated with Grx2 in addition to treatment with 250 µM GSNO had an increased survival rate of 234 ± 32% (Fig. 2F). In presence of LPS-activated BV2 cells, the increased levels of Grx2 led to an enhanced survival rate of A2B5 positive cells compared to •NO-treated cells without Grx2 (214 ± 16%, Fig. 2F). Secretion of •NO by BV2 cells after LPS treatment was measured by the Griess reaction (Fig. 2G). Corroboratively, the •NO scavenger CPTIO improved A2B5 survival with increasing concentrations (Fig. S3C). In additional control experiments, we showed that Grx2 affected neither microglial •NO secretion (Fig. 2G) nor the survival of microglia (Fig. S3D). Furthermore, Grx2 does not increase proliferation (Fig. 2H) or survival of A2B5 positive cells in the absence of BV2 cells (Fig. S3E). Moreover, in our experimental set-up LPS had no effect on the survival rates of microglia (Fig. S3D) or of A2B5 cells that were cultivated without microglia (Fig. S3E). An siRNA-mediated reduction in the levels of the mitochondrial and cytosolic Grx2 isoforms (*GLRX2a*: 28 ± 13%, *GLRX2c*: 33 ± 7%) led to higher cell death rates in both treatment conditions, i.e. GSNO and LPS-activated microglia (Fig. 2I). We further confirmed the intracellular protective functions of Grx2 against GSNO by using HeLa cells overexpressing either cytosolic Grx2c or mitochondrial Grx2a (Enoksson et al., 2005). The calculated IC_{50} value changed from 480 µM in control cells to 610 µM and 990 µM in Grx2c or Grx2a HeLa cells, respectively (Fig. 2J).

Grx2 decreases formation of peroxynitrite

We further investigated the underlying mechanism responsible for protection against oligodendrocytic cell death. Using A2B5 positive cells and OLN93 cells we observed via the Western blot technique that Grx2 inhibits •NO-mediated protein nitration and carbonylation with biological relevance. The increase in intracellular Grx2 levels after incubation of OLN93 cells with 2 µM Grx2 were similar to the increase observed for A2B5 cells (473 ± 113%, Fig. S2E). Formation of nitrotyrosines increased following GSNO treatment (165 ± 14%) compared to controls, whereas the presence of Grx2 decreased its formation to 112 ± 8% (Fig. 3A). The measurement of protein carbonyls revealed a similar pattern (Fig. 3B): While GSNO treatment increased the level of carbonylation to 185 ± 18% compared to controls, the addition of Grx2 resulted in levels comparable to control OLN93 cells (120 ± 15%). This observation was confirmed in A2B5 positive cells (signal intensity for carbonylated proteins was 93% and 162% with or without Grx2, respectively, compared to control cells, Fig. S4A).

Nitrosative and oxidative damage is mainly facilitated by $ONOO^-$. OLN93 cells displayed an almost identical increase in both nitrated (145 ± 17% (- Grx2) and 150 ± 10% (+ Grx2), Fig. 3C) and carbonylated (270 ± 72% (- Grx2) and 239 ± 69% (+ Grx2), Fig. 3D) proteins after $ONOO^-$ challenge via treatment with the $ONOO^-$-donor SIN-1, regardless of the presence of Grx2. We then confirmed that Grx2 protection against SIN-1 induced nitration in A2B5 positive cells is limited as well (170 ± 30% and 183 ± 36% with and without Grx2, respectively, Fig. S4B). Utilization of our newly developed peroxynitrite probe fluorescein-boronate (Rios et al., 2016) in HeLa cells overexpressing Grx2c revealed intracellular inhibition of $ONOO^-$-formation by elimination of $^{\bullet}NO$ as protective Grx2 mechanism decreasing oxidative and nitrosative protein modifications. The amount of $ONOO^-$ went down to 27 ± 4% or 56 ± 7% in Grx2c overexpressing cells compared to wildtype cells treated with GSNO or SIN-1, respectively (Fig. 3E and F). Treatment with Grx2 led to a decreased formation of 77 ± 5% (compared to GSNO treatment) or 91 ± 3% (compared to SIN-1 treatment) of $ONOO^-$. These data were reflected in experiments using A2B5 cells (GSNO + Grx2: 61 ± 9%; SIN-1 + Grx2: 85 ± 7% of $ONOO^-$ compared to cells without Grx2, Fig. 3G and H). Since fluorescein-boronate might also react in presence of peroxides, we demonstrated $^{\bullet}NO$-dependent reactivity in SIN-1-treated A2B5 cells with (44 ± 4%) or without (100%) presence of CPTIO (Fig. 3H). Although H_2O_2 treatment induced some fluorescence, Grx2 treatment did not reduce probe reactivity after incubation of A2B5 cells with H_2O_2 (Fig. S4C). In line, H_2O_2 treatment induced no protein nitration (Fig. S4D). Visualization of cell death induction in OLN93 (Fig. 3I) and A2B5 cells (Fig. 3J) using immunofluorescence confirmed the protective effects of Grx2 against GSNO, but not against SIN-1. Upon treatment with either $^{\bullet}NO$ or $ONOO^-$, the amount of active caspase 3 increased. However, only in the case of $^{\bullet}NO$ treatment did Grx2 attenuate caspase 3 activation (66% or 108% of active caspase 3 positive A2B5 cells compared to cells treated only with GSNO or SIN-1). Moreover, Grx2 displayed no protective effect on the survival rates of A2B5 positive cells treated with different concentrations of SIN-1 (Fig. 3K).

Only holo-Grx2 protects against $^{\bullet}NO$

Next, we aimed to characterize the discovered protective mechanism by testing the activity of different mutants of the Grx2 protein in the above-described assays. Surprisingly, it was not the enzymatic activity of Grx2, but its ability to coordinate an FeS cluster that resulted in its protective effect against $^{\bullet}NO$-mediated cell death. We compared the protective efficacy of Grx2C37S, a mutant that lacks the N-terminal active site

cysteine, and Grx2S38P. Grx2C37S is enzymatically inactive and lacks the ability to coordinate the FeS cluster, whereas Grx2S38P is unable to coordinate the cofactor, but shows an elevated level of enzymatic activity when compared to the wildtype protein (Berndt et al., 2007). These two mutants were neither able to inhibit $ONOO^-$ formation in HeLa cells after GSNO treatment (Grx2C37S: 114 ± 25%; Grx2S38P: 111 ± 9% compared to GSNO treatment, Fig. 4A), nor to affect the amount of protein carbonyls following GSNO treatment (Fig. 4B). In contrast to wildtype Grx2 (decreased intensity of detected protein carbonyls was 140 ± 28% compared to untreated control cells; 208 ± 31% without Grx2 addition), Grx2S38P showed no reduction in the overall level of carbonylated proteins (259 ± 49%). Subsequently, both mutants did not protect A2B5 positive cells against $^{\bullet}NO$ that was released by LPS-activated microglia (Fig. 4C). The survival rate of OLN93 cells that were treated with two additional $^{\bullet}NO$-donors that had different rates of $^{\bullet}NO$ release, NOC5 (t_2 = 25 minutes) and NOC7 (t_2 = 5 minutes), was also not increased by the addition of the Grx2S38P mutant (Fig. 4D). Cells were incubated with the respective $^{\bullet}NO$-donor for 20 minutes and survival rates were determined by the cell Titer Blue assay 24 hours later. NOC7 decreased the survival rate of OLN93 cells to 28% compared to untreated cells. This effect was ameliorated by the addition of wildtype Grx2 (57%), whereas Grx2S38P showed no protective effect (34% surviving OLN93 cells). Because NOC5 showed almost no effect on the survival rate, this experiment demonstrated that the survival of OLN93 cells in our experimental set-up depends solely on $^{\bullet}NO$ treatment.

Disassembly of holo-Grx2 by $^{\bullet}NO$ leads to formation of dinitrosyl-iron-complexes

To unravel the importance of the FeS cluster, we treated holo-Grx2 with various $^{\bullet}NO$-donors: Following the decay of the specific absorbance of the Grx2-bound Fe_2S_2 cluster at 320 nm and 428 nm, we visualized the time-dependent destruction of holo-Grx2 by GSNO (Fig. 5A), SNAP (Fig. 5B), and NOC5 and NOC7 (Fig. 5C). $^{\bullet}NO$-mediated disassembly was more accelerated than the disassembly that occurred following treatment with GSH-disulfide (GSSG) (K_i' [min^{-1}]: GSSG = 4.78 ± 0.52 x 10^{-3}, GSNO = 1.15 ± 0.05 x 10^{-2}). As shown in Fig. 5C, destruction of holo-Grx2 by $^{\bullet}NO$ is concentration-dependent. In addition to UV-VIS spectroscopy, Mössbauer spectroscopy confirmed the disassembly of the cofactor that was coordinated by Grx2 (Fig. 5D). After treatment with GSNO, the signal of the Fe_2S_2 cluster (quadrupole splitting ΔE_Q = 0.60 mm x s^{-1}, isomer shifts δ = 0.27 mm x s^{-1}) was reduced and was split into new sub-signals (1: quadrupole splitting ΔE_Q = 0.66 mm x s^{-1}, isomer shifts δ = 0.56 mm x s^{-1}, 2: quadrupole splitting ΔE_Q = 0.68 mm x s^{-1}, isomer

shifts δ = 0.28 mm x s^{-1}). To determine the reaction rate between holo-Grx2 and •NO, we used data obtained with NOCs because of their known decay rate (t_2NOC5 = 25 min, t_2NOC7 = 5 min, i.e. first order rate constants of 4.6 x 10^{-4} and 2.3 x 10^{-3} s^{-1}). Second order rate constants of 4.48 ± 0.22 x 10^{-2} and 9.36 ± 0.02 x 10^{-2} M^{-1} x s^{-1} for NOC5 and NOC7, respectively, were calculated for the overall reaction demonstrating that the liberation of •NO from NOCs is the rate limiting step. Thereby, we can conclude that the reaction between holo-Grx2 and •NO must be considerably larger, thus in a physiologically meaningful range. EPR spectroscopy identified the formation of dinitrosyl-iron-complexes (DNICs) upon •NO-mediated destruction of holo-Grx2 via a specific signal at g = 2.03 (Fig. 5E,F). Treatment of hGrx2c-expressing *E. coli* cells with GSNO revealed an intracellular time-dependency of DNIC formation with a maximum around three minutes (Fig. 5E). Therefore, we incubated OLN93 cells in the following experiments for three minutes with GSNO. The EPR signal intensity of the OLN93 cells that were treated with Grx2 and GSNO was used as a reference (100%, Fig. 5F). Compared to this condition, OLN93 cells that were treated with Grx2 or GSNO alone displayed just 25 or 32% of the EPR signal, respectively. The signal was further increased to 125% in the presence of MK517, which inhibits the multidrug resistance protein 1 (MRP1), a membrane-bound protein described as an exporter of DNICs (Watts, Hawkins, Ponka, & Richardson, 2006). Its expression in OLN93 and A2B5 cells was verified by immunofluorescence, Western blot, and PCR (Fig. 6 A-C). However, co-treatment of A2B5 cells with Grx2 and MK517 did neither further increase survival rate after GSNO challenge (GSNO/Grx2: 100 ± 6%, GSNO/Grx2/MK517: 103 ± 10%, Fig. 6D), nor further decrease carbonylation rate (98% compared to treatment with GSNO and Grx2 alone, Fig. S4E). MK517 alone showed no increase in DNIC formation (32% signal intensity, Fig. 5F). In comparison to this signal, intensity showed just a minor increase to 49% after additional incubation of OLN93 cells with Grx1, the mammalian glutaredoxin without the ability to coordinate an iron-sulfur cluster. Increased washing conditions did not change the signal intensity (103%), suggesting that intracellular Grx2 was responsible for the DNIC formation, as seen before (Fig. 5E). To further confirm the intracellular origin of the complexes, we again used the Grx2 overexpressing HeLa cells (Grx2c: three-fold higher Grx2 levels, Grx2a: 1.5-fold higher Grx2 levels). We took advantage of the observation that DNICs inhibit glutathione-S-transferases (GST) (Cesareo et al., 2005; Keese, Böse, Mülsch, Schirmer, & Becker, 1997) and measured GST activity in these HeLa cells with or without GSNO treatment. Corroboratively, GST activity decreased in a manner that was dependent on the amount of intracellular Grx2 (Fig. 7A). Accordingly, the incubation of recombinant GST with GSNO

and increasing concentrations of holo-Grx2 *in vitro* demonstrated a Grx2-dependent inhibition of GST activity (Fig. 7B).

Discussion

The activation of microglia, the macrophage-like immune cells of the CNS, is associated with several neurological diseases, including MS (Trapp, 2004). Upon activation, microglia release nitric oxide that is generated by the inducible nitric oxide synthase (Li et al., 2005). Microglia activation via LPS injection into the CNS white matter has been proposed as a promising experimental model of early MS lesions inducing demyelination via increased nitric oxide production (Desai et al., 2016). The term “nitric oxide” represents the three redox-active forms of this important signaling molecule, the nitrosonium cation (NO^+), the nitroxyl anion (NO^-) and the nitric oxide radical ($^{\bullet}NO$) (Stamler, Singel, & Loscalzo, 1992). Nitric oxide reacts with the superoxide radical to form peroxynitrite and with metal centers, including FeS clusters (Foster & Cowan, 1999).

Although many Grxs were characterized as FeS proteins, little is known about their functions and molecular mechanisms. FeS clusters have been hypothesized to act as redox sensors allowing to switch between inactive holo-Grxs and active apo-Grxs (Berndt et al., 2007; Lillig et al., 2005). In addition, FeS Grxs are important for the maintenance of iron homeostasis (Haunhorst et al., 2013; Mühlenhoff et al., 2010) and for FeS cluster biosynthesis (Bandyopadhyay, Chandramouli, & Johnson, 2008; Wingert et al., 2005), where these proteins support the incorporation of FeS clusters into apo-proteins (Mühlenhoff, Gerber, Richhardt, & Lill, 2003). Here, we describe the detoxification of $^{\bullet}NO$ as a new function of the iron cofactor.

Although a Grx2 mutant that lacks the ability to coordinate the FeS cluster but retains enzymatic activity does not show protection, it is possible that the cluster has a redox sensing function because a changed active site composition might inhibit Grx2-specific substrate recognition, which could be important for oligodendroglial survival under the condition of brain inflammation. We have already shown that GSNO might activate Grx2 via the disassembly of the FeS cluster (Hashemy, Johansson, Berndt, Lillig, & Holmgren, 2007). In contrast, Grx1, the second dithiol Grx in vertebrate cells, is inactivated upon GSNO treatment, which indicates their different regulation and functions *in vivo* (Hashemy et al., 2007). Indeed, we found that the expression of these two Grxs in EAE mice is diametrical. Whereas mice suffering from EAE experience a significant reduction of Grx2

transcripts, Grx1 transcript levels increased or were not regulated (Fig. 1 D,E). Although EAE reflects not all aspects of MS (Schuh et al., 2014), increased nitric oxide formation/protein nitration is a common feature (Li, Vana, Ribeiro, & Zhang, 2011). In line, nitrotyrosines were found in oligodendrocytes in EAE (Fig. 1B) as well as in MS patients (Jack et al., 2007).

Free, chelatable iron has been described to be deleterious for brain function. Accumulation of iron is associated with numerous diseases of the CNS, including MS (Rouault, 2013). Here, we add a new aspect to the importance of functional iron homeostasis and FeS cluster biosynthesis for brain function: We demonstrate the important role of protein-bound iron for the protection against •NO-mediated damage of myelin integrity.

Several cofactors of mammalian proteins are utilized as iron sources for the formation of DNICs (Crack, Green, Thomson, & Le Brun, 2014). In *E. coli*, FeS proteins are the major source of protein-bound DNICs (Landry, Duan, Huang, & Ding, 2011). Because an increased level of chelatable iron appears to be dangerous for neural cells, FeS proteins might be the iron source for the formation of DNICs. Although there could be other FeS proteins in the brain that contribute to •NO detoxification, we propose that, based on its unique FeS cluster coordination, Grx2 and most likely also other FeS Grxs are important for oligodendrocyte protection against •NO that is secreted by activated microglia. Mammalian Grx2, as well as the vast majority of all other FeS Grxs coordinate the FeS cofactor via the N-terminal active site cysteines and two molecules of GSH in a dimer (Berndt et al., 2007; Johansson et al., 2007). To our knowledge, Grxs are the only proteins that use non-protein ligands for FeS coordination. This might lead to the formation of free GSH-coordinated DNICs although utilizing a protein-bound FeS cluster. In line, the observed EPR spectrum at g = 2.03 (Fig. 5E,F) indicates the formation of DNICs with thiol-containing ligands (Vanin, Serezhenkov, Mikoyan, & Genkin, 1998) and the loss of GST activity (Fig. 7) is facilitated by binding of these complexes to the GST active site (Cesareo et al., 2005; Keese et al., 1997). Several GSTs bind DNICs, which potentially stores •NO and thereby protect cells against •NO-mediated cell death (Lok et al., 2014). However, only GST P1-1 supports the release of DNICs via MRP1 (Lok et al., 2012). MRP1 requires GSH for the export of iron (Watts & Richardson, 2001), which is most likely secreted as a DNIC (Watts et al., 2006). Both pharmacological and genetic inhibition of MRP1 activity led to increased intracellular levels of DNICs (Lok et al., 2012; Watts et al., 2006). The treatment of OLN93 cells with the MRP1 inhibitor MK571 increased the DNIC signal (Fig. 5F), which further supports the hypothesis that •NO-

mediated disassembly of holo-Grx2 leads to dinitrosysl-diglutathionyl-iron-complexes (DNDGICs).

In contrast to oligodendrocytes and other cell types, the MRP1-mediated efflux of iron and GSH, in the form of DNDGICs, following •NO secretion by activated macrophages induces apoptosis in tumor cells (Lok et al., 2014). Interestingly, Grx2c was first described as a cancer-specific isoform (Lönn et al., 2008). Therefore, it would be interesting to investigate the impact of modulated Grx2 levels on the survival of cancer cells following treatment with •NO-donors. These observations follow recent reports that show that $ONOO^-$ mediates oligodendroglial cell death *in vitro* as well as in MS patients (Jack et al., 2007; Li et al., 2005; Li et al., 2011). We demonstrated the importance of •NO detoxification to prevent the formation of $ONOO^-$ (Fig. 2 and 3). Formation of DNICs was suggested as an important mechanism to prevent $ONOO^-$ formation (Shumaev et al., 2008). We used specific donors of •NO (GSNO, SNAP, NOCs) and $ONOO^-$ (SIN-1) to better define the role of Grx2 in oligodendroglial damage, which is induced by these RNS. Mitochondria are the primary site of peroxynitrite formation and also preferred targets for peroxynitrite-induced damage (Enoksson et al., 2005), suggesting that •NO detoxification in mitochondria is important for cell survival. Indeed, the overexpression of mitochondrial Grx2a provided an increased level of protection against GSNO-mediated cell death than did the overexpression of the cytosolic Grx2 isoform (Fig. 2J). These and other data obtained during this study confirm an intracellular function of Grx2, although externally applied. Important for a potential therapeutic application of GSH-coordinated FeS clusters, the resulting intracellular Grx2 levels were still in a physiological range (max. seven-fold increase). It has been shown before that intravenous injection of another thiol oxidoreductase, Trx1, facilitated anti-inflammatory functions within the mouse CNS (Hattori et al., 2004) indicating that injected FeS-coordinating Grxs might reach the brain and thus oligodendrocytes.

In addition to preventing $ONOO^-$ formation, DNDGICs could provide additional benefits for cell survival, although our data showed only limited increase in the protective effect after inhibition of DNDGIC export. The treatment of cells with these complexes resulted in a decrease in the level of apoptosis (Giliano et al., 2011; Kim, Chung, Simmons, & Billiar, 2000) e.g., via caspase 3 inhibition (Kim et al., 2000). These findings and other observations led to the discovery of a DNDGIC-containing therapeutic agent that is currently in clinical trials (Chazov et al., 2012). This indicates that supply of GSH-coordinated iron-sulfur clusters, e.g. provided by Grx2, represents a feasible new therapeutic approach to transform •NO from a harmful molecule to a beneficial agent without increasing the pool of chelatable iron or further enhancing the levels of DNICs. In

this regard, the recently characterized $[[Fe_2S_2]^{2+}(GS^-)^4]^{2-}$ complex (Qi et al., 2012) is another feasible GSH-coordinated iron-sulfur cluster that might be protective under conditions of neuroinflammation.

Conclusion

Increased nitric oxide production and concomitant nitrosative damage to myelin and OPCs is an early event during neuroinflammatory diseases. Therefore, nitric oxide detoxification is an important tool to protect myelin integrity against inflammatory processes and cellular damage. Although remyelination occurs in initial stages of MS, repair processes fail when the disease progresses (Hampton et al., 2012). It is evident that increased $^{\bullet}NO$ levels in chronic MS limit the efficiency of remyelination by the induction of OPC cell death (Kremer, Aktas, Hartung, & Küry, 2011; Miron et al., 2013; Miron, Kuhlmann, & Antel, 2011). Moreover, instead of transplantation approaches to replace damaged/lost oligodendrocytes, therapeutic strategies promoting endogenous regenerative capacity came into focus (Franklin & Gallo, 2014). Hence, strategies aiming at boosting Grx2 or other GSH coordinated FeS clusters represent an attractive approach to counteract inflammation-driven demyelination.

Acknowledgments

The authors thank Nina Voevodskaya (Department of Biochemistry and Biophysics, Stockholm Universitet, Sweden), Annett Günther and Isaac Hashemy (Karolinska Institute), Bernd Mienert (Max-Planck-Institut für Chemische Energiekonversion), and Christina Wilms and Bastian Bosch (Heinrich-Heine University) for experimental support; Helmut Sies (Heinrich-Heine Universität), Nicolas Rouhier (Université de Lorraine, Nancy, France), and Leda Dimou (Ludwig-Maximilians Universität, Munich, Germany) for valuable discussions. For financial support we thank the graduate school iBrain (K.L.), the Swedish Cancer Society (AH, grant no. 961), the Swedish Research Council (A.H., grant no. KAW 2006.0192), the Research Commission of the Medical Faculty (O.A. and C.B., grant no.06/2012), the Gemeinnützige Hertie Stiftung (O.A. and C.B., grant no. P1120028), the Karolinska Institute (C.B.), and the German Research Foundation (C.H.L., grant no. LI984/3-1 and LI984/4-1; C.B., grant no. BE3259/1-2 and BE3259/6-1). The authors declare no competing financial interests.

Author contributions

Klaudia Lepka, Katrin Volbracht, Eckhard Bill, Reiner Schneider, Thomas Hildebrandt, Jens Ingwersen, Tim Prozorovski, Christopher Horst Lillig, and Carsten Berndt performed

and analyzed experiments; Klaudia Lepka, Rafael Radi, Arne Holmgren, Orhan Aktas, and Carsten Berndt designed the experiments; Natalia Rios and Rafael Radi provided new reagents; Lawrence Steinman and Hans-Peter Hartung provided critical input; Klaudia Lepka, Jack van Horssen, Rafael Radi, Orhan Aktas, and Carsten Berndt wrote the manuscript. All of the authors contributed to and endorsed the submitted version.

References

Bandyopadhyay, S., Chandramouli, K., & Johnson, M. K. (2008). Iron-sulfur cluster biosynthesis. *Biochemical Society transactions, 36*(Pt 6), 1112–1119.

Berndt, C., Hudemann, C., Hanschmann, E.-M., Axelsson, R., Holmgren, A., & Lillig, C. H. (2007). How does iron-sulfur cluster coordination regulate the activity of human glutaredoxin 2? *Antioxidants & redox signaling, 9*(1), 151–157.

Berndt, C., Lillig, C. H., & Flohé, L. (2014). Redox regulation by glutathione needs enzymes. *Frontiers in pharmacology, 5,* 168.

Bräutigam, L., Schütte, L. D., Godoy, J. R., Prozorovski, T., Gellert, M., Hauptmann, G., . . . Berndt, C. (2011). Vertebrate-specific glutaredoxin is essential for brain development. *Proceedings of the National Academy of Sciences of the United States of America, 108*(51), 20532–20537.

Bräutigam, L., Jensen, Lasse Dahl Ejby, Poschmann, G., Nyström, S., Bannenberg, S., Dreij, K., . . . Berndt, C. (2013). Glutaredoxin regulates vascular development by reversible glutathionylation of sirtuin 1. *Proceedings of the National Academy of Sciences of the United States of America, 110*(50), 20057–20062.

Cesareo, E., Parker, L. J., Pedersen, J. Z., Nuccetelli, M., Mazzetti, A. P., Pastore, A., . . . Lo Bello, M. (2005). Nitrosylation of human glutathione transferase P1-1 with dinitrosyl diglutathionyl iron complex in vitro and in vivo. *The Journal of biological chemistry, 280*(51), 42172–42180.

Chazov, E. I., Rodnenkov, O. V., Zorin, A. V., Lakomkin, V. L., Gramovich, V. V., Vyborov, O. N., . . . Vanin, A. F. (2012). Hypotensive effect of Oxacom® containing a dinitrosyl iron complex with glutathione: animal studies and clinical trials on healthy volunteers. *Nitric oxide : biology and chemistry / official journal of the Nitric Oxide Society, 26*(3), 148–156.

Compston, A., & Coles, A. (2002). Multiple sclerosis. *Lancet (London, England), 359*(9313), 1221–1231.

Crack, J. C., Green, J., Thomson, A. J., & Le Brun, Nick E. (2014). Iron-sulfur clusters as biological sensors: the chemistry of reactions with molecular oxygen and nitric oxide. *Accounts of chemical research, 47*(10), 3196–3205.

Desai, R. A., Davies, A. L., Tachrount, M., Kasti, M., Laulund, F., Golay, X., & Smith, K. J. (2016). Cause and prevention of demyelination in a model multiple sclerosis lesion. *Annals of neurology, 79*(4), 591–604.

Enoksson, M., Fernandes, A. P., Prast, S., Lillig, C. H., Holmgren, A., & Orrenius, S. (2005). Overexpression of glutaredoxin 2 attenuates apoptosis by preventing cytochrome c release. *Biochemical and biophysical research communications, 327*(3), 774–779.

Foster, M., & Cowan, J. A. (1999). Chemistry of Nitric Oxide with Protein-Bound Iron Sulfur Centers. Insights on Physiological Reactivity. *Journal of the American Chemical Society*, (121(17)), 4093–4100.

Franklin, R. J. M., & Gallo, V. (2014). The translational biology of remyelination: past, present, and future. *Glia, 62*(11), 1905–1915.

Giliano, N. Y., Konevega, L. V., Noskin, L. A., Serezhenkov, V. A., Poltorakov, A. P., & Vanin, A. F. (2011). Dinitrosyl iron complexes with thiol-containing ligands and apoptosis: studies with HeLa cell cultures. *Nitric oxide : biology and chemistry / official journal of the Nitric Oxide Society, 24*(3), 151–159.

Godoy, J. R., Funke, M., Ackermann, W., Haunhorst, P., Oesteritz, S., Capani, F., Elsässer, H. P., & Lillig, C. H. (2011). Redox atlas of the mouse. Immunohistochemical detection of glutaredoxin-, peroxiredoxin-, and thioredoxin-family proteins in various tissues of the laboratory mouse. *Biochimica et Biophysica Acta- General Subjects 1810*(1), 2-92.

Habig, W. H., Pabst, M. J., & Jakoby, W. B. (1974). Glutathione S-transferases. The first enzymatic step in mercapturic acid formation. *The Journal of biological chemistry, 249*(22), 7130–7139.

Hampton, D. W., Innes, N., Merkler, D., Zhao, C., Franklin, Robin J M, & Chandran, S. (2012). Focal immune-mediated white matter demyelination reveals an age-associated increase in axonal vulnerability and decreased remyelination efficiency. *The American journal of pathology, 180*(5), 1897–1905.

Hanschmann, E.-M., Godoy, J. R., Berndt, C., Hudemann, C., & Lillig, C. H. (2013). Thioredoxins, glutaredoxins, and peroxiredoxins--molecular mechanisms and health significance: from cofactors to antioxidants to redox signaling. *Antioxidants & redox signaling, 19*(13), 1539–1605.

Hart, T. W. (1985). Some observations concerning the S-nitroso and S-phenylsulphonyl derivatives of L-cysteine and glutathione. *Tetrahedron Letters, 26*(16), 2013–2016.

Hashemy, S. I., Johansson, C., Berndt, C., Lillig, C. H., & Holmgren, A. (2007). Oxidation and S-nitrosylation of cysteines in human cytosolic and mitochondrial glutaredoxins: effects on structure and activity. *The Journal of biological chemistry, 282*(19), 14428–14436.

Hattori, I., Takagi, Y., Nakamura, H., Nozaki, K., Bai, J., Kondo, N., . . . Yodoi, J. (2004). Intravenous administration of thioredoxin decreases brain damage following transient focal cerebral ischemia in mice. *Antioxidants & redox signaling, 6*(1), 81–87.

Haunhorst, P., Hanschmann, E.-M., Bräutigam, L., Stehling, O., Hoffmann, B., Mühlenhoff, U., . . . Lillig, C. H. (2013). Crucial function of vertebrate glutaredoxin 3 (PICOT) in iron homeostasis and hemoglobin maturation. *Molecular biology of the cell, 24*(12), 1895–1903.

Hoff, K. G., Culler, S. J., Nguyen, P. Q., McGuire, R. M., Silberg, J. J., & Smolke, C. D. (2009). In vivo fluorescent detection of Fe-S clusters coordinated by human GRX2. *Chemistry & biology, 16*(12), 1299–1308

Hohlfeld, R., & Wekerle, H. (2004). Autoimmune concepts of multiple sclerosis as a basis for selective immunotherapy: from pipe dreams to (therapeutic) pipelines. *Proceedings of the National Academy of Sciences of the United States of America, 101 Suppl 2,* 14599–14606.

Hudemann, C., Lönn, M. E., Godoy, J. R., Zahedi Avval, F., Capani, F., Holmgren, A., & Lillig, C. H. (2009). Identification, expression pattern, and characterization of mouse glutaredoxin 2 isoforms. *Antioxidants & redox signaling, 11*(1), 1–14.

Huehnchen, P., Prozorovski, T., Klaissle, P., Lesemann, A., Ingwersen, J., Wolf, S. A., . . . Steiner, B. (2011). Modulation of adult hippocampal neurogenesis during myelin-directed autoimmune neuroinflammation. *Glia, 59*(1), 132–142.

Ip, C. W., Kroner, A., Bendszus, M., Leder, C., Kobsar, I., Fischer, S., . . . Martini, R. (2006). Immune cells contribute to myelin degeneration and axonopathic changes in mice overexpressing proteolipid protein in oligodendrocytes. *The Journal of neuroscience : the official journal of the Society for Neuroscience, 26*(31), 8206–8216.

Jack, C., Antel, J., Brück, W., & Kuhlmann, T. (2007). Contrasting potential of nitric oxide and peroxynitrite to mediate oligodendrocyte injury in multiple sclerosis. *Glia, 55*(9), 926–934.

Johansson, C., Kavanagh, K. L., Gileadi, O., & Oppermann, U. (2007). Reversible sequestration of active site cysteines in a 2Fe-2S-bridged dimer provides a mechanism for glutaredoxin 2 regulation in human mitochondria. *The Journal of biological chemistry, 282*(5), 3077–3082.

Keese, M. A., Böse, M., Mülsch, A., Schirmer, R. H., & Becker, K. (1997). Dinitrosyl-dithiol-iron complexes, nitric oxide (NO) carriers in vivo, as potent inhibitors of human glutathione reductase and glutathione-S-transferase. *Biochemical pharmacology, 54*(12), 1307–1313.

Kim, Y. M., Chung, H. T., Simmons, R. L., & Billiar, T. R. (2000). Cellular non-heme iron content is a determinant of nitric oxide-mediated apoptosis, necrosis, and caspase inhibition. *The Journal of biological chemistry, 275*(15), 10954–10961.

Kremer, D., Aktas, O., Hartung, H.-P., & Küry, P. (2011). The complex world of oligodendroglial differentiation inhibitors. *Annals of neurology, 69*(4), 602–618.

Landry, A. P., Duan, X., Huang, H., & Ding, H. (2011). Iron-sulfur proteins are the major source of protein-bound dinitrosyl iron complexes formed in Escherichia coli cells under nitric oxide stress. *Free radical biology & medicine, 50*(11), 1582–1590.

Lassmann, H., Brück, W., & Lucchinetti, C. F. (2007). The immunopathology of multiple sclerosis: an overview. *Brain pathology (Zurich, Switzerland), 17*(2), 210–218.

Li, J., Baud, O., Vartanian, T., Volpe, J. J., & Rosenberg, P. A. (2005). Peroxynitrite generated by inducible nitric oxide synthase and NADPH oxidase mediates microglial toxicity to oligodendrocytes. *Proceedings of the National Academy of Sciences of the United States of America, 102*(28), 9936–9941.

Li, S., Vana, A. C., Ribeiro, R., & Zhang, Y. (2011). Distinct role of nitric oxide and peroxynitrite in mediating oligodendrocyte toxicity in culture and in experimental autoimmune encephalomyelitis. *Neuroscience, 184,* 107–119.

Lillig, C. H., Berndt, C., Vergnolle, O., Lönn, M. E., Hudemann, C., Bill, E., & Holmgren, A. (2005). Characterization of human glutaredoxin 2 as iron-sulfur protein: a possible role as redox sensor. *Proceedings of the National Academy of Sciences of the United States of America, 102*(23), 8168–8173.

Lok, H. C., Suryo Rahmanto, Y., Hawkins, C. L., Kalinowski, D. S., Morrow, C. S., Townsend, A. J., . . . Richardson, D. R. (2012). Nitric oxide storage and transport in cells are mediated by glutathione S-transferase P1-1 and multidrug resistance protein 1 via dinitrosyl iron complexes. *The Journal of biological chemistry, 287*(1), 607–618.

Lok, H. C., Sahni, S., Richardson, V., Kalinowski, D. S., Kovacevic, Z., Lane, D J R, & Richardson, D. R. (2014). Glutathione S-transferase and MRP1 form an integrated system involved in the storage and transport of dinitrosyl-dithiolato iron complexes in cells. *Free radical biology & medicine, 75,* 14–29.

Lönn, M. E., Hudemann, C., Berndt, C., Cherkasov, V., Capani, F., Holmgren, A., & Lillig, C. H. (2008). Expression pattern of human glutaredoxin 2 isoforms: identification and characterization of two testis/cancer cell-specific isoforms. *Antioxidants & redox signaling, 10*(3), 547–557.

Miron, V. E., Kuhlmann, T., & Antel, J. P. (2011). Cells of the oligodendroglial lineage, myelination, and remyelination. *Biochimica et biophysica acta, 1812*(2), 184–193.

Miron, V. E., Boyd, A., Zhao, J.-W., Yuen, T. J., Ruckh, J. M., Shadrach, J. L., . . . ffrench-Constant, C. (2013). M2 microglia and macrophages drive oligodendrocyte differentiation during CNS remyelination. *Nature Neuroscience, 16*(9), 1211–1218.

Mühlenhoff, U., Gerber, J., Richhardt, N., & Lill, R. (2003). Components involved in assembly and dislocation of iron-sulfur clusters on the scaffold protein Isu1p. *The EMBO journal, 22*(18), 4815–4825.

Mühlenhoff, U., Molik, S., Godoy, J. R., Uzarska, M. A., Richter, N., Seubert, A., . . . Lill, R. (2010). Cytosolic monothiol glutaredoxins function in intracellular iron sensing and trafficking via their bound iron-sulfur cluster. *Cell metabolism, 12*(4), 373–385.

O'Sullivan, S. A., Velasco-Estevez, M., & Dev, K. K. (2017). Demyelination induced by oxidative stress is regulated by sphingosine 1-phosphate receptors. *Glia.*

Pang, Y., Campbell, L., Zheng, B., Fan, L., Cai, Z., & Rhodes, P. (2010). Lipopolysaccharide-activated microglia induce death of oligodendrocyte progenitor cells and impede their development. *Neuroscience, 166*(2), 464–475.

Prinz, M., Priller, J., Sisodia, S. S., & Ransohoff, R. M. (2011). Heterogeneity of CNS myeloid cells and their roles in neurodegeneration. *Nature neuroscience, 14*(10), 1227–1235.

Qi, W., Li, J., Chain, C. Y., Pasquevich, G. A., Pasquevich, A. F., & Cowan, J. A. (2012). Glutathione complexed Fe-S centers. *Journal of the American Chemical Society, 134*(26), 10745–10748.

Radi, R. (2013). Protein tyrosine nitration: biochemical mechanisms and structural basis of functional effects. *Accounts of chemical research, 46*(2), 550–559.

Rios, N., Piacenza, L., Trujillo, M., Martínez, A., Demicheli, V., Prolo, C., . . . Radi, R. (2016). Sensitive detection and estimation of cell-derived peroxynitrite fluxes using fluorescein-boronate. *Free radical biology & medicine, 101,* 284–295.

Rouault, T. A. (2013). Iron metabolism in the CNS: implications for neurodegenerative diseases. *Nature reviews. Neuroscience, 14*(8), 551–564.

Schneider, R., Koop, B., Schröter, F., Cline, J., Ingwersen, J., Berndt, C., . . . Prozorovski, T. (2016). Activation of Wnt signaling promotes hippocampal neurogenesis in experimental autoimmune encephalomyelitis. *Molecular neurodegeneration, 11*(1), 53.

Schuh, C., Wimmer, I., Hametner, S., Haider, L., van Dam, A.-M., Liblau, R. S., . . . Lassmann, H. (2014). Oxidative tissue injury in multiple sclerosis is only partly reflected in experimental disease models. *Acta neuropathologica, 128*(2), 247–266.

Shumaev, K. B., Gubkin, A. A., Serezhenkov, V. A., Lobysheva, I. I., Kosmachevskaya, O. V., Ruuge, E. K., . . . Vanin, A. F. (2008). Interaction of reactive oxygen and nitrogen species with albumin- and methemoglobin-bound dinitrosyl-iron complexes. *Nitric oxide : biology and chemistry / official journal of the Nitric Oxide Society, 18*(1), 37–46.

Sies, H. (2015). Oxidative stress: a concept in redox biology and medicine. *Redox biology, 4,* 180–183.

Stamler, J. S., Singel, D. J., & Loscalzo, J. (1992). Biochemistry of nitric oxide and its redox-activated forms. *Science (New York, N.Y.), 258*(5090), 1898–1902.

Stoppini, L., Buchs, P. A., & Muller, D. (1991). A simple method for organotypic cultures of nervous tissue. *Journal of neuroscience methods, 37*(2), 173–182.

Trapp, B. D. (2004). Pathogenesis of multiple sclerosis: the eyes only see what the mind is prepared to comprehend. *Annals of neurology, 55*(4), 455–457.

Vanin, A. F., Serezhenkov, V. A., Mikoyan, V. D., & Genkin, M. V. (1998). The 2.03 signal as an indicator of dinitrosyl-iron complexes with thiol-containing ligands. *Nitric oxide : biology and chemistry / official journal of the Nitric Oxide Society, 2*(4), 224–234.

Watts, R. N., & Richardson, D. R. (2001). Nitrogen monoxide (no) and glucose: unexpected links between energy metabolism and no-mediated iron mobilization from cells. *The Journal of biological chemistry, 276*(7), 4724–4732.

Watts, R. N., Hawkins, C., Ponka, P., & Des Richardson, R. (2006). Nitrogen monoxide (NO)-mediated iron release from cells is linked to NO-induced glutathione efflux via multidrug resistance-associated protein 1. *Proceedings of the National Academy of Sciences of the United States of America, 103*(20), 7670–7675.

Wingert, R. A., Galloway, J. L., Barut, B., Foott, H., Fraenkel, P., Axe, J. L., . . . Zon, L. I. (2005). Deficiency of glutaredoxin 5 reveals Fe-S clusters are required for vertebrate haem synthesis. *Nature, 436*(7053), 1035–1039.

Zipp, F., & Aktas, O. (2006). The brain as a target of inflammation: common pathways link inflammatory and neurodegenerative diseases. *Trends in neurosciences, 29*(9), 518–527.

Figure legends

Fig. 1 In EAE mice levels of nitrotyrosine increase and Grx2 levels decrease. Slices of mouse cerebelli that suffered from actively induced experimental autoimmune encephalomyelitis (EAE, chronic phase, day 26) were used to visualize microglia (using anti-Iba1 antibodies, A), nitrated proteins (using anti-nitrotyrosine antibodies, A,B), oligodendrocytes (using anti-Olig2 antibodies, B), oligodendrocyte progenitor cells (using anti-A2B5 antibodies, C), Grx2 (C), and nuclei (using Hoechst, A-C). Arrows mark oligodendrocytes with increased nitration (B) or Grx2 positive A2B5 cells (C). Scale bars: A: 100 µm, B,C: 10 µm). D) Transcript levels of *GLRX2* isoforms and *GLRX1* were measured by qPCR and compared between control (naïve mice) and brain hemispheres after adoptive transfer EAE (chronic disease phase (day 30) of two independent EAE experiments; $n_{control}$ = 7, n_{EAE} = 10). E) Transcript levels of Grx2 isoforms and Grx1 were measured by qPCR and compared between control (pre-onset mice) and cerebellum after actively induced EAE (chronic disease phase (day 26); $n_{control}$ = 5, n_{EAE} = 7). D) Protein extracts obtained from cerebelli during chronic phase after actively induced EAE ($n_{control\ (pre\text{-}onset)}$ = 3, n_{EAE} = 3) were separated by SDS-PAGE and transferred onto a nitrocellulose membrane. Antibodies specific for mouse Grx2 and β-actin were used and bands were quantified using ImageJ. Shown is mean ± SEM, statistics were calculated using Student´s t-test (*: $p<0.05$, ns = not significant).

Fig. 2 Grx2 protects against $^{\bullet}$NO-mediated oligodendroglial cell death. A-D) Organotypic cerebellar slice cultures were treated with 750 µM GSNO or 10 µg/ml LPS in the presence or absence of 2 µM mouse Grx2 or 10 and 25 µM CPTIO. After 24 h, myelin, oligodendroglial progenitor cells (exemplified positive cells are highlighted by arrows), and axons were stained using antibodies that recognized MBP, A2B5, or NFM (scale bars A,D: 100 µm, C: 25 µm). A) Damaged myelin structures were identified using 7 – 8 (GSNO) or 33 – 47 slices (LPS). B) Protection by CPTIO was determined in 3 slices/condition. C) Damage of axonal structures was investigated in 11 - 18 slices. D) The number of A2B5 positive cells was counted in 11 – 12 slices. E,F) Using the cell titer blue assay, the survival rates of A2B5 positive cells after different treatment ± 2 µM Grx2 in addition to 50 - 250 µM GSNO (F: 250 µM GSNO) (n = 5 - 7) or to co-cultivation with

50,000 BV2 cells activated with 1 µg/ml LPS (n = 10) were determined. G) NO release by BV2 cells treated with 1 µg/ml LPS ± 1,000 U/ml INFγ ± 2 µM Grx2 was determined using Griess reagent (n = 6). H) Visualization of BrdU incorporation into DNA of proliferating A2B5 cells (using anti-BrdU and anti-acetylated histone 3 antibodies, scale bar 20 µm) and graphical evaluation (n = 4). I) Survival rates of A2B5 cells incubated with or without Grx2siRNA in presence of either 1 µg/ml LPS activated BV2 cells (n = 5) or 250 µM GSNO (n = 2) measured with the cell titer blue assay. Transcript levels of *GLRX2* isoforms (dashed line: *GLRX2a*, dotted line: *GLRX2c*) were measured by qPCR. J) HeLa cells overexpressing either mitochondrial (HeLaGrx2a) or cytosolic Grx2 isoforms (HeLaGrx2c) were treated with increasing amounts of GSNO. 24 h after treatment, cell survival was determined by XTT assay (n = 36). All data show mean ± SEM, statistics were calculated using ANOVA (with Bonferroni post-test) (A,D) and Student´s t-test (*: $p<0.05$, **: $p<0.005$, ***: $p<0.001$).

Fig. 3 Grx2 protects against oxidative and nitrosative protein damage via inhibition of peroxynitrite formation. OLN93 (A-D,I) HeLa (E,F), or A2B5 cells (G,H,J,K) were incubated with GSNO (A,B,I: 0.5 mM; E,G: 1 mM, J: 50 µM) or SIN1 (C,D,I: 0.5 mM; F,H: 1 mM; J: 50 µM; K: 50 and 100 µM) ± 2 µM Grx2. Directly after treatment, $ONOO^-$-formation was determined using fluorescein-boronate (E-H), after 24 h cell lysates were prepared (A–D), cells were fixed with 4% PFA (I,J), or survival rate was measured using the cell titer blue assay (K). The lysates were separated by SDS-PAGE and transferred onto nitrocellulose membranes, which were then incubated with anti-nitrotyrosine / anti-β-actin antibodies (A,C) or the protein-bound carbonyl groups were derivatized to 2,4-dinitrophenylhydrazone before SDS-PAGE and detection on membranes by anti-dinitrophenyl antibodies (B,D). Western blots were analyzed using ImageJ. The original blot of that one shown in A) is presented in supplementary Fig. S4D. I,J) Fixed cells were stained with anti-active caspase 3 antibodies (green) and nuclei were visualized with Hoechst (blue), scale bars: I: 50 µm (inserts 10 µm), J: 10 µm. All data show mean ± SEM (A: n = 4, B: n = 7-8, C: n = 4, D: n = 3, E: n = 3, F: n = 3, G: n = 3, H: n = 2, K: n = 11-18).

Fig. 4 FeS cluster coordination is crucial for Grx2´s protection against $^{\bullet}$NO. A) OLN93 cells were incubated with the Grx2 mutants C37S and S38P (2 µM) for 24 h and challenged with 1 mM GSNO together with fluorescein-boronate. $ONOO^-$-formation was

determined and compared to cells treated with GSNO alone (n = 3). B) Carbonyl groups in protein lysates were obtained from OLN93 cells that were treated with 500 µM GSNO ± either 2 µM Grx2 wildtype or Grx2S38P. They were derivatized to 2,4-dinitrophenylhydrazone before SDS-PAGE and detection on membranes by anti-dinitrophenyl antibodies. The amount of protein carbonyls was analyzed using ImageJ (n = 3). C) A2B5 cells were co-cultured with LPS (1 µg/ml) -activated BV2 cells and incubated ± 2 µM Grx2 (n = 10), Grx2C37S (n = 6), or Grx2S38P (n = 12) and surviving cells compared to cells treated with LPS alone (n = 9) were determined by the cell titer blue assay. D) OLN93 cells were treated with 5 mM NOC5 or NOC7 for 25 min with or without 2 µM Grx2 wildtype or 2 µM Grx2S38P. Surviving OLN93 cells were determined by the cell titer blue assay (n = 2). Mean ± SEM is shown, statistics were calculated using ANOVA (with Bonferroni post-test) (***: $p<0.001$), ns = not significant).

Fig. 5 Disassembly of holo-Grx2 leads to formation of dinitrosyl-iron-complexes. A) 150 µM human Grx2 was incubated with 5 mM GSNO in a sealed UV/VIS cuvette. At indicated time points, UV/VIS spectra were recorded. B) 250 µM human Grx2 was incubated with either 5 mM of GSH, GSSG, GSNO, or SNAP in sealed UV/VIS cuvettes. Decrease in absorbance at 428 nm was followed in a UV/VIS photospectrometer using 250 µM untreated hGrx2 as reference. C) 50 µM mouse Grx2 was incubated in 96 plate wells with 2 or 5 mM NOC5 or NOC7. The decrease in absorbance at 428 nm was recorded using a plate reader. D) Mössbauer spectra at 80 K of 3.3 mM human Grx2 (upper spectrum, quadrupole splitting ΔE_Q = 0.60 mm x s^{-1}, isomer shifts δ = 0.27 mm x s^{-1}) and 2.3 mM hGrx2 treated with 10 mM GSNO for 2 h (lower spectra, dashed line: quadrupole splitting ΔE_Q = 0.66 mm x s^{-1}, isomer shifts δ = 0.56 mm x s^{-1}, dotted line: quadrupole splitting ΔE_Q = 0.68 mm x s^{-1}, isomer shifts δ = 0.28 mm x s^{-1}, solid line: overlay of the two sub spectra). E) EPR spectra at 20 K of *E. coli* cells, *E. coli* cells overexpressing human Grx2 without GSNO treatment, or after 3 and 30 min of treatment with 1 mM GSNO and calculated concentrations of dinitrosyl-iron-complexes formed in *E. coli* cells overexpressing human Grx2 treated with 1 mM GSNO for indicated time points. F) 20 Mio OLN93 cells were incubated for 2 h with or without 100 µM mouse Grx2 or mouse Grx1 and 20 µM MK-571, an inhibitor of MRP1. Before freezing and EPR spectroscopy (9.64 GHz, 1 mW, 7.5 G modulation, 20 K), cells were washed once or twice with PBS and incubated with or without 5 mM GSNO for 3 min.

Fig. 6 Oligodendroglial cells express multidrug resistance protein1 (MRP1). A) Immunofluorescence of fixed OLN93 cells using anti-MRP1 antibodies (green). Nuclei were counterstained with Hoechst (blue), scale bar 50 µm. B) Western blot analyses of OLN93 and A2B5 cell lysates detecting MRP1 (190 kDa) using specific antibodies. C) PCR products obtained by qPCR using a specific MRP1 primer pair in OLN93 and A2B5 samples, but not in negative controls. D) Using the cell titer blue assay, the survival rates of A2B5 positive cells treated with 100 µM GSNO and 2 µM Grx2 ± 20 µM of the MRP1 inhibitor MK-571 were determined (n = 4, mean ± SEM). Statistics were calculated using Student´s t-test (ns = not significant).

Fig. 7 Dinitrosyl-iron-complex-induced inhibition of glutathione-S-transferase (GST) depends on Grx2 concentration. A) HeLa wildtype cells and HeLa cells overexpressing the mitochondrial isoform Grx2a (150% Grx2 compared to wt) or the cytosolic isoform Grx2c (300% Grx2 compared to wt) were incubated with 2 mM GSNO for 5 min. GST activity was measured via the 1-chloro-2,4-dinitrobenzene (CDNB) method and compared to HeLa without GSNO treatment. GST activity was plotted against Grx2 concentration in HeLa cells (n = 3). B) Recombinant GST was incubated with 2 mM GSNO in the presence of 5 and 50 µM hGrx2. Afterwards GST activity was determined using the CDNB method (n = 3). Data are mean ± SEM.

Fig. 1

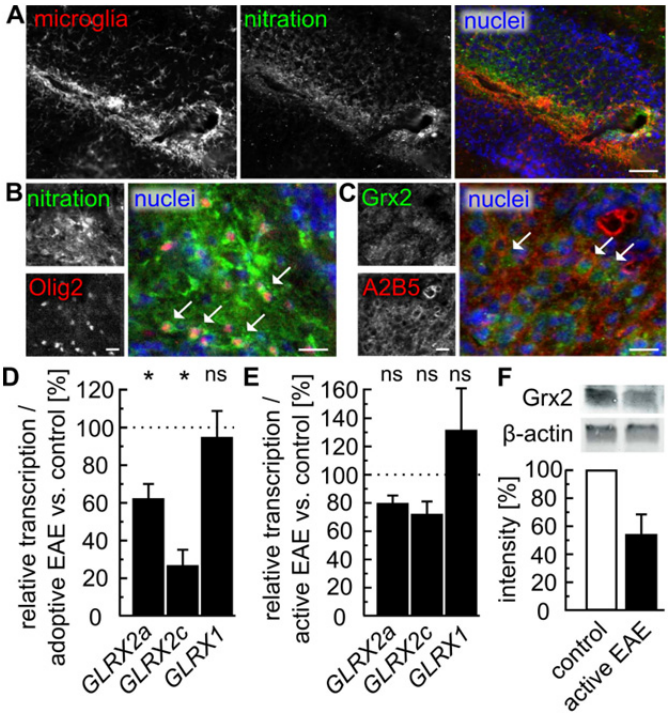
A
microglia
nitration
nuclei
B
nitration
nuclei
Olig2
C
Grx2
nuclei
A2B5
D
relative transcription / adoptive EAE vs. control [%]
* * ns
GLRX2a
GLRX2c
GLRX1
E
relative transcription / active EAE vs. control [%]
ns ns ns
GLRX2a
GLRX2c
GLRX1
F
Grx2
β-actin
intensity [%]
control
active EAE

Fig. 2

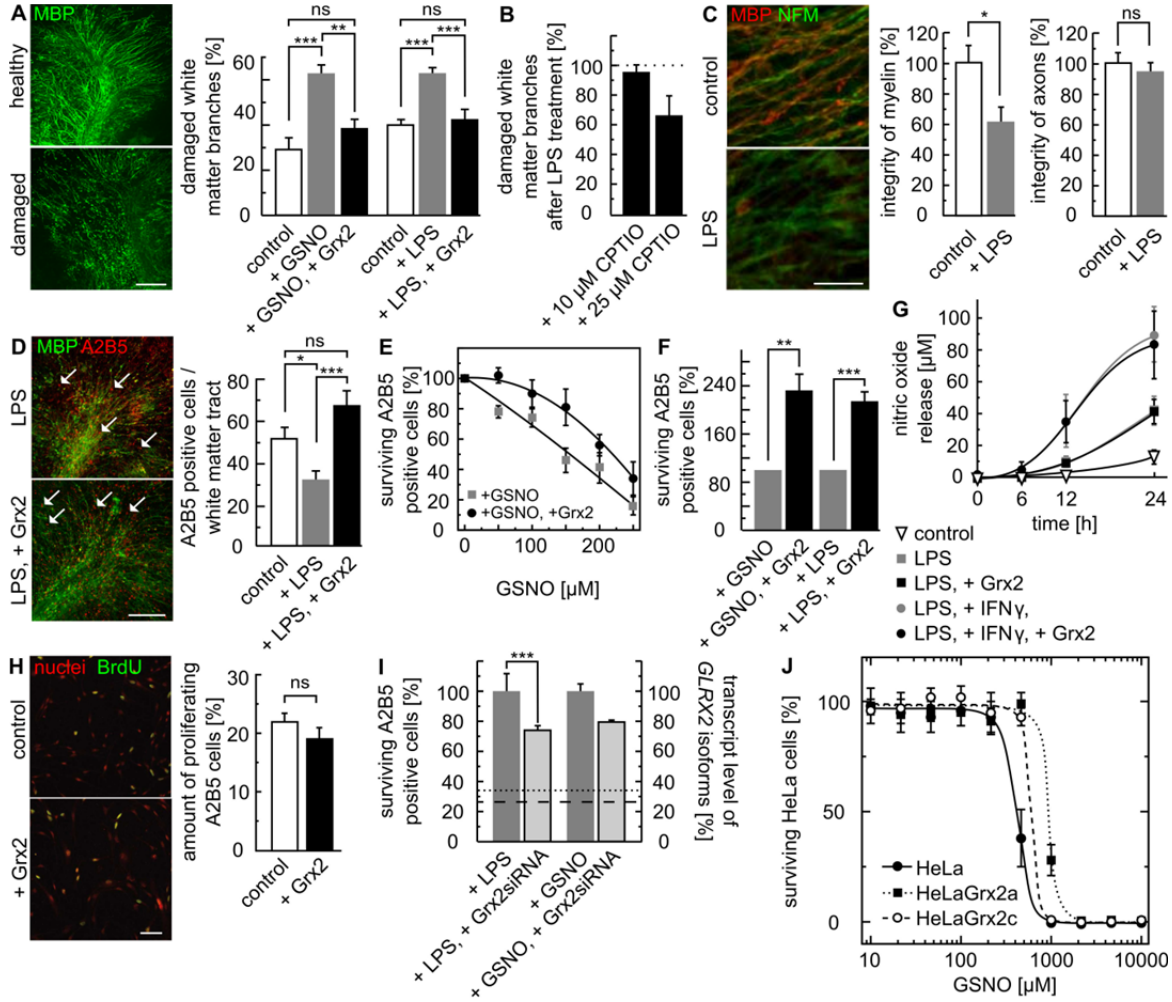
A
MBP
healthy
damaged
damaged white matter branches [%]
control
+ GSNO
+ GSNO, + Grx2
+ LPS
+ LPS, + Grx2
B
damaged white matter branches after LPS treatment [%]
+ 10 µM CPTIO
+ 25 µM CPTIO
C
MBP NFM
control
LPS
integrity of myelin [%]
integrity of axons [%]
D
MBP A2B5
LPS
LPS, + Grx2
A2B5 positive cells / white matter tract
E
surviving A2B5 positive cells [%]
+GSNO
+GSNO, +Grx2
GSNO [µM]
F
surviving A2B5 positive cells [%]
G
nitric oxide release [µM]
time [h]
control
LPS
LPS, + Grx2
LPS, + IFNγ,
LPS, + IFNγ, + Grx2
H
nuclei BrdU
control
+ Grx2
amount of proliferating A2B5 cells [%]
I
surviving A2B5 positive cells [%]
transcript level of GLRX2 isoforms [%]
+ LPS
+ LPS, + Grx2siRNA
+ GSNO
+ GSNO, + Grx2siRNA
J
surviving HeLa cells [%]
HeLa
HeLaGrx2a
HeLaGrx2c
GSNO [µM]

Fig. 3

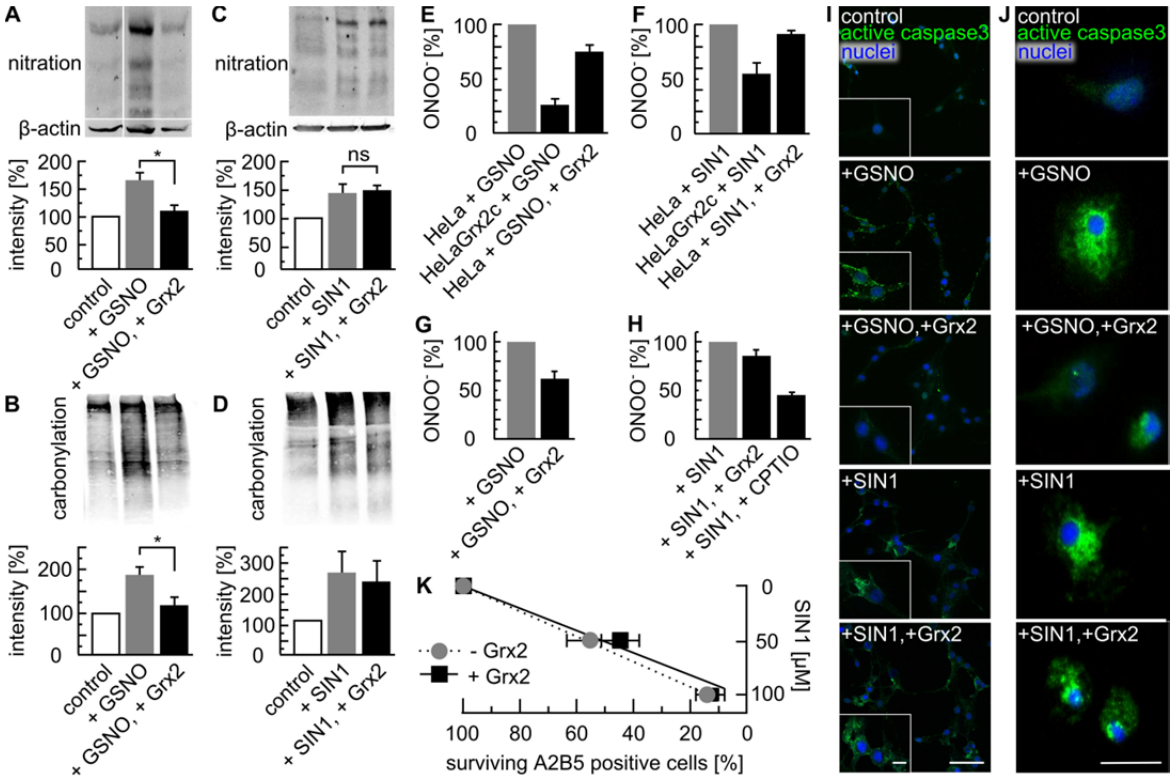
A
nitration
β-actin
intensity [%]
control
+ GSNO
+ GSNO, + Grx2
B
carbonylation
C
ns
+ SIN1
+ SIN1, + Grx2
D
E
ONOO- [%]
HeLa + GSNO
HeLaGrx2c + GSNO
HeLa + GSNO, + Grx2
F
HeLa + SIN1
HeLaGrx2c + SIN1
HeLa + SIN1, + Grx2
G
H
+ SIN1, + CPTIO
I
control
active caspase3
nuclei
+GSNO
+GSNO,+Grx2
+SIN1
+SIN1,+Grx2
J
K
- Grx2
+ Grx2
SIN1 [µM]
surviving A2B5 positive cells [%]

Fig. 4

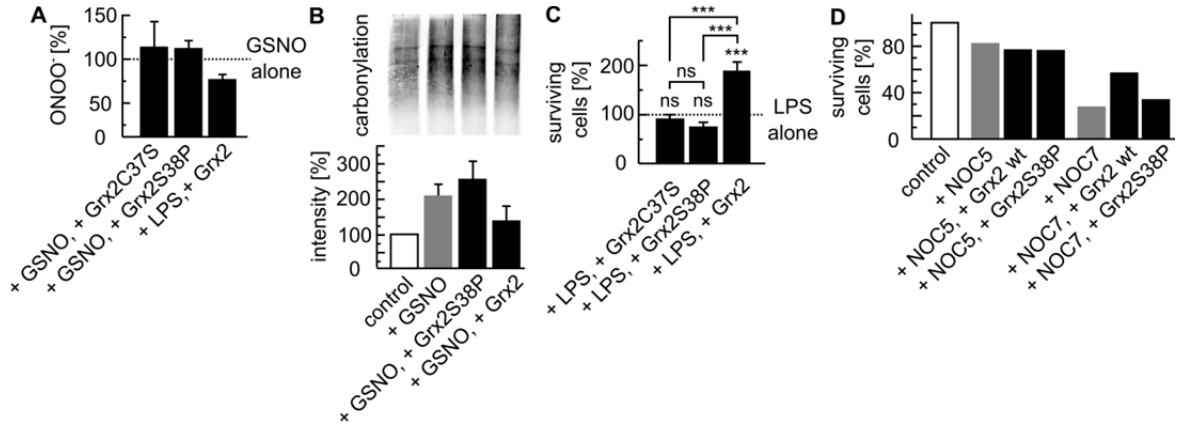
A
ONOO- [%]
GSNO alone
+ GSNO, + Grx2C37S
+ GSNO, + Grx2S38P
+ LPS, + Grx2
B
carbonylation
intensity [%]
control
+ GSNO
+ GSNO, + Grx2S38P
+ GSNO, + Grx2
C
surviving cells [%]
ns
***
LPS alone
+ LPS, + Grx2C37S
+ LPS, + Grx2S38P
+ LPS, + Grx2
D
surviving cells [%]
control
+ NOC5
+ NOC5, + Grx2 wt
+ NOC5, + Grx2S38P
+ NOC7
+ NOC7, + Grx2 wt
+ NOC7, + Grx2S38P

Fig. 5

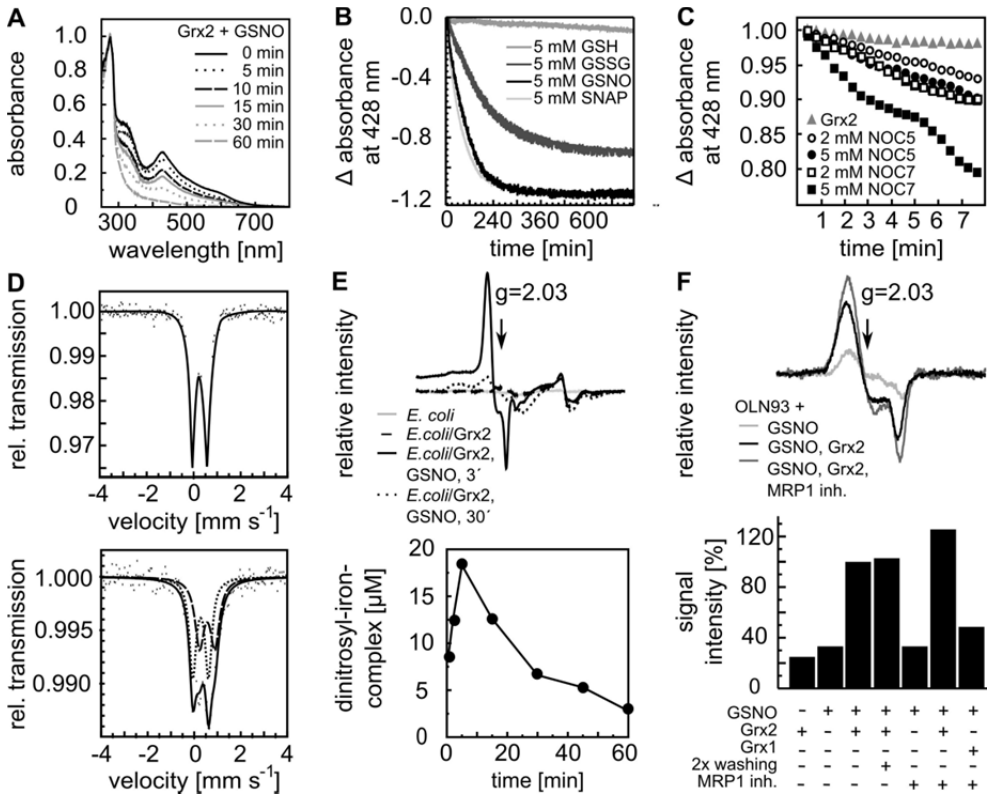
A
absorbance
Grx2 + GSNO
0 min
5 min
10 min
15 min
30 min
60 min
wavelength [nm]
B
Δ absorbance at 428 nm
5 mM GSH
5 mM GSSG
5 mM GSNO
5 mM SNAP
time [min]
C
Δ absorbance at 428 nm
Grx2
2 mM NOC5
5 mM NOC5
2 mM NOC7
5 mM NOC7
time [min]
D
rel. transmission
velocity [mm s-1]
E
relative intensity
g=2.03
E. coli
E.coli/Grx2
E.coli/Grx2, GSNO, 3´
E.coli/Grx2, GSNO, 30´
dinitrosyl-iron-complex [µM]
time [min]
F
relative intensity
g=2.03
OLN93 +
GSNO
GSNO, Grx2
GSNO, Grx2, MRP1 inh.
signal intensity [%]
GSNO
Grx2
Grx1
2x washing
MRP1 inh.

Fig. 6

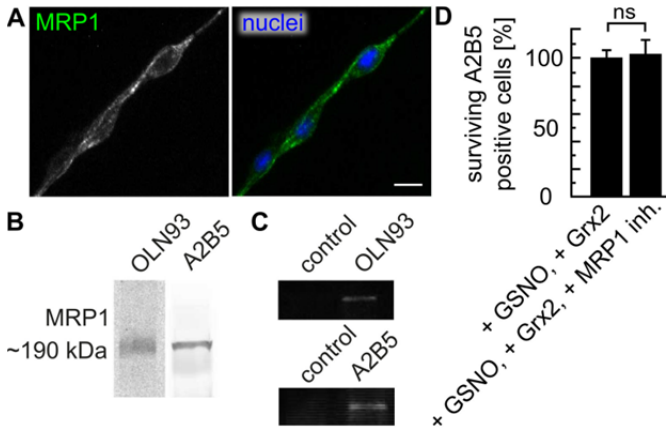
A
MRP1
nuclei
B
OLN93
A2B5
MRP1
~190 kDa
C
control
OLN93
control
A2B5
D
surviving A2B5 positive cells [%]
ns
+ GSNO, + Grx2
+ GSNO, + Grx2, + MRP1 inh.

Fig. 7

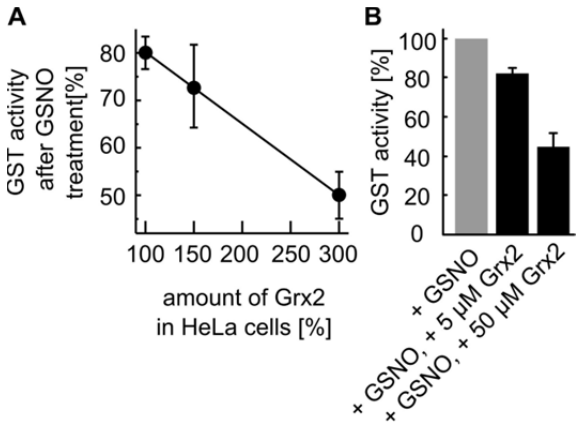
A
GST activity after GSNO treatment[%]
80
70
60
50
100 150 200 250 300
amount of Grx2 in HeLa cells [%]
B
GST activity [%]
100
80
60
40
20
0
+ GSNO
+ GSNO, + 5 µM Grx2
+ GSNO, + 50 µM Grx2

Supplement

Fig. S1 Purity of isolated A2B5 cells. A2B5 positive cells were visualized by anti-A2B5 antibodies (green). Quantification (mean ± SEM, n = 5) was performed by comparison to all cells visualized by Hoechst (blue). Scale bar 20 µm.

Fig. S2 Recombinant Grx2 is taken up by oligodendroglial cells. Organotypic cerebellar slice cultures (A,C), A2B5 cells (B,D) and OLN93 cells (E) were incubated with 2 µM Grx2. Recombinant Grx2 was visualized by anti-his-tag antibodies (A,B), mature oligodendrocytes by anti-MBP antibodies (A), and oligodendroglial progenitor cells by anti-A2B5 antibodies (B). Scale bars 50 (A) and 10 µm (B). C) Western blot analyses were performed with lysates obtained from slices (n = 4), A2B5 cells (n = 4), and OLN93 cells (n = 6) incubated with or without 2 µM Grx2 using anti-mouse Grx2 and anti-β-actin antibodies. Quantification (mean ± SEM) was performed using ImageJ.

Fig. S3 Control experiments for •NO treated oligodendrocytes. Effect of GSNO treatment on Grx2 expression in A2B5 positive cells (A) and OLN93 cells (B) was measured by qPCR (A, n = 3) or Western blot analyses (B, n = 3, quantification was performed using ImageJ). Survival rates of A2B5 positive cells treated with 250 µM GSNO with or without 10 or 50 µM of the NO scavenger CPTIO (C, n = 3), as well as BV2 cells (D, n = 3) and A2B5 positive cells (E, n = 3) treated with or without 1 µg/ml LPS and / or 2 µM Grx2 were determined 24 h after treatments with the cell titer blue assay. Shown are mean ± SEM.

Fig. S4 Protection of A2B5 cells against damages by Grx2 and MRP1 inhibition. A2B5 cells were incubated with 250 µM (A) or 50 µM (E) of the $^{\bullet}$NO-donor GSNO or 50 µM of the $ONOO^-$-donor SIN1 (B) ± 2 µM Grx2 (A,B,E) ± 20 µM of the MRP1 inhibitor MK-571 (E). Cell lysates were investigated for carbonylated (A and E, after derivatization of carbonyl groups to 2,4-dinitrophenylhydrazone before SDS-PAGE) and nitrated proteins (B) detected via Western blots using anti-dinitrophenyl antibodies (A, n = 2; E, n = 1) or anti-nitrotyrosine antibodies (B, n = 3) and analyzed using ImageJ. D) OLN93 cells were incubated with 0.5 mM H_2O_2 or GSNO ± 2 µM Grx2 and protein nitration was visualized via Western blot analysis using anti-nitrotyrosine antibodies. Data are mean ± SEM.

Fig. S1

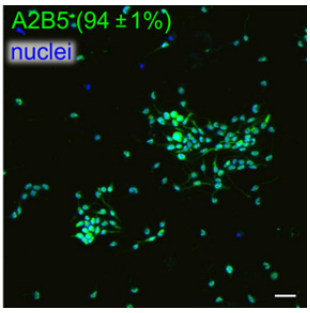
A2B5 (94 ± 1%)
nuclei

Fig. S2

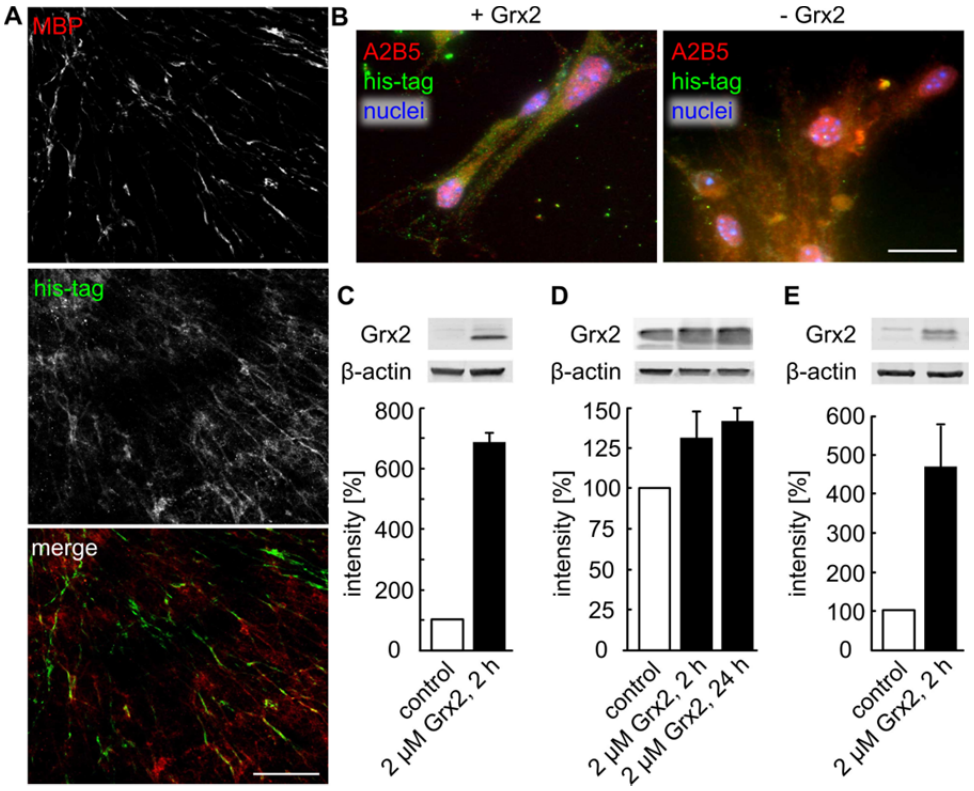
A
MBP
his-tag
merge
B
+ Grx2
- Grx2
A2B5
his-tag
nuclei
C
D
E
Grx2
β-actin
intensity [%]
control
2 µM Grx2, 2 h
2 µM Grx2, 24 h

Fig. S3

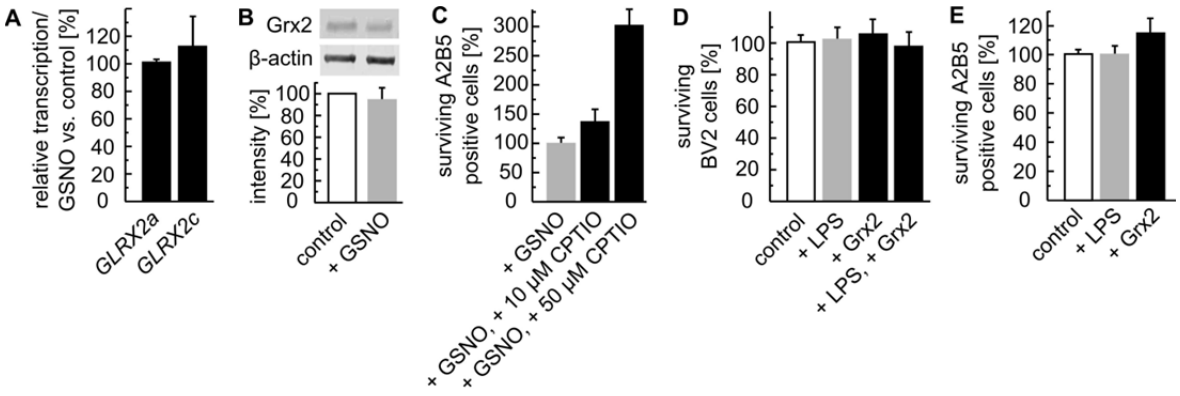
A
relative transcription/ GSNO vs. control [%]
120
100
80
60
40
20
0
GLRX2a
GLRX2c
B
Grx2
β-actin
intensity [%]
100
80
60
40
20
0
control
+ GSNO
C
surviving A2B5 positive cells [%]
300
250
200
150
100
50
0
+ GSNO
+ GSNO, + 10 µM CPTIO
+ GSNO, + 50 µM CPTIO
D
surviving BV2 cells [%]
100
80
60
40
20
0
control
+ LPS
+ Grx2
+ LPS, + Grx2
E
surviving A2B5 positive cells [%]
120
100
80
60
40
20
0
control
+ LPS
+ Grx2

Fig. S4

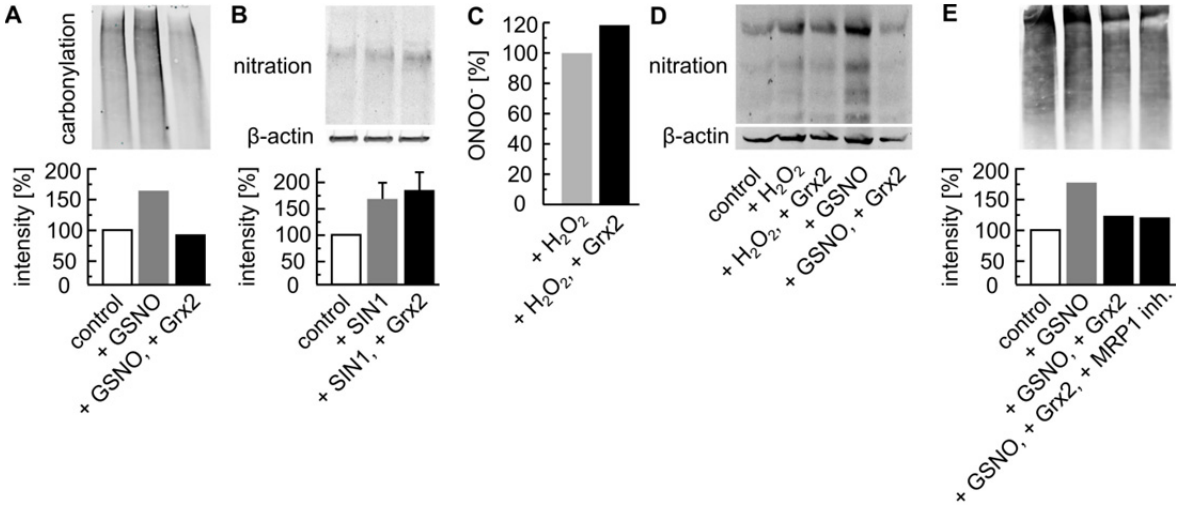
A
carbonylation
intensity [%]
200
150
100
50
0
control
+ GSNO
+ GSNO, + Grx2
B
nitration
β-actin
intensity [%]
200
150
100
50
0
control
+ SIN1
+ SIN1, + Grx2
C
ONOO- [%]
120
100
80
60
40
20
0
+ H2O2
+ H2O2, + Grx2
D
nitration
β-actin
control
+ H2O2
+ H2O2, + Grx2
+ GSNO
+ GSNO, + Grx2
E
intensity [%]
200
150
100
50
0
control
+ GSNO
+ GSNO, + Grx2
+ GSNO, + Grx2, + MRP1 inh.

7. Acknowledgements

First, I would like to thank Prof. Dr. Orhan Aktas for his supervision and for the opportunity to work on this project in the Department of Neurology and Prof. Dr. Dieter Willbold for the support and for accepting the task as referee.

Many thanks to my co-supervisor Dr. Carsten Berndt for his support through my PhD. Thanks for showing complete confidance in my work and for providing opportunities to collaborate with groups all over the world. Also big thanks to Dr. Tim Prozorovski for the interesting and motivating discussions. I'd like to thank all members of the AG Aktas and all current and former colleagues of the Life Science Center for helping me during both the productive and unproductive times. Especially Thomas (my lab-mate; THKL), Christine and Julia; thank you for the backup and all the fun and delicious times. I will never forget. Thanks to Katrin Volbracht for the help on establishing the *in vitro* and *ex vivo* assays. Further, many thanks to all colleagues and friends who read, discussed, corrected and thereby improved this thesis.

Thanks to all collaborators for supporting my work with helpful discussions and for the great time in their labs. Especially, I would like to thank Dr. Jack van Horssen and his group for their help by providing human MS material and for the establishment of the histological stainings. Thanks to Prof. Dr. Eckhard Bill for the opportunity to perform EPR measurements. Thanks to Prof. Dr. Roland Lill and to Dr. Ulrich Mühlenhoff for the help with the protein activity measurements. Thanks also to Prof. Dr. Rafael Radi and Natalia Rios for providing the Fluorescein-boronate probe.

For Financial Support I would like to thank the iBrain Graduate School from the Heinrich-Heine-University Düsseldorf, the priority program SPP1710 of the German Research Foundation and the Biogen GmbH.

Der größte Dank gebührt meinen Eltern, die mich meine gesamte Ausbildung hindurch stets unterstützt haben und ohne die es nicht möglich gewesen wäre. Allen Freunden, besonders Patrick und meiner kleinen Schwester Anna, danke ich, dass sie in allen Lebenslagen für mich da waren und da sind.

8. Declaration

Ich versichere an Eides Statt, dass die Dissertation von mir selbstständig und ohne unzulässige fremde Hilfe unter Beachtung der "Grundsätze zur Sicherung guter wissenschaftlicher Praxis an der Heinrich-Heine-Universität Düsseldorf" erstellt worden ist.

Die Dissertation wurde weder in dieser noch in einer abgewandelten Form bereits einer anderen Fakultät vorgelegt.

Ich habe bisher keine erfolglosen Promotionsversuche unternommen.

Düsseldorf, den 10. Januar 2017

_____

(Klaudia Lepka)